

REGIONAL GROUNDWATER GEOCHEMISTRY ON THE
NIAGARA PENINSULA

NATURAL AND ANTHROPOGENIC SOURCES CONTROLLING
REGIONAL GROUNDWATER GEOCHEMISTRY ON THE
NIAGARA PENINSULA

(Thesis Format: Monograph)

by

CAITLIN A. SMAL, B.SC.

School of Geography and Earth Sciences
Graduate Program in Earth and Environmental Sciences

A Thesis Submitted to the School of Graduate Studies in Partial
Fulfillment of the Requirements for the Degree Master of Science

McMaster University © Copyright by Caitlin A. Smal, 2016

MASTER OF SCIENCE (2016)
Earth and Environmental Sciences

McMaster University
Hamilton, Ontario

TITLE: Natural and Anthropogenic Sources Controlling Regional Groundwater
Geochemistry on the Niagara Peninsula

AUTHOR: Caitlin Alicia Smal (nee. McEwan), B.Sc. (Brock University)

SUPERVISORS: Dr. Gregory F. Slater, McMaster University
Dr. Stewart M. Hamilton, Ontario Geological Survey

PAGES: xvi, 288.

ABSTRACT

Groundwater chemistry on the Niagara Peninsula has been identified as highly mineralized in comparison to groundwaters collected from the same bedrock formations elsewhere in southern Ontario. Three geochemical zones were discerned using hierarchical cluster analysis and other geochemical and isotopic methods. The Escarpment Zone, located along the Niagara and Onondaga Escarpments, is characterized by unconfined aquifer conditions, parameters reflective of surficial contaminants, including road salt, and elevated HCO_3^- , DOC, NO_3^- , coliform bacteria and tritium. In contrast, in the Salina Zone thick, low-permeability sediments and gypsiferous bedrock results in highly mineralized groundwaters with Ca- SO_4 geochemical facies and elevated S^{2-} , Ca^{2+} , Mg^{2+} , K^+ , Na^+ , SO_4^{2-} , Cl^- , Br^- , Sr^{2+} , NH_4^+ and CH_4 . The Guelph Zone contains the lowest electrical conductivity of the three zones and elevated F^- . Outliers exist with groundwater geochemistry that differs from the local geochemical zone and the host aquifer. These sites have elevated SO_4^{2-} (>1000 to 5200 mg/L) with depleted $\delta^{34}\text{S}_{\text{SO}_4}$ (-2.2 to 14.3‰ VCDT) signatures that differs starkly from Devonian and Silurian evaporites (~20 to 32 ‰) in the host formations. This exogenic SO_4 was identified in a cross-formational northeast – southwest linear trend crossing three major groundwater flow systems. The lack of down-stream impact in these systems and tritium groundwater ages that are typically only decades old indicate a young, non-geological origin and implicate anthropogenic activities. Additionally, nine samples were identified with elevated methane concentrations and $\delta^{13}\text{C}_{\text{CH}_4}$ signatures within the thermogenic range. As thermogenic methane is not produced within shallow aquifers and would be short-lived in the presence of the ubiquitous sulfate, these samples imply recent upward migration of methane from depth through vertical conduits. Taken together, the evidence supports large-scale upward movement of fluids in the centre of the Niagara geochemical anomaly and more sporadic upward transport of gases over a wider area of the peninsula. The most likely vector is through

corroded and leaking casings or boreholes of abandoned (century) gas wells that are common across the peninsula.

ACKNOWLEDGEMENTS

I could not be here today without the support and help of several people. First, I would like to thank my supervisors, Dr. Greg Slater and Dr. Stew Hamilton. Greg, I am thankful for your support, encouragement and patience these past couple of years. Our meetings have encouraged me when I felt overwhelmed and your guidance with my thesis is much appreciated. Stew, thank you for all of the leadership and guidance over the last couple of years. I would not where I am today without you, and the opportunities you have given me. Your enthusiasm for geochemistry and hydrogeology is inspiring, and encouraged me to pursue this Master's thesis. Thank you for the guidance during the sampling program for this thesis and providing me with the opportunity to study this thesis and as well as insight and passionate discussion over the course of this thesis.

I would like to thank the members of the Environmental Organic Geochemistry group, particularly my office mates Mark, Corey, Kelly, Margot, Dave and Sian for their support and laughs over the last couple years. My time at McMaster University would not have been the same without you. I wish to express a sincere thank you to Corey Goad and Allyson Brady in particular for their assistance with lab work. Thank you for answering any questions I had when beginning new methods and for teaching me on the instruments. Finally, I would like to thank Jennie Kirby. Jennie, without you my sampling for my thesis would not have been complete. Thank you for managing and ordering the hundreds of sample bottles I needed on such short notice and teaching me on the instruments. Your excellent organization, guidance and patience made my thesis much less stressful and much more enjoyable.

Thank you to my crew leaders and fellow field assistants for their hard work collecting the samples for this thesis. Kayla, Steph, Neal, Jason, and Alex, thank you for the fun memories and the hard work last summer. I would like to sincerely

thank Stephanie Fudge for her hard work preparing, shipping and doing quality control on station and sample data in the past two years, and for her excellent organization during the sampling program. Thank you to Jayme Campbell from the Niagara Peninsula Conservation Authority for his local insight on Niagara's hydrogeology and resources, as well as cooperation and leadership during the monitoring well sampling program portion of this thesis. Jayme, sampling with you was fun and informative, and I really appreciate all the assistance and support you have provided over the past couple of years. Thank you to Abigail Burt for insight on the Quaternary sediments in Niagara, and for drilling all those monitoring wells that we sampled over the last few years!

My lab work, field work and writing would not have been completed without the unwavering support of my family and friends. I want to express my sincerest gratitude to my husband, Conrad, for his loving and unwavering support. Conrad, your support and love made the distance, long hours, and thesis writing easy and enjoyable, and you have always been there to support me. Thank you for always supporting my dreams and being a patient ear to talk to. Thank you to my parents and in-laws for their support during this time. Mom and Dad, you have always believed in me and never doubted my ability, and have lifted me up when I have become discouraged. Thank you to my sister Kirsten, and all my friends for your support and love during the completion of my thesis. Your interest in my research has helped me stay encouraged during the course of the field work, lab work and writing of this thesis.

TABLE OF CONTENTS

Abstract	iii
Acknowledgements	v
List of Tables	x
List of Figures	x
List of Appendices	xvi
Chapter 1: Introduction	1
Chapter 2: Background	6
2.1 Study Area Location	6
2.2 Geology	8
2.2.1 Quaternary Sediments	10
2.2.2 Regional Geologic Setting	11
2.2.3 Bedrock Geologic Units	14
2.2.4 Geologic Features	25
2.3 Hydrogeology	29
2.4 Previous Hydrogeochemical Research	34
2.4.1 Abandoned Gas Wells	34
2.4.2 Formational Waters	36
2.4.3 Shallow Groundwater Systems	36
2.4.4 Inorganic Geochemistry of Southern Ontario Groundwater.	41
2.4.5 Sulfur and Carbon Cycling in Groundwater Systems	41
2.4.6 Chloride – Bromide (Cl/Br) Ratios	44
Chapter 3: Methods	47
3.1 Site Determination	47
3.2 Sample Collection	50
3.3 Hydrogeological Testing	53

3.4 Sample Analysis	54
3.4.1 Field Measurement Techniques	54
3.4.2 Inorganic Geochemistry	57
3.4.3 Nitrogen and Bacterial Parameters	59
3.4.4 DOC and DIC Concentrations	60
3.4.5 Isotopic Analysis	62
3.5 Physical Well Locations and Quality Control Procedures	69
3.6 Statistical Analysis	71
3.7 Geochemical Modelling	72
Chapter 4: Results	74
4.1 Field Parameters and Inorganic Geochemistry	74
4.2 Regional Groundwater Chemistry Multivariate Statistics	81
4.2.1 Hierarchical Cluster Analysis (HCA)	82
4.3 Groundwater Chemistry of Clusters	88
4.3.1 Saturation Indices	94
4.3.2 Chloride-Bromide Ratios	97
4.4 Stable Isotope Geochemistry	99
4.4.1 Oxygen and Hydrogen Isotopes and Tritium of Water	99
4.4.2 Sulfur Isotopes	103
4.4.3 Carbon Isotopes	114
4.5 Dissolved Gasses	121
4.6 Case Study: Norfolk Quarry Biogeochemistry	122
Chapter 5: Discussion	126
5.1 Geological Context of the Niagara Geochemical Anomaly	129
5.2 Regional Hydrogeology of the Niagara Peninsula	140
5.3 Escarpment Zone Geochemical Grouping	148
5.3.1 Bedrock Geochemistry, Escarpment Zone	150

5.3.2 Influence of Biogeochemical Cycling on Groundwater Chemistry	153
5.4 Salina Zone Geochemical Grouping	165
5.4.1 Bedrock Geochemistry, Salina Zone	167
5.4.2 Influence of Biogeochemical Cycling on Groundwater Chemistry	173
5.5 Guelph Zone Geochemical Grouping	176
5.5.1 Bedrock Geochemistry and Biogeochemical Cycling	177
5.6 Exceptions and Outliers within Geochemical Groupings	179
5.6.1 Exogenic SO ₄ -rich, δ ³⁴ S _{SO₄} -depleted fluids	179
5.6.2 Exogenic Thermogenic Methane	182
5.6.3 Biogenic Methane	184
5.6.4 Additional Outliers	187
5.6.5 Case Study, Norfolk Quarry	188
Conclusion	191
References	195
Appendices	210

LIST OF TABLES

Table 4.1: Descriptive statistics for general chemistry parameters from bedrock wells on the Niagara Peninsula	76
Table 4.2: Calculated hardness values for samples	81
Table 4.3: Median geochemical concentrations and isotopic values for each cluster	86
Table 4.4: Correlation of cluster groupings and water-types	87
Table 4.5: Average enriched tritium (E^3H), $\delta^{18}O_{H_2O}$ and $\delta^2H_{H_2O}$ for each cluster	103

LIST OF FIGURES

CHAPTER 2

Figure 2.1: Groundwater sample locations within the study area	9
Figure 2.2: (top) Geological cross-section of sedimentary units and sediments on the Niagara Peninsula (Menzies and Taylor, 1988), (bottom) Drift thickness and Bedrock Escarpments on the Niagara Peninsula	12
Figure 2.3: Composite log of Quaternary sediments on the Niagara Peninsula (from Burt, 2015)	13
Figure 2.4: Geological cross-sections of the Niagara Escarpment and Onondaga Escarpments (courtesy of F. Brunton, 2016)	22
Figure 2.5: Stratigraphic Sequences of the geological units on the Niagara Peninsula (courtesy of F. Brunton, 2016)	23
Figure 2.6: Geological Map of the Onondaga Escarpment, Quarries and Mines (from Steele and Haynes, 2000)	24

Figure 2.7: Buried bedrock channels on the Niagara Peninsula (from Flint and Lolcama, 1986)	27
Figure 2.8: Location of Karst belts in southern Ontario (from Brunton, 2013) ...	29
Figure 2.9: Potentiometric groundwatersheds on the Niagara Peninsula (from NPCA, 2011 and Matheson, 2012)	33
Figure 2.10: Buried bedrock channels and groundwater flow direction on the western Niagara Peninsula (from Campbell and Burt, 2015)	34
Figure 2.11: Location of gas and petroleum wells on the Niagara Peninsula ...	35
Figure 2.12: $\delta^{18}\text{O}_{\text{H}_2\text{O}}$ and $\delta^2\text{H}_{\text{H}_2\text{O}}$, $\delta^{34}\text{S}_{\text{SO}_4}$ and $\delta^{18}\text{O}_{\text{SO}_4}$, and $\delta^{13}\text{C}_{\text{DIC}}$ of formation brines from Paleozoic formations in southern Ontario (from Skuce et al., 2015)	37
Figure 2.13: Isotopic fractionation due to lake evaporation from the Great Lakes basin (from Jasecho et al., 2014)	39
Figure 2.14: Movement of modern groundwater and stagnation of Pleistocene-aged groundwater underlying thick clay (from McIntosh and Walter, 2006)	40
Figure 2.15: $\delta^{13}\text{C}$ and $\delta^{18}\text{O}$ of DIC from the Salina Formation at the Domtar gypsum mine in Caledonia, Ontario (from O'Shea, 1988)	43

CHAPTER 3

Figure 3.1: Treatment system for a domestic well sampled as a part of this study.....	48
Figure 3.2: Obtaining static water level and well depth measurements from a well	49
Figure 3.3: A well pit with an unsecure sanitary seal well cap	50
Figure 3.4: Morning calibration station from pH, conductivity and dissolved oxygen	52
Figure 3.5: Sample bottles collected, field probes used, and field filtration equipment at a field site	53
Figure 3.6: Field measurement techniques for hydrogen sulfide and alkalinity.	56

Figure 3.7: Dissolved Inorganic Carbon (DIC) measurement comparison	63
Figure 3.8: Dissolved Organic Carbon (DOC) measurement comparison	64

CHAPTER 4

Figure 4.1: Spatial distributions of field parameters measured during collection of groundwater samples	77
Figure 4.2: Map of the distribution of concentrations of major cations Mg^{2+} , Ca^{2+} , Na^+ and K^+	78
Figure 4.3: Map of the distribution of concentrations of major ions HCO_3^- , SO_4^{2-} , Cl^- and Sr^{2+}	79
Figure 4.4: Map of geochemical concentrations of minor constituents As^{3+} , B , Fe^{2+} and F	80
Figure 4.5: Linkage distances between clusters defined using Hierarchical Cluster Analysis (HCA)	85
Figure 4.6: Spatial location of geochemical clusters defined by HCA	87
Figure 4.7: Water-types overlain on the subcropping Paleozoic bedrock	89
Figure 4.8: Piper Tri-Linear Diagrams for clusters defined using HCA	90
Figure 4.9: Box plots subdivided by cluster for bicarbonate, hydrogen sulfide, sulfate, Total Dissolved Solids (TDS) and pH	91
Figure 4.10: Box plots subdivided by cluster for calcium, magnesium, sodium, chloride and bromide	92
Figure 4.11: Water-type facies represented in each cluster	93
Figure 4.12: Box and Whisker plots of saturation indices for minerals commonly found in sedimentary bedrock units subdivided by cluster	95
Figure 4.13: Spatial distribution of gypsum and calcite saturation indices for samples in the study area	96
Figure 4.14: Spatial distribution of the dolomite saturation index for samples collected within the study area	97

Figure 4.15: Chloride – Bromide ratio plots for Group A (a) and Group B (b)	100
Figure 4.16: Water Isotopes of samples collected as a part of this study plotted on the Global Meteoric Water Line and Great Lakes Meteoric Water Line	104
Figure 4.17: Maps of $\delta^{18}\text{O}_{\text{H}_2\text{O}}$ (‰) and $\delta^2\text{H}_{\text{H}_2\text{O}}$ (‰) of groundwater samples collected on the Niagara Peninsula	105
Figure 4.18: Distribution of the Deuterium Excess for groundwater samples in the study area	106
Figure 4.19: Chart of Conductivity ($\mu\text{S}/\text{cm}$) vs $\delta^{18}\text{O}_{\text{H}_2\text{O}}$ (‰)	106
Figure 4.20: Distribution of enriched tritium values (TU) in the study area	107
Figure 4.21: Tritium values (in TU) vs $\delta^{18}\text{O}_{\text{H}_2\text{O}}$ (‰) for samples	107
Figure 4.22: $\delta^{34}\text{S}_{\text{SO}_4}$ (x-axis) and $\delta^{34}\text{S}_{\text{S}^{2-}}$ (y-axis) isotopic signatures (‰) for all groundwater samples with sulfide concentrations >0.3 mg/L	108
Figure 4.23: (a) $\delta^{34}\text{S}_{\text{SO}_4}$ (x-axis) and $\delta^{18}\text{O}_{\text{SO}_4}$ (y-axis) isotopic signatures (‰) for all groundwater samples organized by cluster, (b) inset map of boxed area in (a)	109
Figure 4.24: Spatial locations of (a) $\delta^{18}\text{O}_{\text{SO}_4}$ (‰) and (b) $\delta^{34}\text{S}_{\text{SO}_4}$ (‰) from samples collected on the Niagara Peninsula	110
Figure 4.25: Map of spatial locations of $\delta^{34}\text{S}_{\text{H}_2\text{S}}$ (‰) from samples collected on the Niagara Peninsula	111
Figure 4.26: $\delta^{34}\text{S}$ isotopic values (‰) of (a) sulfate and (b) sulfide compared to concentrations of sulfate in samples collected	112
Figure 4.27: $\delta^{34}\text{S}$ isotopic values (‰) of (a) sulfate and (b) sulfide compared to concentrations of sulfide in samples collected	113
Figure 4.28: $\delta^{13}\text{C}$ (‰) of DOC vs $\delta^{13}\text{C}$ (‰) of DIC	115
Figure 4.29: (a) Concentration of DIC compared with $\delta^{13}\text{C}$ of DIC (‰) (b) Spatial distribution of $\delta^{13}\text{C}$ of DIC (‰)	116
Figure 4.30: (a) Concentration of DOC compared with $\delta^{13}\text{C}$ of DOC (‰) (b) Spatial distribution of $\delta^{13}\text{C}$ of DOC (‰)	117
Figure 4.31: Spatial locations and sample ID's of wells sampled for $\delta^{13}\text{C}$ of methane (‰) overlain on the subcropping geology	118

Figure 4.32: (a) $\delta^{13}\text{C}$ (‰) of CH_4 vs. DOC concentration and (b) HCO_3^- concentration	119
Figure 4.33: (a) $\delta^{13}\text{C}$ (‰) of CH_4 vs. $\delta^{13}\text{C}$ of DIC (‰) (b) CH_4 concentration vs. $\delta^{13}\text{C}$ of CH_4 (‰)	120
Figure 4.34: Comparison between laboratory and field measurements of methane concentration from collected samples	121
Figure 4.35: Changes in concentrations and isotopic values of geochemical parameters across a transect of groundwater from exposed bedrock at the Norfolk Quarry, near Port Dover, Ontario	124 - 125

CHAPTER 5

Figure 5.1: Geochemical Zones defined using results of HCA overlain on (a) drift thickness and (b) the Paleozoic Geology	128
Figure 5.2: Comparison between Sulfate concentrations (mg/L) on the Niagara Peninsula and in the same formations elsewhere in southern Ontario	132
Figure 5.3: Comparison between Magnesium concentrations (mg/L) on the Niagara Peninsula and in the same formations elsewhere in southern Ontario	133
Figure 5.4: Comparison between Calcium concentrations (mg/L) on the Niagara Peninsula and in the same formations elsewhere in southern Ontario	134
Figure 5.5: Comparison between Light Rare Earth Elements (LREE) concentrations (mg/L) on the Niagara Peninsula and in the same formations elsewhere in southern Ontario	135
Figure 5.6: Comparison between DOC concentrations (mg/L) obtained from bedrock wells on the Niagara Peninsula and from bedrock formations in southern Ontario	136
Figure 5.7: Longitudinal plots of SO_4^{2-} , Ca^{2+} and Mg^{2+} for the Salina group transecting from Lake Huron in the west to the Niagara River in the east	137
Figure 5.8: Longitudinal plots of SO_4^{2-} , Ca^{2+} and Mg^{2+} for the Silurian carbonate units transecting from Lake Huron in the west to the Niagara River in the east	138

Figure 5.9: Longitudinal plots of SO_4^{2-} , Ca^{2+} and Mg^{2+} for the Devonian carbonate units transecting from Lake Huron in the west to the Niagara River in the east	139
Figure 5.10: Bedrock topography on the Niagara Peninsula	144
Figure 5.11: (a) Tritium and (b) $\delta^{18}\text{O}_{\text{H}_2\text{O}}$ isotopic signatures within groundwater catchments (Matheson, 2012) on the Niagara Peninsula	145
Figure 5.12: (a) Bicarbonate concentrations (mg/L) and (b) Conductivity ($\mu\text{S}/\text{cm}$) in wells located near the Fonthill ice contact delta complex	146
Figure 5.13: Water levels in the Chippawa (Niagara Falls) Channel from Lake Erie to the Niagara River	147
Figure 5.14: Elevated Nitrate concentrations plotted on a Cl/Br mass ratio chart (a) and spatial plot (b)	156
Figure 5.15: Tritium values plotted on a Cl/Br mass ratio chart (a) and spatial plot (b)	157
Figure 5.16: Nitrate, Nitrite and Ammonia concentrations (mg/L) on the Niagara Peninsula	158
Figure 5.17: $\delta^{18}\text{O}_{\text{SO}_4}$ vs $\delta^{34}\text{S}_{\text{SO}_4}$ chart for samples from each cluster on the Niagara Peninsula with sources of sulfate and their respective isotopic ranges	163
Figure 5.18: Water colour in Geochemical Zones on the Niagara Peninsula..	164
Figure 5.19: (a) SO_4^{2-} concentrations plotted on a chloride concentration vs. Cl/Br mass ratio chart. (b) Location of elevated SO_4^{2-} concentrations in Niagara	168
Figure 5.20: Hardness (mg/L CaCO_3) vs Alkalinity (mg/L CaCO_3) plot by cluster	171
Figure 5.21: (a) Ca^{2+} (x-axis) vs. SO_4^{2-} (y-axis) plot and (b) Ca^{2+} (x-axis) + Mg^{2+} vs. SO_4^{2-} (y-axis) chart	172
Figure 5.22: $\delta^{13}\text{C}_{\text{DIC}}$ and $\delta^{34}\text{S}_{\text{SO}_4}$ isotopic compositions overlain on the groundwatersheds on the Niagara Peninsula	175
Figure 5.23: Exogenic sulfate samples collected on the Niagara Peninsula ...	182
Figure 5.24: Location of exception and outliers within geochemical groupings	189

LIST OF APPENDICES

Appendix A: Field Parameters	211
Appendix B: Station Locations and Geologic Units	215
Appendix C: Station and Well Information	221
Appendix D: Major Ion Chemistry	226
Appendix E: Bacterial and Nitrogen Parameters	231
Appendix F: Dissolved Gases and Carbon Species	236
Appendix G: Minor Constituents – B, PO ₄ , Si, Sr, B, Fe and I	241
Appendix H: Trace Constituents – Ag, Al, As, Ba, Be, Bi, Cd	246
Appendix I: Trace Constituents – Ce, Co, Cr, Cs, Cu, Dy, Er	251
Appendix J: Trace Constituents – Eu, Ga, Gd, Hf, Hg, Ho, La	255
Appendix K: Trace Constituents – Li, Lu, Mn, Mo, Nb, Nd, Ni	260
Appendix L: Trace Constituents – Pb, Pr, Rb, Sb, Sc, Se, Sm	265
Appendix M: Trace Constituents – Sn, Ta, Tb, Th, Ti, Tl, Tm	270
Appendix N: Trace Constituents – U, V, W, Y, Yb, Zn, Zr	275
Appendix O: Isotopic Parameters	280
Appendix P: Water Type and Cl/Br Ratios	285

Chapter 1: Introduction

Groundwater is a source of drinking water for 2.9 million users in southern Ontario (Singer, 2003). In areas where fresh, abundant groundwater is plentiful, rural residents obtain domestic water from wells completed in shallow, high permeability sediments and bedrock aquifers. Groundwater obtained from bedrock aquifers in most places in southern Ontario is of good quality, with sufficient capacity for domestic use (Singer, 2003). Natural water quality problems in groundwater obtained from drilled wells in bedrock are normally the result of dissolved constituents of mineralogical origin and their subsequent modification by redox processes; including high sulfate from evaporite minerals, dissolved methane produced in shallow bedrock aquifers, hardness from carbonate dissolution, hydrogen sulfide from organic reduction of sulfate and dissolved trace metals from the host bedrock.

The Ambient Groundwater Geochemistry program of the Ontario Geological Survey (OGS) provides novel opportunities for the study and characterization of bedrock groundwater and the sources of its chemical constituents in southern Ontario (Hamilton et al., 2011; Hamilton, 2015). The program collects raw groundwater samples from domestic, farm and monitoring wells in accessible parts of the province to allow mapping of groundwater geochemistry. The uniform spatial distribution of samples, robust chemical characterization and consistency of sampling protocols allows for the determination of geochemical signatures relating to the water bearing zone in rock or the screened interval in overburden from which the samples were obtained. In most cases, wells sampled are drilled to and ‘completed’ at either the bedrock interface aquifer ± 1 m from the bedrock surface (i.e. the ‘contact’ aquifer) or into the sub-cropping bedrock unit. In a small number of cases, wells were drilled through the subcropping bedrock unit and completed in a deeper bedrock unit.

The OGS identified locations of poor water quality in bedrock groundwater upon completion of the Ambient Groundwater Geochemical sampling in southern Ontario. One such region is on the Niagara Peninsula, where many rural residents have resorted to the use of cisterns and trucked-in water because of the poor quality of groundwater in the carbonate-bedrock aquifer. The anomalous geochemical nature of the bedrock aquifers on the Niagara Peninsula was first described by Hamilton et al. (2011) as 2 different systems, the Selkirk-Grimsby anomaly and the Welland anomaly. Matheson (2012) treated the entire Niagara Peninsula as one system, delineating 4 groundwater groupings based on the stable isotopes of water and tritium.

Following the results of the southern Ontario portion of the Ambient Groundwater Sampling Program (Hamilton, 2015) and an undergraduate thesis on the Niagara Peninsula geochemical anomaly (Matheson, 2012), it was determined that more study was required. Additional sampling at a higher density (~4x) was carried out in the summer of 2015 (McEwan et al., 2015) and a large-scale analytical program was completed. This thesis describes further research, using these data, on the source of anomalous geochemical conditions in bedrock groundwater on the Niagara Peninsula.

This Master's thesis was completed in cooperation and with the support of the OGS. Sampling efforts in the western Peninsula in the summer of 2015 was lead in part by the author and the results of geochemical samples are presented in this study. A collaborative study between the OGS and the Niagara Peninsula Conservation Authority (NPCA) allowed for the extension of the study area eastwards to the Niagara River at a lower density.

The objectives of this study are specific to the Niagara Peninsula and are as follows;

- 1) To identify sources of anomalous groundwater chemistry
- 2) To understand controls on spatial variations in groundwater chemistry

- 3) To characterize redox processes influencing the geochemical assemblage in bedrock groundwater
- 4) To determine if surficial and/or deep subsurface anthropogenic influences have affected groundwater quality
- 5) To understand regional hydrogeological conditions and their role in influencing the geochemical assemblage of samples

This study aims to understand the sources of poor water quality in bedrock aquifers to aid in decision-making for rural communities and homeowners on the Niagara Peninsula who currently rely on wells with poor quality and/or expensive treatment systems or cisterns.

Possible hypotheses as to the sources of the anomalous groundwater chemistry in bedrock on the Niagara Peninsula include: (a) water rock interaction, including gypsum dissolution, dedolomitization reactions and carbonate dissolution, (b) variations in the thickness of low permeability clay and silt sediments protecting the aquifer from surface contamination (c) karst influencing the rate at which surface waters can enter the aquifer, and (d) the influence of up to century-old, corroding and abandoned gas wells in the southern portion of the peninsula allowing gas or water to move into shallow aquifers from deeper strata.

Water-rock interaction is believed to be a dominant process controlling groundwater chemistry in the bedrock aquifers on the Niagara Peninsula. The dissolution of high solubility gypsum and anhydrite in the Salina Group adds dissolved sulfate and calcium to groundwater. Carbonate dissolution can also occur in areas with exposure to the atmosphere, such as karst terrains. It is hypothesized that carbonate dissolution is occurring where bedrock is exposed at surface in the northern and southern Niagara Peninsula (Brunton and Dodge, 2008). The influence of terrestrial sulfides on groundwater chemistry is suggested to play a role in the southwestern and southeastern Niagara Peninsula (Matheson, 2012). To investigate this hypothesis, sulfur isotopes samples were

collected in the 2015 sampling program for analysis of dissolved sulfate and sulfide. With increases in elemental concentrations of redox-sensitive parameters in bedrock aquifers, it is expected that microbial metabolic activity will affect the relative proportions of these species. Geochemical and isotopic tracers are commonly used to trace metabolic reactions in groundwater systems, and are used in this study.

Drift thickness can prevent the downward infiltration of fresh precipitation to recharge groundwater aquifers. On the central Niagara Peninsula, thick clay units infill bedrock troughs and buried bedrock valleys, acting as aquitards in restricting the recharge and movement of groundwater. As a result, late Pleistocene, early Holocene aged groundwater remains in the Wainfleet area (Matheson, 2012). Where drift is absent or thin, rapid recharge of snow-melt and rain can occur, especially during the winter months. Locations with thin drift are susceptible to surface contamination, especially where karst and epi-karst bedrock is present.

Matheson (2012) suggested that abandoned wells provide the most viable explanation for the source of the highly mineralized groundwater on the Niagara Peninsula and contribute additional bicarbonate, reduced sulfides and organic material to the shallow groundwater systems. With increased data collection as a part of this study, this hypothesis is investigated. Southwestern Ontario has a history of hydrocarbon production dating back to 1858 (Skuce et al., 2015) when the first commercial oil well was installed near Oil Springs, Ontario. Not long after in 1866, the first 'sour gas' (i.e. rich in hydrogen sulfide) was found in Port Colborne, Ontario, within the bounds of the current study area. The spread of hydrocarbon production in southern Ontario occurred rapidly in the late 19th Century, with thousands of wells installed prior to the monitoring and regulation of well construction and abandonment procedures in Ontario (Skuce, 2013). Abandoned 'century' gas wells are unused, abandoned and corroding due to the presence of hydrogen sulfide in shallow-intermediate depth bedrock aquifers (Skuce et al., 2015). It should be noted that although gas wells may appear to be

abandoned as reported by the Ontario Ministry of Natural Resources, many wells are still used by landowners but not reported to the regulating agencies (J. Warbick, P. Comm, 2015).

This investigation was completed using a broad geochemical and isotopic characterization of samples; including major ions, trace elements, field parameters, bacteriological parameters; stable isotopes of carbon, sulfur and water and tritium. 17 sample bottles were collected at 156 domestic and farm wells, monitoring wells, and abandoned water wells across the Niagara Peninsula for the interpretation of geochemical changes.

Thesis Structure

Following the introduction, Chapter 2 provides background information on the location, geology, and hydrogeology of the study area, defines past hydrogeochemical research on the Niagara Peninsula, and the biogeochemical processes responsible for the geochemical evolution of bedrock groundwater. Chapter 3 describes the methods used for sample preparation, sample collection, sample analysis, and data processing in this study. Chapter 4 presents the results of this study, followed in Chapter 5 by the discussion of the results and its place in past research. Chapter 6 provides a summary of the findings of this study and suggestions for future work.

Chapter 2: Background Information

The primary intent of this chapter is to provide context, including the geological and hydrogeological setting, for the regional bedrock groundwater geochemical data discussed in this study. This will also include a discussion of regional hydrogeochemical investigations completed to date on the Niagara Peninsula and concepts relating to geochemical and isotopic signatures seen in these waters.

2.1 Study Area Location

The primary study area encompasses the Niagara Escarpment to the north, Lake Erie to the south, Hamilton to the west and the Niagara River in the east (Figure 2.1). Two samples were taken below the Niagara Escarpment as part of a complimentary sampling program, and were included with results of this study for geochemical context. The study area is within Universal Transverse Mercator (UTM) Zone 17N using the 1983 North American Datum (NAD83) projection between the latitudes of 42°47'34" N and 43°13'36" N and longitudes of 79°20'32" W and 80°12'14" W. It has an approximate surface area of 3300 km², with land usage dominated by agriculture and livestock, rural residential areas and forested areas. Communities in the study area include (from east to west) Pelham, Wainfleet, Lowbanks, Dunnville, Lincoln, Smithville, Cayuga, Grimsby, Binbrook, Hamilton, Caledonia, Hagersville and Port Dover. The Welland Canal provides a linkage for ship transport between Lake Ontario and Lake Erie, and extends 43 km from St. Catharines to Port Colborne.

As a result of collaborative efforts with the NPCA, the study area was extended eastwards to the Niagara River, with monitoring well sampling from 18 locations providing geochemical characterization. The eastern study area is located within the latitudes of 42°47'34" N and 43°13'36" N and longitudes of 78°54'31" W and 79°20'32" W. The sampling area in the eastern peninsula is at a lower density,

but yields similar geochemical trends from field parameter observations. Most samples were collected south of (i.e. above) the Niagara Escarpment, with the exception of two samples located close to Lake Ontario. Major municipalities in the eastern Niagara Peninsula include the Town of Port Colborne, the City of Welland, the City of Thorold, the City of St Catharines, the Town of Niagara-on-the-Lake, the City of Niagara Falls, and the Town of Fort Erie.

The western study area for this thesis was subdivided into 5 x 5 km spatial cells, with the goal of attaining one geochemical sample from a bedrock well in each cell to delineate spatial changes in groundwater chemistry. This goal was successfully attained, as in every 5 by 5 km node across the western study area, 1 geochemical and isotopic sample set was taken from a well completed in the bedrock aquifer or the “overburden–bedrock contact” aquifer. The majority of samples collected were from domestic wells and farm wells, some of which were disused but not decommissioned. Homeowners with domestic wells drilled to bedrock were contacted and asked if they were willing to participate in the scientific study; if they agreed, then the raw, untreated groundwater was sampled from their well. Groundwater samples were collected at regular intervals from Port Dover in the west to just west of Welland in the east (Figure 2.1) in the summer of 2015 following Ambient Groundwater Geochemistry Program sampling protocols (Hamilton, 2015 – Supporting Document). Additional sampling using the protocols and methods of the Ambient Groundwater Geochemistry Program (Hamilton et al., 2010; Hamilton, 2015) was completed in the eastern Niagara Peninsula in collaboration with the NPCA. This sampling was completed in monitoring wells mostly (~80%) installed by the OGS as part of the three-dimensional Quaternary mapping project of the Niagara Peninsula, with support from the NPCA (Burt, 2014). Several Provincial Groundwater Monitoring Network (PGMN) wells were sampled on the peninsula that are managed by local conservation authorities. The monitoring well sampling in the summer and early

fall of 2015 provided high-quality, geo-referenced ‘golden spike’ samples supporting the domestic well sampling.

The study area encompasses 4 conservation authorities: The NPCA, the Grand River Conservation Authority, the Long Point Conservation Authority and the Hamilton Conservation Authority, each responsible for their own Source Protection Areas (NPCA, 2014; Lake Erie Region Source Protection Committee, 2015a, Lake Erie Region Source Protection Committee, 2015b; Halton-Hamilton Source Protection, 2015; Figure 2.1). The Niagara Peninsula Source Protection Area (NPSPA) comprises the largest portion of the study area, with a total area of 2,430 km² and over 450,000 residents (NPCA, 2013). The NPSPA has 3 main drainage areas; the Lake Ontario Drainage area (40%), Niagara River Drainage area (55%) and Lake Erie Drainage area (5%). The largest watershed in the NPSPA is the Welland River watershed, with a watershed area of approximately 1050 km² (NPCA, 2013). This watershed is located centrally in the study area, extending from the headwaters at the NPSPA boundary near Ancaster in the west to the Niagara River near Niagara Falls in the east. Connection between surface water and groundwater is minimal in the Welland River watershed (NPCA, 2013), as the majority of the watershed lies on the low-permeability, primarily glaciolacustrine deposits of the Haldimand Clay Plain.

2.2 Geology

This section provides an overview of the geological controls influencing groundwater flow and chemistry of ambient bedrock groundwater on the Niagara Peninsula. It discusses the subcropping bedrock geology, Quaternary glacial sediments and prominent geologic features of the Niagara Peninsula south of the Niagara Escarpment.

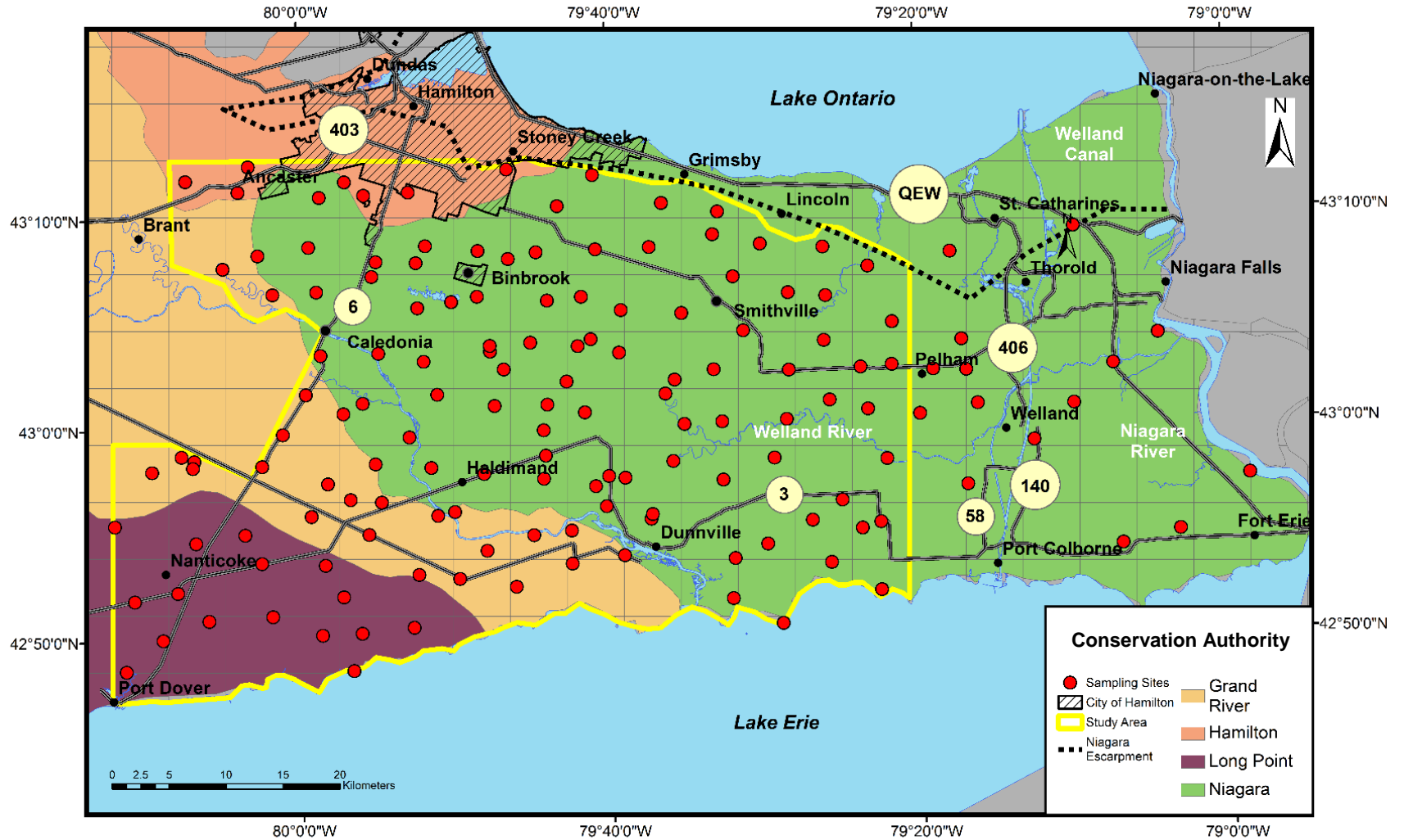


Figure 2.1: Groundwater sample locations from domestic wells, monitoring wells, springs and Conservation Authorities within the study area.

2.2.1 Quaternary Sediments

Detailed descriptions of Quaternary glacial sediments on the Niagara Peninsula have been provided by Burt (2014, 2015), Menzies and Taylor (1998) and Feenstra (1981). For the purposes of this study, a short description of the major sediment groups deposited in glacial and post-glacial periods within the study area will follow. The OGS is currently undertaking a 3-D Mapping Program to refine the location of buried bedrock valleys, glacial features, and sediments present on the Niagara Peninsula (Burt, 2014; Burt 2015; Campbell and Burt, 2015). Glacial cover is thinnest (Figure 2.2) at the crest of the Niagara and Onondaga escarpments (Menzies and Taylor, 1998) and thickens in the Salina trough, which is a bedrock low between the two escarpments trending from Brantford to Welland along the strike of the Salina Group (F.R. Brunton, P. Comm., 2014).

A composite log was drafted by Burt (2015) (Figure 2.3) describing the major stratigraphic units present on the Niagara Peninsula. The current understanding of depositional events on the Niagara Peninsula consists of 4 depositional periods including two ice advances represented by two till units within the stratigraphic framework (Menzies and Taylor, 1998).

Burt describes the Lower Drift unit as being the oldest unit, comprising sand, silt and locally gravel and ranging in thicknesses from several metres in the Salina bedrock trough to a few centimetres on the Niagara and Onondaga Escarpments (Burt, 2015). This unit includes glacial features such as drumlins south of the Onondaga Escarpment and potentially eskers in some locations (Burt, 2015). This unit was described as correlating with the Wentworth or Catfish Hill – Wentworth Till (Feenstra, 1981). Overlying the Lower Drift unit is the Lower Glaciolacustrine unit composed of clay, silty clay and clayey silt deposited following the retreat of Wentworth ice and the subsequent formation of glacial Lake Warren and Whittlesey (Burt, 2015). The Halton Drift was deposited during

the advance and retreat of Halton ice, and includes a wide range of sediment types. The Halton Drift mainly contains of silt and clay, with some stones close to the Niagara Escarpment. This unit is the thickest stratigraphic unit in the Niagara Region (Menzies and Taylor, 1998). The Fonthill ice contact-delta complex in the east-central part of the study area is a prominent topographical landform on the Niagara Peninsula formed along the Halton ice margin. The Fonthill ice contact-delta complex is composed of gravelly sand, sand, and silty sand overlying silty diamiction and glaciolacustrine silt and clay (Burt, 2015). The Upper Glaciolacustrine unit contains rhythmically bedded silt and clay in the western Niagara Peninsula and clay in the central and eastern Niagara Peninsula deposited under deep-water lake conditions (Burt, 2015).

Glaciolacustrine units formed under deep-water lake conditions located between the Niagara and Onondaga Escarpments are collectively referred to as the Haldimand Clay (Figure 2.3) (Menzies and Taylor, 1998). Clays on the Niagara Peninsula have high smectite content and are susceptible to swelling. The Wainfleet bog is a large peat deposit north of the Onondaga Escarpment near the Port Colborne – Wainfleet area deposited in a glaciolacustrine setting in deep water, lake conditions (Menzies and Taylor, 1998). Near Dunnville and Lowbanks, a coarse sand sub-facies of the Upper Glaciolacustrine unit is found in some locations (Menzies and Taylor, 1998).

2.2.2 Regional Geologic Setting

The Bedrock Strata of the Niagara Peninsula was deposited during the Paleozoic Era when inland seas covered much of what is now southern Ontario. During the Paleozoic, regional tectonic events had 2 major influences on the lithology and development of sedimentary strata; the addition of clastic material, and the development of a foreland basin now known as the Appalachian Basin. The Niagara Peninsula lies within the Appalachian Basin, east of the Algonquin Arch

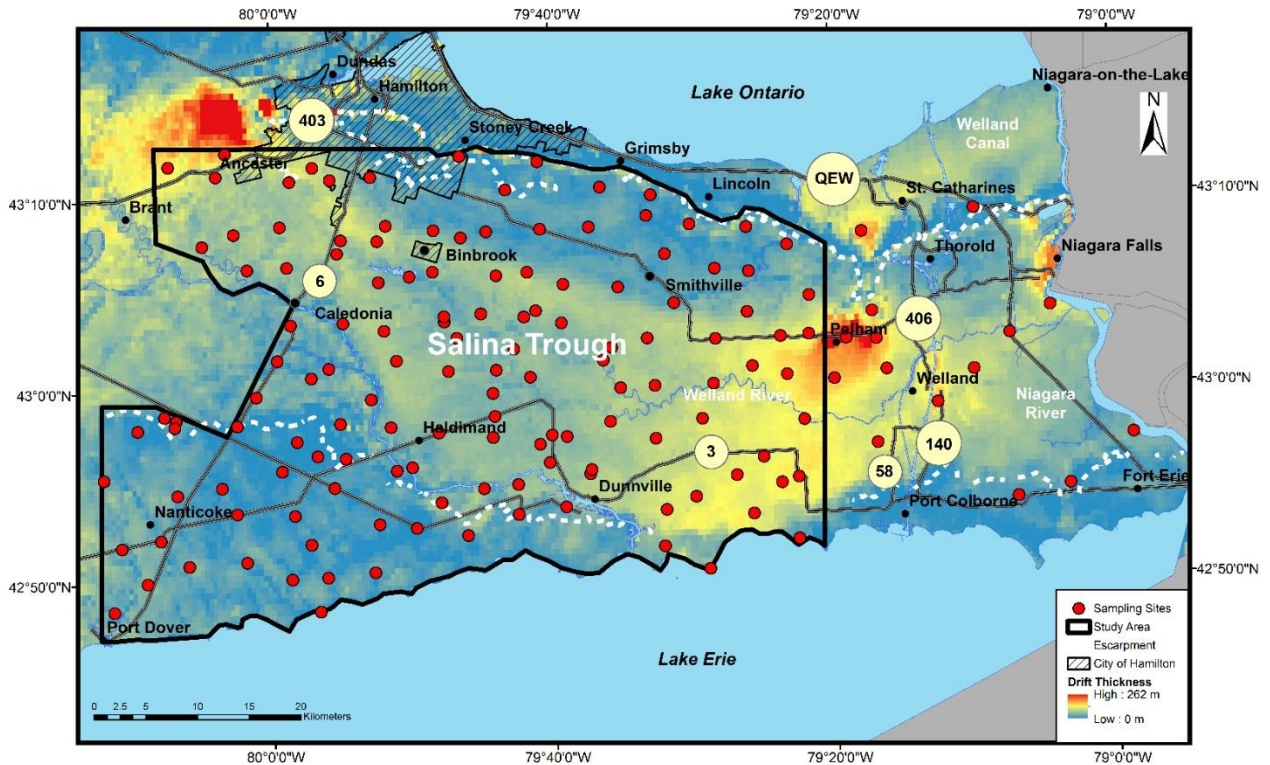
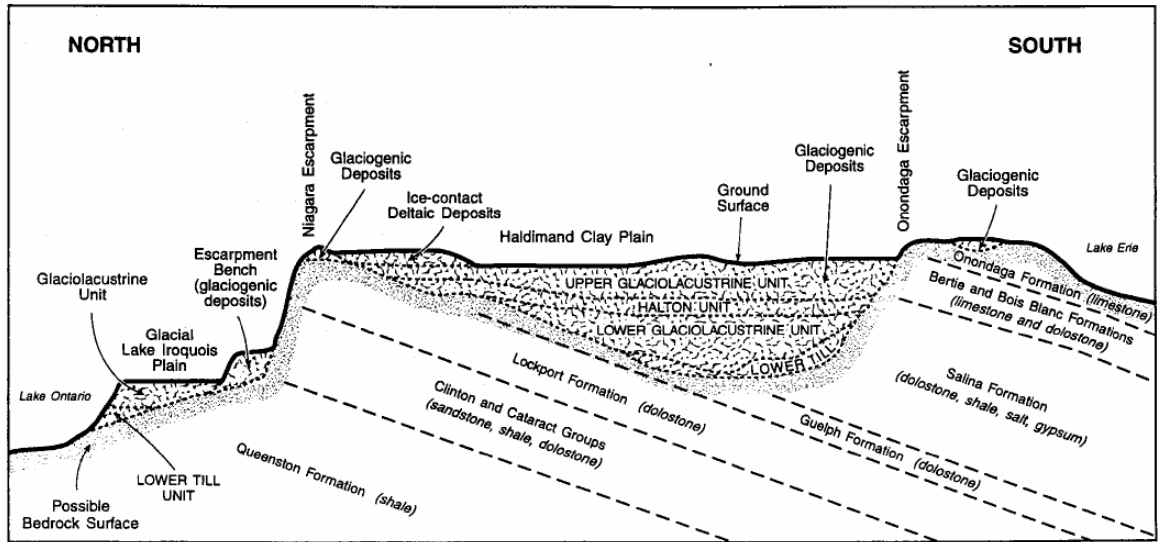


Figure 2.2: (a) Geological cross-section of sedimentary units and quaternary sediments on the Niagara Peninsula (from Menzies and Taylor, 1998) (b) Map of drift thickness and sample locations in the study area (data from Gao et al., 2006).

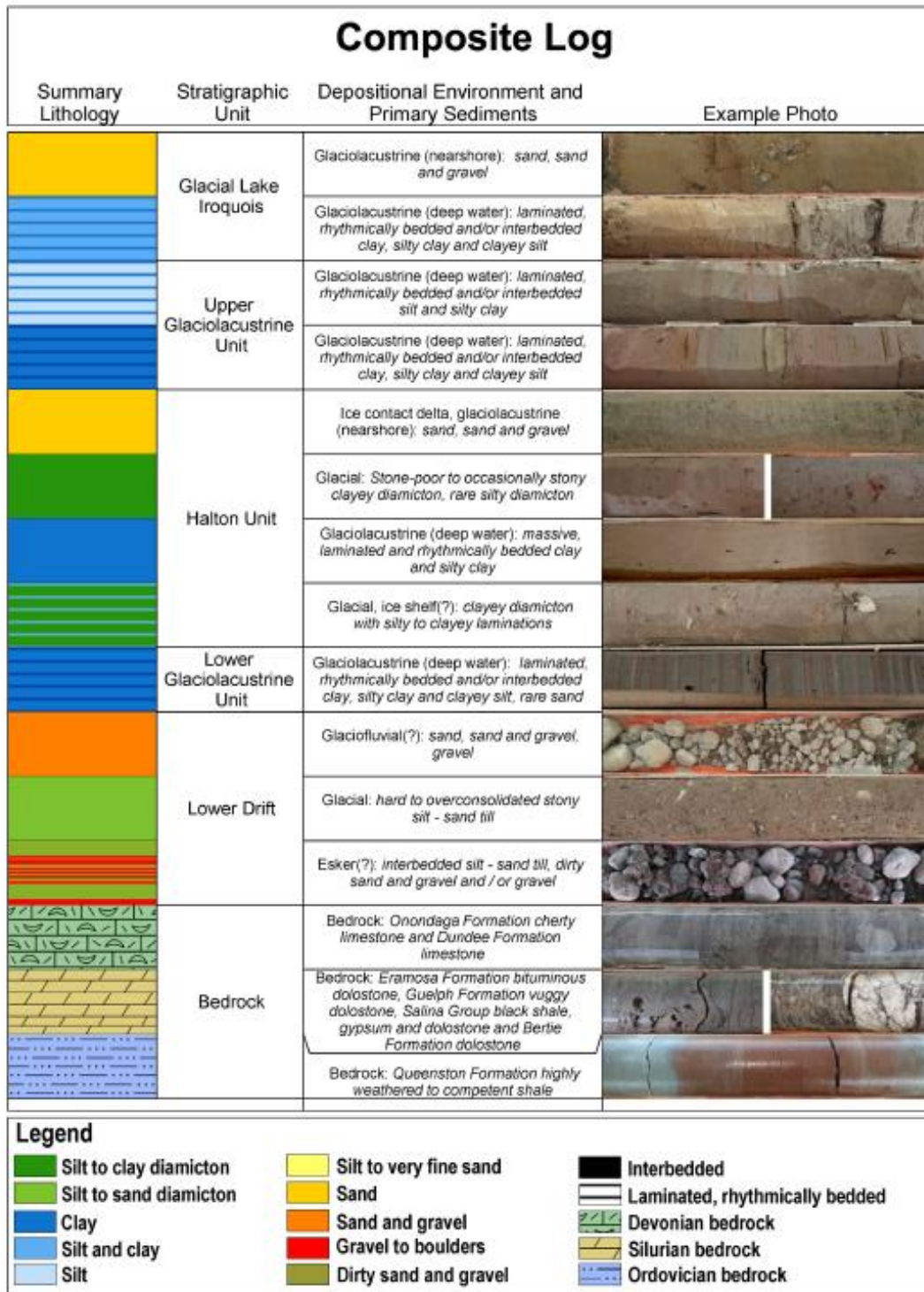


Figure 2.3: Composite log of the Quaternary sediments on the Niagara Peninsula (from Burt, 2015)

(Armstrong and Carter 2010; Johnston et al. 1992), which is a northeast-trending tectonic ridge, active from the Precambrian through the Paleozoic.

The axis of the Algonquin Arch trends through the centre of southern to southwestern Ontario. West of the Algonquin Arch is the Michigan Basin, an intercratonic basin formed directly on the craton by processes not related to orogenic activity (Johnston et al., 1992). Paleozoic rocks deposited in the Appalachian Basin are folded and lithologically variable due to orogenic events in the Paleozoic along the continental margin. In comparison, Paleozoic rocks west of the Algonquin arch have less variable lithology as they were deposited in a calmer, tectonically stable setting (Johnston et al., 1992). The Niagara Escarpment is a prominent geological feature that dominates the landscape of southern Ontario and northern New York State. The Niagara Peninsula subdivides Ordovician geological strata north of the Niagara Escarpment from Silurian and Devonian geological strata to the south. The escarpment was formed from the erosion of soft shale and carbonate bedrock under a resistant dolostone cap rock (Gao, 2011).

2.2.3 Bedrock Geologic Units

Subcropping bedrock on the Niagara Peninsula is characterized by sedimentary dolostones, limestones, evaporites and shales of Devonian to Silurian age. These sedimentary rocks overlie the Precambrian basement and dip 3 to 12 m/km southwest, dip increasing with depth (Armstrong and Carter, 2010). Thicknesses of sedimentary units in the Appalachian Basin are up to 13 000 m, in comparison to thicknesses of only 1525 m along the Algonquin Arch just west of the Niagara Peninsula (Johnston et al., 1992). Geologic deposits in the Niagara Peninsula have a higher proportion of clastic material than the Michigan Basin west of the Algonquin Arch, due to increased influence of orogenic activity (Johnson et al., 1992).

Sedimentary bedrock units exposed on surface within the study area include the Lower Silurian Clinton-Cataract Group and Lockport Formation, the Upper Silurian Salina Group and Bertie (Bass Islands) Formation, and the Devonian Oriskany, Bois Blanc, Onondaga and Dundee Formations (Figure 2.2 and 2.4) (Armstrong and Carter, 2010; Armstrong, 2007). Recent revisions in stratigraphic nomenclature has redefined the Lockport Formation as a Group, designated the Goat Island and Gasport members within the previous Lockport Formation as Formations, designated the Eramosa as a Formation within the Lockport Group, and included the Guelph Formation within the larger Lockport Group (F. Brunton, P.Comm., 2016, Figures 2.4 and 2.5). The Eramosa Formation subcrops quaternary sediments in many areas north of the Guelph Formation (F. Brunton, P.Comm., 2016). Recent revisions in stratigraphic nomenclature were not published prior to the completion of this thesis, and thus although included in the descriptions of the units, traditional nomenclature published up to date is used in figures and descriptions later in this work.

For the purposes of this thesis, only the geologic strata subcropping south of the Niagara Escarpment will be discussed in detail. It is noted that two wells sampled as a part of this thesis obtain groundwater from the Ordovician Queenston Formation, a red, slightly calcareous to non-calcareous, locally gypsiferous shale unit formed in a delta complex under non-marine to shallow marine environments (Johnston et al., 1992).

2.2.3.1 Clinton and Cataract (Medina) Groups

The Lower-Silurian Clinton Group on the Niagara Peninsula includes the following stratigraphic units (youngest to oldest); the Decew, Rochester, Irondequoit, Reynales, Neagha and Thorold Formations. The Lower-Silurian Cataract Group is composed of the following units (from youngest to oldest); the Grimsby, Cabot Head, Manitoulin and Whirlpool Formations (Armstrong and Carter, 2010). Recent stratigraphic revisions rename the Cataract Group as the

Medina Group, and include the Neagha and Thorold Formations as a part of this Group (F. Brunton, P. Comm, 2016; Figure 2.4 and 2.5).

The Whirlpool Formation consists of fine-grained, massive to interbedded sandstone. The Whirlpool Formation is overlain by the Manitoulin Formation west of Grimsby, and the Cabot Head Formation east of Grimsby where the Manitoulin Formation pinches out. The Manitoulin Formation consists of moderately fossiliferous dolostone and shale units with abundant chert nodule presence. The Cabot Head Formation contains non-calcareous shales, and is considered to be a prominent regional aquitard (Brunton, 2009). Overlying the Cabot Head Formation is the Grimsby Formation, a thick unit (approx. 15 m) on the Niagara Peninsula containing interbedded red shales and sandstones.

The Thorold Formation is characterized by sandstones formed in a shallow marine environment exhibiting hummocky cross-stratification, trace marine fossils, cross-bedding and laminations. Some researchers suggest the Thorold Formation should be reassigned to the Cataract group, and this has been supported by recent stratigraphic revisions (Brett et al., 1995; F. Brunton, P. Comm, 2016). The Neagha Formation is a thin (maximum thickness= 2 m), locally-isolated shale unit with limestone interbeds outcropping from the Niagara River to Grimsby along the Niagara Escarpment (Johnston et al., 1992). The Reynales Formation overlies the Thorold and Neagha Formations, and is characterised by argillaceous dolostones and dolomitic limestones. Recent work has led to revisions in nomenclature for the Reynales Formation, subdividing the upper portion of the formation into 3 units; the Merritton (Fossil Hill), Williamson, and Rockway Formations (Brett et al., 1995; Brunton, 2008; Brunton, 2009). The Merritton Formation acts as a regional aquitard, confining groundwater flow upwards from the Cabot Head Formation and permitting the development of karst-influenced bedrock aquifers in the overlying Gasport Formation (Brunton, 2009). Discontinuously overlying the Merritton Formation is the Williamson Shale, a thin unit dividing the Merritton Formation from the Rockway Formation. The

Rockway Formation is a 1-2 m thick argillaceous dolomicrite unit (Brunton, 2009). Overlying the Reynales Formation is the Irondequoit Formation, a coarser-grained, fossiliferous unit with crinoids and bryozoan-dominated bioherms deposited in a high-energy, shoal environment. The overlying Rochester Formation is a fossiliferous, bioturbated, calcareous shale exhibiting the highest faunal diversity of all Silurian strata in the Niagara Peninsula (Johnston et al., 1992). The youngest unit in the Clinton group is the Decew Formation. The Decew Formation is an argillaceous dolostone with a sharp erosional boundary separating it from the overlying Lockport Formation (Johnston et al., 1992).

2.2.3.2 Lockport Group (nee. Formation)

The Lower-Silurian Lockport Group (Amabel Formation – Bruce Peninsula) (Figure 2.4 and 2.5) comprises two subunits based on lithology, the Goat Island Member (Ancaster and Vinemount beds) and the Gasport member. Recent researchers have found the Vinemount lithofacies correlates with the Eramosa Formation, not the Goat Island Formation as previously thought (Brunton, 2009). The placement and lithological definition of the overlying Eramosa Formation has been debated in the past 2 decades. Previous researchers thought of the Eramosa Formation as part of the Lockport and Amabel Formations (Bolton, 1957), or part of the Lockport Formation but not the Amabel Formation (Johnston et al., 1992), as part of the Guelph Formation (Sandford, 1969) or as a formation within the Lockport Group (Brett et al., 1995, Armstrong and Carter, 2010). The Stone Road, Reformatory Quarry, and Vinemount members of the Eramosa Formation were defined by Brunton, 2009, in a field study identifying lithological units influencing groundwater in Guelph, Ontario. For the purposes of this study, the Eramosa Formation will be regarded as a part of the Lockport Group, however the Lockport Group may be referred to as the Lockport Formation in figures and text within this thesis. The Eramosa Formation is a petroleum source rock and reservoir, contains bitumen, abundant pyrite, sphalerite and galena from sulfide mineralization, and can be subject to karstification when exposed to the

surface (Brunton, 2009). Oxidation of pyrite in the organic-rich Eramosa Formation can lead to an increase in acidity of groundwater within this formation (Kunert et al., 1998). In most cases when covered by quaternary sediments or the overlying Guelph Formation, the Eramosa Formation is a regional aquitard (Brunton, 2009). The Goat Island member of the Lockport Formation consists of very fine to fine argillaceous dolostone with chert nodules and vugs filled with gypsum, calcite or fluorite. The Gasport member consists of dolostone and dolomitic limestone, with minor argillaceous dolostone.

2.2.3.3 Guelph Formation

The Guelph Formation consists of medium to thickly bedded, fine- to medium-crystalline dolostones that are tan to brown in colour (Armstrong and Carter, 2010). The Guelph Formation is considered to be a bedrock aquifer near its contact with Quaternary-aged sediments, as the Guelph Formation exhibits well developed intergranular, intercrystalline and vuggy porosity at shallow depths (<10 m from bedrock surface) (Armstrong and Carter, 2010). Northwest of the study area, the Guelph Formation is an important aquifer for the City of Guelph, Ontario (Brunton, 2009).

2.2.3.4 Salina Group

The Salina Group strata are characterized by thinly bedded, argillaceous dolostones with intermittent shale layers and gypsum nodules in the subcropping geology on the Niagara Peninsula (Armstrong and Dodge, 2007; Armstrong and Carter, 2010). In the Michigan Basin, the Salina Group are dominated by cyclic evaporite units, where carbonates are overlain by gypsum and halite and capped by shales units. The Salina Group has a higher component of clastic materials in the Appalachian Basin than in the Michigan Basin, with less presence of evaporites (Armstrong and Carter, 2010). Gypsum is present instead of anhydrite in water-bearing units due to hydration reactions with groundwater replacing the anhydrite (Armstrong and Carter, 2010).

The Salina Group is sub-divided into 8 units of formational rank; the *G Unit*, *F Unit*, *E Unit*, *D Unit*, *C Unit*, *B Unit*, *A-2 Unit*, and *A-1 Unit*. The G Unit is not present on the Niagara Peninsula, and thus will not be described or mapped in this study. The F Unit is the subcropping formation in the Salina Group near Wainfleet (Oil and Gas Well Record T004907, Armstrong and Carter, 2010) and consists of dark shales with pink and blue anhydrite nodules (later altered to gypsum) in the upper portion and interbedded shales, anhydrite and dolostones in the lower portion. Below the F Unit is the E unit, a dolostone unit with some gypsum nodules and interbedded shale. The D unit is not present in core logs from the Niagara Peninsula (Armstrong and Carter, 2010). The C unit is a consistently thick (thickness =23 m), dolostone to red-green shale unit with anhydrite nodules and a lower anhydrite bed. The B Unit is a thick, salt-bearing unit in the Michigan Basin with an anhydrite bearing zone near the bottom of the formation (Armstrong and Carter, 2010). Halite is not currently present on the Niagara Peninsula in any units of the Salina Group. The A-2 and A-1 Units contain thick carbonate sequences (limestone and dolostone) overlying evaporites containing anhydrite (Armstrong and Carter, 2010).

The evaporites of the Salina Group have been mined on the Niagara Peninsula since the early 1880's. Gypsum production on the Niagara Peninsula amounted to 16.3 % of the total Canadian production in 1987, with production commencing from 3 mines; the Domtar Construction Materials operation near Caledonia, the Canadian Gypsum Company in Hagersville, and Westroc Industries in Drumbo (Haynes et al., 1989). Since the mid 1990's, production of gypsum has ceased at the Domtar mine in Caledonia and the flooded Westroc Industries mine in Drumbo (Steele and Haynes, 2000). In 2016, gypsum mining is ongoing at only one location, the Canadian Gypsum Company (CGC) mine near Hagersville, ON (Figure 2.6).

2.2.3.5 Bass Islands Formation and Bertie Formation

From Dunnville (east) to Hagersville (west), the Bass Islands Formation overlies the younger Bertie Formation and are regarded as different units (Armstrong and Carter, 2010). Outside of the transect, the Bass Islands and Bertie Formations are largely regarded as lithologically and stratigraphically equivalent. The Bass Islands Formation comprises very fine to crystalline dolostones with minor anhydrite beds and some thin sandstone beds. The Bertie Formation comprises dark brown to light grey dolostones with minor shale and laminations (Armstrong and Carter, 2010). The Bass Islands and Bertie Formations are the primary units forming the Onondaga Escarpment, and are exposed at surface in several locales (Haynes and Parkins, 1991; Armstrong, 2007). The Bass Islands and Bertie Formations have little primary porosity, however paleokarst features, open joints, and sand-filled features suggest karst may have an influence on groundwater movement in the area (Armstrong, 2007; Armstrong and Carter, 2010). The Bertie Formation along the Onondaga Escarpment is a major contributor of aggregates and crushed stone in Southern Ontario (Haynes and Parkins, 1991). As of 2000, three major quarries existed on the Bertie Formation; the Port Colborne Quarry, Ridgemount Quarry and Law Quarry (Figure 2.6) (Steele and Haynes, 2000).

2.2.3.6 Oriskany Formation

In a few select locations within the study area (Armstrong and Dodge, 2007), the lower Devonian Oriskany Formation sandstone overlies infilled paleo-sinkholes formed by the collapse of Silurian units as a result of salt dissolution during the Paleozoic. Oil Staining is present in 2 quarries near Cayuga and natural gas from this formation has been encountered during drilling in Lake Erie (Armstrong, 2007; Armstrong and Carter, 2010).

2.2.3.7 Bois Blanc Formation

The Bois Blanc strata are composed of cherty (up to 90% of rock volume), fine to medium grained, fossiliferous, bioturbated limestone and dolostone with

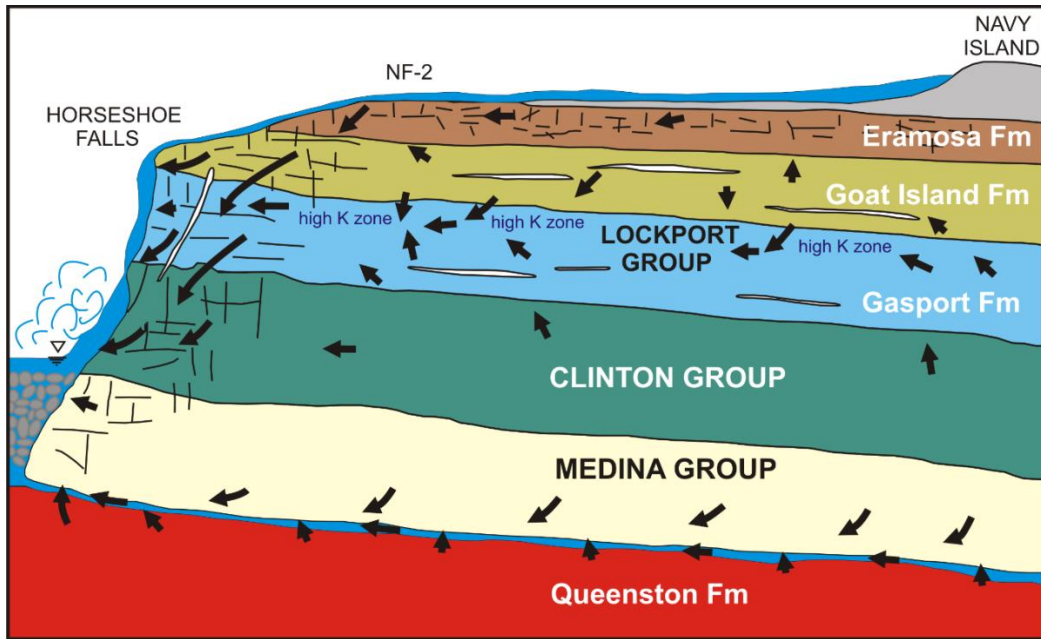
abundant sand grains in the lower part of the formation (Armstrong, 2007). The Bois Blanc Formation ranges in thickness from 3 m to 50 m, and has low porosity, with the exception of the contact aquifer between bedrock and overburden (Armstrong and Carter, 2010).

2.2.3.8 Onondaga Formation

The Onondaga Formation is a middle-Devonian, brown, fine - medium grained, cherty, fossiliferous limestone (Armstrong, 2007). The Onondaga Formation is considered to be equivalent to the Amherstburg Formation in the Michigan Basin, and in parts of the eastern Niagara Peninsula may be time-equivalent to the Lucas Formation (Armstrong and Carter, 2010). The Onondaga Formation is exposed at many locations in the study area, including Hemlock Creek near Selkirk, Ontario (Armstrong and Carter, 2010). The Onondaga Formation is a major aquifer in the study area, and contains sulfurous water where confined by overlying bedrock or glacial sediments and fresh water where unconfined by porous sediments or exposed at surface (Armstrong and Carter, 2010).

2.2.3.9 Dundee Formation

The Dundee Formation overlies the Onondaga Formation in the southwestern study area, near Port Dover, Ontario. It is characterized by medium to thickly-bedded, fossiliferous limestones with some dolostone presence (Armstrong, 2007). The Dundee Formation contains crude oil in some porous cavities, as observed in a quarry near Port Dover, Ontario and in a monitoring well sampled as a part of this study (Armstrong and Carter, 2010). Secondary porosity produced from the collapse of parts of the Dundee Formation due to dissolution of salt beds in the underlying Salina Group locally provides a major source of permeability in the unit (Armstrong and Carter, 2010).



Period	Remainder of Southwestern Ontario	Niagara Peninsula	
		West	East
Devonian	Port Lambton Group		
	Kettle Point Fm		
	Hamilton Group		
	Dundee Fm		Dundee Fm
	Detroit River Gp	Anderdon Mbr Lucas Fm	Lucas Fm Moorehouse Mbr Clarence Mbr Edgecliffe Mbr
	Amherstburg Fm	Amherstburg Fm	
	Sylvania Fm	Formosa reef	
Silurian	Bois Blanc Fm	Bois Blanc Fm	
	Bass Islands Fm	Bass Islands Fm	Akron Mbr Williamsville Mbr Scajaquada Mbr Falkirk Mbr Oatka Mbr
	Salina Group	Salina Group	Bertie Fm

Figure 2.4: Geological cross-sections of the Niagara Escarpment (top) and Onondaga Escarpment (bottom). Cross-sections were drafted using recent unpublished stratigraphic nomenclature, courtesy of F. Brunton (2016).

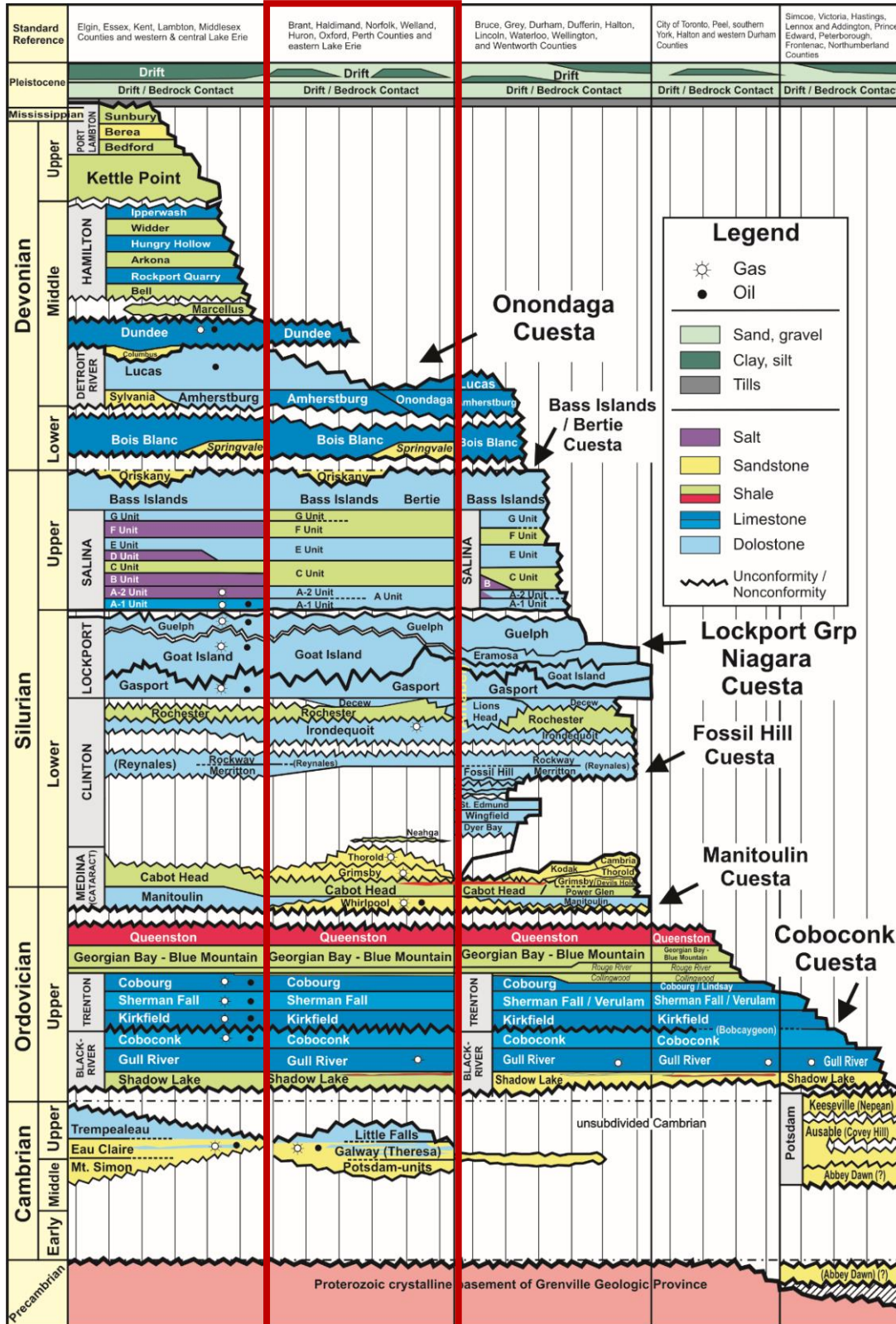


Figure 2.5: Stratigraphic sequences of the geological units on the Niagara Peninsula (outlined in red). Cross-sections were drafted using recent unpublished stratigraphic nomenclature, courtesy of F. Brunton (2016).

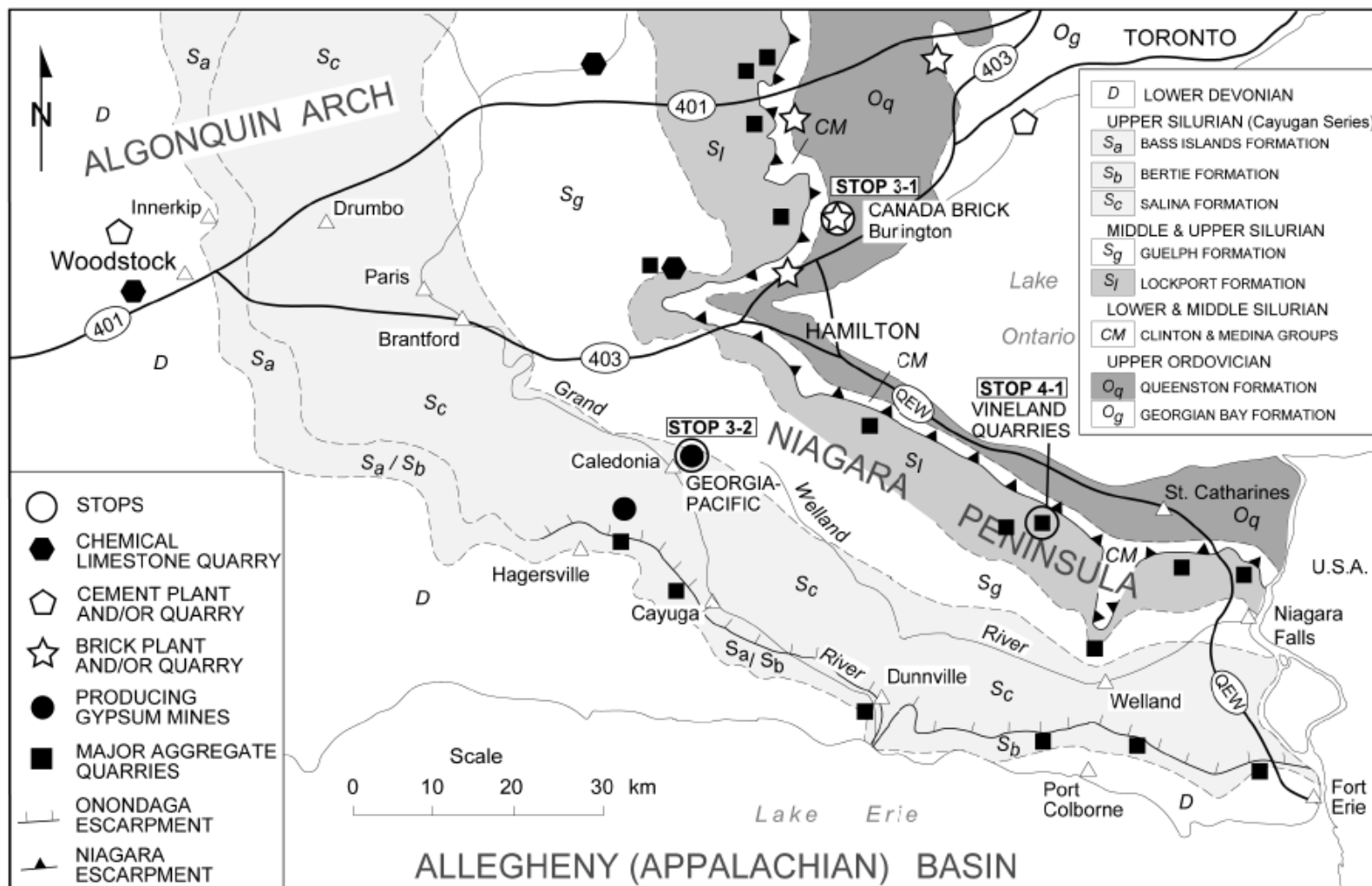


Figure 2.6: Geological Map of the Onondaga Escarpment with the location of gypsum mines and stone quarries in 2000 (Steele and Haynes, 2000).

2.2.4 Geologic Features

2.2.4.1 Bedrock Topographic Features

Major bedrock features on the Niagara Peninsula include the Niagara and Onondaga Escarpments forming topographic highs, the Salina Trough (a bedrock low present in the Salina Group) and four buried bedrock channels (Fig. 2.7) including the Erigan Channel, the Chippawa-Niagara Falls Channel, the St. David's Channel and the Crystal Beach Channel.

The Niagara Escarpment is a prominent landscape feature in southern Ontario with an east-west orientation from Rochester, New York, to Hamilton, Ontario and a northerly orientation from there to the Bruce Peninsula near Tobemory, Ontario (Armstrong and Carter, 2010). The Niagara Escarpment exposes mid to lower Silurian carbonates and shales along its flanks, and provides excellent exposure of rock formations present in southern Ontario. The Onondaga Escarpment has a lower surface relief than the Niagara Escarpment, with a maximum relief of 5 metres south of Port Colborne (Menzies and Taylor, 1998). However, it is extensive as a bedrock topographic feature, as much of it is buried along the southern margin of the Salina trough.

The entrance to the Erigan buried bedrock channel was first discovered by Spencer (1907) to be located east of Lowbanks, on the shore of Lake Erie (Flint and Lolcama, 1986). The Erigan bedrock channel runs from Lowbanks to Lake Ontario, widens as it crosses the Salina Group, and separate into two tributaries near Wainfleet. In the area between Fonthill and St. John's, the Erigan bedrock channel was historically presumed to separate into three channels, the western, northern and eastern outlets (Flint and Lolcama, 1986). The extent, boundaries and aquifer potential of the Erigan Channel are currently being mapped by a collaborative project between the OGS and the NPCA (Campbell and Burt, 2015) and boundaries are being redefined. Campbell and Burt present a new bedrock channel from preliminary mapping and geophysical surveys, the Chippawa –

Niagara Falls Channel. Groundwater flow was suggested to occur from Lake Erie to Lake Ontario along the Eriqan Channel, with little recharge, as determined by tritium measurements (Campbell and Burt, 2015). A cone of depression is present in the Chippawa – Niagara Falls Channel from decades of dewatering at the Welland Canal Townline Tunnel (Campbell and Burt, 2015).

The Crystal Beach Channel and St. David's channel are two smaller bedrock topographic lows in the eastern portion of the study area, near Crystal Beach/ Stevensville and Niagara Falls/ Queenston, respectively (Flint and Lolcama, 1985). The Crystal Beach Channel was discovered to be relatively shallow, with loosely defined boundaries in a study of bedrock topography by Gao (2011).

The Salina Trough, also termed the Brantford-Welland Trough (Gao, 2011) is a bedrock topographic low present in the Salina Group from Woodstock to the Niagara River in Canada, and likely extends further into New York State (Gao, 2011). The Salina Trough is bounded by the Niagara Escarpment to the north and the Onondaga Escarpment to the south.

2.2.4.2 The Presence of Karst

Karst refers to landscapes and bedrock features formed by the dissolution of carbonates and evaporites with low initial primary porosity during groundwater flow through fractures, fissures and joints. Solution enhancement of joints (kluftkarren), bedding planes and fissures, often known collectively as fractures by hydrogeologists, leads to the formation of large secondary porosity features such as channels and conduits (Ford & Williams, 2013). Although the presence of karst landscape at the surface is the only karst feature often recognized by hydrogeologists (Ford & Williams, 2013), subsurface karst geomorphology plays an important role for groundwater flow and transport in many systems. High solubility alone is not sufficient to produce karst as specific lithological characteristics of the rock and connection to a water source are needed for solution enhancement (Ford & Williams, 2013). The presence or absence of a

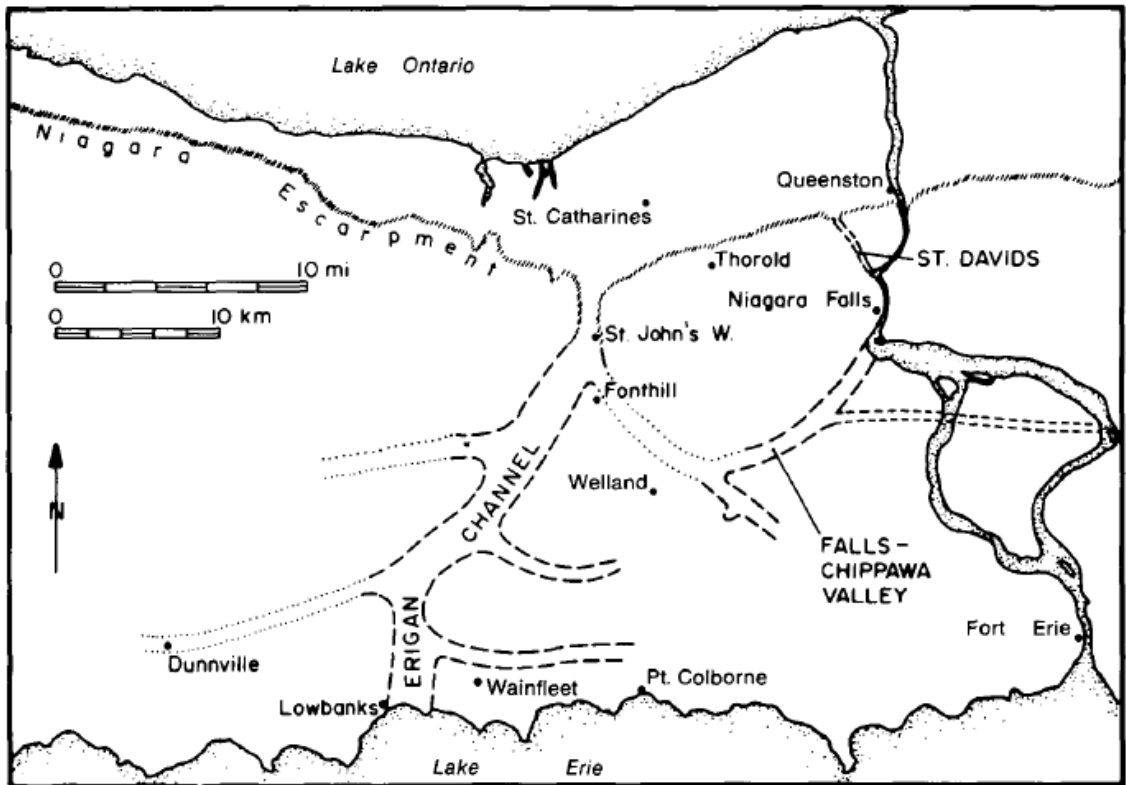


Figure 2.7: Buried bedrock channels on the Niagara Peninsula (from Flint and Lolcama, 1985). Boundaries of buried bedrock channels were being re-assessed at the time of publication of this thesis (Burt, 2015; Campbell and Burt, 2015).

carbonate-rich till overlying the bedrock can determine the likelihood of karstification and dissolution of bedrock units (Kunert et al., 1998). Karst development occurs most prominently in open-system, vadose zones above the water table; however vuggy and cavernous porosity can also develop more slowly below the water table where water unsaturated with respect to calcite/dolomite dissolves the bedrock along joints planes (Kunert et al., 1998). Pre-glacial karst features in Southern Ontario are not always apparent at surface due to erosion and alteration by past advancing and retreating ice sheets and infill of cavities by Quaternary sediments (Brunton, 2013).

A relationship between the location of buried bedrock valleys and topographic highs such as escarpments and cuestas (e.g. Onondaga Escarpment, Niagara Escarpment) and the probability of locating karst features exists in southern Ontario (Figure 2.8). Sinkhole development occurs where groundwater flow can erode, dissolve and transport sediments infilling pre-glacial solution-enhanced joints and cavities (Brunton, 2013), as can often be observed near recharge areas at the top of escarpments. A study by Perrin et al. in Cambridge, Ontario found that karst develops when glacial drift is thin (Figure 2.8), and this observation was supported by OGS mapping from 2005 – 2007 (Brunton, 2013).

The bedrock elevation difference along buried valleys prior to glacial infilling of sediments creates groundwater hydraulic gradients driving the movement of fresh, unsaturated groundwater from the top of the valley to the base (Cole et al., 2009). The productivity of City of Guelph pumping wells in the Amabel and Guelph Formations correlates with the distance of the well from a buried bedrock valley, suggesting a relationship between karst and buried bedrock valley formation (Cole et al., 2009). Additionally, spatial differences in lithology within the same formation can influence the susceptibility of karst development. This phenomenon is apparent in the lithological change from limestone to dolostone in the Lucas Formation north of London, ON, where Canada's largest known breathing well zone occurs (Freckelton, 2013; Brunton, 2013).

Historically, predictions of groundwater contamination and groundwater management were made on the assumption that groundwater flow is laminar and homogeneous following Darcy's Law through porous media (Boyer and Pasquarell, 1999). However, it is now widely recognized that karstic groundwater flow does not follow this model. Karst aquifers are particularly susceptible to groundwater contamination from surface sources due to their high flow velocities and short residence times in conduit networks, and lack of natural filtering by porous media (Ford & Williams, 2013; Mahler et al., 2000). The heterogeneity of karst aquifers can cause contamination from a source to occur in a well

connected by conduits, where another well located within a few metres may not have any contamination (Mahler et al., 2000).

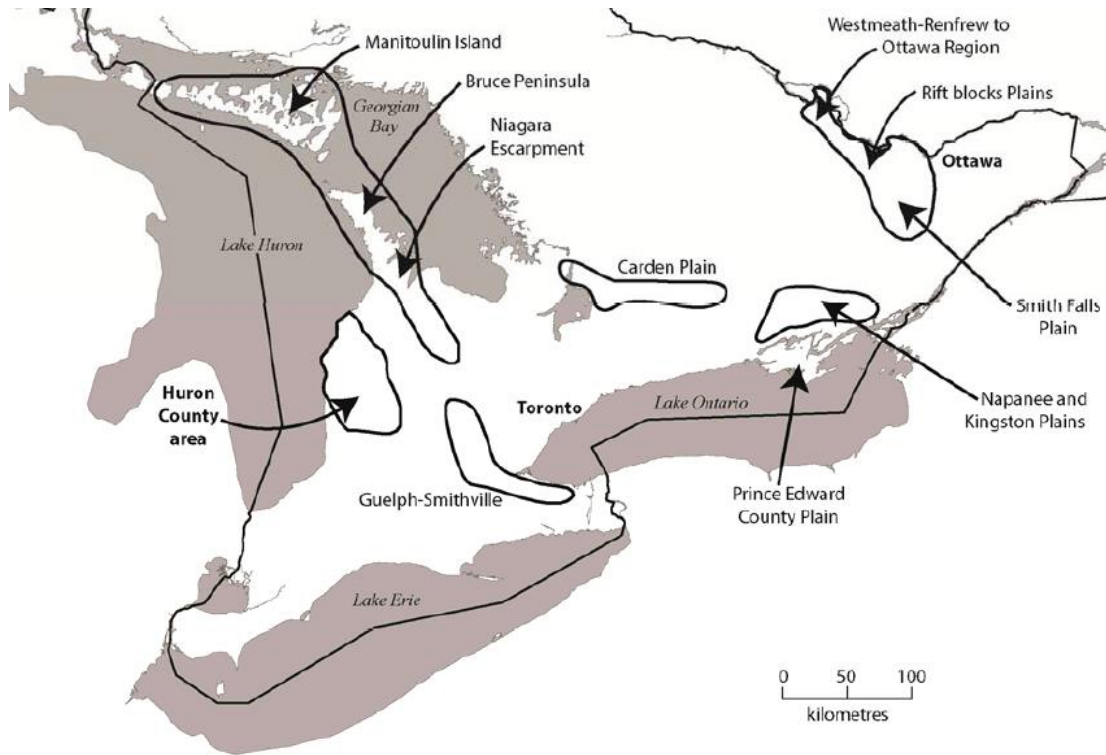


Figure 2.8: Location of known karst belts in southern Ontario (Brunton, 2013).

Secondary and tertiary porosity provides the main mechanism for groundwater flow in Silurian carbonates on the Niagara Peninsula. Evidence for secondary and tertiary porosity in the Guelph Formation of the Niagara Peninsula was found as well-connected bedrock jointing, cavernous pores, and vuggy porosity (Worthington, 2002). Thus, it is imperative that a thorough understanding of the location of karst and mechanisms of karst formation on the Niagara Peninsula is considered for interpretation of data.

2.3 Hydrogeology

Approximately 77,000 persons rely on groundwater wells or cisterns for their drinking water in the Niagara Peninsula Source Water Protection Area (NPCA,

2011). The population using domestic well water from bedrock formations on the Niagara Peninsula is likely lower than this number, as residents rely on other sources for drinking water due to long-term, persistent water quality issues. It was observed during sampling in 2010 and 2015 that a large percentage of rural residents obtain drinking water from private cisterns due to water quality issues in groundwater obtained from the Salina and Guelph Formations.

This section will introduce current research on the hydrogeologic system, groundwater flow direction, and transmissivities values for bedrock aquifers on the Niagara Peninsula. An understanding of hydraulic gradients, flow direction and groundwater recharge areas will aid in the interpretation of geochemical data collected for this study.

The fine-textured, low permeability glacial sediments collectively referred to as the Haldimand Clay has been classified as an aquitard (NPCA, 2011) and covers a large portion of the study area. These sediments restrict the movement of groundwater downwards, and have reported hydraulic conductivities of 7×10^{-7} m/s to 2×10^{-10} m/s (NPCA, 2011) where unweathered. Groundwater recharge in these low-permeability regimes is very slow (Novakowski and Lapcevic, 1988). However, where the overburden is thin, the Haldimand Clay is reported to be highly weathered with interconnected fractures up to a depth of 5 m, providing a mechanism for fast groundwater recharge to bedrock (Jagger Hims Ltd., 2004). In cases where overburden cover is absent, such as at the crests of the Niagara and Onondaga Escarpments, groundwater recharge can occur directly through solution-enhanced cavities, conduits and fractures within the carbonate bedrock. Regional groundwater studies on the Niagara Peninsula have classified the bedrock groundwater systems as four main aquifers; the surficial overburden, Guelph-Lockport Formation, the Onondaga/Bois Blanc Formation and the “Contact-zone aquifer” (Novakowski and Lapcevic, 1998). Dolomites and dolomitic limestones were reported to have the highest hydraulic conductivities of bedrock units in a study that correlates bedrock type and hydraulic conductivity

(Hobbs et al., 2008). The Guelph-Lockport Formation and Onondaga/Bois Blanc Aquifers are confined to unconfined, depending on the presence of overlying Quaternary sediments overlying the bedrock. The contact-zone aquifer is assumed to be confined under thick, low transmissivity Quaternary sediments, and includes the areas in the Salina Trough and south of the Onondaga Escarpment. For the sake of simplicity, the bedrock groundwater system is considered here as one connected aquifer: confined under thick low-permeability sediments, semi-confined to unconfined where drift is 5 m or less due to the presence of weathering and fractures, or unconfined where no drift is present. Bedrock groundwater flow directions will be presented on a regional scale as one system.

Groundwater flow direction is controlled by bedrock topographic highs where modern recharge infiltrates and flows down gradient to topographic lows. In southern Ontario, modern recharge infiltrates on the crest of the Niagara Escarpment and on glacial moraines and discharges in topographic lows, such as lakes (Hobbs et al., 2008). Major recharge areas (Figure 2.9) are found on the Niagara and Onondaga Escarpments (Matheson, 2012) and the Fonthill ice contact-delta complex (Figure 2.9).

Groundwater flow is mainly horizontal in the Lockport-Guelph Aquifer, to the southeast, and follows major bedding plane fractures (Zanini et al., 2000). Where solution conduits and other karst features are present, groundwater flow may be controlled locally at surface and at depth (Worthington, 2002), even where karst features are infilled by quaternary deposits. Zanini et al. studied groundwater movement and general chemistry from waters obtained at several depths in the Eramosa and Lockport Formations near the town of Smithville, ON. They state that in some areas the Eramosa Formation acts as a shallower, discrete aquifer, divided from the lower Lockport members by a low permeability Vinemount member; however, in other areas the Lockport member can be considered one

aquifer due to similar electrical conductivity measurements and isotopic data at various depths.

Groundwater flows north and south from the bedrock topographic highs of the Onondaga and Niagara Escarpments (Figure 2.9). A drainage divide exists in the northern study area in the Lockport and Guelph Formations, dividing groundwater flow direction from northwards towards the crest of the Niagara Escarpment to southwards towards the Salina trough. Groundwater movement is primarily to the southeast in the western Salina trough. Where buried valley systems are present (Figure 2.10), groundwater elevation decreases with distance northward from Lake Erie toward the Welland River. There is a regional potentiometric high in the Erigan channel near the Fonthill ice contact-delta complex, which forms a regional recharge area. In the Chippawa – Niagara Falls channel near the Welland Canal Townline Tunnel, 40+ years of dewatering has caused a large cone of depression in the surrounding area (Campbell and Burt, 2015). Buried bedrock channels are infilled with quaternary sediments, and, except in the Fonthill and Townline Tunnel areas just described, may provide a regional 'sink' for groundwater movement north to the Niagara Escarpment (Nowakowski and Lapcevic, 1988). Groundwater samples collected from the Erigan and Chippawa-Niagara Falls buried channels were found to have consistently low tritium content, suggesting little recharge from Lake Erie (Campbell and Burt, 2015).

Transmissivities for bedrock units in the study area range from; 2×10^{-4} m/s, 1.8×10^{-4} m/s and 1.4×10^{-4} m/s in the Lockport, Amabel and Guelph Formations (Singer et al., 2003), from 6×10^{-4} to 1×10^{-5} m/s in the Salina Group (Jagger Hims Ltd., 2004), 3.6×10^{-4} m/s in the Bass Islands/Bertie Formation, 4.7×10^{-4} in the Bois Blanc Formation (Singer et al., 2003) and 1.9×10^{-6} m/s in the Onondaga Formation (Jagger Hims Ltd., 2004).

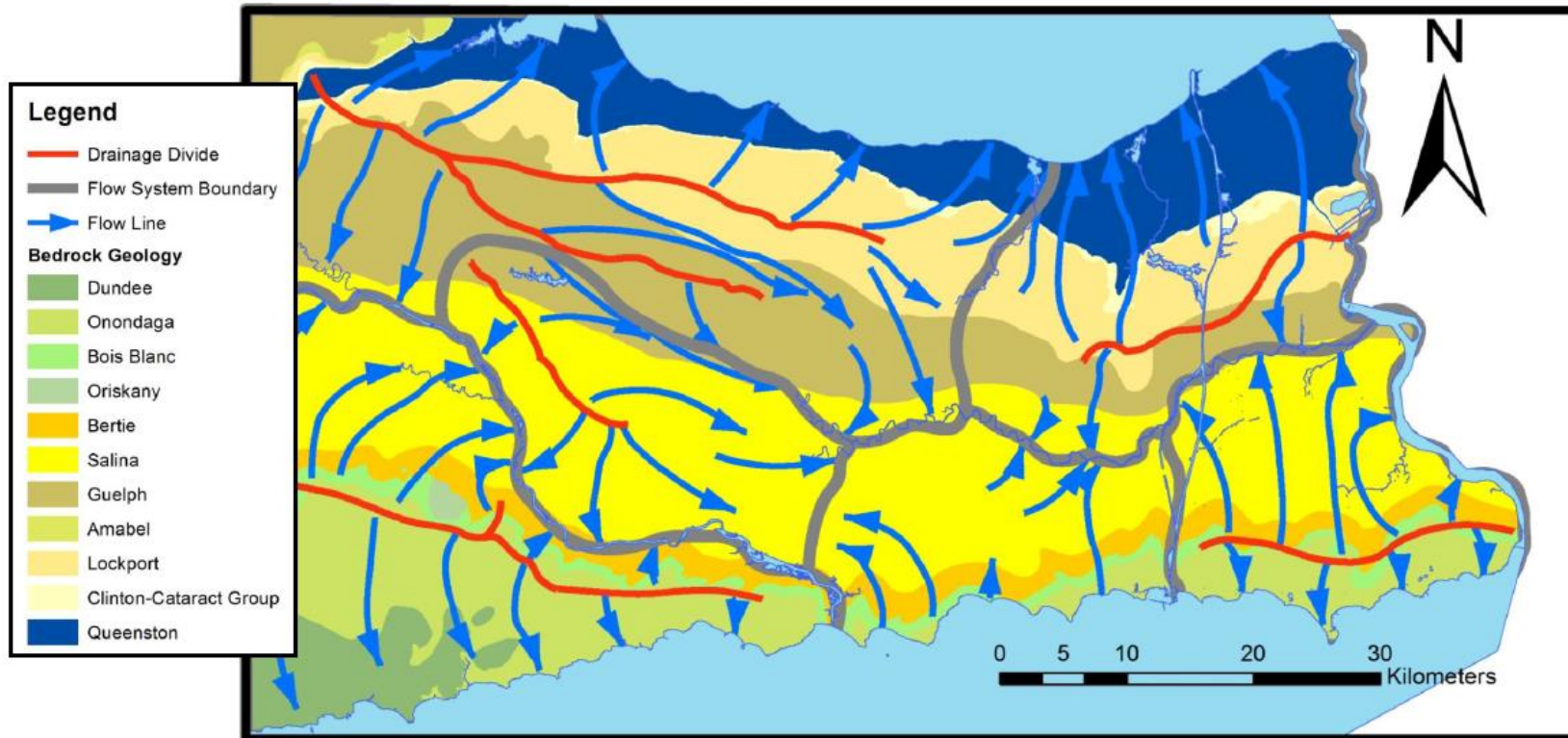


Figure 2.9: Groundwatersheds (recharge catchments) and groundwater flow directions overlying sub-cropping bedrock formations (from Matheson, 2012).

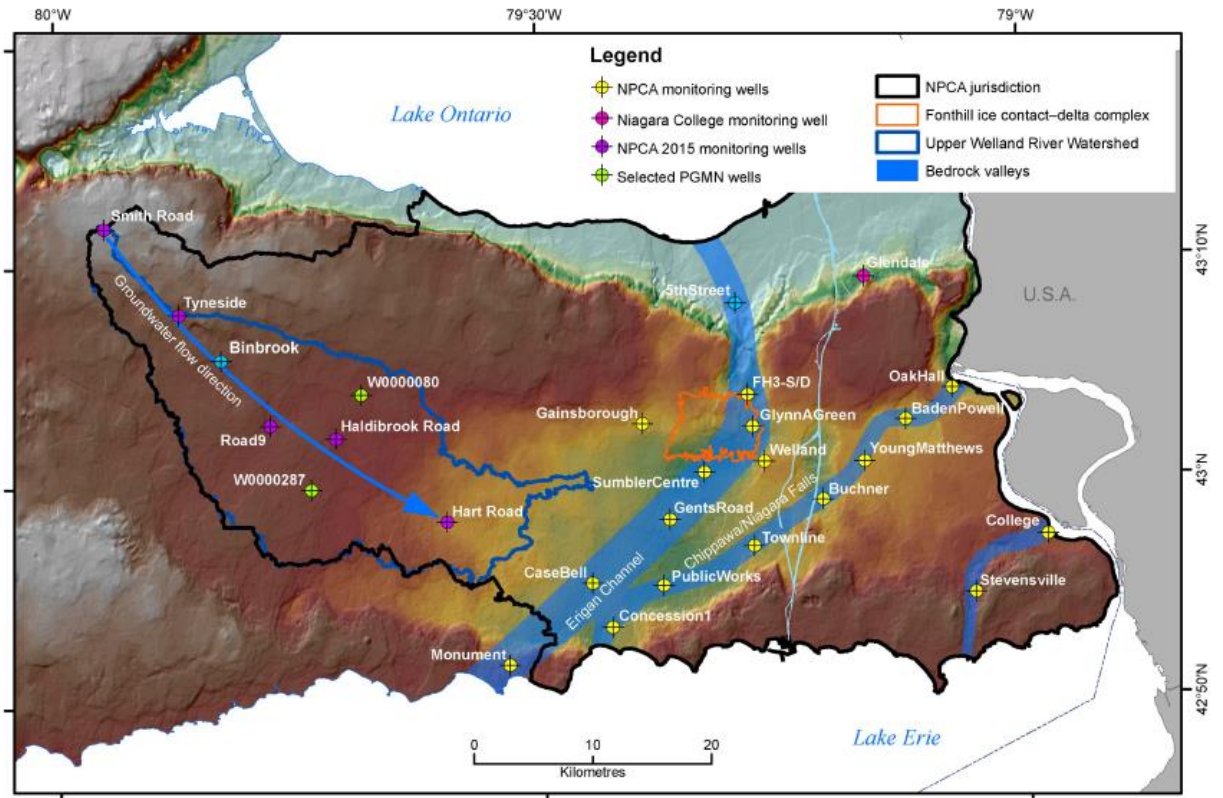


Figure 2.10: The Erigan, Chippawa-Niagara Falls and Crystal Beach buried bedrock channels on the Niagara Peninsula. Estimated groundwater flow direction on the western Peninsula is indicated by the blue arrow on the map. All monitoring wells shown were sampled as a part of this study (from Campbell and Burt, 2015).

2.4 Previous Hydrogeochemical Research

The regional characterization of southern Ontario groundwaters has been studied by several researchers over the past century. Relevant research and geochemical studies will be discussed further to place this research in the greater context of regional geochemical work on shallow and deep bedrock aquifers conducted in southern Ontario to date.

2.4.1 Abandoned Gas Wells

The presence of corroding well casings in ‘century’ gas wells on the Niagara Peninsula (Figure 2.11) may provide conduits for the upwards migration of

thermogenic methane and deeper, brine-impacted groundwater from depth to shallow aquifers.

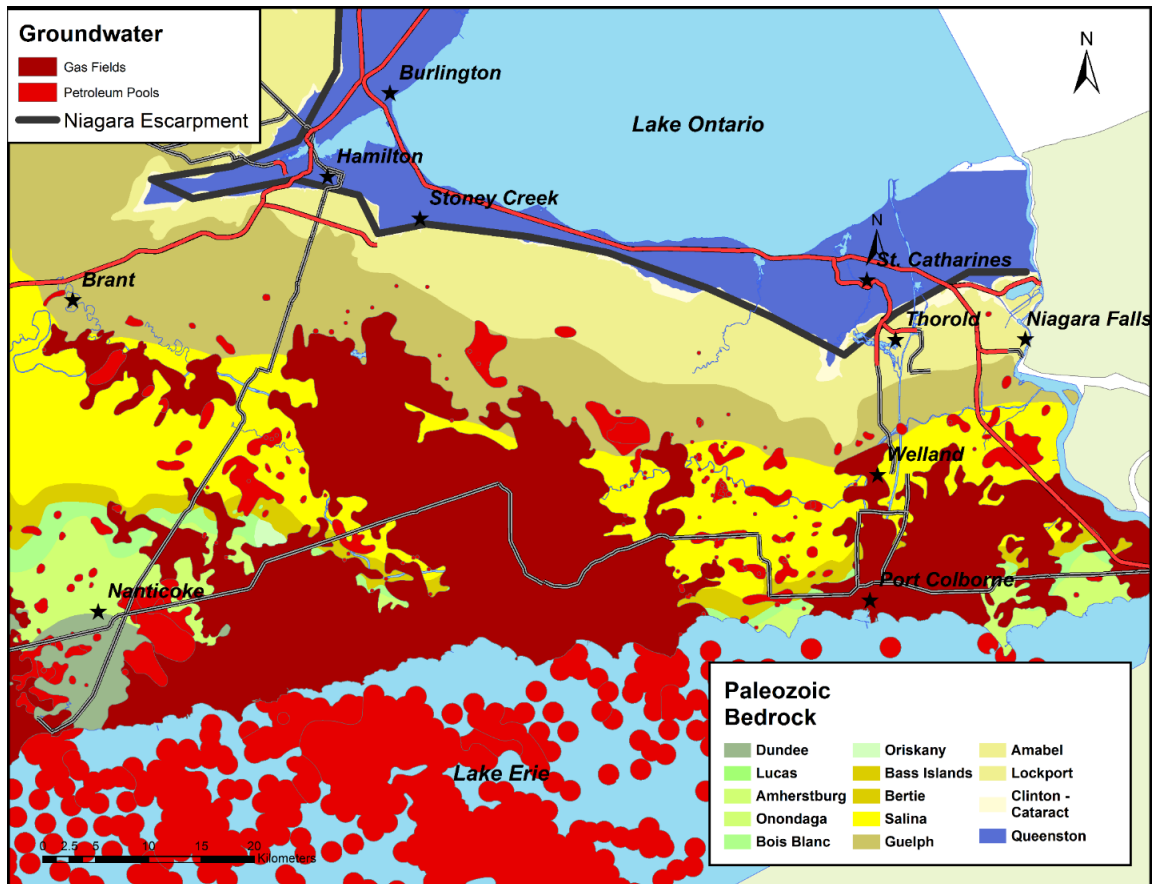


Figure 2.11: Location of gas and petroleum fields on the Niagara Peninsula.

Recently, researchers at the Ontario Ministry of Natural Resources and the University of Western Ontario developed a geochemical tool for the identification of corroded portions of well casings drilled to depth through several formations (Skuce et al., 2015). The tool was an effort to provide a cost-effective method of determining the stratigraphic origin of the leakage based on a geochemical and isotopic characterization of deep, formational groundwater. If upward gradients in corroded well casings are contaminating shallow aquifers, an understanding of deep brine groundwater geochemistry from Paleozoic bedrock formations in southern Ontario is essential. The shallowest reported brines in Paleozoic bedrock occur in the Salina A-1 and A-2 units and the Guelph Formation, with

lithologic and isotopic similarities and evidence of mixing with meteoric waters (Skuce et al., 2015). Overlying saline brine groundwater is an intermediate sulfur water system characterized by high concentrations of hydrogen sulfide, found at depths of 250 to 400 m below ground surface (bgs; Skuce et al., 2015).

2.4.2 Formational Waters

Dollar et al (1991) and Chapman et al., (2013) used isotopic tracers to characterize the groundwater geochemistry from saline groundwaters found at depth in the formations underlying southern Ontario in the Michigan Basin and the northern Appalachian Basin. The study was designed to assess waters from all lithological units for $\delta^{18}\text{O}_{\text{H}_2\text{O}}$ and $\delta^2\text{H}_{\text{H}_2\text{O}}$, and $^{87}\text{Sr}/^{86}\text{Sr}$ for lithological trends between and within formations. All geochemical samples collected for $\delta^{18}\text{O}_{\text{H}_2\text{O}}$ and $\delta\text{D}_{\text{H}_2\text{O}}$ from deep water brines plot to the right and below the Global Meteoric Water Line (GMWL), indicative of isotopic exchange reactions between formational waters and the host carbonate bedrock. Skuce et al. (2015) expanded on research done by Dollar et al. (1991) and had similar findings subdivided by formations with a larger suite of isotopic parameters, including $\delta^{18}\text{O}_{\text{H}_2\text{O}}$ and $\delta^2\text{H}_{\text{H}_2\text{O}}$, $\delta^{34}\text{S}_{\text{SO}_4}$ and $\delta^{18}\text{O}_{\text{SO}_4}$, $\delta^{13}\text{C}_{\text{DIC}}$, $^{87}\text{Sr}/^{86}\text{Sr}$, $\delta^{34}\text{Cl}$ and $\delta^{81}\text{Br}$ (Figure 2.12). Results for $\delta^{13}\text{C}$ of DIC and $\delta^{34}\text{S}$ and $\delta^{18}\text{O}$ of sulfate do not show major differences between formations, especially in shallow aquifer systems where multiple sulfur and carbon sources may be present (Skuce et al., 2015).

2.4.3 Shallow Groundwater Systems

Evaporation over the Great Lakes is seasonal, with 90% of evaporation occurring between September and March when the polar jet stream is present over southern Ontario (Jasecho et al., 2014). This phenomenon allows for evaporated air from the Great Lakes to be precipitated as lake-effect snow in snow-belt regions. Evaporation from the great lakes has a deuterium excess, shifting groundwater signatures affected by winter precipitation and subsequent infiltration above and to the left of the meteoric water line (Jasecho et al., 2014,

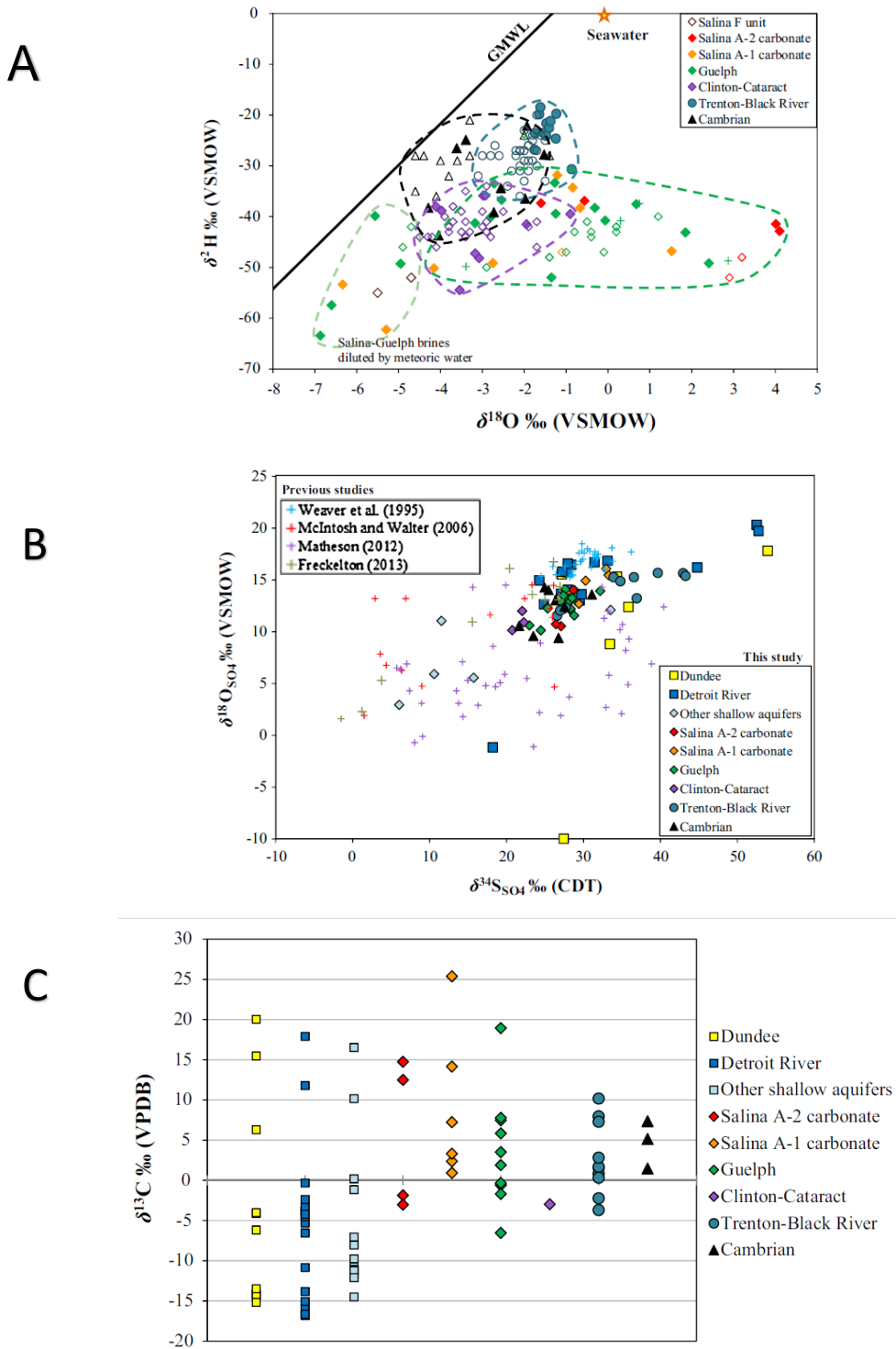


Figure 2.12: $\delta^{18}\text{O}_{\text{H}_2\text{O}}$ and $\delta^2\text{H}_{\text{H}_2\text{O}}$, $\delta^{34}\text{S}_{\text{SO}_4}$ and $\delta^{18}\text{O}_{\text{SO}_4}$, and $\delta^{13}\text{C}_{\text{DIC}}$ of formation brines from Paleozoic formations in southern Ontario (from Skuce et al., 2015)

Figure 2.13). Matheson (2012) attributed the strong deuterium excess seen in Niagara Peninsula groundwater to a high proportion of winter recharge. Ice cover on Lake Erie restricts the evaporation of surface water in the months of February and March, during which the historically maximum average ice cover of 85% is recorded (Jasecho et al., 2014). Ice cover is decreasing 1.3% per year, which may contribute to a higher amount of lake effect snow over snow-belt regions.

In the summer months, warm, humid, air masses transport evaporated water from the Gulf of Mexico to southern Ontario where it falls as precipitation, and prevents the evaporation of lake water from the Great Lakes (Jasecho et al., 2014). Although monthly precipitation in the summer months (April – August) is comparable to monthly winter precipitation on the Niagara Peninsula, summer precipitation is utilized as evapotranspiration and is not available as a surplus for infiltration. In the winter months, infiltration is most important during the winter snowmelt, as cooler temperatures hold snow cover in storage until warmer temperatures promote snowmelt infiltration during the spring freshet. Based on the precipitation data for Simcoe, ON, just west of the study area, a Simcoe Meteoric Water Line, $\delta^2\text{H} = 7.5 (\delta^{18}\text{O}) + 12.6$, was created to represent local values (Desaulniers et al., 1981). Modern groundwater recharge generally has $\delta^{18}\text{O}$ signatures of -11 ‰ to -8 ‰ and $\delta^2\text{H}$ signatures of -190 ‰ to -80 ‰ in southern Ontario (McIntosh and Walter, 2006; Hobbs et al., 2008; Husain et al., 2004; Clayton et al., 1966).

The presence of late Pleistocene, early Holocene-aged groundwater in Silurian rocks of the Salina Group was first noted by Clayton (1966) when he reported that deep formational waters have an isotopic composition of -13 to -9 ‰ for $\delta^{18}\text{O}$, characteristic of mixing between formational brines and glacial water precipitated under cooler climate conditions. Hydraulic loading of ice sheets during past Pleistocene glaciation re-directed regional groundwater flow in the Michigan and Appalachian Basins and provided a component of recharged water

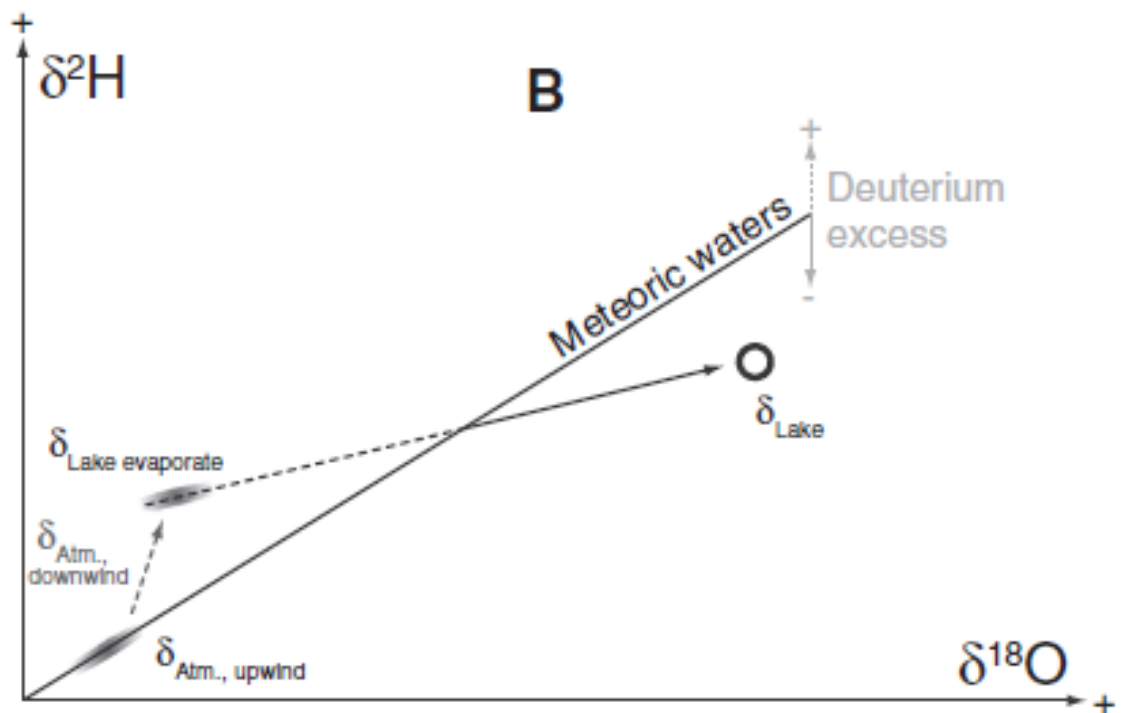


Figure 2.13: Isotopic fractionation due to lake evaporation from the Great Lakes basin (from Jasecho et al., 2014).

at depth, supressing underlying saline groundwaters (Figure 2.14; McIntosh and Walter, 2006). Desaulniers et al (1981) and Matheson (2012) provided evidence for 9000 BP to 11000 yr. BP, Pleistocene groundwater in the Wainfleet area of the Niagara Peninsula confined under a thick layer of glaciolacustrine clay. These Pleistocene waters remain in the area due to slow recharge through mainly unoxidized, thick clay units (Figure 2.14), stagnant flow conditions less than 0.08 cm/yr (Desaulniers et al., 1981) and the presence of bedrock lows in the area including the Salina bedrock trough and the Erigan buried bedrock channel (Hamilton et al., 2015). Pleistocene sediments stored in aquifers under thick, relatively impermeable Quaternary sediments deposited during the last glaciation under Lake Erie (Drimmie et al., 1993) may contribute to a glacially-mixed signal in southern Niagara groundwater, as similar potentiometric surfaces suggest groundwater movement from under Lake Erie to inland Wainfleet.

Pleistocene groundwaters are found in the Michigan, Illinois, Appalachian and Forest City sedimentary basins in southern Ontario and the north-western United States. Depleted isotopic signatures of -13.5 to -17 ‰ have been reported in several confined aquifers including values of -14 to 17 ‰ in the Wainfleet area of the Niagara Peninsula (Desaulniers et al., 1981) and -13.5 to -14.7 ‰ in the Alliston Aquifer north of Toronto in southern Ontario (Aravena et al., 1995). The samples from the Alliston groundwater may have a component of mixing with shallower, meteoric waters, as the isotopic signatures fall slightly above the accepted $\delta^{18}\text{O}$ values for late Pleistocene, early Holocene groundwaters of -15 ‰ to -20 ‰ (Desaulniers et al., 1981; Aravena et al., 1995); however other sources estimate the range of glacial meltwaters as being between -11 ‰ and -25 ‰ (Hobbs et al., 2008; McIntosh and Walter, 2006).

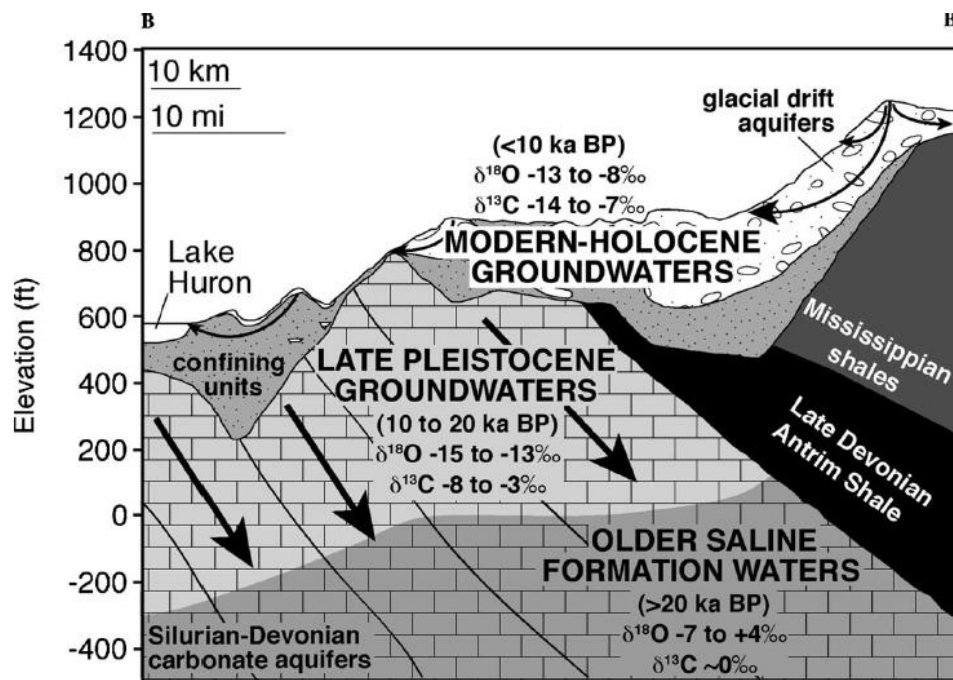


Figure 2.14: Conceptual model of the movement of modern groundwater and stagnation of Pleistocene-aged groundwater underlying thick clay confining units (McIntosh and Walter, 2006).

2.4.4 Inorganic Geochemistry of Southern Ontario Groundwater

In Hamilton, ON, multi-level well sampling identified CaSO₄ type groundwater with Total Dissolved Solids (TDS) values ranging from 480 to 15,100 mg/L from depths ranging from 5 to 65 m below ground surface (Hobbs et al., 2008). TDS values of <1000 mg/L are indicative of fresh water, values between 1000 and 10,000 mg/L are classified as brackish water, values between 10,000 and 100,000 mg/L are considered saline and values >100,000 are brine groundwaters (Hobbs et al., 2008). CaSO₄/CaMgSO₄ groundwaters are typically found downgradient below confining layers of glaciolacustrine clay or shale layers, while recharge areas in glacial overburden and shallow bedrock units are dominated by groundwater of CaMgHCO₃⁻ water type, with Ca²⁺ + Mg²⁺ versus alkalinity molar ratios of 1:2, characteristic of carbonate mineral dissolution (McIntosh and Walter, 2006). CaMgSO₄, NaHCO₃ and NaCl waters are commonly associated with microbial redox reactions and water-rock/water-soil interactions.

2.4.5 Sulfur and Carbon Sources in Groundwater Systems

Sulfur isotopes are useful for source determination in groundwater systems, as they can be used to distinguish between various sources of sulfide and sulfate. Natural sources of sulfur compounds in groundwater include gypsum and terrestrial sulfides (including pyrite and sphalerite) from sedimentary rocks and sulfate from brines at depth and may have differing ratios for formational and meteoric waters. For example, sulfate associated with Na-Ca-Cl brines from the Canadian Shield typically have positive $\delta^{34}\text{S}$ and $\delta^{18}\text{O}$ values, whereas sulfate associated with the oxidation of reduced sulfur compounds in shallow groundwaters in the same geological formation typically have lower, and potentially negative $\delta^{34}\text{S}$ and $\delta^{18}\text{O}$ values (Frape et al., 1984).

The atmospheric and oceanic sulfate isotopic composition at the time of deposition and early diagenesis is preserved in marine evaporite units, and is

consistent worldwide over a given time period due to the slow circulation and mixing of ocean currents (Fritz et al., 1988). Presently, the $\delta^{34}\text{S}$ value of sulfur and oxygen are 20 ‰ CDT and 9.5 ‰ VSMOW, respectively. During the Silurian period, isotopic compositions of marine evaporites were observed to be between +26 and +32 ‰ for $\delta^{34}\text{S}$, and +12.5 and +15 ‰ for $\delta^{18}\text{O}$ from cores and quarry exposures of the Silurian Salina group in southern Ontario (Fritz et al., 1988). Other studies of isotopic ratios of marine evaporites from Devonian-Silurian groundwater in the Michigan Basin report $\delta^{34}\text{S}$ values of +24.9 to +28.7 ‰ (McIntosh and Walter, 2006). Samples of evaporites from a gypsum mine in Caledonia, ON, within the study area for this thesis, had a narrow isotopic range for sulfate of +27.1 ‰ to +29 ‰ $\delta^{34}\text{S}$ (Fritz et al., 1988).

$\delta^{13}\text{C}_{\text{DIC}}$ values for the dolomitic shales with minor amounts of gypsum located in the Caledonia Domtar gypsum mine (O'Shea et al., 1988), are shown in Figure 2.15. $\delta^{13}\text{C}$ of DIC in groundwater between +0.5 ‰ and -4 ‰ may be influenced by carbonate dissolution, as Paleozoic carbonates generally have isotopic compositions close to the carbonate reference standard Pee Dee Belemnite (PDB). Soil CO_2 generally has isotopic compositions between -21.9 ‰ and -23 ‰ in North America (McIntosh and Walter, 2006; Skuce, 2013). Where soil CO_2 is in equilibrium with carbonate dissolution, isotopic values of DIC fall between -14 and -11 ‰ under open and closed conditions (McIntosh and Walter, 2006).

The source of methane in groundwater is determined using several methods that include, in decreasing order of common use, carbon and hydrogen isotopic signatures of methane, the presence or absence of higher hydrocarbons, ^{14}C dating and/or genetic testing to determine the microbial populations present in an aquifer. The use of isotopes for the differentiation of microbially-mediated methane from thermogenic methane produced at depth has gained interest in the past few decades. Biogenic methane production is usually characterized by $\delta^{13}\text{C}$ below -60 ‰, very reducing environments, and a lack of electron acceptors more energetically favourable to microbial populations.

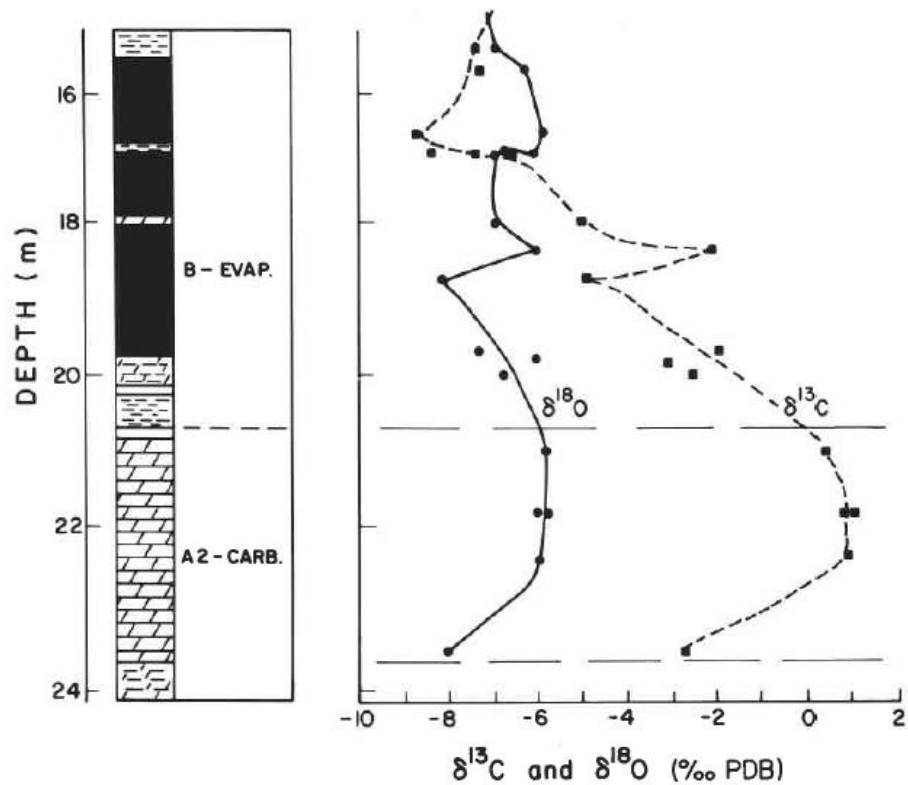


Figure 2.15: $\delta^{13}\text{C}$ and $\delta^{18}\text{O}$ of DIC from the Salina Group at the Domtar gypsum mine in Caledonia, Ontario (O'Shea et al., 1988).

Microbial methane in southern Ontario was noted to be present in Devonian shales in southwestern Ontario (McIntosh et al., 2014; Hamilton et al., 2015) and the Alliston Aquifer north of Toronto, ON (Aravena et al., 1995).

In contrast, thermogenic methane is isotopically heavier than biogenic methane, with isotopic ratios for $\delta^{13}\text{C}$ of CH_4 observed to range from -50 ‰ to -37 ‰ in southern Ontario. The $\delta^{13}\text{C}_{\text{CH}_4}$ of three gas samples from private wells, two in bedrock and one in overburden, near the north shore of Lake Erie collected by Barker and Fritz (1981) were determined to range from -29.8 ‰ to -37 ‰, therefore falling above the upper limit of biogenic methane (-50 ‰; Barker & Fritz, 1981). These samples are from the Haldimand-Norfolk region, to the west of the current study area. Deep natural gas deposits in the area have an isotopic range of -36 ‰ to -44.4 ‰, and have been found in groundwater in the area in prior

studies (Barker and Fritz, 1981). The presence of thermogenic methane in these samples is thought to result from leaking oil and gas wells (McIntosh et al., 2014). The explanation listed by the authors for the isotopic values of $\delta^{13}\text{C}$ greater than -36 ‰ in samples is due to partial methane oxidation of thermogenic, natural gas methane sources by methanotrophs (Barker & Fritz, 1981).

2.4.6 Chloride – Bromide (Cl/Br) Ratios

Chloride and bromide have been used to differentiate both anthropogenic and naturally occurring sources of dissolved salts by many researchers (Davis et al., 1998; Grasby and Betcher, 2002; Alcalá and Custodio., 2008; Mullaney et al., 2009; Katz et al., 2011; Warner et al., 2012; Llewellyn, 2014; Johnston et al., 2015) because of their conservative nature in low-salinity groundwaters. Almost all bromine in natural groundwater systems occurs in the form of bromide, sources of which include agricultural applications, evaporite minerals, and local precipitation with halogens derived from seawater. Chloride is naturally more abundant than bromide by 40 – 8000 times (Davis et al., 1998). Defined ranges of Cl/Br Ratios have been delineated by various researchers, providing a fingerprint for attributing contamination or other sources of halogens in groundwater to their source of origin. For example, shallow groundwater beneath septic systems have Cl/Br mass ratios between 300 – 600 (Davis et al., 1998) and are often high in dissolved nitrate, nitrite, ammonia, chloride, sodium, potassium, DOC and boron with depleted dissolved oxygen (Katz et al., 2011). Like shallow groundwater systems, deeper aquifers can be affected by surface contamination where karstic conduits or anthropogenic pathways such as corroded well casings allow short circuiting between strata and the transport of shallow groundwater to depth (Llewellyn, 2014; Warner et al., 2012). Where electron acceptors are available, many septic contaminants are susceptible to biogeochemical conversion from one species to another. However, ‘conservative’ tracers such as chloride and bromide do not phase-convert and can provide a

fingerprinting mechanism that is useful for attributing the source of a potential suite of contaminants, especially if used in conjunction with other methods such as isotopic tracers (or artificial sweeteners).

The Cl/Br ratio of precipitation is dependent on the range in seasonal temperatures and the distance from coastal regions. Cl/Br Ratios in rainfall and recharge water have been extensively studied and were found to be close to, or below, the Cl/Br Ratio of seawater (290 ± 4) when precipitation falls close to the coast (Katz et al., 2011). As evaporated seawater is carried inland, Cl/Br ratios of local precipitation decrease from that of seawater to reported values as low as 50 in the continental United States. Local precipitation is thought to be the main contributor to Cl/Br ratios of approximately 120 in Lake Superior, the largest freshwater lake in North America (Davis et al., 1998). Based on these ranges, local precipitation within the study area of this thesis is assumed to be within the range of 50 – 160 for chloride concentrations less than 5 mg/L. Other sources of chloride and/or bromide in groundwater systems include; deep Appalachian Basin Brines (ABB), halite dissolution, road salt, water softener systems, and human and animal food additives. Waters with high Total Dissolved Solids concentrations, including Cl > 10 mg/L, correlating to an Appalachian Basin Brine Cl/Br signature were discovered in studies initiated to determine the baseline water quality in shallow aquifers prior to fracking activities in the Appalachian Basin of the northeastern United States. ABB Cl/Br Signatures can be discriminated from halite dissolution (Cl/Br ratio > 1000, Mullaney et al., 2009) by their low Cl/Br signature (C/Br ratio approximately 50 - 300, Johnston et al., 2005) and are distinguished from dilute groundwater by Cl concentrations exceeding 10 mg/L. Only a small component of brine input (<10%) in the shallow aquifer system is required for the impartation of an ABB signature, as demonstrated by the Salt Spring site in the northeastern United States, with a brine component of 7%, elevated TDS, and sulfate concentrations lower than 50 mg/L (Warner et al., 2012). The Appalachian Basin Brine Cl/Br signature derives

from seawater evaporation during the Silurian (Warner et al., 2012; Llewellyn, 2014; Johnston et al., 2015) resulting in the enrichment of Br⁻ in the residual seawater from Br⁻ exclusion during halite saturation and precipitation (Warner et al., 2012), followed by subsequent geochemical mixing and evolution. Bedded halite deposits are primarily found in the lower formations of the Upper Silurian Salina Group, however the spatial extent of halite deposits within the unit pinch out in areas, as noted east of Susquehanna County in eastern Pennsylvania (Llewellyn, 2014). The ABB Cl/Br signature extends past the regional extent of halite-bearing units in the Salina Group, as well as in overlying Devonian carbonate units, suggesting both the lateral and vertical migration of ABB brines over geologic time (Llewellyn, 2014).

Halite has a low Br content in its crystal lattice and its impact on pristine groundwater is to increase the Cl/Br ratio. Halite influences on groundwater include: evaporite dissolution in the bedrock formation, road salting activities during the winter months in cold climates, animal feed supplements and salt-licks and septic systems through the use of water softener systems (backwash brines) and food additives. Thomas (2000) reported a strong association between Cl/Br Ratios above 400 and septic effluent in a study of the Central Glacial Deposits aquifer located near Detroit, Michigan.

Chapter 3: Methods

This section describes the methods used during site determination, sample collection, hydrogeological testing, field calibration, field measurement of geochemical parameters and laboratory analysis. This thesis had a large field work component, and thus the methods used for site determination and sample collection will be explained in detail.

3.1 Site Determination

The need for re-sampling at past sites and higher density sampling in the Niagara Region and Haldimand Country was identified following the results of the Ambient Groundwater Geochemistry Program conducted in 2010 (Hamilton et al., 2011). Samples were collected across the peninsula from a 5 x 5 km grid from wells completed in bedrock or in the bedrock–overburden contact aquifer.

Almost all contact with domestic well owners was unannounced. Upon arrival at a potential sampling site, the homeowner was asked 1) to confirm that they have a water well drilled to bedrock and 2) if they would allow sampling for research purposes, as per the Ambient Groundwater Geochemistry program sampling protocol (Hamilton et al., 2010; Hamilton 2015). The homeowner was asked about the accessibility of a sampling point that would yield raw, untreated well water. If the homeowner expressed concern or doubt about the possibility of treatment, softener test-strips were used and an inspection of the plumbing and treatment system (Figure 3.1) was carried out with the homeowner's consent. In many cases, residential water supplies are obtained from cisterns or holding tanks and, often in these cases, the pre-existing well on the property has been abandoned. In some cases, homeowners did not decommission such wells, but removed all plumbing and left wells unused. In a few cases, when no other bedrock water well within the 5 by 5 km grid was available for sampling, unused domestic wells were sampled using the same sampling procedures as for

monitoring wells (i.e., purging of at least 3 well volumes). With the identification of a bedrock water well on the property and after permission had been obtained, a short interview was conducted. The well-owner was asked about the age and depth of the well, if there is an access point to allow sampling of water before treatment, what water treatment systems are in place, and their subjective observations about the quality and quantity of their well water. Monitoring wells were sampled following the successful purge of 3 well volumes in most cases, however, where this was not possible due to low flow conditions, casings were purged of standing water at least once and sampled upon recovery.



Figure 3.1: A typical treatment system for a domestic well sampled as a part of this study. Untreated groundwater was always collected, often from the base of the pressure tank.

Prior to sampling, an inspection of the well was conducted and measurements made. Measurements include diameter of the well casing, the distance the well

casing projects from surface (stickup), depth of the well and the static water level prior to the start of sampling (Figure 3.2).



Figure 3.2: Obtaining static water level and depth measurements from a domestic well.

In cases where the well cap could not be removed because it was buried, there was a sanitary seal or was otherwise inaccessible, static water levels from the Ministry of Environment and Climate Change water-well records were used. Signs of any compromised well-head security were noted and the type of well cap used was recorded. Pictures of the well-head, well cap, plumbing system and sampling set-up were taken (Figure 3.3).



Figure 3.3: An unsecure well in a well pit. Signs of water damage from flooding is apparent on the sides of the well pit. Well locations were determined using a global positioning system device and transferred into geographic information software (ESRI®ArcGIS®). 120 samples were collected in the summer of 2015 from domestic and farm wells and 7 samples were collected from several groundwater-fed springs. 29 monitoring wells were sampled in the study area using consistent sample collection protocols. 26 additional quality-control samples (blanks, standards and duplicates) were submitted with the collected samples for laboratory analyses, for a total of 182 samples.

3.2 Sample Collection

Static water level measurements were taken prior to purging and the water level tape was decontaminated after measurement. At the monitoring wells, manual water level measurements were taken regularly during purging to support measurements recorded on a transducer. In the few cases where spring samples were taken, they were obtained at the source of the groundwater discharge (the primary vent) by syringe-sampling or with the use of a peristaltic pump.

A three-point calibration of pH was carried out each day prior to groundwater sampling using pH 4, pH 7 and pH 10 calibration standards (Figure 3.4). Conductivity was calibrated at the beginning of the field season, and checked every morning to ensure readings were within 5% of the calibration standard. Oxidation–reduction potential was not calibrated, and not used as a definitive geochemical parameter. Dissolved oxygen (DO) was calibrated each morning using a two-point calibration of dissolved oxygen in an active yeast solution (0% DO) and shaken water (100% DO).

At each sample site, 17 bottles for geochemical, isotopic and gas analyses were collected (Figure 3.5) and a number were later shipped to various laboratories for analysis. Others were analyzed shortly after data collection in the field, or analyzed in-house at McMaster University. Samples were collected for the following analyses: major cations, anions and trace elements, mercury (Hg), iodide (I⁻), bacteria (total and fecal coliforms), nitrogen parameters (e.g., total Kjeldahl nitrogen (TKN), organic nitrogen, ammonia (NH₃/NH₄⁺), nitrate/nitrite (NO₃⁻/NO₂⁻), colour, dissolved gases, including methane (CH₄) and carbon dioxide (CO₂), dissolved organic carbon (DOC), total organic carbon (TOC), dissolved inorganic carbon (DIC) and total inorganic carbon (TOC). Bacteria samples (total and fecal coliforms) were collected in 250 mL sterile HDPE bottles prepared with sodium thiosulfate pentahydrate (Na₂S₂O₃ • 5H₂O) for preservation. NO₃⁻, NO₂⁻, organic nitrogen, TKN, NH₃, DOC, DIC and colour samples were collected in 60 mL HDPE bottles. Isotopic samples include analyses for $\delta^{18}\text{O}_{\text{H}_2\text{O}}$, $\delta^{18}\text{O}_{\text{SO}_4}$, $\delta^2\text{H}_{\text{H}_2\text{O}}$, $\delta^{34}\text{S}_{\text{SO}_4}$, $\delta^{34}\text{S}_{\text{H}_2\text{S}}$, $\delta^{13}\text{C}_{\text{DIC}}$, $\delta^{13}\text{C}_{\text{DOC}}$, $\delta^{13}\text{C}_{\text{CH}_4}$ and enriched tritium (H₃).

Time-sensitive samples, including total and fecal coliforms, nitrogen parameters, TOC/TIC and colour, were shipped daily for analysis within 48 hours of sample collection. Field analyses include alkalinity, dissolved hydrogen sulfide (H₂S) and dissolved oxygen (DO). Anions, cation/metals, mercury, DOC/DIC, $\delta^{13}\text{C}_{\text{DIC}}$ and

$\delta^{13}\text{C}_{\text{DOC}}$ samples were pressure filtered using a 0.45 μm Millipore™ Durapore® polyvinylidene fluoride (PVDF) filter at each site. In the case of turbidity; alkalinity, hydrogen sulphide (H_2S^-), $\delta^{18}\text{O}_{\text{SO}_4}$, $\delta^{34}\text{S}_{\text{SO}_4}$ and $\delta^{34}\text{S}_{\text{H}_2\text{S}}$ samples were also filtered. Cation/metal samples were acidified to 1% by volume ($\text{pH} < 2$) using J.T. Baker® UltraPure nitric acid (HNO_3).



Figure 3.4: Morning calibration station for pH, Conductivity and Dissolved Oxygen.

Hg samples were acidified to 2 % by volume using Fisher Chemical Optima™ grade hydrochloric acid (HCl) shortly after sample collection. Iodide (I^-) samples were collected in 60 mL polyethylene bottles preserved with 3% 0.2 M nickel acetate ($\text{Ni}(\text{CH}_3\text{COO})_2$) to precipitate NiS, which eliminates a potential analytical interference. $\delta^{34}\text{S}_{\text{SO}_4}$ and $\delta^{34}\text{S}_{\text{H}_2\text{S}}$ samples were prepared with 2 mL saturated zinc acetate dehydrate ($\text{C}_4\text{H}_6\text{O}_4\text{Zn} \cdot 2 \text{H}_2\text{O}$) in each 250 mL sample bottle prior to sampling. Samples collected for $\delta^{13}\text{C}_{\text{DIC}}$ and $\delta^{13}\text{C}_{\text{DOC}}$ were heated to 450 °C and then “fixed” with saturated mercuric chloride (HgCl_2) prior to sampling to eliminate biological activity after sample collection. $\delta^{13}\text{C}_{\text{DIC}}$ and $\delta^{13}\text{C}_{\text{DOC}}$ samples were collected in 40 mL amber VOA glass vials, capped with an open top, white

polypropylene cap with standard 0.125-inch-thick PTFE lined silicone septum. An additional PTFE/rubber septum was placed below the cap of each sample bottle to insure a tight seal and, prevent the loss of gasses after sampling.



Figure 3.5: Sample bottles collected, field probes used and field filtration equipment at a field site.

3.3 Hydrogeological Testing

In collaboration with the Niagara Peninsula Conservation Authority (NPCA), geochemical sampling to support the objectives of this thesis was undertaken concurrently with hydraulic testing on monitoring wells in the Upper Welland River watershed and Erigan Buried Valley system. Hydraulic testing methods included single-well pumping and recovery tests, injection testing, and determination of hydrogeological parameters including transmissivity. Hydraulic

testing by the NPCA was completed with the objectives of understanding (1) the Upper Welland River subgroundwatershed system, and (2) the buried valley bedrock groundwater systems in the eastern part of the study area. Detailed investigation of transmissivity and well recovery are outside the scope of this thesis.

3.4 Sample Analysis

Sample analysis occurred in the field for time sensitive and volatile parameters, and in various laboratories. Samples for methane concentrations and carbon isotopes of methane and CO₂ were analyzed at McMaster University by the author.

3.4.1 Field Measurement Techniques

Field measurement of hydrogen sulfide was determined to be the best technique for obtaining accurate and consistent concentrations (Hamilton et al., 2007) and thus was the method used in this study. The detection limit of the hydrogen sulfide field kit used (HACH Sulfide Color Disc Test Set, Model HS-WR) is 0.01 mg/L (S²⁻), and the maximum concentration measurable without field dilution is 11.25 mg/L (S²⁻). In cases where the hydrogen sulfide concentration exceeded 11.25 mg/L (S²⁻), samples were diluted in a syringe using 4 parts distilled water and 1-part sample water. The diluted sample water was then used for measurement and the concentration obtained was multiplied by 5. Hydrogen sulfide was detected using the field method at 79% of sites within the study area, with concentrations ranging from <0.01 mg/L to 41.25 mg/L.

During sampling at all sites, alkalinity was measured for the determination of bicarbonate values using a HACH alkalinity field kit (Model AL-DT) (Figure 3.6). Alkalinity is defined as the capacity for solutes in water to neutralize acid, measured using the titration with a strong acid solution to a low pH end-point, which signifies that all solutes contributing to alkalinity have reacted (Hem, 1985).

The immediate measurement of these parameters is critical for obtaining accurate bicarbonate (HCO_3^-) concentrations, because the partitioning of gases after atmospheric exposure changes the CO_2 composition of the groundwater sample. The HACH alkalinity field kit has a range of measurement of 10 to 4000 mg/L, reported generally as mg/L CaCO_3 with the assumption carbonate alkalinity makes up all of the alkalinity, provided the pH is below 9.5. Carbonate alkalinity derives from dissolved carbon dioxide, calcium carbonate and bicarbonate species formed through the dissolution of carbonates and input of CO_2 from the atmosphere. In some cases, alkalinity can also be made up from non-carbonate species, the main species including; hydroxide, silicate, borate, and organic ligands (Hem, 1985). These cases only occur when the pH is greater than 9.5, or when waters have significant amounts of natural gas, petroleum or dissolved organic carbon. Minor contributions to alkalinity also result from species such as NH_4 , and HS^- .

Field-measurement of dissolved methane and carbon dioxide were measured in the field laboratory 24 hours after sample collection. Methane samples, collected in 1L glass bottles, were filled to 600 mL and stored upside down after sampling and allowed to equilibrate to room temperature. After equilibration, gas parameters were measured in the headspace using an RKI Eagle 2 portable multi-gas meter. The determination of methane concentrations using the field method is based on Henry's Law for ideal fluids; most volatile gases will partition out of water to a degree based on their gas-water solubility constant. This constant is dependent on the temperature of the air and the barometric pressure on the day of sample measurement. The temperature of the water in the gas samples (room temperature) was measured using the temperature function on a YSI optical dissolved oxygen probe. Calibration of high-level methane was carried out weekly, because high gas concentrations damage the low-level sensor. Measurement of dissolved oxygen was completed in the field using an YSI optical DO sensor.



Figure 3.6: Training summer students on the proper usage of HACH field kits for alkalinity (mg/L CaCO_3) and Hydrogen Sulfide (mg/L as S^{2-}).

3.4.1.1 Methane Concentrations

In addition to the field measurements, methane concentrations were also determined in lab to allow comparison of the two methods and for analytical completeness. Methane samples for lab analysis involved gentle filling of an intermediary container (usually the tritium bottle) with groundwater followed by immediate extraction of 30 mL of water using a syringe. A fine needle was then added to the syringe and the water was injected into a 60 mL, HgCl_2 -fixed evacuated bottle through a butyl septum. The samples were stored upside down prior to analysis.

Lab Analysis was completed at McMaster University in the Environmental Organic Geochemistry Lab by the author for all samples collected in the summer of 2015. Methane concentrations were determined using a SRI 8610C Gas Chromatograph equipped with an on-column injector with carrier EPC and PeakSimple data system. A standard curve with a minimum acceptable

regression value of 0.99 was completed each day using a minimum of 3 CH₄ and CO₂ standards. Duplicate samples and certified standards were run approximately every 5 samples for quality control purposes. Methane was measured as 'peaks' on the SRI using a flame ionization detector (FID), which measures the concentration of an organic parameter in a gas stream, and the standard curve regression line was for calculating methane concentrations. The SRI 8610C Gas Chromatograph has the capability to measure other gasses including CO₂, N₂ and water vapour through the use of a thermal conductivity detector (TCD), however standards for these parameters were not available and thus results from TCD measurement were not used.

3.4.2 Inorganic Geochemistry

Immediately following sample collection, samples were kept cool at approximately 4°C and shortly thereafter shipped to several environmental laboratories for analysis. Geochemical analyses of major and minor anions and cation concentrations, trace metal concentrations, dissolved organic carbon, and mercury concentrations were completed at Geoscience Laboratories in Sudbury, Ontario, Canada. Cation concentrations, excluding mercury, were analyzed using either Inductively Coupled Plasma-Atomic Emission Spectroscopy (ICP-AES) or Inductively Coupled Plasma-Mass Spectroscopy (ICP-MS). Concentrations of elements analyzed by ICP-AES were determined by a Teledyne Leeman Laboratories Prodigy ICP-AES-Dual View instrument with the halogens (chlorine (Cl), Bromine (Br), and Iodine (I)) option (Geolabs method reference codes: IAX-CUS, IAW-CUS, IAW-200) (Pamer, 2007). The precision for this method is better than 10% of the true value of the sample at concentrations exceeding the lower limit of quantification (LLoQ)², defined as the average of procedural blank plus 10 times its standard deviation (Freckelton, 2013). The accuracy for elements by the method was found to be better than 5 % for most elements (Pamer, 2007). The primary reference materials for the IAW-200 method code are BIGMOOSE and

TM-15.2 (method code IAW-200) Certified Reference Materials (CRMs) from Environment Canada (Hargreaves, 2014). Analysis of elements by ICP-MS (Geolabs reference codes: IMX-CUS and IMW-100) were determined using a Perkin Elmer Elan 9000 ICP-MS instrument for open and closed-beaker digestions. Precision and accuracy is within 10% for most elements close to the limit of quantification (LoQ), and improves to between 2% and 8% with higher concentrations of elements (Burnham, 2008). Precision exceedances above 10% were reported for the following elements; Sb, Bi, Mo, Sn, W, and possibly Cu, Hf, Pb, Ni and Zn, due to sample heterogeneity in solid-media duplicates and contamination due to sample preparation. Accuracy exceedances were found for several elements (Er, Hf, Lu, Pr, Tb, U and Y) above 10% but below 15% of the reference value (Burnham, 2008). Quality-control materials used for the monitor the precision and accuracy of ICP-MS data include the Certified Reference Material (CRM) SLRS-5 (river water reference material for trace element analysis distributed by the National Research Council of Canada) and in-house quality-control materials (QCMs). The use of Certified Reference Materials allows for determination of precision and accuracy, however they are expensive and all elements of interest may not be present in concentrations higher than detection from one reference material. To overcome these shortcomings, a round-robin study of QCMs was completed by Geoscience Laboratories researchers to assess accuracy in samples routinely used to monitor within and between batch variations (Burnham et al., 2012).

Anion concentrations were determined using a dual-pump system Dionex model ICS-3000 Ion Chromatograph (IC) (Geolabs reference method ICW-100 or ICW-CUS). Three IC analytical methods were used; the carbonate method, hydroxide method and dual-analysis method. The carbonate method produces results in less than 10 minutes per sample, except in the case of high anionic concentrations where serial dilutions are required to bring the anion within the analytical range of the method. The hydroxide method is best for water samples

with low anionic content and low salt and sulfur contents. In cases where the low detection limits of the hydroxide method and large range of concentrations of the carbonate method were required, the dual-analysis method was available (Pamer, 2011).

Total mercury concentrations were determined by Atomic Fluorescence Spectroscopy at the Geoscience Laboratories. Sample solutions initially undergo a bromine/chloride overnight digestion to remove any organic material and release mercury into solution. Prior to analysis, digestion is halted using a solution of hydroxylamine hydrochloride ($\text{NH}_4\text{OH}\cdot\text{HCl}$) and then aspirated and mixed by the instrument to release the mercury species to Hg^0 . Precision and accuracy for mercury measurements was determined to be less than 8% when several solutions of known concentration of mercury were prepared for quality control purposes (Pamer, 2008).

3.4.3 Nitrogen and Bacterial Parameters

Bacterial Samples (Total and Fecal Coliforms) were analyzed by SGS Laboratories in Lakefield, Ontario, Canada within 48 hours of sample collection. Total Coliform counts were determined within 48 hours of sample collection using the simultaneous determination of Total Coliform, Escherichia Coli and background bacteria in aqueous, soil and sludge samples by membrane filtration method (SGS Method Reference Code: MTH-MICRO-1), based on the Ontario Ministry of the Environment MICROMFDC-E3407A method. Fecal Coliform counts were determined using membrane filtration methods (SGS Method Reference Code: MTH-MICRO-4) based on the Standard Methods membrane filter technique 9222 D (Standard Methods for the Examination of Water and Wastewater 21st Edition). Nitrogen Species (NO_3^- , NO_2^- , NH_3/NH_4 , TKN and Organic Nitrogen) were analyzed within 7 days of sample collection. Nitrate (NO_3^- as N) and Nitrite (NO_2^- as N) were determined by Ion Chromatography (SGS Method Reference Code: ME-CA-[ENV]IC-LAK-AN-001) following the United

State's Environmental Protection Agency method 300.1 for determination of inorganic anions in drinking water by ion chromatography (Hautman and Munch, 1997). Ammonia/Ammonium (NH_3/NH_4) was determined using a Skalar Segmented Flow Autoanalyzer (SHS Method Reference Code: ME-CA-ENVISEA-LAK-AN-007) with the method derived from the Standard Methods 4500-NH₃G protocol (Standard Methods for the Examination of Water and Wastewater 21st Edition). Total Kjeldahl Nitrogen (TKN as N) was determined using a Skalar Segmented Flow Autoanalyzer (SGS Method Reference Code: ME-CA-[ENV]SFA-LAK-AN-002) method derived from the Standard Methods protocols 4500-N C & 4500-NO₃⁻ F (Standard Methods for the Examination of Water and Wastewater 21st Edition).

3.4.4 DOC and DIC Concentrations

Dissolved Organic Carbon (DOC) and Dissolved Inorganic Carbon (DIC) were determined by several labs for operational reasons (e.g. concentrations were required at the time of $\delta^{13}\text{C}_{\text{DIC/DOC}}$ analysis) and to allow comparison with previous years. Analysis by three laboratories was completed for both parameters to assess differences in measurement between sample collection procedures, filtering techniques and laboratory measurements.

Dissolved Organic Carbon (DOC) and Dissolved Inorganic Carbon (DIC) samples were submitted for analysis to Geoscience Laboratories in Sudbury, Ontario, and analyzed using the methods for Total Organic Carbon (TOC) and Total Inorganic Carbon (TIC) (Pamer, 2015). DOC measurements were provided in the development stage for information purposes only, and do not represent a certified product by Geolabs (Geoscience Laboratories). Samples were filtered into 60 mL polyethylene bottles using a 0.45 μm Millipore™ Durapore® polyvinylidene fluoride (PVDF) filter and kept cool until analysis. Samples were analyzed using a Shimadzu TOC-L CPH/CPN configured with Type B halogen scrubber and high salts combustion tube followed by analysis on a Shimadzu

Turntable ASI-L autosampler equipped for high suspended solids and with sparging module. The determination of DOC/TOC values follows the traditional method of calculating the difference between the measured total carbon (TC) and inorganic carbon (IC) concentrations. To determine the TC content, the sample is introduced into a TC combustion tube, where carbon-bearing compounds are converted to CO₂ and transferred to the gas analyzer for measurement. To determine the IC content, the sample is reacted with a small amount of 25% w/v phosphoric acid and sparged with carrier gas for reaction with the inorganic fraction of carbon-bearing compounds (Pamer, 2015).

Analysis of Dissolved Organic Carbon (DOC) and Dissolved Inorganic Carbon (DIC) concentrations was completed in conjunction with isotopic analysis at HATCH Laboratories, in Ottawa, Ontario. Samples were filtered and collected in full, 40 mL amber glass TraceClean EPA vials with double septum caps treated with HgCl₂ prior to sample collection. Samples were analyzed at HATCH using an OI Analytical Aurora Model 1030W TOC Analyzer with a model 1088 Autosampler, interfaced to a Finnigan Mat DeltaPlusXP isotope ratio mass spectrometer for analysis by continuous flow (HATCH website, University of Ottawa). Data was normalized by three internal standards, and an analytical precision of 2% of the concentration (ppm) was reported.

TOC and TIC concentrations were also determined at SGS analytical laboratories on unfiltered samples. The method used a Skalar Segmented Flow Analyzer (SGS Method Reference Code: ME-CA-[ENV]EWL-LAK-AN-023) based on the Standard Methods 5310C protocol (Standard Methods for the Examination of Water and Wastewater 21st Edition). Both TOC and TIC have a minimum detection limit of 0.1 mg/L for this analytical technique but the reported detection limit for 2015 data is 1 mg/L.

A comparison between laboratory measurements of DIC/TIC (Figure 3.7) and DOC/TOC (Figure 3.8) was completed following quality control checks on each

dataset. Samples run at HATCH laboratories for DIC show excellent precision but a positive drift (a 'roleover') relative to alkalinity (mg/L as C) for DIC concentrations greater than 50 ppm, and therefore above the normal range of samples routinely submitted to HATCH labs (S. Hamilton, P. Comm., 2015). Therefore, this may be an instrumentation problem related to concentrations outside the calibration envelope. Concentrations for DIC/TIC determined by SGS and Geolabs show results similar to each other, with Geolabs expressing better precision (Figure 3.7). Due to these factors, Geolabs data were used for DIC concentrations for the completion of this study.

DOC concentrations (Figure 3.8) at Geoscience Laboratories (Geolabs) were limited by a high detection limit of 2.85 ppm that prevented DOC determination on approximately 80% of samples. However, even above this concentration, the Geolabs DOC concentrations did not produce reliable results (Figure 3.8), as this data was provided in the developmental stage for the method for information purposes only. DOC/TOC concentrations at both SGS labs and Hatch labs have lower detection limits of 1 ppm and 0.2 ppm, respectively. Comparison between the analytical data shows a better correlation between SGS and Hatch samples, with higher precision demonstrated for the Hatch DOC concentrations as determined by plotting the duplicate pairs against one another. Therefore, the HATCH DOC concentrations are used in this study due to the higher analytical precision, lower detection limit, and better correlation with another lab's results.

3.4.5 Isotopic Analysis

Isotopic tracers are among the most useful tools for interpretation of geochemical signatures in groundwater systems. Isotopic parameters analyzed for the completion of this study include; oxygen and hydrogen isotopes of water ($\delta^{18}\text{O}$ and $\delta^2\text{H}$), Enriched tritium (E^3H) of water, oxygen and sulfur isotopes of sulfate ($\delta^{18}\text{O}$ and $\delta^{34}\text{S}$), sulfur isotopes of sulfide ($\delta^{34}\text{S}$), carbon isotopes ($\delta^{13}\text{C}$) of

Dissolved Inorganic Carbon (DIC) Concentrations (ppm) Analytical Comparison

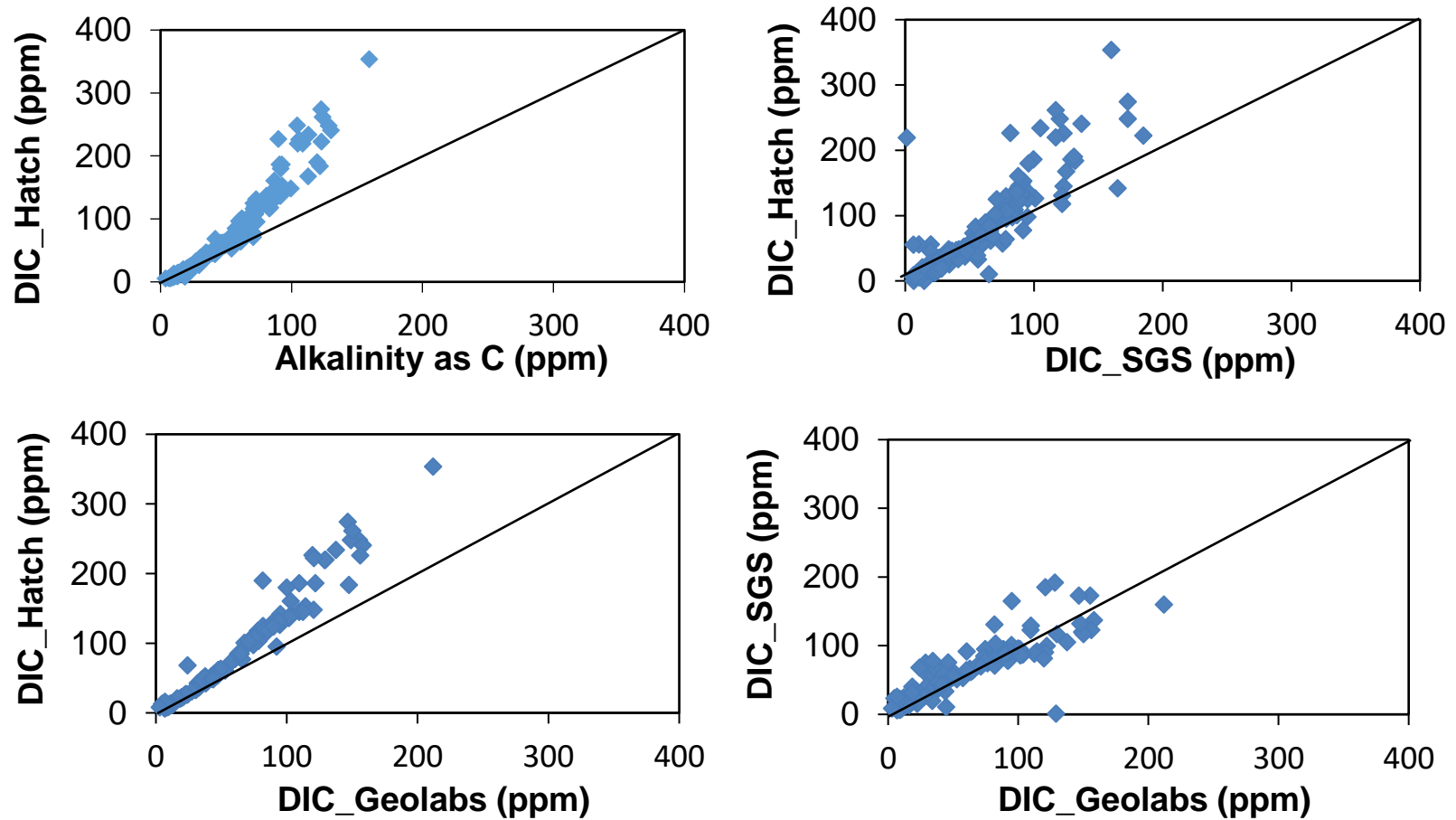


Figure 3.7: Comparison between Dissolved Inorganic Carbon (DIC) Concentrations measured in field (a) and at three respective laboratories (b, c, and d).

Dissolved Organic Carbon (DOC) Concentrations (ppm) Analytical Comparison

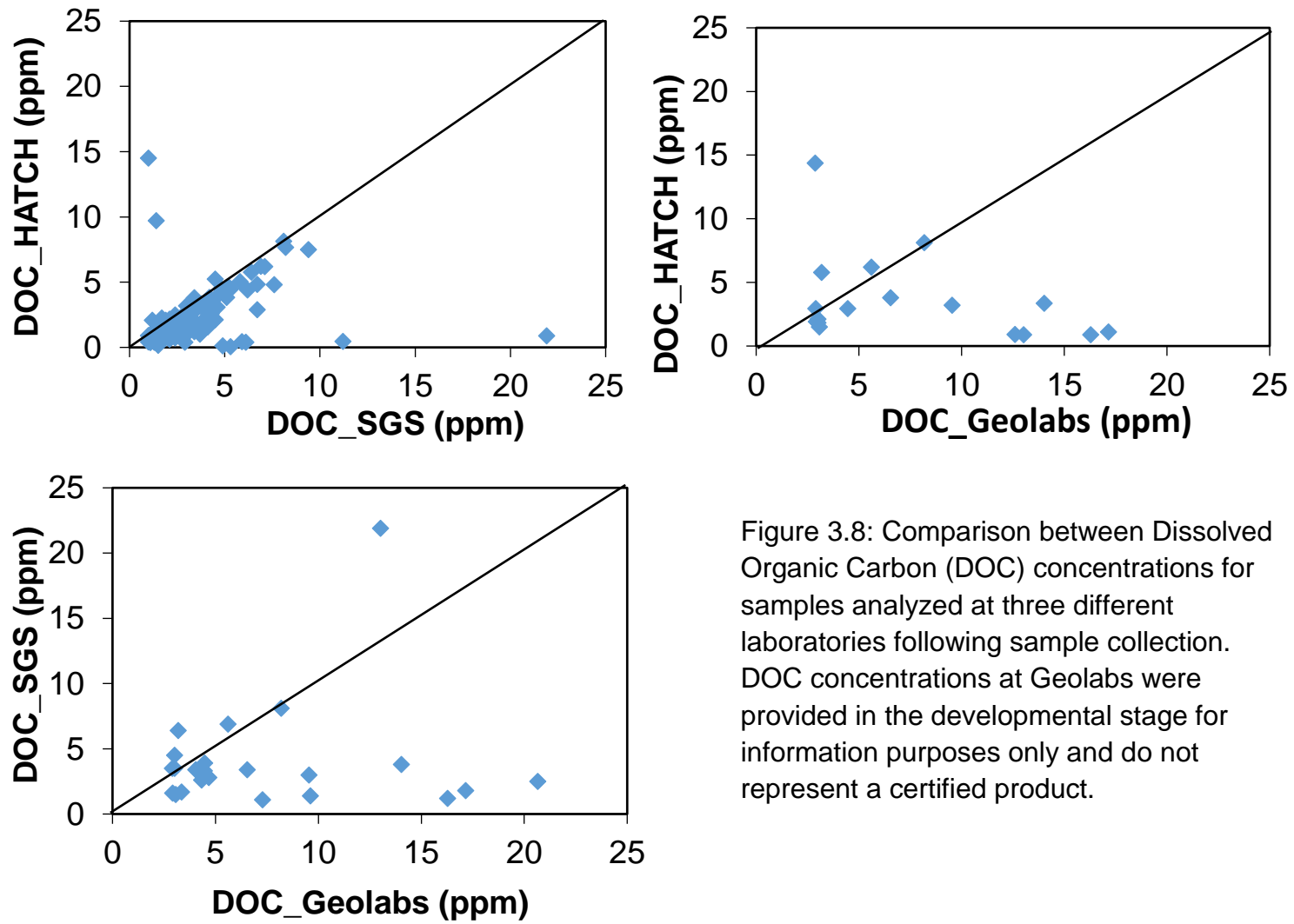


Figure 3.8: Comparison between Dissolved Organic Carbon (DOC) concentrations for samples analyzed at three different laboratories following sample collection. DOC concentrations at Geolabs were provided in the developmental stage for information purposes only and do not represent a certified product.

dissolved organic carbon (DOC), and dissolved inorganic carbon (DIC), and carbon isotopes of methane ($\delta^{13}\text{C}$).

Delta notation (δ) is conventionally used to represent differences in the absolute values of two isotopes of an element compared to a standard (Freidman & O'Neil, 1977). Standard delta notation is represented by the equation:

$$\delta (\text{‰}) = \left(\frac{R_{\text{sample}} - R_{\text{standard}}}{R_{\text{standard}}} \right) \times 1000$$

Where R represents the ratio of heavy to light isotopes and standard represents the corresponding ratio in the international reference standard for that material. Stable isotope ratios and their corresponding standards used in this study include $^{18}\text{O}/^{16}\text{O}$ and $^2\text{H}/\text{H}$ (standard: Vienna Standard Mean Ocean Water), $^{13}\text{C}/^{12}\text{C}$ (standard: Vienna Pee Dee Belemnite) and $^{34}\text{S}/^{32}\text{S}$ (standard: Canyon Diablo Troilite). Analytical results are corrected, evaluated and reported relative to these standards (IT2, P.Comm., 2015).

The isotopic fractionation produced by differences between the ratio of the heavy and light isotopes of the element can provide insight on abiotic and biological processes occurring in the studied environment (Clark and Fritz, 1997). A positive δ value is isotopically enriched in the heavier isotope for the element relative to the standard, whereas a negative δ value is isotopically depleted in the heavier isotope, or enriched in the lighter isotope relative to the standard (Freidman & O'Neil, 1977). Additionally, differences in δ between two species in a geochemical environment is described by the fractionation factor (α) between the two substances (Freidman & O'Neil, 1977). The fractionation factor, or isotopic effect, describes the abiotic and biologically-mediated partitioning of isotopes driven by energetic favourability and kinetic isotope effects (Clark and Fritz, 1997). Biologically mediated isotope fractionation is usually larger than abiotic fractionation, due to the preference of the lighter, more energetically

favourable isotope for microbial metabolism. Following metabolic processing of redox-sensitive parameters, the product becomes isotopically depleted, whereas the reactant becomes isotopically enriched (Clark and Fritz, 1997). The relative isotopic values for a parameter can give insight into the metabolic processes and natural sources of dissolved constituents in an aquifer (Clark and Fritz, 1997).

Samples collected for tritium, water isotopes ($\delta^{18}\text{O}$ and $\delta^2\text{H}$), sulfur isotopes of sulfate and sulfide ($\delta^{34}\text{S}$ and $\delta^{18}\text{O}$) and carbon isotopes of DIC, DOC and CH_4 ($\delta^{13}\text{C}$) were submitted to external laboratories, or measured at McMaster University by the author of this thesis. Samples were reported relative to certified reference standards.

3.4.5.1 Water Isotopes

Stable isotopic analyses of water isotopes ($\delta^{18}\text{O}$ and $\delta^2\text{H}$) were completed at Isotopic Tracer Technologies Inc. in Waterloo, Ontario using a Picarro CRDS Isotopic Water Analyzer (Model L1102-i). This instrumentation includes a high precision autosampler used to make small injections into the vapourizer, along with a vapourization module that is used for converting the liquid water sample to the gas phase at 140°C , avoiding any possible fractionation that commonly occur with other methods. The precision reported by Isotopic Tracer Technologies Inc. for $\delta^{18}\text{O}$ and $\delta^2\text{H}$ are ± 0.1 ‰ and ± 0.6 ‰, respectively. There are no quantification methods or detection limits (DL) for this type of analysis.

3.4.5.2 Enriched Tritium

Enriched tritium was measured to determine groundwater age for each sample across the study area. The method used for determining tritium composition for groundwater samples includes collection of 250 mL of water in an air-tight sample bottle with little headspace, enrichment by electrolysis and measurement by scintillation counting. The analytical precision for enriched tritium analysis is ± 0.8 Tritium Units (TU).

3.4.5.3 Sulfur Isotopes

Prior to sample collection, a small amount (2 mL) of zinc acetate was added to both sulfide and sulfate $\delta^{34}\text{S}$ sample bottles to 'fix' the sulfide as ZnS. Samples were kept cool following sampling, and subsequently shipped to Isotope Tracer Technologies Inc. for sample preparation and analysis. Samples were filtered in the lab through a 0.45 μm cellulose nitrate filter to collect the white ZnS precipitate and the residual fluid was processed for sulfate. The operational limits of the ZnS collection and analysis method limited $\delta^{34}\text{S}_{\text{H}_2\text{S}}$ determination to cases where H_2S concentration was above 0.3 mg/L. Where sulfide concentrations were field measured to be between 0.3 and 1.0 mg/L, an additional 1-litre sample bottle with 8 mL of zinc acetate was collected for analysis. Where samples had sulfide concentrations greater than 1 mg/L, the 1 litre bottle was not required as enough ZnS material could be recovered from the 250 mL $\delta^{34}\text{S}_{\text{SO}_4}$ bottle.

The determination of $\delta^{34}\text{S}$ of sulfate involves sample pre-treatment, precipitation and collection of BaSO_4 and combustion of the BaSO_4 to SO_2 for analysis by Isotope-Ratio Mass Spectrometry (IRMS). Pre-treatment of dissolved sulfate in water is dependent on the sulfate concentration, as determined in the lab either chromatographically or with a commercially available test kit. Samples with sulfate concentrations greater than 50 mg/L (98% of samples analyzed) were directly precipitated using Barium Chloride ($\text{BaCl}_2 \cdot \text{H}_2\text{O}$) and agitated. After allowing the sample to settle, treatment for carbonates was completed by acidification of the sample using a 10% HCl solution to a pH between 3-4.

The BaSO_4 slurry was then analyzed following combustion to SO_2 and measurement on a CarloErba EA+ MAT-253 IRMS system for $\delta^{34}\text{S}$ and a TCA coupled with a DeltaPlus XL IRMS system for $\delta^{18}\text{O}$. Samples with sulfate concentrations less than 50 mg/L initially passed through an ion exchange resin, removing sulfate from water prior to release by an NaCl eluent. After the ion exchange procedure, samples with low sulfate concentrations follow the same

precipitation and measurement procedure as higher SO_4^{2-} concentration samples. The analytical precision reported for sulfur and oxygen isotopic ratios are 0.3 ‰ and 0.2 ‰ respectively.

3.4.5.4 Carbon Isotopes of DIC and DOC

$\delta^{13}\text{C}$ of DIC and DOC were determined at G.G. Hatch Stable Isotope Laboratory in Ottawa, Ontario. A quantity of sample was drawn through the septum of the sample bottle with a syringe, injected into a reaction chamber and mixed with 5% phosphoric acid to release the inorganic carbon as CO_2 . A helium carrier gas then transports this through a chemical and Nafion™ trap to scrub any water remaining in the gas. Sample preparation for dissolved organic carbon was completed in a similar fashion, with the substitution of phosphoric acid with persulfate solution to release the organic carbon. Following the transport and cleaning of these two respective gases, samples were analyzed using a DeltaPlus Advantage isotope mass ratio spectrometer coupled with a Conflo III. Analytical precision reported for $\delta^{13}\text{C}$ of DIC and DOC is 0.2 ‰.

3.4.5.5 Carbon Isotopes of Methane

$\delta^{13}\text{C}$ of methane was analyzed at McMaster University by the author for samples with high methane concentrations measured in the field, and in lab (see below). Due to analytical constraints of the method and sample volume collected, only samples with methane concentrations greater than 30 $\mu\text{mol/L}$ were analyzed.

Samples analyzed for $\delta^{13}\text{C}$ of CH_4 were collected in 60 mL glass bottles that were pre-burnt and fixed with 2 drops of Mercuric Chloride (HgCl_2) (Fisher Scientific: CAS No. 7487-94-7) capped with a butyl septum stopper prewashed with NaOH and crimped with a 20 mm aluminium seal. Sample bottles were also pre-evacuated prior to sample collection to eliminate sources of contamination from ambient air during bottle preparation and sampling. 30 mL of sample was collected in each 60 mL bottle to provide an equal ratio of air to headspace

for ease in methane calculations. It is assumed that all dissolved methane partitioned into air from the water following sample collection, as the Henry's Law Constant (air-water partitioning coefficient) for methane is small ($K_H = 1.4 \times 10^{-3}$, Sander, 2015).

Samples analyzed for $\delta^{13}\text{C}$ of CH_4 were manually injected into a Finnigan MAT Delta plus Gas Chromatograph – Isotope Ratio Mass Spectrometer (CG/IRMS) with volumes ranging from 100 μL to 1000 μL , depending on methane concentration pre-determined by lab analysis (see below). Following sample injection, the gaseous sample was passed through a GS-Q Com 0.32 mm US6537022H column at 250°C for CO_2 and CH_4 . Analytical peaks determined following gas separation in the column were quantified using certified reference standards of methane and carbon dioxide to a precision of 0.5 ‰ $\delta^{13}\text{C}$ for both parameters. Standards of methane at several concentrations and volumes were run for quality control prior to the start of analysis and after every 5 samples during analysis.

3.5 Physical Well Locations and Quality Control Procedures

Each sample location was assigned a specific Station ID and Sample ID that are henceforth used to represent that sample in this study. In many cases, the Sample ID and Station ID are the same, which indicates that the sample was taken from a station new in 2015 and not from a station sampled in previous years. In some cases, wells and springs from earlier sampling (mostly in 2010) in the Ambient Groundwater Geochemistry Program were revisited for investigation of temporal changes. Samples and stations at the well or spring were georeferenced with UTM coordinates (NAD83, Zone 17N) using a GPS.

The depth of the well sampled and the geological source of the water was determined at the OGS using the Ontario Ministry of the Environment Water Well Records, a Digital Elevation Model (DEM), existing geological maps by the OGS

and information collected on site through manual measurements or discussion with the homeowner.

Extensive analytical quality control (QC) protocols were carried out prior to, during and after sample collection and analysis. 15% of samples submitted to all labs for analysis were for QC; including duplicates, field blanks and field standards. Duplicate samples were randomly and simultaneously collected at certain station locations amounting to at least 1 in 20 samples. Field blanks were prepared using ultrapure distilled and deionized water and treated with the same preservatives and procedures as collected samples. Certified reference or in-house bulk standards with known concentrations for most parameters were sequenced throughout all batches.

In addition to standards, duplicates and blanks, analytical quality was assured with the determination of charge balance between major cations and anions. As aqueous solutions are electrically neutral, when analyzing full suites of major ions, the determination of apparent deviations from electroneutrality via calculation of the percentage charge balance error (CBE) can indicate sources of analytical error. The charge balance error of a sample can be calculated using the following equation;

$$\text{CBE (\%)} = \frac{(\sum \text{cations} - \sum \text{anions})}{(\sum \text{cations} + \sum \text{anions})} \times 100$$

A positive number is indicative of an excess of cations and a negative error of an excess in anions. Common sources of charge balance errors include (Fritz, 1994); the use of lab alkalinity instead of field alkalinity (usually a positive error), insufficient or lack of filtering of metals (negative error), or errors in lab analysis of parameters. For the 165 samples collected as a part of this thesis, including field duplicates, 145 (88%) have charge balance errors below 10%. Only 4 samples

have charge balance errors above 15% (15-AG-100, 15-AG-121, 15-AG-095 and 15-AG-112), the worst of which was 17.2%. For further information on QC procedures for station and sample information see; Hamilton et al. (2007), Hamilton and Braunder (2008), Hamilton and Freckelton (2009), Hamilton et al. (2010, 2011), Freckelton and Hamilton (2013), Colgrove et al (2014) and McEwan et al. (2015).

3.6 Statistical Analysis

Descriptive statistics were completed on the Niagara Peninsula groundwater samples for all major ions, isotopes and field parameters. Hierarchical Cluster Analysis (HCA) was chosen as the multivariate statistical method used during the completion of this thesis. Hierarchical Cluster Analysis was used to divide samples into categories, or clusters, based on geochemical facies. The use of multivariate statistics provides insight on biogeochemical reactions occurring within the study area.

For HCA preparation, chemical parameters were excluded on the basis of five factors; (a) additive parameters including conductivity and TDS, (b) highly censored parameters (i.e. those with a large proportion of samples below the detection limit) including NO_3^- , NO_2^- , DO, PO_4^{2-} , Al^{3+} , dissolved gasses and trace elements, (c) parameters with missing data from several sampling locations (d) parameters with little regional variation, and (e) parameters exhibiting repetition with, or similarities to other parameters e.g. DIC, which mirrors HCO_3^- . Bacterial parameters were excluded from analysis on the basis of a high percentage of data falling below the detection limit; and isotopic data were excluded on the basis of missing data from several sites at the time of analysis. In HCA, samples must have a complete set of data for all parameters or must be excluded entirely from the analysis. As localized variations occur within small areas in the study, the replacement of missing values with averaged local data was not deemed acceptable. Censored data (samples with values lower than the detection limit)

need to be represented as a value for multivariate statistical analysis. It was decided that censored data would be replaced with the positive value of the detection limit in this study, following the methods of Cloutier et al., 2008.

Hierarchical Cluster Analysis was completed in Statistica (StatSoft©) using the Euclidean distance measure and Ward's linkage Method. The use of both methods is common in hydrochemical studies (Cloutier et al., 2008; Guler et al., 2004; Freckelton et al., 2013) for the determination of similarities between sites (Euclidean distance measure) and the subsequent linkage of samples through the analysis of variance in distances between groupings. The Euclidean distance method links the most similar samples together first and then subsequently continues grouping samples based on chemical similarities as displayed on a dendrogram.

Descriptive statistics were used to determine the skewness of data. All geochemical parameters used in the HCA show a positively skewed distribution. Parameters with highly positive skewness were determined to be non-normally distributed, and were log-transformed (Cloutier et al., 2008). Ca^{2+} , HCO_3^- , SO_4^{2-} and F^- exhibited close to normal frequency distributions and low positive skewness values, and thus were not log-distributed. Log-distributed and normally-distributed variables were then standardized and z-scores manually calculated by the equation $z = (x_i - \bar{x}) / s$; (x_i = sample value, \bar{x} = mean, s = standard deviation), as done commonly in multivariate statistical analyses (Cloutier et al., 2008; Guler et al., 2002, Schot and van der Wal., 1992). Standardization centres the mean of data on zero with standard deviations of +3 to -3, reducing the preferential weighting of parameters with higher magnitude data during the calculation of Euclidean Distances.

3.7 Geochemical Modelling

The PHREEQC module of the geochemical modelling program Aquachem (Waterloo Hydrogeologic, 2015) was used for the calculation of groundwater

saturation indices (SI) for Niagara Peninsula samples using input parameters including temperature, pH, conductivity, and major ion chemistry. Saturation indices were calculated for minerals commonly present in local bedrock units including; calcite, dolomite, gypsum, anhydrite, fluorite, pyrite, hematite, goethite, halite and quartz. Saturation indices are used to demonstrate the state of saturation of a constituent in equilibrium with water. The saturation index of a sample is expressed by the equation $SI = \log (IAP/KSP)$, where IAP is the ion-activity product and KSP is the solubility product. Water-types or hydrogeochemical facies were determined for all samples using Aquachem geochemical software for all samples based on the greatest relative concentrations of major ions.

Chapter 4: Results

The regional dataset for the Niagara Peninsula groundwater sampling program contains 182 samples; 26 of which are field blanks, standards and duplicate samples. A total of 156 observation sites were sampled in the summer of 2015 from a combination of primarily domestic and monitoring wells, in addition to a few springs located within the boundaries of the study area. An almost full and uniform density of groundwater sampling was achieved in the western Niagara Peninsula as a part of the initial sampling program, and was supported by monitoring well sampling in the eastern Niagara Peninsula as a part of a collaborative program with the NPCA. All samples collected, listed with spatial locations, concentration data and isotopic parameters are presented in the Appendices of this thesis.

This chapter summarizes the isotopic and major ion geochemical data collected and analyzed as a part of this study. For relevance and simplicity, only geochemical parameters controlling major geochemical and biological processes are discussed in this chapter. The full listing of all 97 geochemical and isotopic parameters for each sample is provided in the Appendix. Geochemical samples are presented as members of clusters defined using the multivariate statistical technique Hierarchical Cluster Analysis, and in some cases, by hydrogeochemical facies defined by the dominant anion and cation of each sample.

4.1 Field Parameters and Inorganic Geochemistry

Regionally, water samples had an average temperature of 11.2 °C and a median temperature of 11.0 °C, with values ranging between 9.2 °C and 15.0 °C. Temperatures at the higher range (>13°C) are not representative of groundwater temperature, but instead due to temperature increase during low-flow sampling of monitoring well samples. Conductivity values on the Niagara Peninsula had an average value of 2462 $\mu\text{S}/\text{cm}$ ($\sigma = 1631 \mu\text{S}/\text{cm}$), with a median value of 2219

$\mu\text{S/cm}$ (Figure 4.1). A large range of positively-skewed conductivity values were present in samples collected on the Niagara Peninsula (min = 264 $\mu\text{S/cm}$; max = 10706 $\mu\text{S/cm}$) with higher values found in the central portion of the study area from groundwater obtained from the Salina and Guelph Formations. Regionally, water samples have an average pH of 7.33 and a median pH of 7.15 (min = 6.50; max = 8.42). pH was more alkaline in the central Niagara Peninsula within the Salina and Guelph Formations (Figure 4.1), and trended towards neutral to slightly acidic in the southwestern and northern study area.

The oxidation-reduction potential (ORP) averages -98.2 mV (Eh ~ 102 mV) and has a median value of -94.2 mV (Eh ~ 106) with a minimum of -320 (Eh ~ -120) and a maximum of 177 (Eh ~ 377). Positive readings are found in the western, southwestern and northern portions of the study area. Table 4.1 presents basic descriptive statistics for all 156 groundwater samples collected at observation sites in the summer of 2015 for 20 geochemical parameters commonly found in natural waters. Statistical values are given in concentration, reported in mg/L.

Figures 4.2 - 4.4 present the distributions of major ions in groundwater across the study area. Ca^{2+} , Mg^{2+} , Na^+ , K^+ , SO_4^{2-} , B and Cl^- are all elevated in the central Peninsula, originating from bedrock beneath thick, low-permeability glacial sediments in the Salina trough. The distribution of elevated Cl^- is refined to an area north of the currently defined contact between the Salina and Guelph Formations, however the Paleozoic stratigraphic boundaries are currently being redefined, and it is likely that lower units of the Salina Group extend northward to include the area exhibiting elevated Cl^- concentrations mapped on the current Guelph/Eramosa Formation (F. Brunton, P. Comm., 2016). Additionally, elevated Cl^- concentrations exist in an anomalous area in Salina Group in the central part of the study area, covering a smaller spatial area than other anomalous major ion parameters. Elevated HCO_3^- concentrations are located in the northern and southwestern peninsula and the western Salina and Guelph Formations. HCO_3^- concentrations in the eastern and central Salina and Guelph Formations are

Descriptive Statistics for the Groundwater Samples								
Parameter	Unit	ODWS	Mean	Median	Minimum	Maximum	Standard Deviation	Skewness
S ²⁻	mg/L		2.59	0.03	-0.01	41.25	7.37	3.9
Ca ²⁺	mg/L		302	256	-0.20	843	198	0.4
Mg ²⁺	mg/L		118	78.1	-0.48	902	114	2.9
K ⁺	mg/L		8.24	7.04	0.68	44.1	5.32	3.4
Na ⁺	mg/L		131	82.0	1.57	1140	168	3.5
HCO ₃ ⁻	mg/L		266	239	20.0	810	177	0.6
SO ₄ ²⁻	mg/L	500*	1180	1020	0.64	5200	935	0.7
Cl ⁻	mg/L	250*	180	31.7	0.54	2950	421	4.4
Br ⁻	mg/L		1.66	0.16	-0.02	32.3	4.54	4.8
F ⁻	mg/L	1.5	0.78	0.70	-0.01	3.16	0.54	1.2
B	mg/L		0.71	0.37	0.02	6.14	0.97	2.8
Fe ²⁺	mg/L	0.3*	0.72	0.24	-0.07	9.51	1.29	3.9
Sr ²⁺	mg/L		8.94	10.2	0.01	51.51	6.84	2.1
Si ⁴⁺	mg/L		5.40	4.95	1.07	14.9	2.23	1.6
DOC	mg/L	5*	1.82	1.36	0.16	8.13	1.54	1.9
DIC	mg/L		79.1	57.4	5.22	354	70.1	1.2
NH ₄ ⁺	mg/L		0.41	0.29	0.04	2.37	0.42	2.1
As ³⁻	mg/L	0.025	0.002	0.001	0.000	0.02	0.003	3.0
Li ⁺	mg/L		0.095	0.290	0.040	2.37	0.420	-4.2
Mn ²⁺	mg/L	0.05*	0.070	0.045	0.001	0.52	0.090	2.8

Table 4.1: Descriptive statistics for general chemistry parameters from bedrock wells on the Niagara Peninsula. Descriptive statistics were used for normalization of sample data for multivariate statistics. The Ontario Drinking Water Standards (ODWS) is provided for each parameter for comparison to mean and median values. * indicates an Aesthetic Objective (AO).

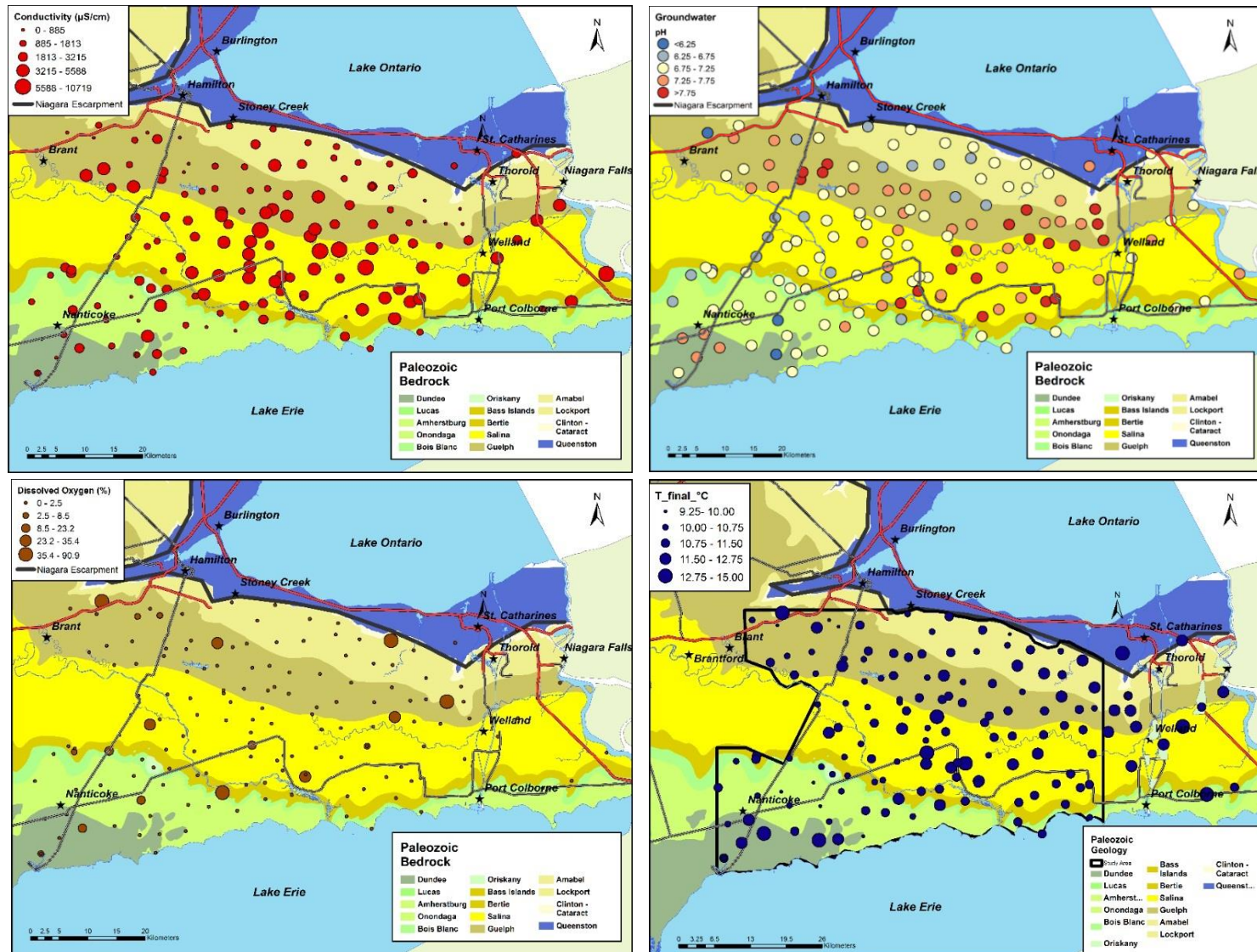


Figure 4.1: Spatial distributions of field parameters; including Conductivity ($\mu\text{S/cm}$), pH, Dissolved Oxygen (%) and Temperature ($^\circ\text{C}$) measured during collection of groundwater samples overlain on the Paleozoic Geology.

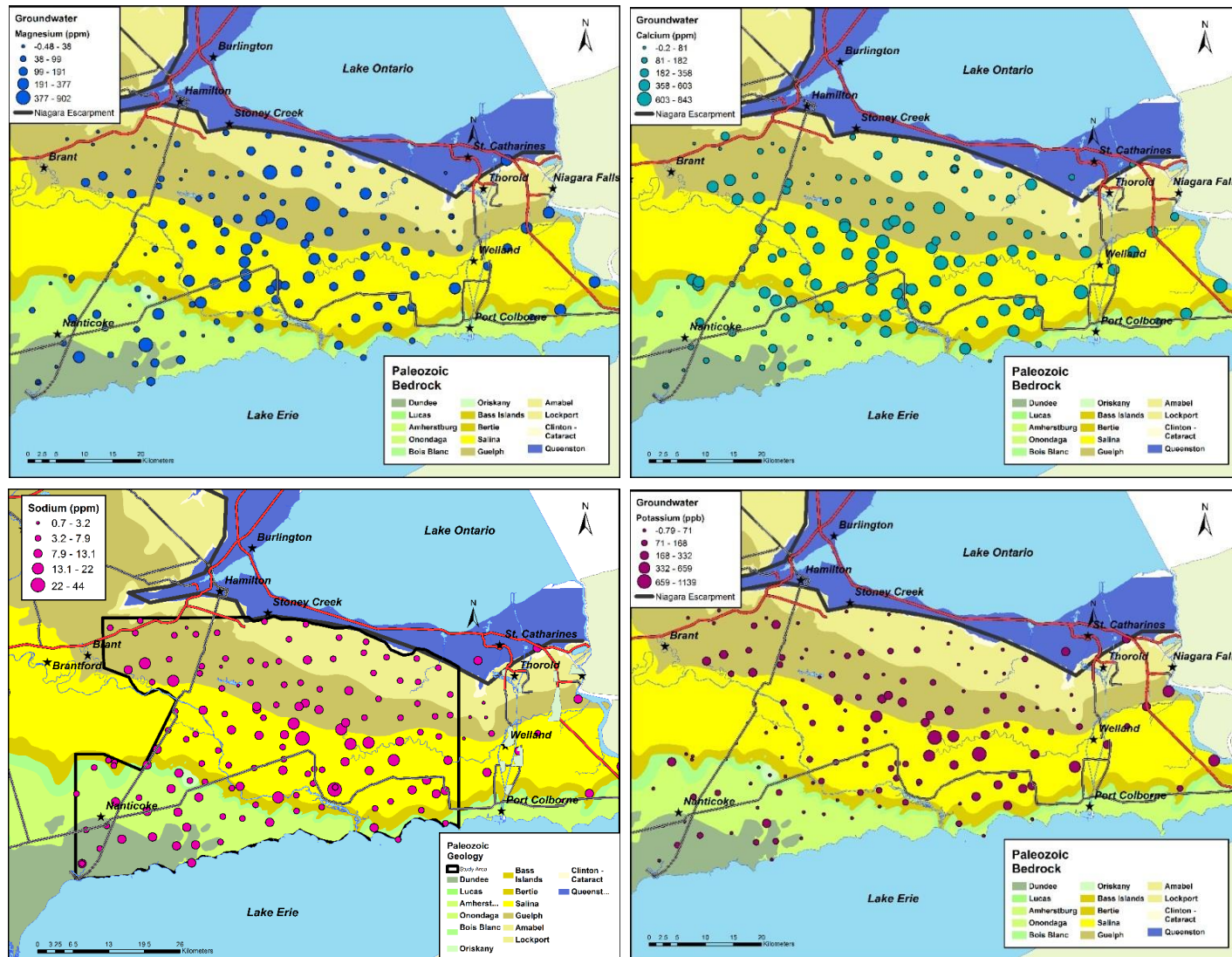


Figure 4.2: Geochemical concentrations of major cations Mg^{2+} (ppm), Ca^{2+} (ppm), Na^+ (ppm) and K^+ (ppb) from groundwater samples collected in the summer of 2015.

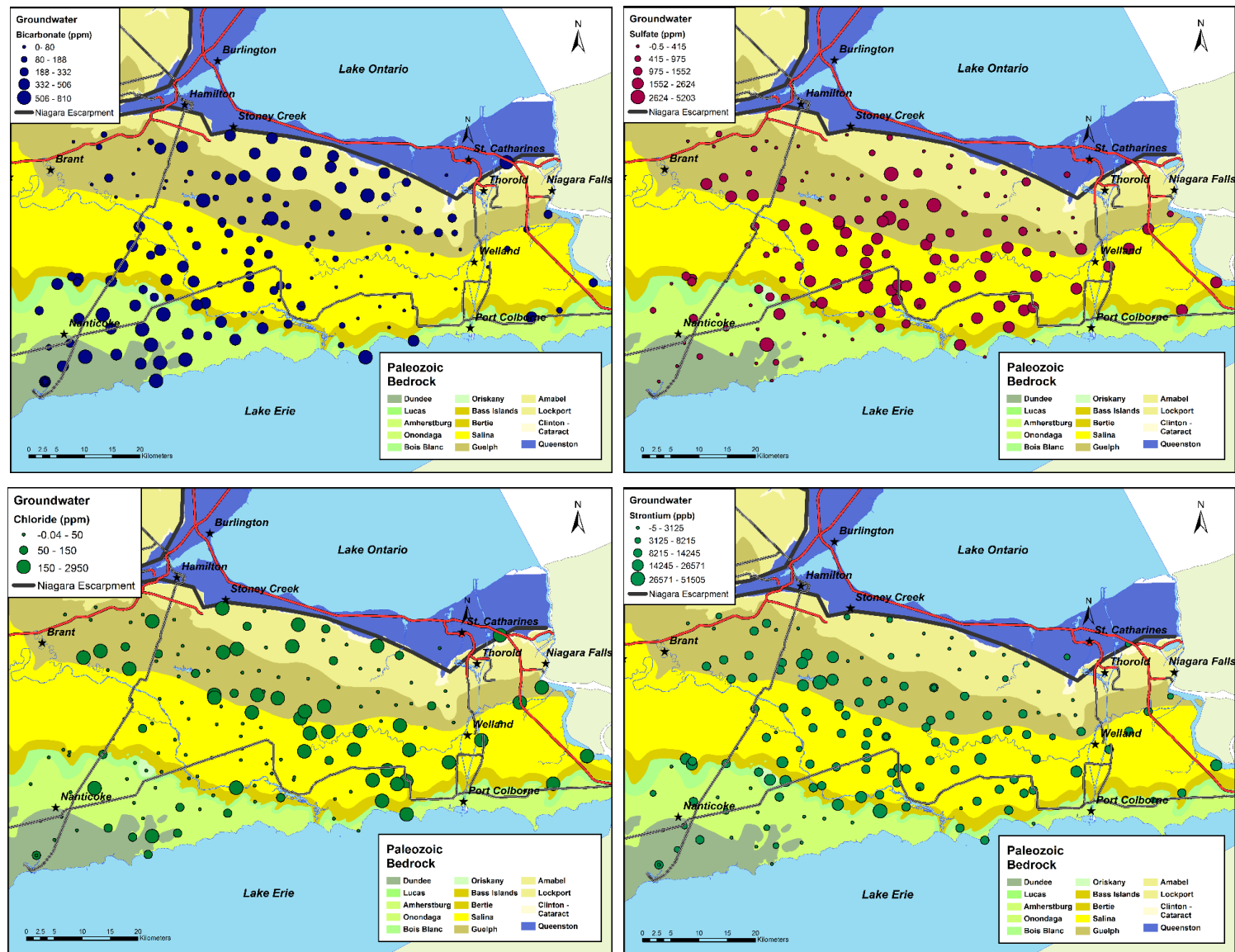


Figure 4.3: Geochemical concentrations of major ions HCO_3^- (ppm), SO_4^{2-} (ppm), Cl^- (ppm) and Sr^{2+} (ppb) from groundwater samples collected in the summer of 2015.

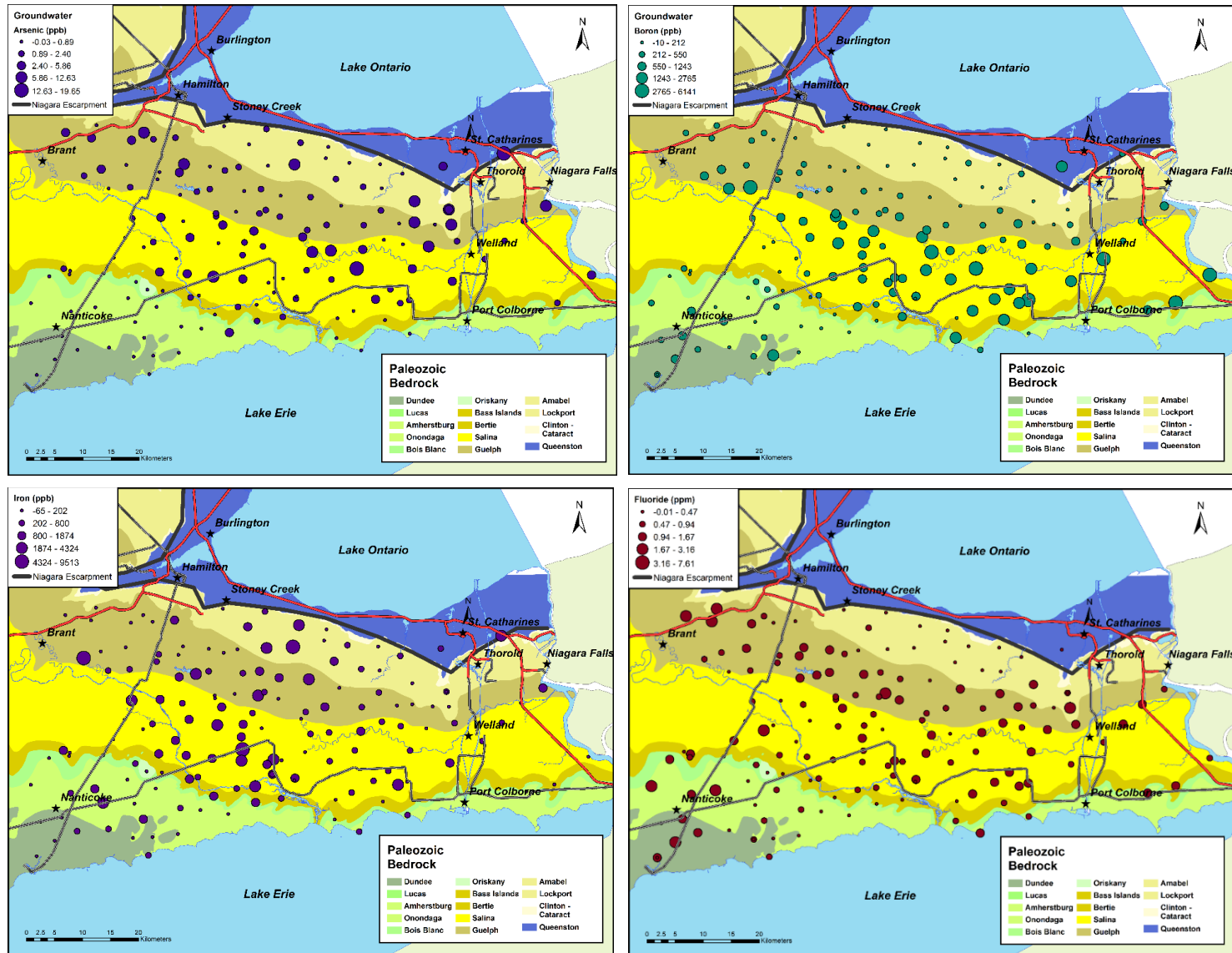


Figure 4.4: Geochemical concentrations of minor constituents As (ppb), B (ppb), Fe (ppb) and F (ppm) from groundwater samples collected in the summer of 2015.

uncharacteristically low for carbonate terrains, suggesting the removal of HCO_3^- through precipitation may be occurring in this area. An almost even distribution of elevated F^- concentrations along the Guelph Formation in Niagara implicates fluoride-bearing minerals (i.e. Fluorite) in the Guelph or Eramosa Formations. Table 4.2 presents the hardness values calculated for all samples using the equation $[\text{CaCO}_3] = 2.5 [\text{Ca}^{2+}] + 4.1 [\text{Mg}^{2+}]$ (in mg/L). As shown in the table, 93% of all samples are classified as ‘very hard water’ (hardness > 180 mg/L). Low HCO_3^- concentrations in the eastern and central Salina and Guelph Formations indicate a significant component of non-carbonate hardness, likely derived from the dissolution of gypsum or anhydrite contributing Ca^{2+} but not HCO_3^- to the groundwater geochemical matrix.

Hardness Scale		Number of Samples	Percentage (%)
0 to 60 mg/L	Soft Water	2	1
60 to 120 mg/L	Moderately Hard Water	4	2
120 to 180 mg/L	Hard Water	6	4
>180 mg/L	Very Hard Water	153	93
Total Number of Samples		165	

Table 4.2: Calculated hardness values for samples collected on the Niagara Peninsula. 93% of samples have very hard water, with hardness values exceeding 180 mg/L as CaCO_3 .

4.2 Regional Groundwater Chemistry Multivariate Statistics

To analyze the large quantity of data collected as a part of this thesis, a multivariate statistical technique, Hierarchical Cluster Analysis (HCA), was used for the determination of correlations between samples. Multivariate statistical techniques provide a method for classifying groundwater samples by composition using input parameters that commonly include major ions and other elements of significance within the groundwater system. Multivariate statistical techniques for geochemical classification allow the user to choose parameters of importance

that may not be represented in more rigid water-classification techniques; or to exclude parameters that may not be geochemically significant. This provides a significant advantage over other geochemical classification techniques such as water-type classifications based on the 6 major ions; HCO_3^- , SO_4^{2-} , Cl^- , Na^+ , Mg^{2+} and Ca^{2+} (Ashley and Lloyd, 1978).

Hierarchical Cluster Analysis (HCA) was used to determine similarities between samples in a population based on multiple parameter linkages. HCA places samples into clusters based on similarities in chemical composition that are represented by linkage distances in multi-dimensional (i.e. multiparameter) space. The greater the linkage distance, the less similarity there is between groups of chemically associated samples to mean and median values of each parameter.

4.2.1 Hierarchical Cluster Analysis (HCA)

A total of 16 parameters were chosen for use in HCA; S^{2-} , Ca^{2+} , Mg^{2+} , K^+ , Na^+ , HCO_3^- , SO_4^{2-} , Cl^- , Br^- , F^- , B , Fe^{2+} , Sr^{2+} , Si^{4+} , DOC and NH_4^+ . These parameters were chosen based on their relative abundance in natural groundwater, and their ability to distinguish biogeochemical reactions and water-rock interaction. The classification of samples into clusters defined using cluster analysis relies on a visual interpretation of the dendrogram. The placement of the phenon line used for cluster subdivision is subjective and based on the interpreter's ability to understand the data. For this dataset, 7 clusters yielded the best subdivision of geochemically distinct groupings, and thus the location of the phenon line was selected at a linkage distance of approximately 11. The locations of the clusters, which are defined as A1-A3 and B1-B4, are shown on the dendrogram in Figure 4.5. These clusters were used in the remainder of this study to subdivide and classify groundwater samples. Placing the phenon line at a linkage distance between approximately 38 and 95 yielded two clusters, referred to as Group A and Group B in this study (Figure 4.5). In Group A, A1 and A2 have a slightly

stronger linkage to one another prior to connection with A3 (Figure 4.5). Group B consists of clusters B1, B2, B3 and B4. B3 and B4 show a strong geochemical relationship demonstrated by their low linkage distance and are separated from the linked clusters B1 and B2 by a linkage distance of approximately 35 (Figure 4.5). The tree diagram (Figure 4.5) indicates that clusters B3 and B4 and clusters B1 and B2 show a similar geochemical signature distinct from the other groupings. The large linkage distance separating Group A and Group B suggests an entirely different geochemical composition for each of the two groups, likely resulting from differences in geological and biogeochemical sources controlling the respective groundwater chemistry.

Table 4.3 presents the median values for geochemical parameters used in HCA for each cluster along with isotopic data, bacterial parameters and selected well data. Lower median values relative to other clusters are underlined, and higher values relative to other clusters are bolded. Elevated total dissolved solids (TDS), SO_4^{2-} , Ca^{2+} , Mg^{2+} , and Cl^- concentrations distinguish Group A from Group B. Mineralized groundwater chemistry in Group A, found primarily in the Salina Group, has groundwater chemistry representative of gypsum dissolution in a carbonate bedrock aquifer under confined conditions. Elevated Enriched Tritium and Cl/Br Ratios in B1 and B3 indicate a potential influence of recent recharge impacted by road salt applications or septic influence. B2 and B4 are less mineralized than Group A, however have average fluoride concentrations approaching the Minimum Acceptable Concentration (MAC) of 1.5 mg/L.

Samples obtained from the Silurian Salina Group almost exclusively consist of the groups A1 and A3 with geochemical facies Ca- SO_4 , except in the westernmost study area, where recent recharge contributes to a geochemical signature characteristic of clusters B1, B4 and A2. The mineralized clusters A1 and A3 have elevated concentrations of S^{2-} , Ca^{2+} , Mg^{2+} , K^+ , Na^+ , SO_4^{2-} , Cl^- , Br^- , Sr^{2+} , NH_4^+ and CH_4 . Groundwaters from A1 and A3 have slightly more isotopically depleted $\delta^{18}\text{O}_{\text{H}_2\text{O}}$ and $\delta^2\text{H}_{\text{H}_2\text{O}}$ signatures than other clusters

suggesting potential influences of old, glacially-mixed groundwaters as well as groundwater influenced by winter precipitation. The source(s) of isotopically depleted groundwater in portions of the study area will be expanded on in the following chapter. The conductivities of A1 and A3 are the highest of any groups, with median values of 3858 $\mu\text{S}/\text{cm}$ and 3466 $\mu\text{S}/\text{cm}$, respectively. Cluster A2 has high concentrations of SO_4^{2-} , however, the presence of significantly higher HCO_3^- concentrations and a higher proportion of Mg- SO_4 geochemical facies differentiates groundwater chemistry (Table 4.3 - 4.4). A2 is characterized by elevated concentrations of Ca^{2+} , Mg^{2+} , K^+ , SO_4^{2-} , Fe^{2+} , Sr^{2+} and Si^{4+} and has an intermediate median conductivity of 2700 $\mu\text{S}/\text{cm}$ relative to other clusters.

In close proximity to the Niagara and Onondaga Escarpments, groundwater samples obtained from Silurian and Devonian carbonate formations under minimal overburden cover have geochemical assemblages reflective of B1 and B3 (see drift thickness, Figure 2.2). B1 and B3 are rich in HCO_3^- and DOC, have high median Cl/Br Ratios and contain NO_3^- and total coliform counts in some samples. Median conductivity values for B1 and B3 groundwaters are 1116 $\mu\text{S}/\text{cm}$ and 1466 $\mu\text{S}/\text{cm}$, respectively. Ca-Mg- HCO_3 water-types represent the highest proportion of samples in B1 and B3, followed by the Ca-Mg- SO_4 geochemical facies (Table 4.4). Groundwater samples classified to clusters B1 and B3 have high tritium and isotopically enriched $\delta^{18}\text{O}_{\text{H}_2\text{O}}$ and $\delta^2\text{H}_{\text{H}_2\text{O}}$ signatures indicating the presence of recent recharge in these waters. Low relative concentrations of S^{2-} , Ca^{2+} , Mg^{2+} , Na^+ , SO_4^{2-} , Br^- , F^- , Sr^{2+} , Fe^{2+} and CH_4 are present in B1 and B3, displaying similar chemistry to cluster B4 present in the Guelph Formation and in the south-western portion of the Niagara Peninsula. B4 has the lowest median conductivity of any group in the study area of 982.5 $\mu\text{S}/\text{cm}$, and a variety of geochemical facies, including Ca- SO_4 , Ca- HCO_3 , Mg- SO_4 and Na- HCO_3 and Na- SO_4 (Table 4.3 - 4.4). Elevated concentrations of F^- , low Cl/Br Ratios and isotopically enriched median $\delta^{34}\text{S}_{\text{SO}_4}$ and $\delta^{18}\text{O}_{\text{SO}_4}$ compositions are the most notable differences between B4 and B1 and B3. B2

appears to be strongly controlled by the bedrock chemistry of the Guelph Formation. Nearly all samples classified in cluster B2 fall within the boundaries of the Guelph Formation from Ancaster in the west to Niagara Falls in the east (Figure 4.6). The predominant geochemical facies of B2 is Ca-SO₄, with groundwater chemistry characterized by high concentrations of Na⁺, S²⁻ and NH₄⁺, low concentrations of K⁺, HCO₃⁻ and DOC and the most alkaline pH values in the study area (Table 4.2 - 4.4). The median conductivity is relatively low at 1647 μS/cm and is reflective of the low TDS (1450 μS/cm).

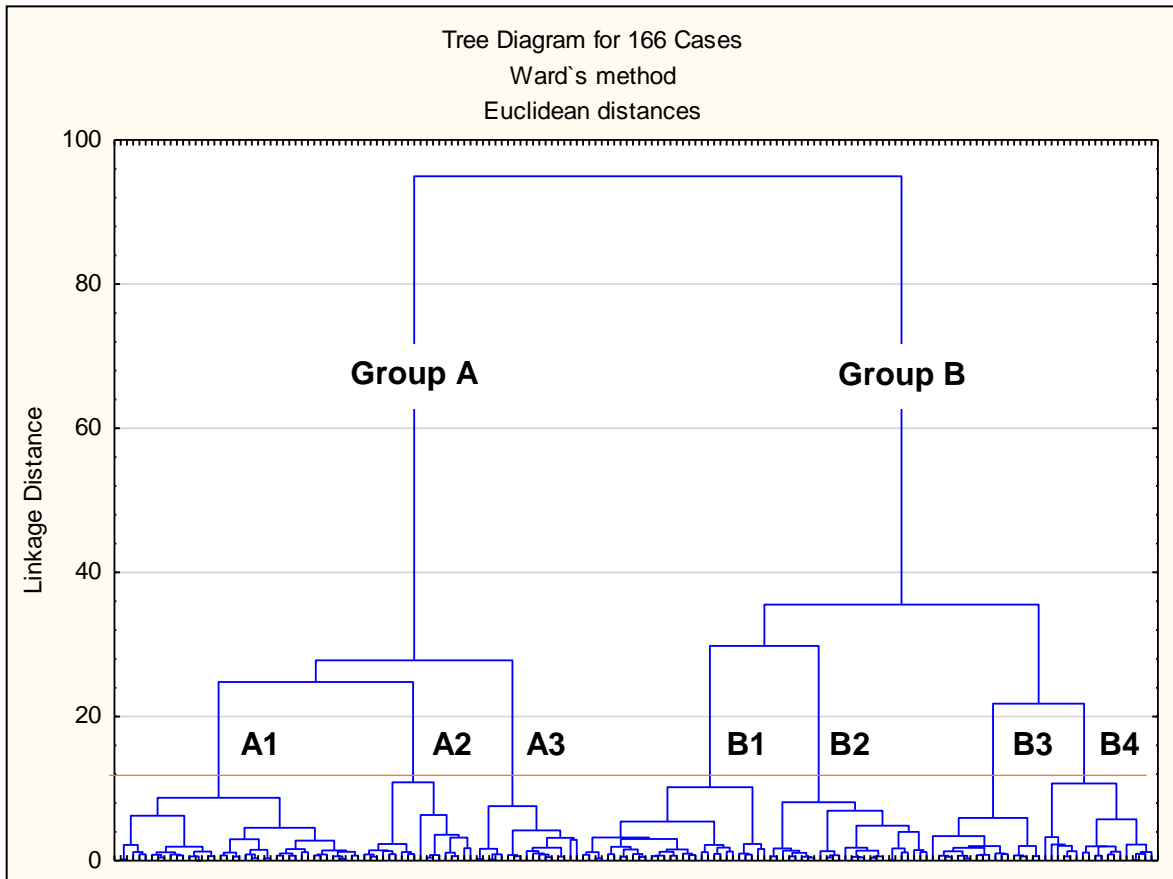


Figure 4.5: Linkage distances between clusters defined using Hierarchical Cluster Analysis (HCA). A linkage distance of 11 was used for subdividing clusters into 7 groupings.

Geochemical Characteristics of each Cluster (median in mg/L)								
Parameter	Unit	A1	A2	A3	B1	B2	B3	B4
Number		38	18	17	30	26	18	18
S ²⁻	mg/L	0.11	0.05	5.25	0.04	0.11	<u>0.01</u>	0.03
Ca ²⁺	mg/L	484	449	502	131	169	<u>116</u>	<u>98.9</u>
Mg ²⁺	mg/L	151	196	150	63.2	67.9	<u>26.4</u>	<u>24.4</u>
K ⁺	mg/L	8.59	7.94	9.45	6.45	<u>5.96</u>	6.88	<u>5.78</u>
Na ⁺	mg/L	168	76.6	125	41.7	101	<u>33.0</u>	46.8
HCO ₃ ⁻	mg/L	<u>79.0</u>	441	201	446	<u>124</u>	354	221
SO ₄ ²⁻	mg/L	2100	1810	1830	<u>296</u>	812	<u>115</u>	<u>225</u>
Cl ⁻	mg/L	43.3	27.6	283	60.1	24.9	30.4	<u>12.9</u>
Br	mg/L	0.53	0.18	2.01	0.10	0.27	0.07	<u>0.06</u>
F ⁻	mg/L	0.84	0.53	0.70	<u>0.36</u>	0.88	<u>0.29</u>	1.28
B	mg/L	1.15	0.24	0.82	<u>0.08</u>	0.41	<u>0.08</u>	0.31
Fe ²⁺	mg/L	0.77	1.12	<u>-0.07</u>	0.61	0.34	<u>-0.07</u>	0.61
Sr ²⁺	mg/L	10.9	10.8	11.4	<u>2.05</u>	9.51	<u>1.64</u>	7.94
Si ⁴⁺	mg/L	4.95	6.62	4.82	4.92	4.55	<u>0.00</u>	3.54
DOC	mg/L	1.60	2.75	2.00	2.55	<u>1.50</u>	3.10	1.80
NH ₄ ⁺	mg/L	0.55	0.23	0.57	0.20	0.27	<u>0.08</u>	0.17

Isotopic, Gaseous and Field Parameter Characteristics of each Cluster								
Parameter	Unit	A1	A2	A3	B1	B2	B3	B4
Tritium	TU	<u>0.82</u>	4.74	2.32	11.3	1.34	11.6	<u>0.42</u>
18O_H2O	‰	<u>-10.4</u>	-9.98	<u>-10.4</u>	-9.84	<u>-10.4</u>	-9.73	-10.1
2H_H2O	‰	<u>-69.0</u>	-64.7	<u>-68.3</u>	-64.2	<u>-69.1</u>	-64.2	-65.7
18O_SO4	‰	12.1	10.2	12.5	8.97	11.4	<u>7.60</u>	12.9
34S_SO4	‰	25.4	16.8	26.0	<u>11.6</u>	21.2	15.5	25.5
34S_S2	‰	21.9	3.50	4.40	<u>-11.7</u>	-0.78	<u>-9.25</u>	-8.18
13C_CH4	‰	-34.4		-37.5	<u>-65.7</u>	-39.7	<u>-64.5</u>	<u>-63.6</u>
13C_DIC	‰	-9.54	-13.2	-12.8	<u>-14.2</u>	-9.82	<u>-14.6</u>	-11.5
13C_DOC	‰	-27.1	-26.7	<u>-27.6</u>	-27.0	-26.6	<u>-27.3</u>	-26.5
pH		7.42	<u>6.80</u>	7.01	<u>6.94</u>	7.63	7.05	7.17
Temp	°C	11.1	10.9	11.1	11.0	11.1	<u>10.7</u>	10.8
DO	%	0.00	0.00	0.00	0.00	0.00	0.00	0.00
CO2	%_sat	<u>0.04</u>	1.58	0.22	1.06	<u>0.05</u>	0.76	0.11
CH4	%_sat	1.92	<u>0.46</u>	2.73	<u>0.34</u>	0.91	<u>0.45</u>	0.56
NO3	mg/L	-0.006	-0.006	-0.006	0.0005	-0.006	0.25	-0.006
Coliforms (T)	Count	1	<u>0</u>	1	1	<u>0</u>	7	1
Cl/Br Ratio		<u>205</u>	310	216	1160	<u>203</u>	709	<u>158</u>
Cl/Br Ratio (mass)		<u>91.2</u>	138	95.6	448	<u>87.6</u>	315	<u>63.4</u>
Well depth	ft	91.0	49.1	81.2	<u>44.5</u>	83.5	<u>46.5</u>	90.5
Drift Thickness	M	78.0	33.5	62.0	<u>21.0</u>	77.4	<u>25.0</u>	67.5
TDS	mg/L	3350	2500	3150	1200	1450	900	<u>800</u>

Table 4.3: Median geochemical concentrations and isotopic values for each cluster. High concentrations/ values are bolded, and low concentrations and/or values are underlined.

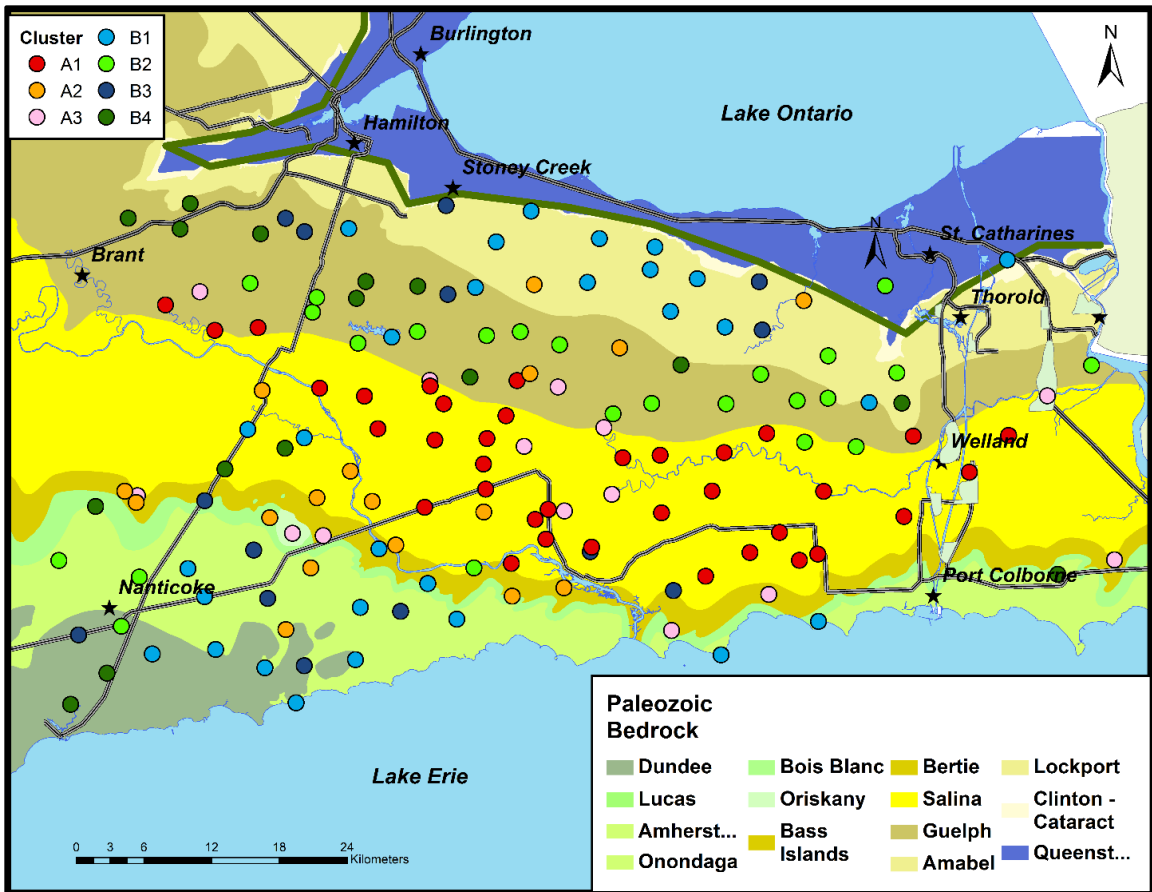


Figure 4.6: Spatial location of geochemical clusters defined by HCA.

Cluster	Ca-HCO ₃	Ca-SO ₄	Ca-Cl	Mg-HCO ₃	Mg-SO ₄	Mg-Cl	Na-HCO ₃	Na-SO ₄	Na-Cl
A1		34	1						3
A2		11			7				
A3		16	1						
B1	10	8	1	5	5	1			
B2	1	17		3	1			2	2
B3	8	5		1	1		2		1
B4	3	6			2		4	3	

Table 4.4: Correlation of cluster grouping and Water-Types defined using AquaChem software.

4.3 Groundwater Chemistry of Clusters

HCA is a powerful data classification method used for understanding regional variations and trends in a large dataset. With the defined clusters in mind, the traditional geochemical facies and major ion geochemistry of groundwater samples collected on the Niagara Peninsula will be presented.

Figure 4.7 illustrates the spatial location of groundwater samples classified to each geochemical facies. The Ca-SO₄ geochemical facies is the predominant water-type in samples collected from the Salina trough bedrock low located in the Salina and Guelph Formations. Secondary geochemical facies characterizing groundwater chemistry include Ca-Cl in the Salina Group, and Mg-SO₄, Ca-HCO₃, Mg-SO₄ and Mg-HCO₃ groundwater in the Guelph Formation.

Groundwater samples collected in the northern and southwestern Niagara Peninsula have a mixed geochemical signature, with the presence of several geochemical facies including Ca-HCO₃, Mg-HCO₃, Ca-SO₄ and Mg-SO₄.

The difference in chemical composition between Group A and Group B is illustrated in two separate piper plots (Figure 4.8). Group A shows less chemical variability than Group B and is dominantly characterized by Ca-Mg-SO₄ groundwater compositions. With the exception of some samples in A2, all samples in Group A have very low HCO₃⁻ in proportion to the total anion proportion. Groundwater samples in A1 and A3 have a higher Cl⁻ composition, whereas samples from A2 have a higher proportion of HCO₃⁻. The cation abundances indicate a higher proportion of Mg²⁺ in A2, and a relatively higher proportion of Na⁺ in A1 and A3. Groundwaters from Group B appear to be geochemically mixed, with high anion abundances of HCO₃⁻ and SO₄²⁻, and high cation abundances of Ca²⁺ and Mg²⁺. Many samples fall near the middle of the tri-linear diagrams for both cations and anions, showing more equal abundances of the major ions. Box-plots of major ions, trace elements, pH and TDS illustrate differences in concentrations of parameters between major groups, as well as

between clusters (Figure 4.9 and 4.10). The range of concentrations for each parameter in each cluster is represented by the minimum and maximum values (ie. whiskers) and the blue boxes, representing the 25th to 75th percentile. Figure 4.11 shows the proportion of each geochemical facies that comprise the 7 clusters defined using HCA. In Group A (A1, A2 and A3) Ca-SO₄ groundwater dominates with a secondary component of high salinity groundwater (Na-Cl and Ca-Cl facies) in groups A1 and A3, and Mg-SO₄ groundwater in group A2. Group B (B1, B2, B3, B4) has a higher proportion of Ca-HCO₃ groundwater, with secondary components of Ca-SO₄ groundwater present in clusters B2 and B4. Group B has greater variability of groundwater types than Group A, with geochemical facies Ca-Cl, Mg-HCO₃, Mg-SO₄, Mg-Cl, Na-HCO₃, Na-SO₄ and Na-Cl all comprising a minor proportion of samples in 1 or more clusters.

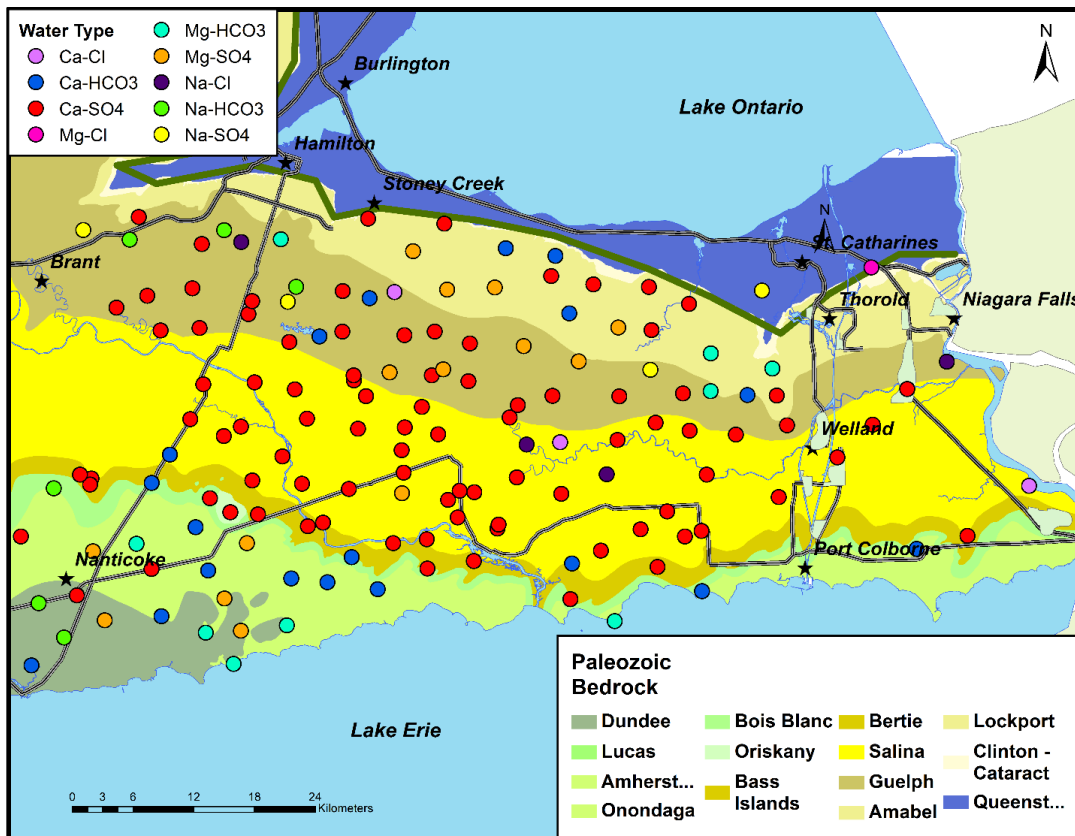
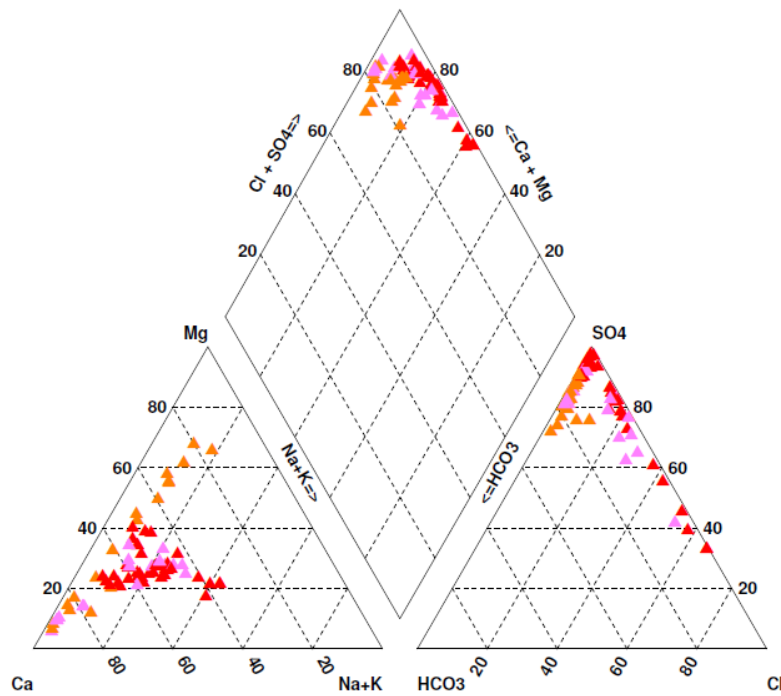


Figure 4.7: Water type spatial distribution in the study area.

Group A



Group B

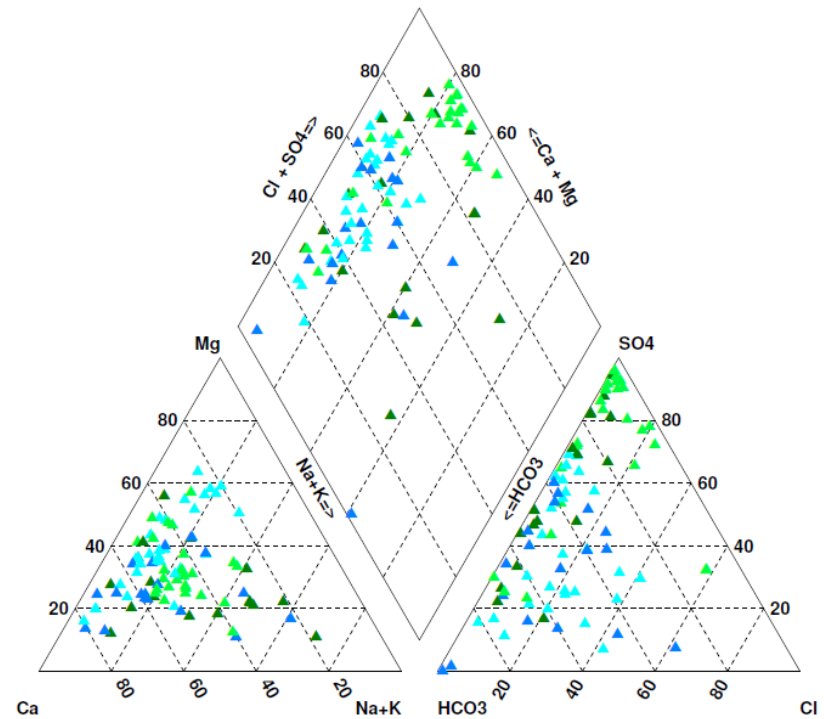


Figure 4.8: (a) Piper Tri-Linear Diagrams for Group A (Clusters A1, A2 and A3) and Group B (Clusters B1, B2, B3 and B4) defined using HCA.

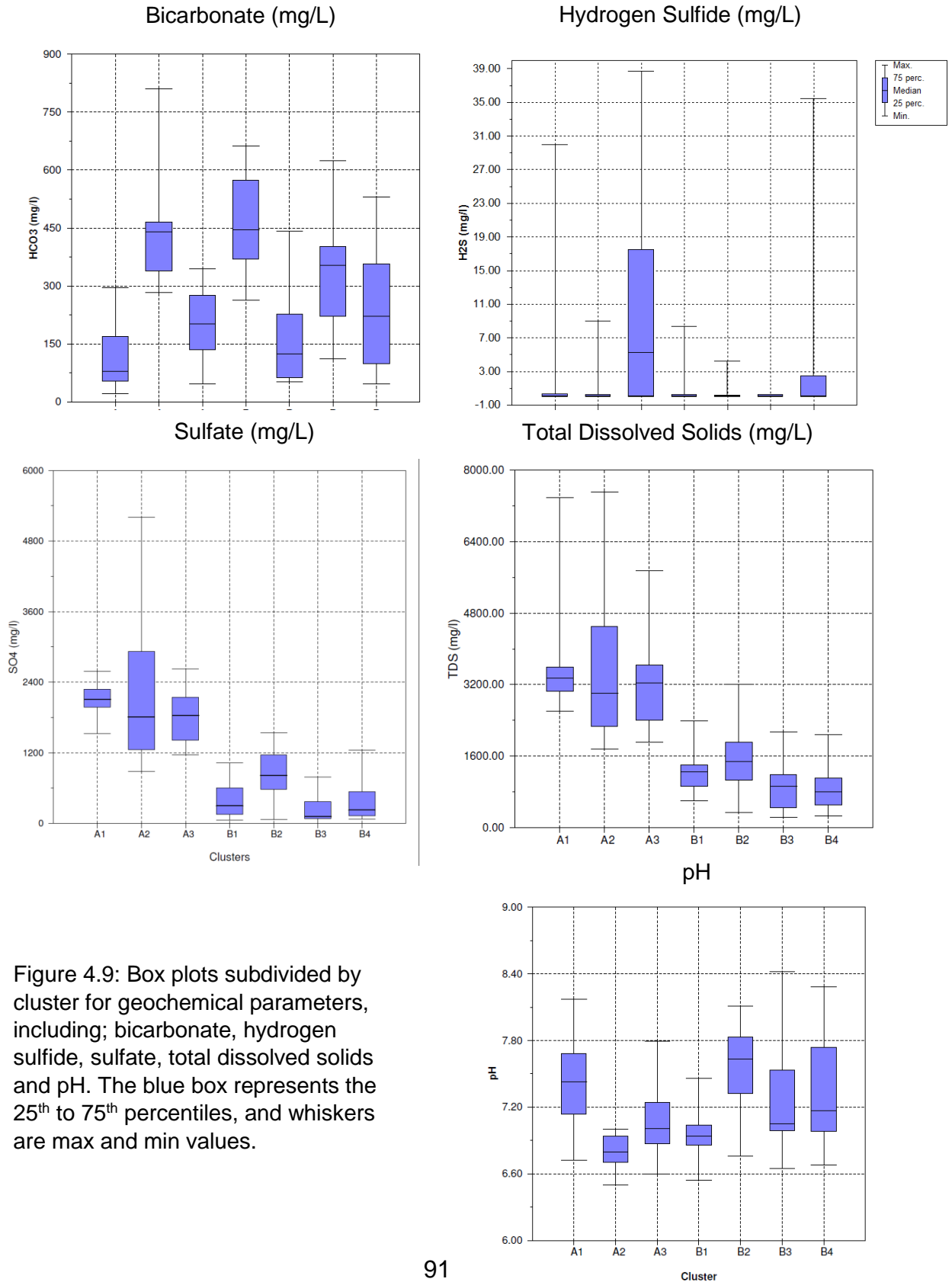


Figure 4.9: Box plots subdivided by cluster for geochemical parameters, including; bicarbonate, hydrogen sulfide, sulfate, total dissolved solids and pH. The blue box represents the 25th to 75th percentiles, and whiskers are max and min values.

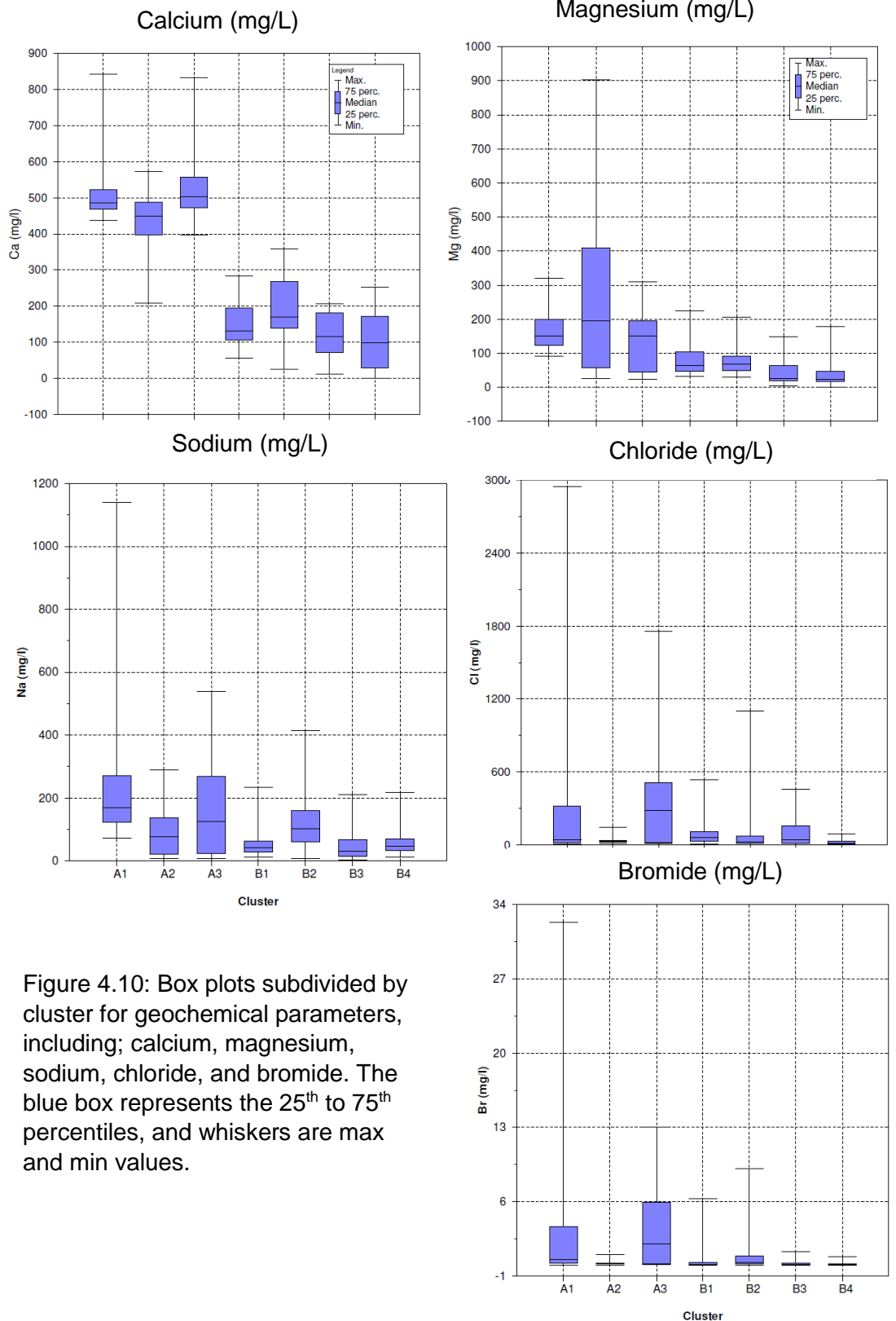


Figure 4.10: Box plots subdivided by cluster for geochemical parameters, including; calcium, magnesium, sodium, chloride, and bromide. The blue box represents the 25th to 75th percentiles, and whiskers are max and min values.

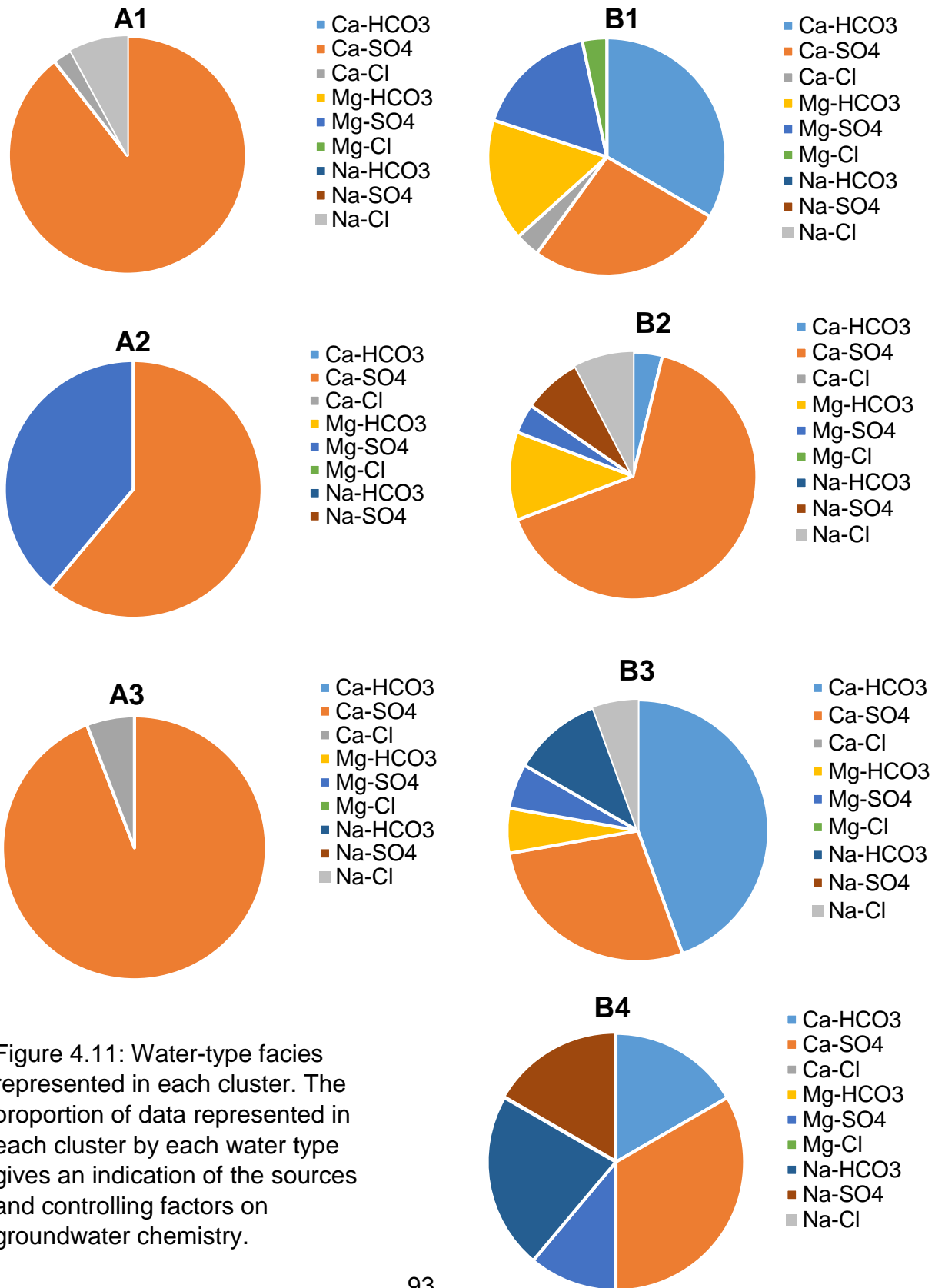


Figure 4.11: Water-type facies represented in each cluster. The proportion of data represented in each cluster by each water type gives an indication of the sources and controlling factors on groundwater chemistry.

4.3.1 Saturation Indices

Saturation Indices were calculated using PHREEQC modelling in Aquachem software for all groundwater samples using the pH, major ion concentrations, total dissolved solids, and water temperature of each sample. The Saturation Index is an indicator of the degree of saturation of the respective mineral in water. A positive Saturation Index ($SI > 0$) is indicative of supersaturation; resulting in the precipitation of the mineral out of solution. Samples with a negative Saturation Index are undersaturated with regard to the mineral ($SI < 0$), and may result in corrosion of the plumbing systems in water wells. Samples with a Saturation Index near 0 are saturated, and are neither precipitating out of solution or dissolving into solution.

Box and Whisker plots for saturation indices of minerals commonly associated with carbonate groundwaters are given in Figure 4.12 for each cluster. From Figure 4.12, it is apparent that sulfate minerals, specifically gypsum and anhydrite, approach saturation for groundwater samples obtained from A1 and A3. Nearly 50 % of samples in A1 and A3 are at saturation or supersaturated with respect to calcite, indicating calcite precipitation is prominent in the Salina Trough region of the Niagara Peninsula. Spatial plots of saturation indices for calcite, dolomite and gypsum (Figures 4.13 – 4.14) show samples at saturation with respect to calcite located in the Salina Trough, as well as the south-western portion of the Peninsula. Fewer samples in the Salina Trough reach dolomite saturation, likely due to the influence of dedolomitization occurring from the dissolution of gypsum and subsequent dissolution of dolomite. Samples undersaturated for calcite and dolomite are found in the Lockport Formation and Dundee Formation.

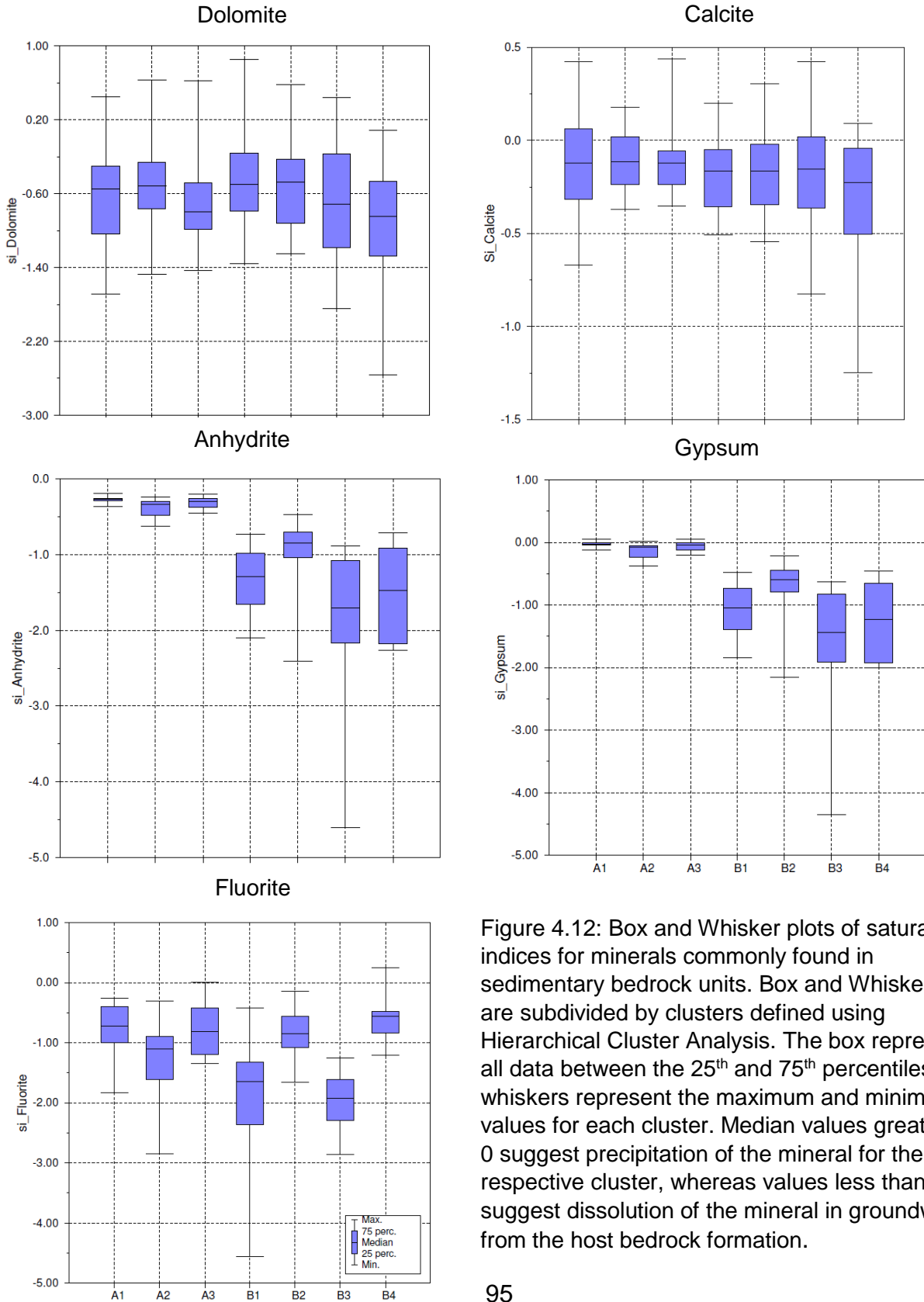


Figure 4.12: Box and Whisker plots of saturation indices for minerals commonly found in sedimentary bedrock units. Box and Whisker plots are subdivided by clusters defined using Hierarchical Cluster Analysis. The box represents all data between the 25th and 75th percentiles, and whiskers represent the maximum and minimum values for each cluster. Median values greater than 0 suggest precipitation of the mineral for the respective cluster, whereas values less than 0 suggest dissolution of the mineral in groundwater from the host bedrock formation.

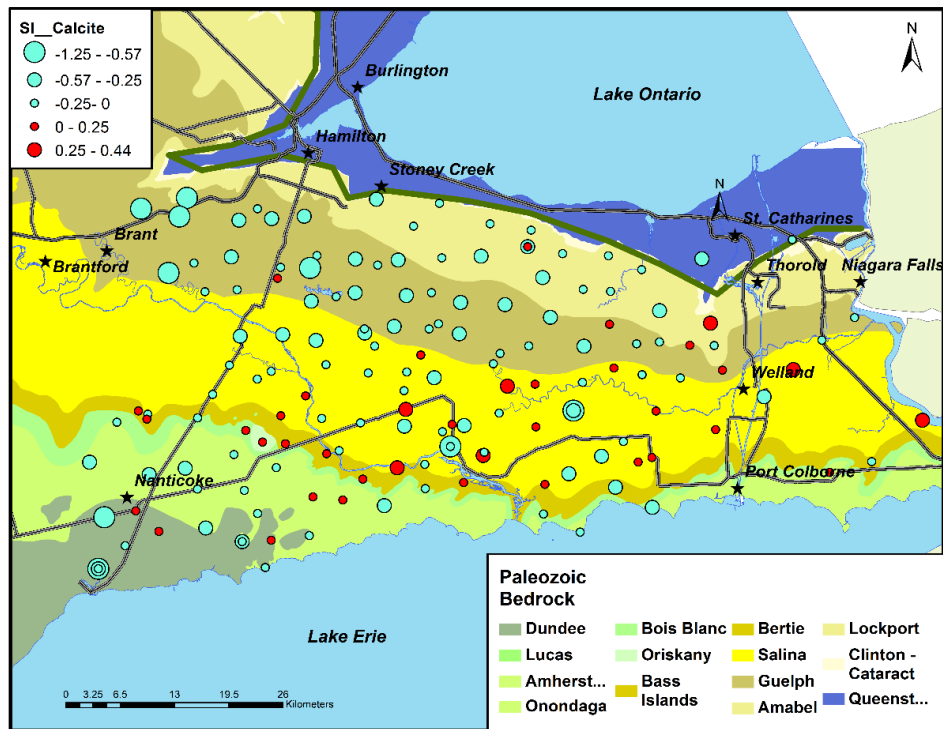
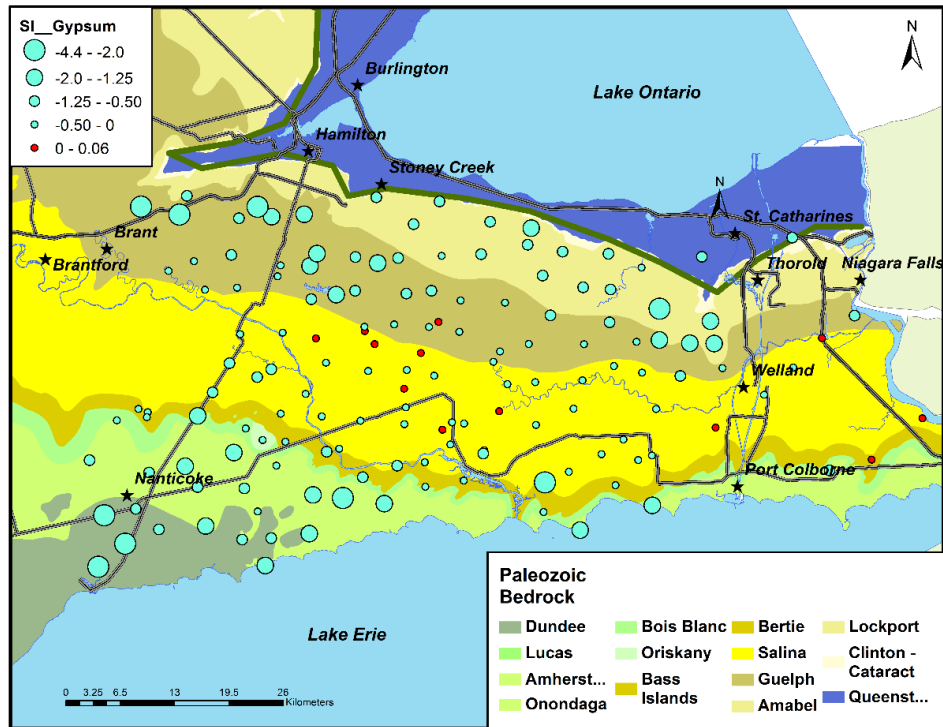


Figure 4.13: Spatial distribution of saturation indices of Gypsum and Calcite calculated using PHREEQC modelling in Aquachem software. Blue circles represent undersaturation and red circles represent supersaturation

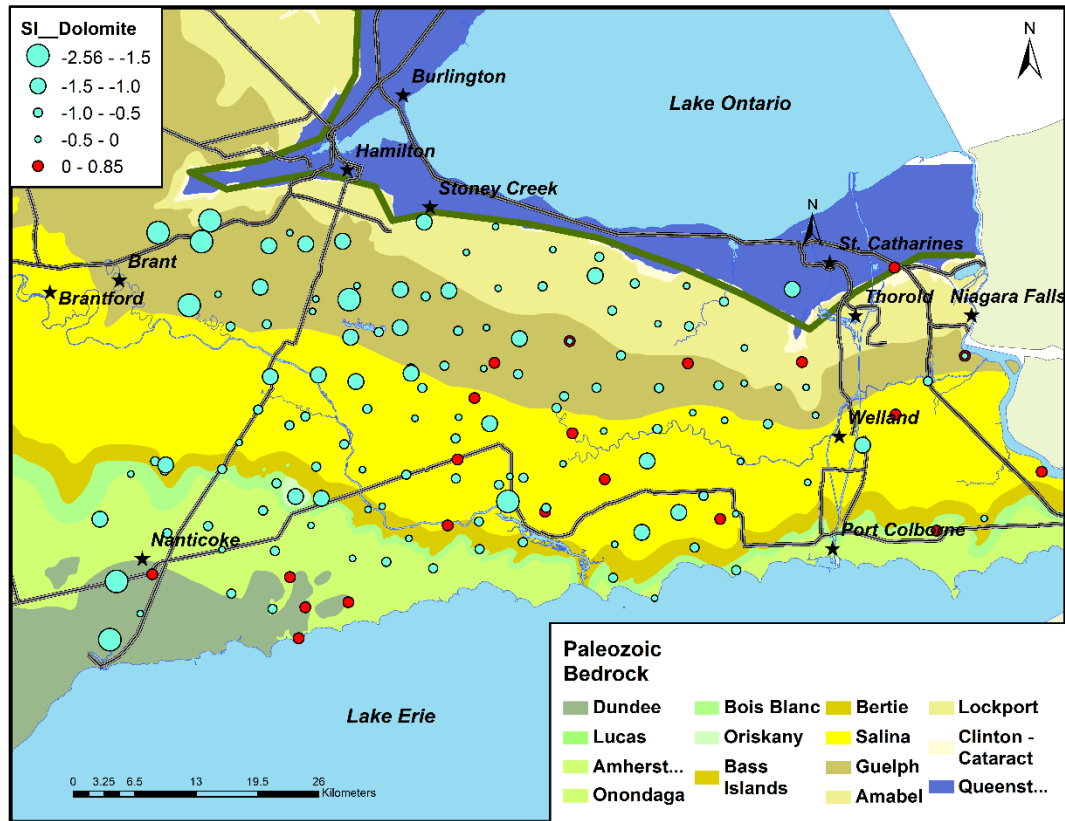


Figure 4.14: Spatial distribution of the saturation index of Dolomite calculated using PHREEQC modelling in Aquachem software. Blue circles represent undersaturation (i.e. dissolution) and red circles represent supersaturation (i.e. precipitation).

4.3.2 Chloride-Bromide Ratios

When Cl/Br Ratios are used in conjunction with other geochemical indicators, including associations with other chemical constituents, isotopic evidence and Na/K ratios used for the differentiation between septic and animal waste (Katz et al., 2011), the identification of septic influence on groundwater can be discerned.

For this study, we will use the Cl/Br Ratio mixing lines constructed by Katz et al. (2011), who compiled historical Cl/Br data from a large number of samples from monitoring and domestic groundwater wells in the United States. The Dilute Groundwater (DG) – Appalachian Basin Brine (ABB) mixing line plotted on Figure 4.15 was created by averaging the Cl/Br ratios for four waters from the Niagara

Peninsula listed in the Oil and Gas Well geochemical database (Skuce et al., 2014).

The distribution of data from the Niagara Peninsula organized by cluster is plotted on Figure 4.15. Cl/Br ratios are plotted by mass on the y-axis, and the chloride concentration is plotted in mg/L on the x-axis. The lines, boxes and circles on the chart represent the various Cl/Br mixing lines for sources labelled on the diagram. As shown on Figure 4.15, most samples within Group A on Niagara Peninsula fall along the DW - ABB mixing line, with chloride concentrations greater than 10 mg/L. Low chloride concentrations ($\text{Cl}^- < 10 \text{ mg/L}$) along this line can be attributed to recent recharge of local precipitation. The appearance of low Cl/Br Ratios correlating with high Cl^- concentrations is rare in southwestern Ontario, elsewhere only occurring in Ordovician Shales outside of the study area (S. Hamilton, personal comm., 2015), although the presence of samples falling along the dilute groundwater – ABB mixing line is commonly found in Ordovician – Devonian shallow carbonate aquifers in New York and Pennsylvania (Warner et al., 2012; Llewellyn, 2014; Johnston et al., 2015) and in the carbonate rock aquifer in southern Manitoba (Grasby and Betcher, 2002) . Although some samples from all clusters fall on the DG - ABB mixing line, A1 and A3 have the largest proportion of samples with high chloride concentrations on the line.

Samples located within the black box on Figure 4.15 represent samples with Cl/Br Ratios indicative of septic waste, or agricultural applications. The grey line represents the theoretical mixing trend between dilute groundwater and septic waste. A large proportion of samples from B1 and B3 are located along the septic waste mixing line and a few samples from A2. A number of samples follow the Dilute Groundwater (DG) – Halite mixing line, marked in orange. A few samples fall in an area overlapping with the range identified for septic waste or fall slightly below the DG - Halite mixing line. Samples within the overlapping range may contain chloride from softener systems discharged into septic waste or are mixed

samples with origins from road salt, fertilizer application and septic systems. Similarly, it is difficult to discern the influences in the cloud of samples with Cl between 10 and 100 mg/L that fall in the area between the DG - ABB and septic mixing lines. As the Niagara Peninsula is located inland from the coast by several hundred kilometres, it is unlikely that seawater influences groundwater composition here, despite some sample falling on the seawater mixing line. More likely, waters falling within this range are mixed samples, with an ABB component and a component influenced by recent recharge or anthropogenic contamination.

Samples falling along the DG – ABB mixing line are located primarily in the central and eastern Salina Group and Bass Islands Formation and the southern half of the Guelph Formation near the contact with the Salina Group. There are also a number that occur near Lake Erie in the Devonian Onondaga and Dundee Formations. Septic and halite signatures are seen in the northern and southwestern parts of the Peninsula where there is minimal glacial overburden capping the bedrock and interface aquifers. The dilute groundwater signature is primarily seen in the central and northern reaches of the Guelph Formation.

4.4 Stable Isotope Geochemistry

This section presents the isotope geochemistry for stable isotopes $\delta^{18}\text{O}$ and $\delta^2\text{H}$ of water, $\delta^{18}\text{O}$ and $\delta^{34}\text{S}$ of sulfate, and $\delta^{13}\text{C}$ of dissolved organic carbon, dissolved inorganic carbon and methane for samples collected in this study. Results of enriched tritium analysis will be presented in conjunction with water isotope data. A complete database of isotopic results for each sample is presented in the appendix.

4.4.1 Oxygen and Hydrogen Isotopes and Tritium of Water

The oxygen and hydrogen isotopic compositions ($\delta^{18}\text{O}_{\text{H}_2\text{O}}$ and $\delta^2\text{H}_{\text{H}_2\text{O}}$) of groundwater samples are reported in permil (‰) relative to the Vienna Standard Mean Ocean Water (vSMOW) protocol and presented below (Figure 4.16)

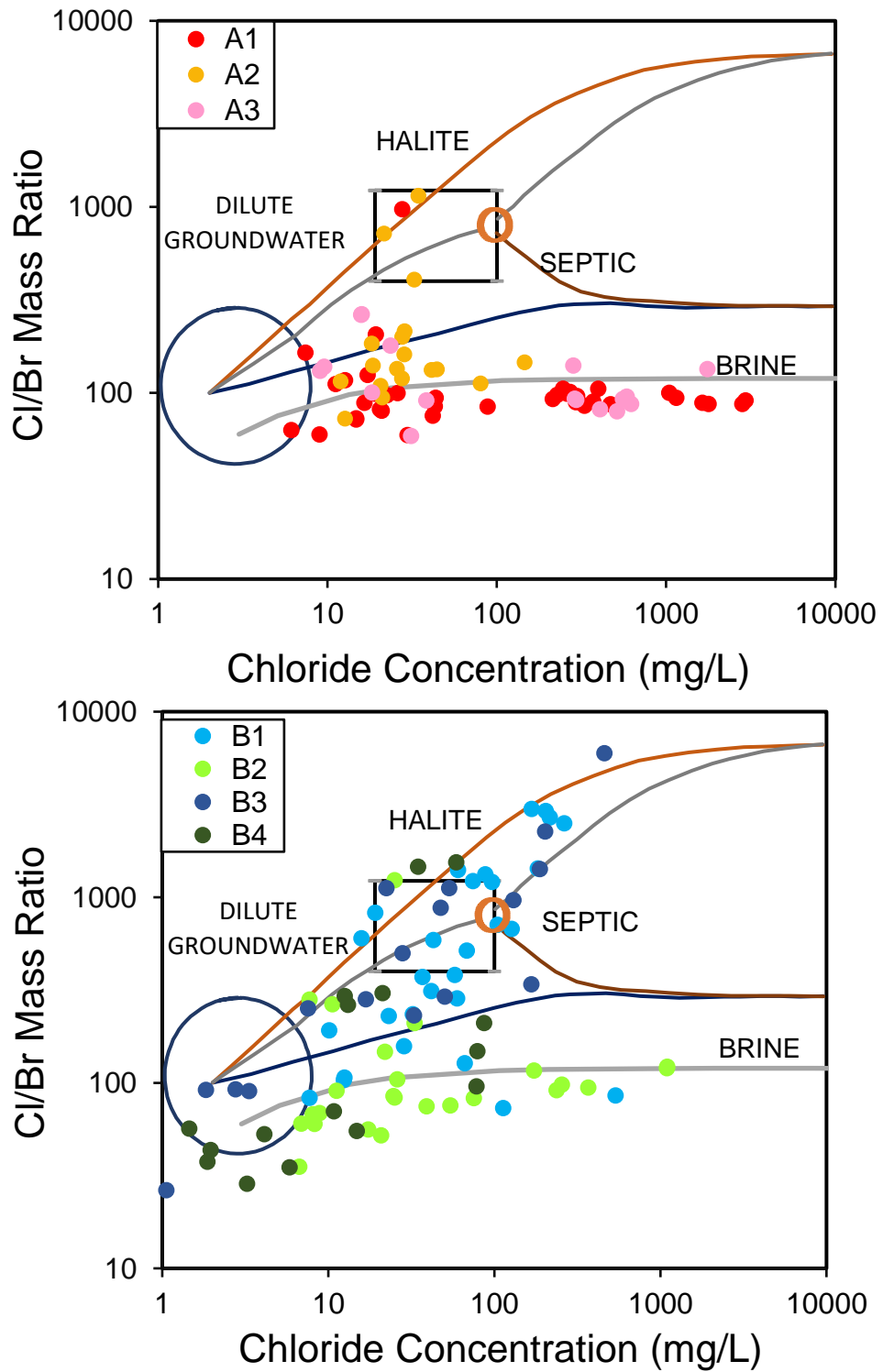


Figure 4.15: Cl/Br Mass Ratio plot for cluster subdivisions in Group A (a) and Group B (b). Samples falling along lines or within shapes on the plot represent a classification based on source (lines and Cl/Br regions are from Katz et al. 2011).

with the Global Meteoric Water Line (GMWL) ($\delta^2\text{H} = 8 [\delta^{18}\text{O}] + 10$; Craig, 1961) and Great Lakes Meteoric Water Line (GLMWL) ($\delta^2\text{H} = 7.1 [\delta^{18}\text{O}] + 1.0$; Longstaffe et al., 2011). Local precipitation data are presented from the International Atomic Energy Agency (IAEA) monitoring location in Simcoe, Ontario, located 8.5 km west of the southwestern boundary of the study area (IAEA, 2011). Based on this dataset, average monthly oxygen and hydrogen isotopic compositions for the winter months (October to March) from 1975 to 1982 were observed to be within the ranges of -29.8 to -8.3 ‰ for $\delta^{18}\text{O}_{\text{H}_2\text{O}}$ and -192 to -50 ‰ for $\delta^2\text{H}_{\text{H}_2\text{O}}$. Corresponding data for the summer months (April to September) in those years ranged from -13.5 to -1.6 ‰ for $\delta^{18}\text{O}_{\text{H}_2\text{O}}$ and -95 to -9 ‰ for $\delta^2\text{H}_{\text{H}_2\text{O}}$. The trend to isotopically depleted values during the winter months reflects the seasonal variation in temperature and therefore the $\delta^{18}\text{O}_{\text{H}_2\text{O}}$ and $\delta^2\text{D}_{\text{H}_2\text{O}}$ of precipitation in temperate, continental climates (Clark, 2015).

Simcoe has a Local Meteoric Water Line (LMWL) of; $\delta^2\text{H} = 7.8 [\delta^{18}\text{O}] + 9.4$, a Winter Local Meteoric Water Line (WLMWL) of $\delta^2\text{H} = 8.4 [\delta^{18}\text{O}] + 18.2$, and a Summer Local Meteoric Water Line (SLMWL) of $\delta^2\text{H} = 7.5 [\delta^{18}\text{O}] + 6.3$. The LMWL for Simcoe, ON is remarkably close to the GMWL, which is plotted in Figure 4.16 relative to all data samples organized by clusters defined using HCA.

The strong deuterium excess of 18.2‰ exhibited in the Winter Local Meteoric Water Line is typical of precipitation derived from a source with low humidity and is almost twice the average global deuterium excess of 10‰ formed under average humidity of 85% (Clark, 2015). The Niagara Peninsula is located between Lakes Erie and Ontario, two of the World's largest freshwater lakes and which commonly contribute to lake effect snowfall in southern Ontario. It is likely that winter precipitation on the Niagara Peninsula is partially derived from lake effect snow from Lake Erie to the south and southwest and less so from Lake Ontario to the north and northeast.

The $\delta^{18}\text{O}$ and $\delta^2\text{H}$ isotopic compositions for groundwater samples fall within the range of -15.6 ‰ to -8.2 ‰, and -107.1 ‰ to -56.9 ‰, respectively (Figure 4.17). The most isotopically depleted value for $\delta^{18}\text{O}$ is -15.6 ‰ and was obtained from the Salina Group. The deuterium excess for groundwater samples obtained on the Niagara Peninsula ranges from 5.1 to 18.1, with an average value of 14.8 (Figure 4.18), which is indicative of a component of lake-effect snow and/or glacial-aged water.

Depleted isotopic compositions may include a component of glacial meltwater as the most negative values approach the estimate range for Pleistocene water (<-15 ‰, Hamilton et al., 2015; MacIntosh and Walter, 2006; Husain et al., 2004; Clayton et al., 1966). High conductivity values ($\mu\text{S}/\text{cm}$) observed in $\delta^{18}\text{O}$ depleted groundwater (Figure 4.19) suggests the presence of stagnant, glacial-aged groundwater with a highly mineralized character. The highest value for $\delta^{18}\text{O}$ (-8.2 ‰) in the study area occurred from sample 15-AG-008, obtained from a quarry spring in the Dundee Formation.

Enriched tritium (E^3H) for groundwater samples range from below the detection limit (<0.8) to 30.15 TU. Two zones of elevated tritium concentrations occur on the Niagara Peninsula along the Niagara and Onondaga Escarpments (Figure 4.20). These bedrock topographic highs are groundwater recharge areas for bedrock flow systems on the Peninsula and are subject to recent recharge (Hamilton, 2015). Areas in the Niagara Peninsula showing high enriched tritium also show enriched $\delta^{18}\text{O}$ signatures (Figure 4.21). Average enriched tritium, $\delta^{18}\text{O}$ and $\delta^2\text{H}$ isotopic compositions are given for each cluster in Table 4.5. B1 and B3 have the highest tritium concentrations and the most enriched $\delta^{18}\text{O}$ signatures, suggesting modern recharge dominates water chemistry. The presence of a large component of winter-derived precipitation and/or older waters precipitated under cold-climate conditions is supported for A1 and A3, as they are the most isotopically depleted in $\delta^{18}\text{O}$ with low enriched tritium values.

Although the average $\delta^{18}\text{O}$ values for A1 (-11.16 ‰) and A3 (-11.05 ‰) are within the range of modern precipitation, a localized region of isotopically depleted $\delta^{18}\text{O}$ and $\delta^2\text{H}$ signatures in the central Wainfleet region (Figure 4.17) and potentiometric surfaces similar to groundwater residing under thick clay Lake Erie bottom sediments may show influence of the migration of Pleistocene-aged groundwater inland.

Cluster		E^3H	$\delta^{18}\text{O}$	$\delta^2\text{H}$
A1		0.8	-11.2	-73.8
A2		6.2	-10.0	-64.8
A3		4.6	-11.1	-73.0
B1		10.6	-9.9	-64.5
B2		1.6	-10.6	-69.8
B3		11.5	-9.8	-65.1
B4		4.0	-10.2	-67.1

Table 4.5: Average enriched tritium (E^3H , in TU), $\delta^{18}\text{O}_{\text{H}_2\text{O}}$ and $\delta^2\text{H}_{\text{H}_2\text{O}}$ for each HCA Cluster.

4.4.2 Sulfur Isotopes

Sulfur isotopic compositions are useful for the determination of the origin of sulphur-bearing species in groundwater and for insight into biogeochemical reactions where sulfur-mediating bacteria and sulphur minerals are present. Sulfur ($\delta^{34}\text{S}_{\text{SO}_4}$) and oxygen ($\delta^{18}\text{O}_{\text{SO}_4}$) isotopic compositions of sulfate were measured for all groundwater samples, and sulfide isotopic composition ($\delta^{34}\text{S}_{\text{S}_2}$) were measured for all samples with sulfide concentrations greater than 0.3 mg/L (Figure 4.22). The isotopic compositions of $\delta^{34}\text{S}_{\text{SO}_4}$ and $\delta^{18}\text{O}_{\text{SO}_4}$ on the Niagara Peninsula range from -3.3 to 45.1 ‰ and -5.5 to 18.4 ‰, respectively. $\delta^{34}\text{S}_{\text{SO}_4}$ and $\delta^{18}\text{O}_{\text{SO}_4}$ have a positive correlation and are approximately linear in the central part of their range but the data become more spaced out in the more isotopically enriched and depleted parts of the range (Figure 4.23). The spatial distributions of $\delta^{34}\text{S}_{\text{SO}_4}$, $\delta^{18}\text{O}_{\text{SO}_4}$ and $\delta^{34}\text{S}_{\text{S}_2}$ are given in Figures 4.24 and 4.25.

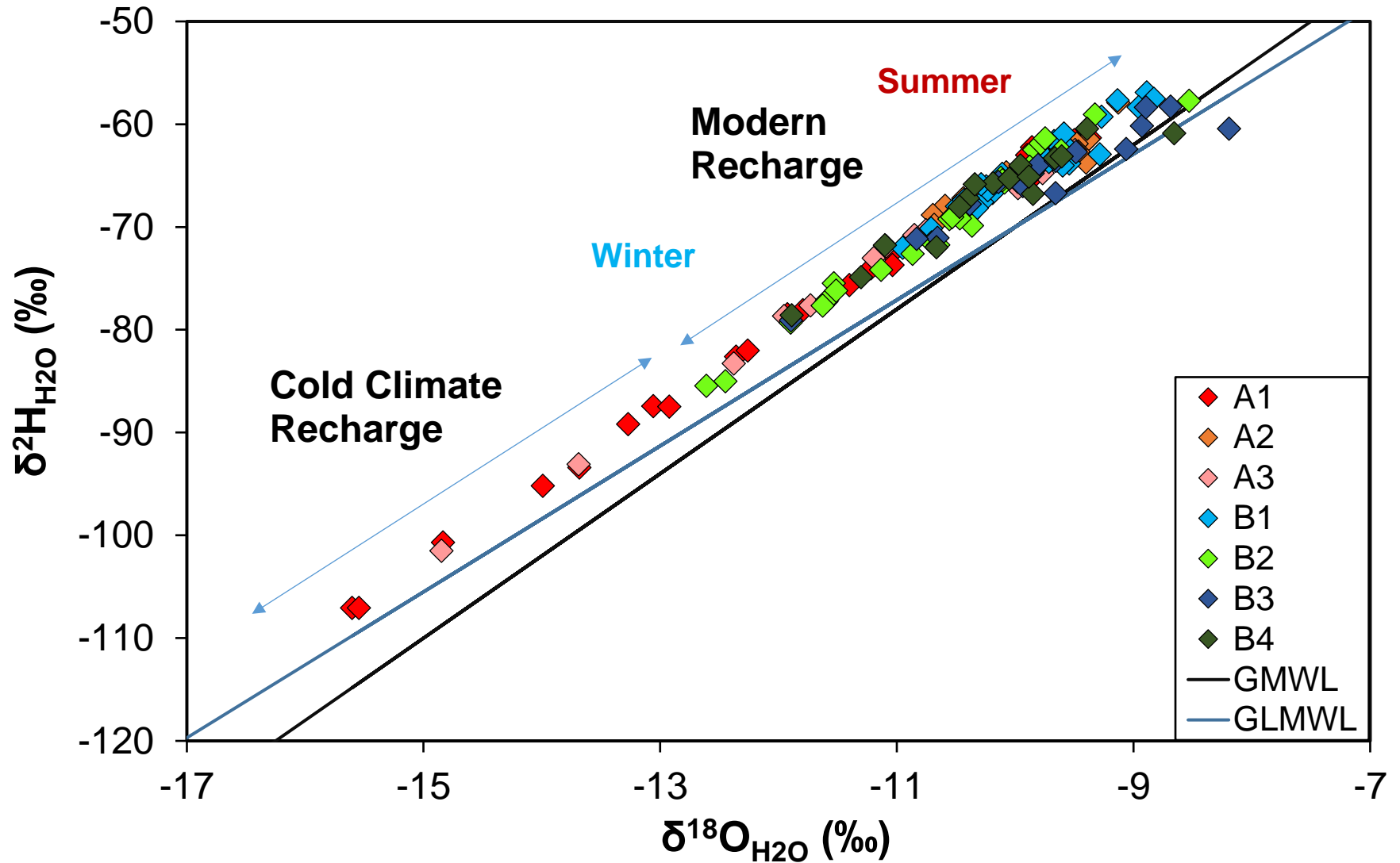


Figure 4.16: (a) Water isotopes of samples collected as a part of this study plotted on the Global Meteoric Water Line (black) and Great Lakes Meteoric Water Line (blue). Samples are plotted by cluster defined using HCA.

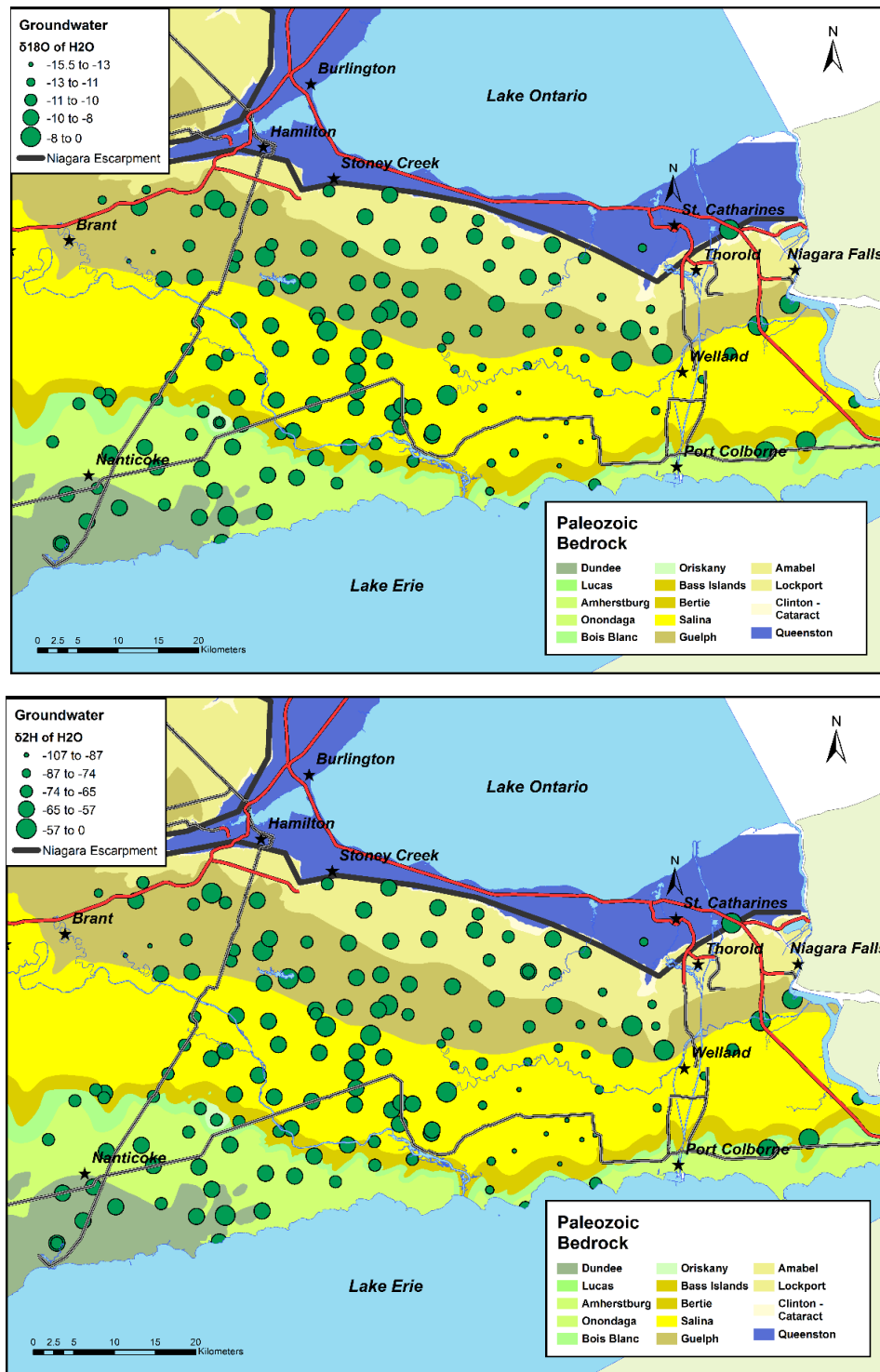


Figure 4.17: (a) $\delta^{18}\text{O}_{\text{H}_2\text{O}}$ (‰) and (b) $\delta\text{D}_{\text{H}_2\text{O}}$ (‰) of groundwater samples collected on the Niagara Peninsula from bedrock wells. Smaller dots represent isotopically depleted samples representative of cooler climate recharge, whereas larger dots represent meteoric precipitation and water-rock interaction.

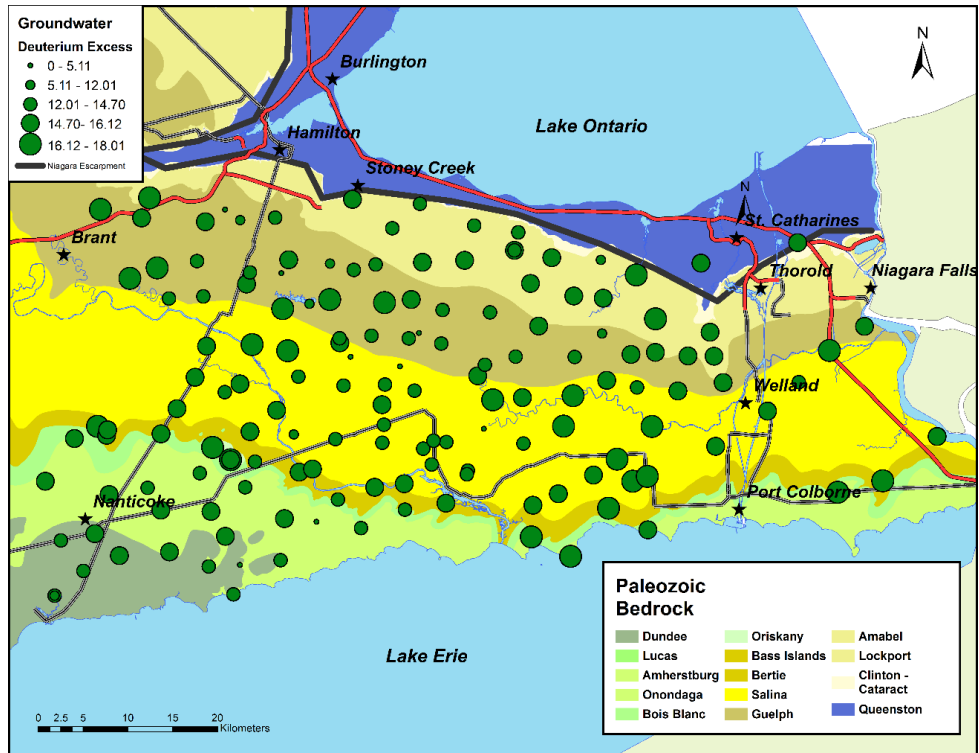


Figure 4.18: Distribution of the Deuterium excess for groundwater samples in the study area. Larger symbols signify higher deviance from the GMWL.

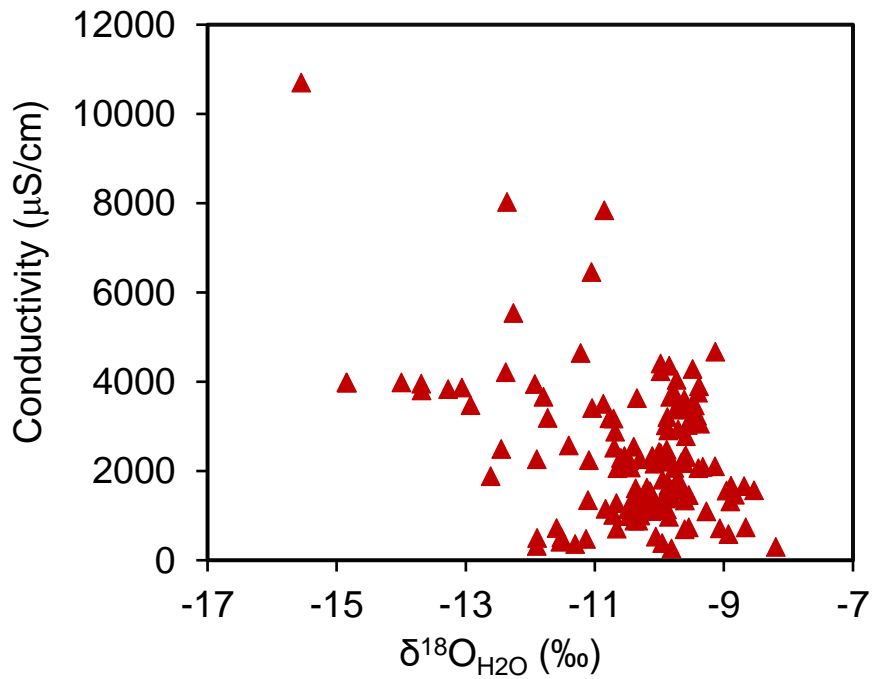


Figure 4.19: Conductivity ($\mu\text{S}/\text{cm}$) vs $\delta^{18}\text{O}_{\text{H}_2\text{O}}$ (‰).

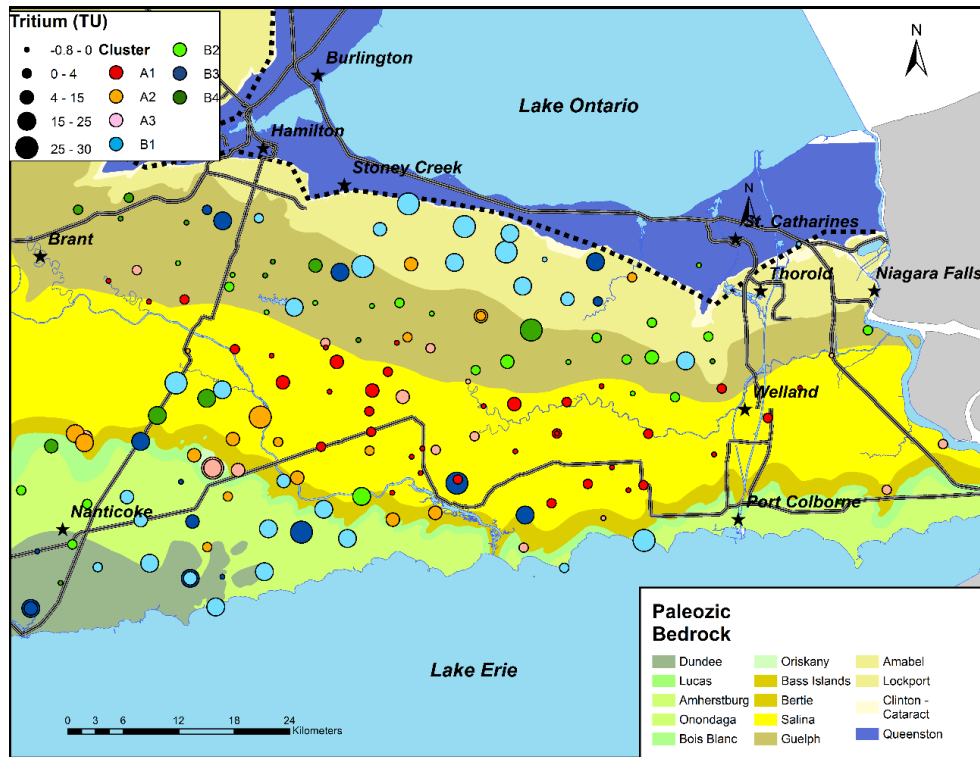


Figure 4.20: Map of the distribution of tritium values (TU) across the study area by cluster.

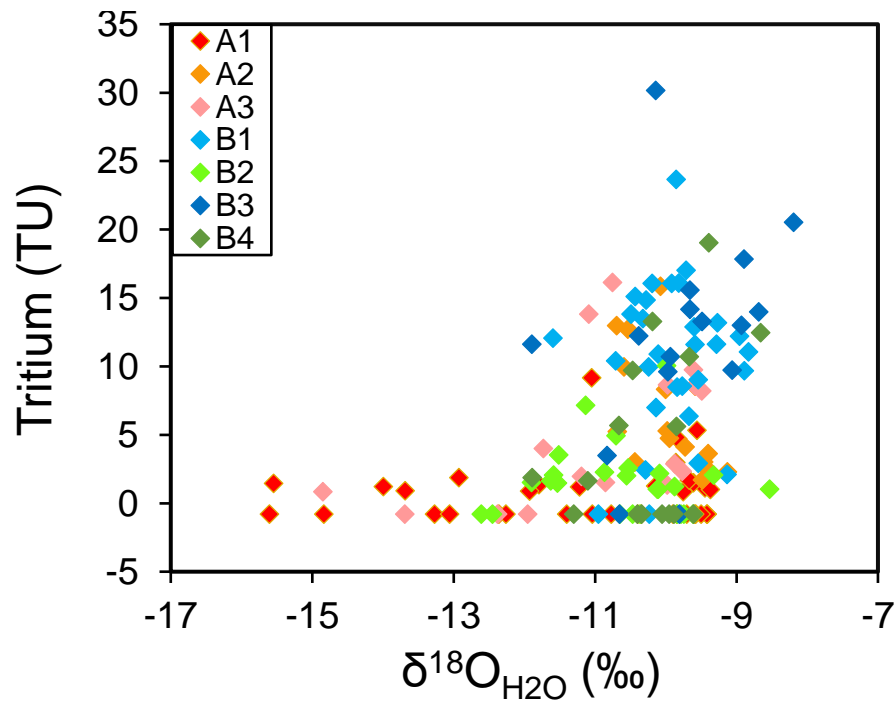


Figure 4.21: The relationship between $\delta^{18}\text{O}_{\text{H}_2\text{O}}$ isotopic signatures (‰) and Tritium (TU) for groundwater samples grouped according to HCA clusters.

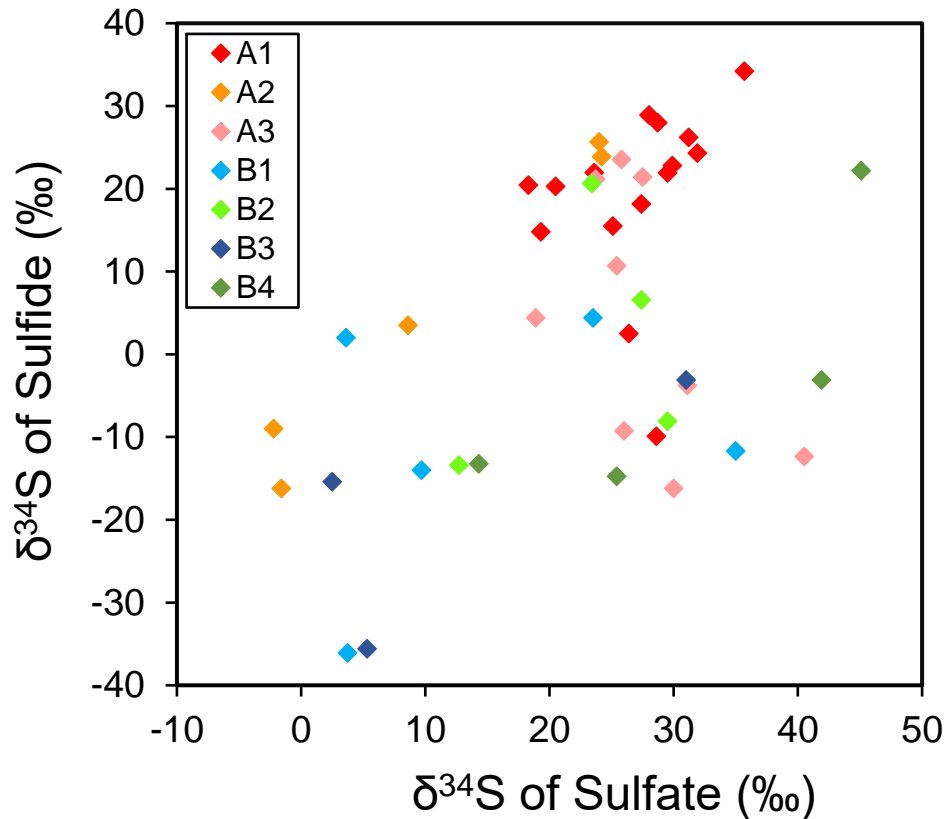


Figure 4.22: $\delta^{34}\text{S}_{\text{SO}_4}$ (x-axis) and $\delta^{34}\text{S}_{\text{S}_2}$ (y-axis) isotopic signatures (‰) for all groundwater samples with sulfide concentrations >0.3 mg/L organized by cluster.

The relationship between sulfur isotopes and the concentration of sulfate in groundwater samples is shown in Figure 4.26. Figure 4.26 also illustrates the differences between the geochemical and isotopic composition of clusters, and that each cluster falls within a small range of geochemical and isotopic values. A2 displays a large range of isotopic values, and a sub-cluster of 7 samples with high sulfate concentrations associated with isotopically depleted values for $\delta^{34}\text{S}_{\text{SO}_4}$. In most samples, A1 and A3 have high sulfate concentrations associated with isotopically enriched $\delta^{34}\text{S}_{\text{SO}_4}$ compositions. B2 and B4 have samples falling along the whole range of $\delta^{34}\text{S}_{\text{SO}_4}$ isotopic compositions and display a wide range of sulfate concentrations up to a maximum of 2000 ppm.

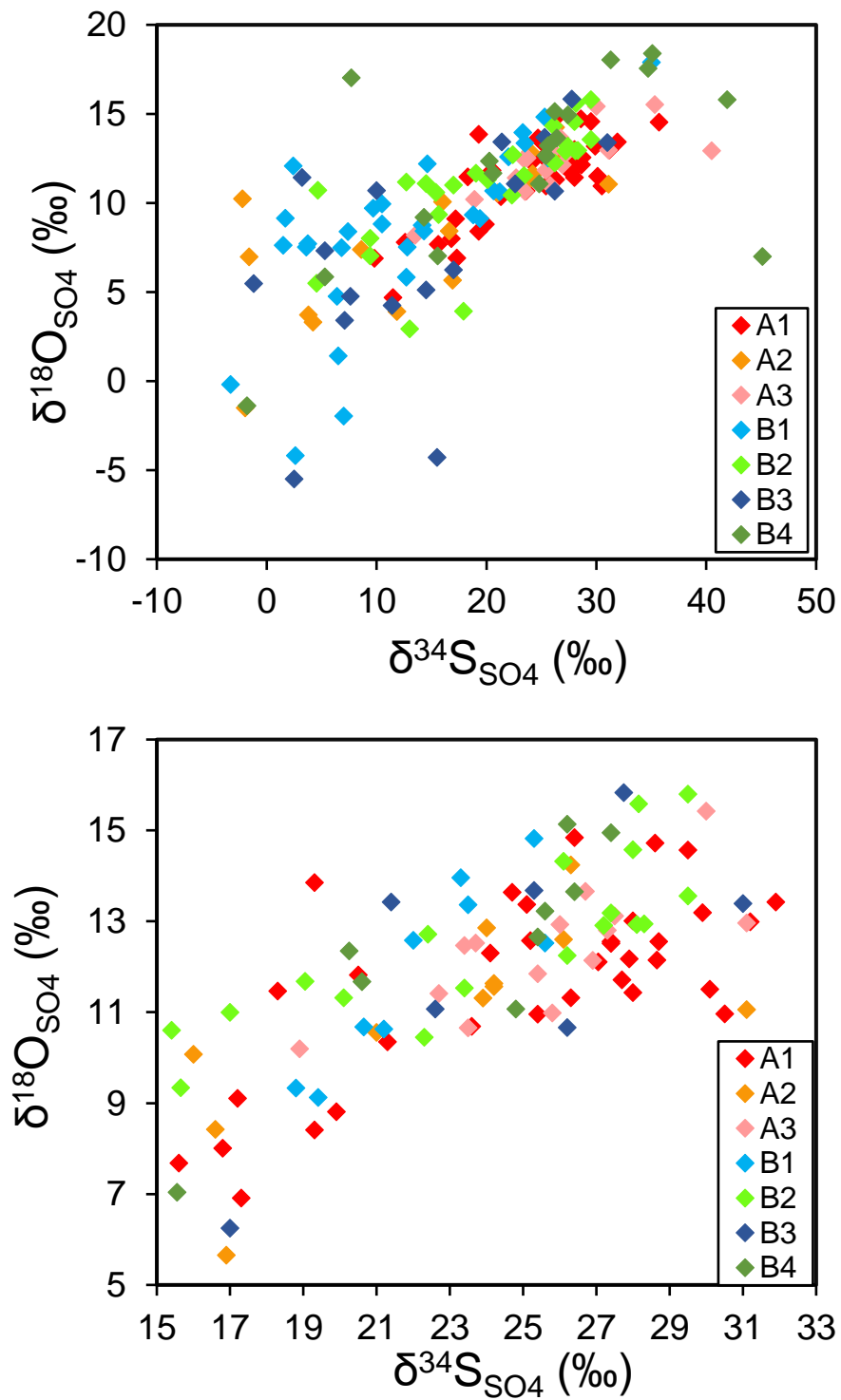


Figure 4.23: (a) $\delta^{34}\text{S}_{\text{SO}_4}$ (x-axis) and $\delta^{18}\text{O}_{\text{SO}_4}$ (y-axis) isotopic signatures (‰) for all groundwater samples organized by cluster. (b) inset map of boxed area in Figure 4.26 (a).

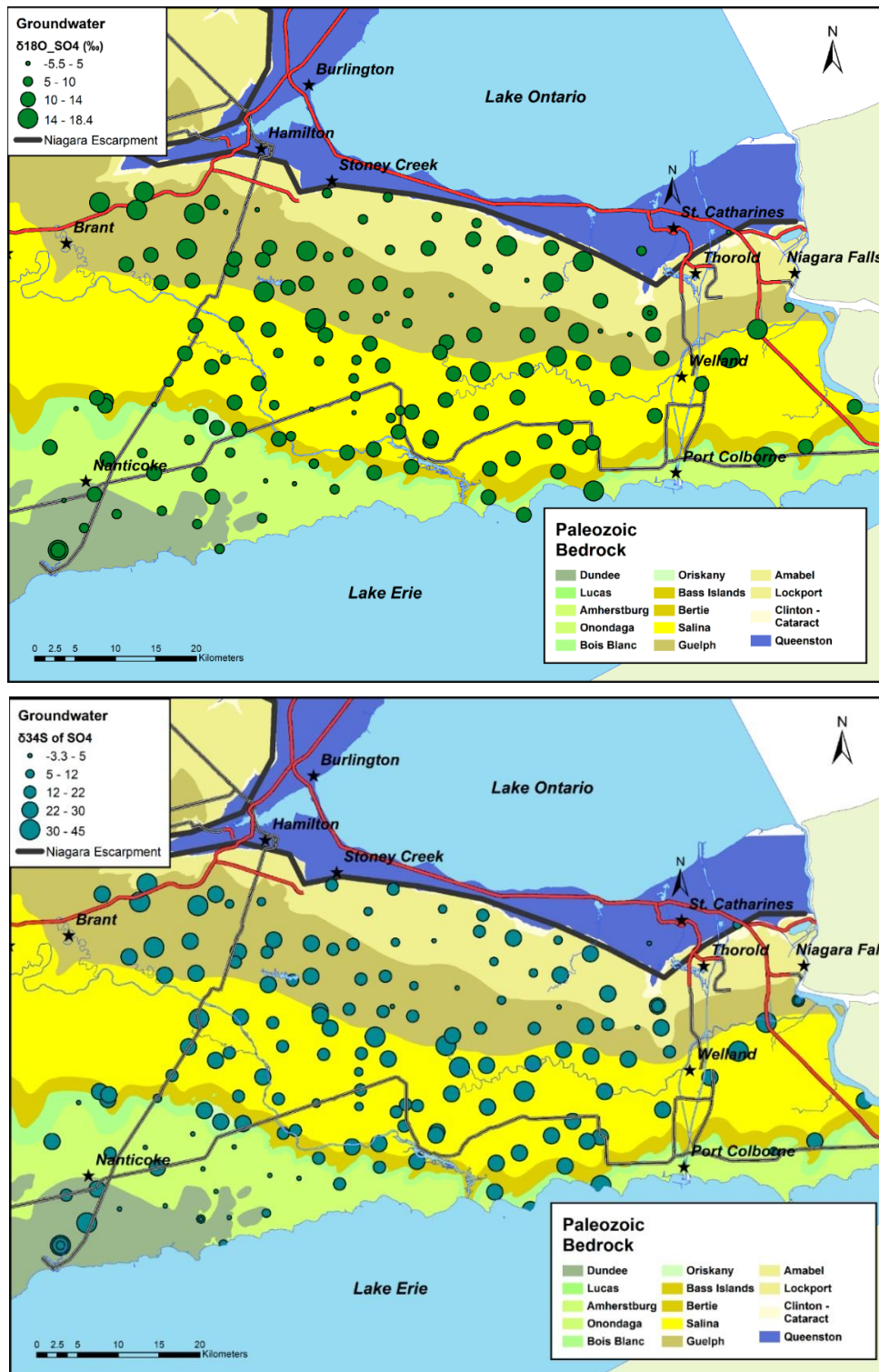


Figure 4.24: Spatial locations of (a) $\delta^{18}\text{O}_{\text{SO}_4}$ (‰) and (b) $\delta^{34}\text{S}_{\text{SO}_4}$ (‰) from samples collected on the Niagara Peninsula.

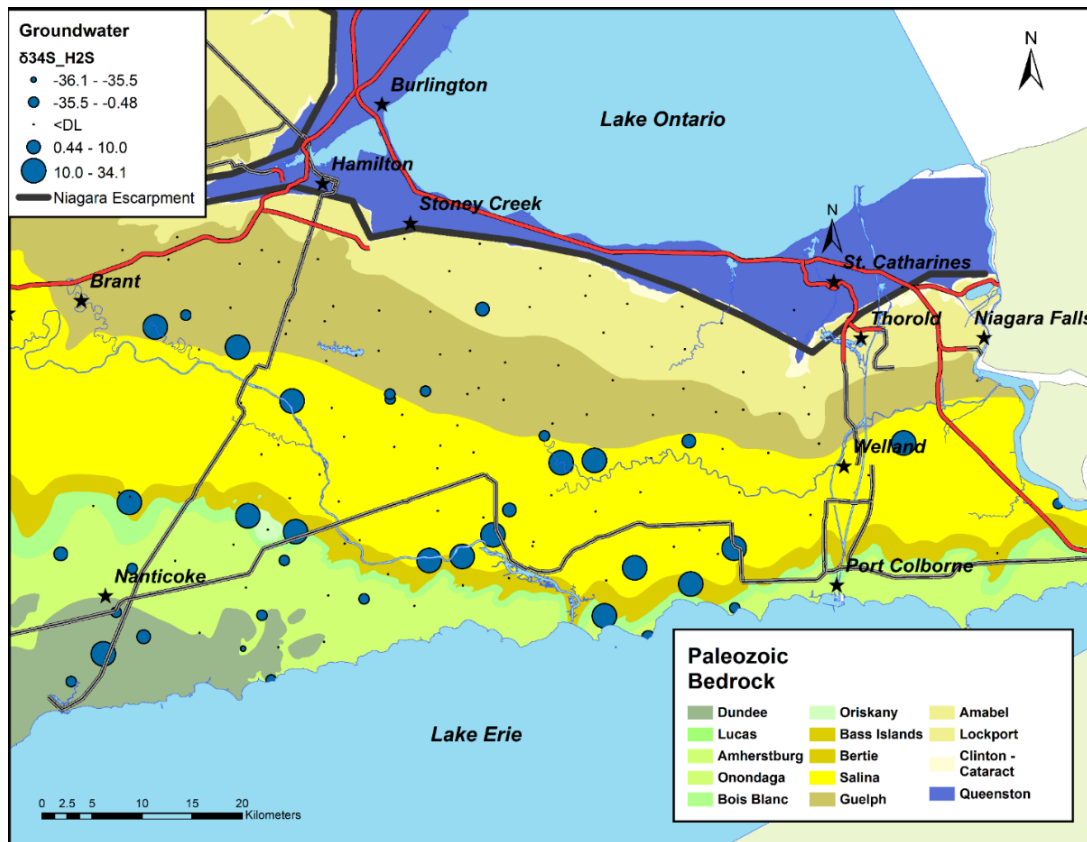


Figure 4.25: Spatial locations of $\delta^{34}\text{S}_{\text{H}_2\text{S}}$ (‰) from samples collected on the Niagara Peninsula. Samples were only collected for $\delta^{34}\text{S}$ of sulfide when field-measured hydrogen sulfide concentrations exceeded 0.3 mg/L as S^{2-} due to analytical restraints.

B1 and B3 have the lowest sulfate concentrations in the study area, and trend towards isotopically depleted $\delta^{34}\text{S}_{\text{SO}_4}$ compositions. Samples in Figure 4.27 show similar cluster associations between sulfide concentrations (ppm) and $\delta^{34}\text{S}_{\text{S}^{2-}}$ and $\delta^{34}\text{S}_{\text{SO}_4}$. For samples with detectable sulphide, $\delta^{34}\text{S}_{\text{SO}_4}$ shows a bimodal distribution in concentration, whereby one group of samples are isotopically depleted ($\delta^{34}\text{S}_{\text{SO}_4}$ -3.3 to 15 ‰) and another with higher H_2S concentrations is enriched ($\delta^{34}\text{S}_{\text{SO}_4}$ 22 to 45.1 ‰). A similar but less pronounced bimodal distribution is seen in $\delta^{34}\text{S}_{\text{S}^{2-}}$ with the break-point between the two modal groups at about -10‰.

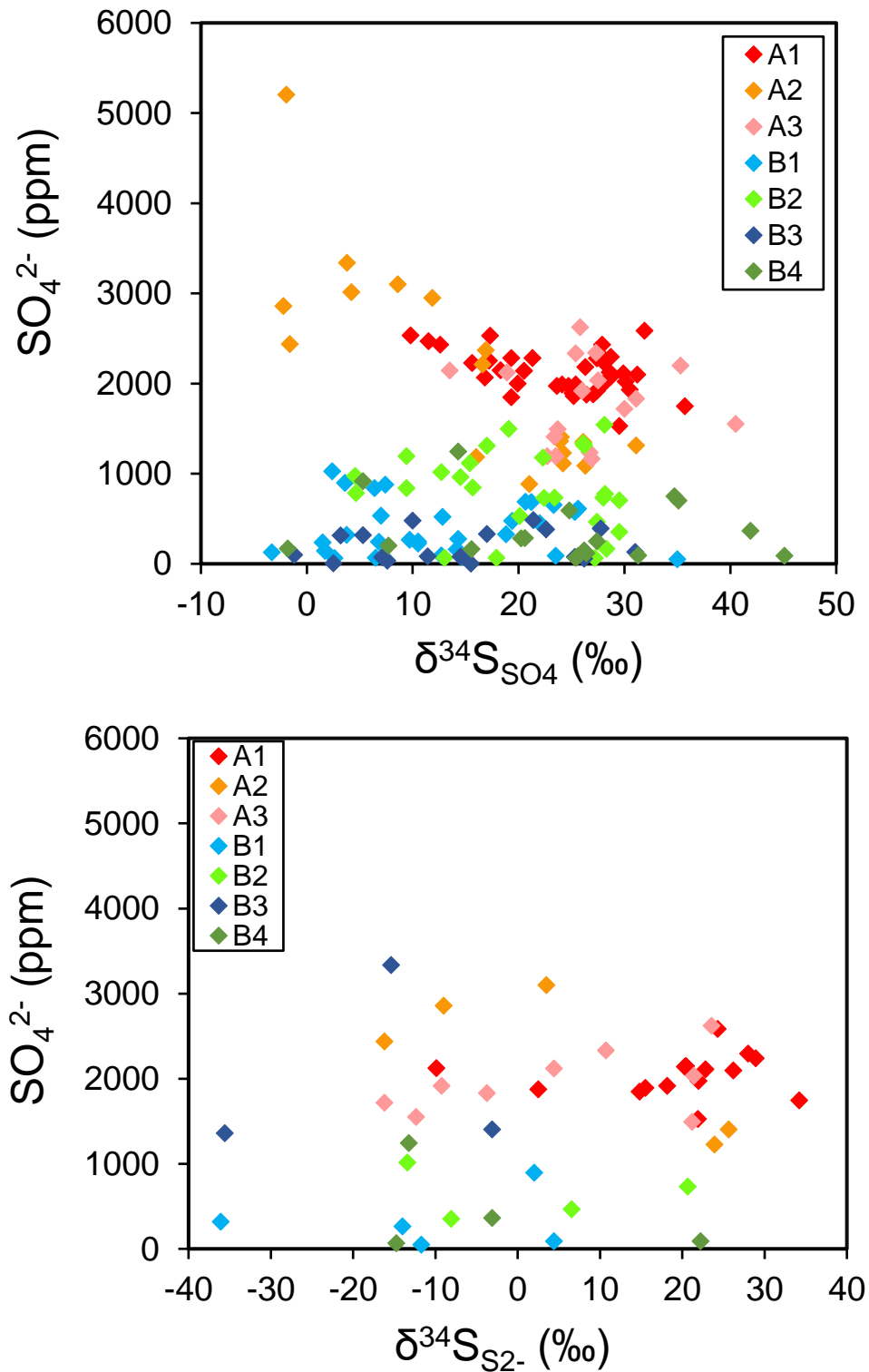


Figure 4.26: $\delta^{34}\text{S}$ isotopic values (‰) of (a) sulfate and (b) sulfide (x-axis) compared to concentrations of sulfate (ppm) in samples collected on the Niagara Peninsula.

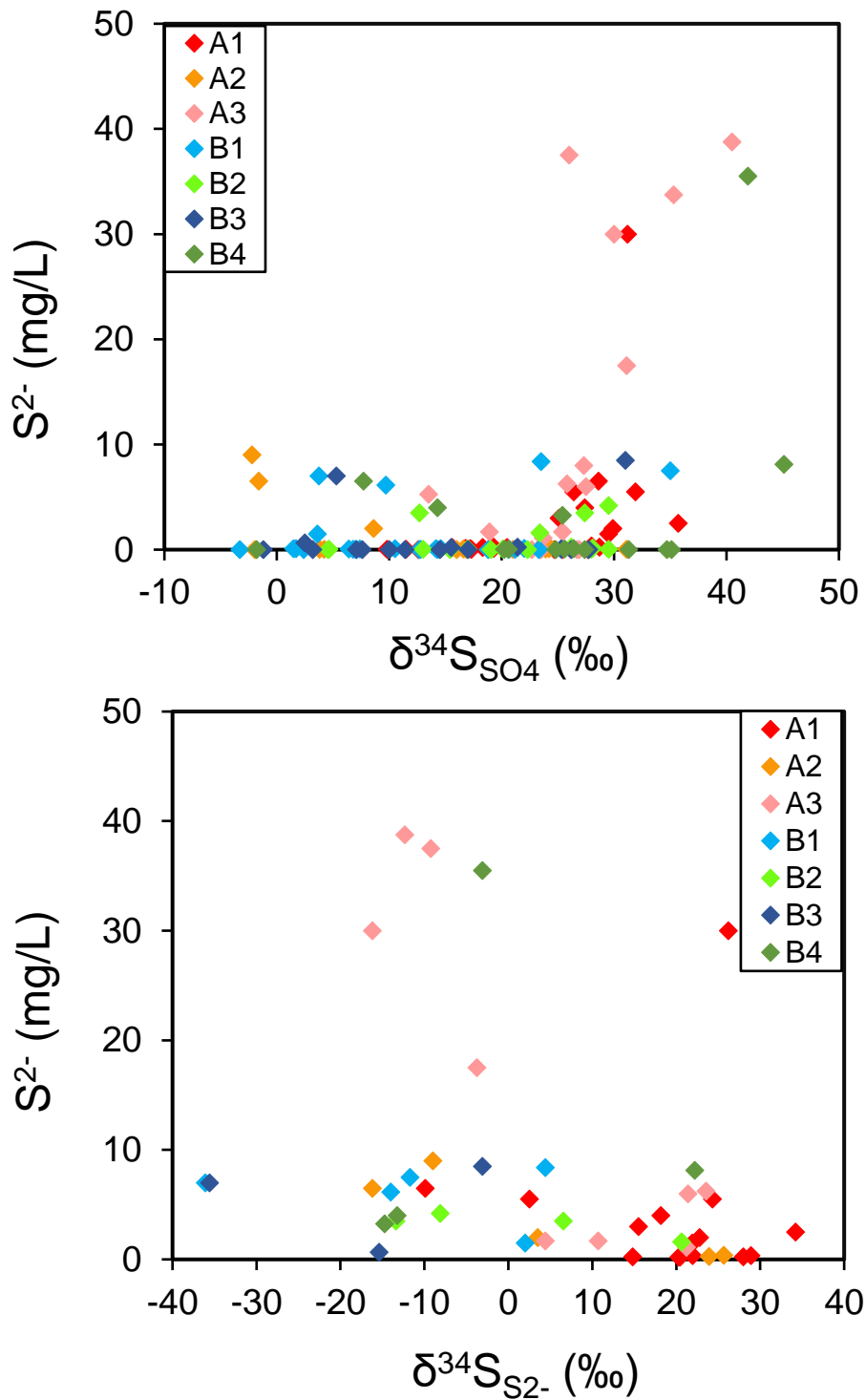


Figure 4.27: $\delta^{34}S$ isotopic values (‰) of (a) sulfate and (b) sulfide (x-axis) compared to concentrations of sulfide (mg/L) in samples collected on the Niagara Peninsula.

4.4.3 Carbon Isotopes

The carbon isotopes of DIC, DOC and methane (CH₄) are presented in this section. $\delta^{13}\text{C}$ isotopic compositions for DIC and DOC were measured for all groundwater samples (Figure 4.28). The range of $\delta^{13}\text{C}_{\text{DIC}}$ for groundwater samples in the study area is between -22.05 and 0.3 ‰, with a mean isotopic composition of -11.8 ‰. The association between DIC concentrations and isotopic values is shown in Figure 4.29. It is apparent a correlation between isotopically depleted $\delta^{13}\text{C}_{\text{DIC}}$ values and high concentrations of DIC (ppm) exists, particularly in clusters A2, B1 and B3. Most samples from cluster A1 fall within the $\delta^{13}\text{C}$ isotopic range of -10 and -5 ‰, exhibiting the strongest association between low DIC concentrations and isotopically enriched $\delta^{13}\text{C}$ signatures (Figure 4.29). Groundwater samples from cluster A3, B2 and B4 are characterized by fewer extremely high DIC concentrations (>100 ppm) and a large range of $\delta^{13}\text{C}$ values.

The spatial distribution of $\delta^{13}\text{C}_{\text{DIC}}$ signatures indicates a relationship between the proximity of bedrock escarpments with thin sediment cover and the $\delta^{13}\text{C}_{\text{DIC}}$ value of groundwater samples (Figure 4.29). Groundwater samples obtained near the crests of the Niagara and Onondaga Escarpments have isotopically depleted $\delta^{13}\text{C}_{\text{DIC}}$ values, whereas samples obtained from the Salina bedrock trough under thick, relatively impermeable drift cover typically have $\delta^{13}\text{C}_{\text{DIC}}$ values between -10 and 0 ‰.

There is no strong relationship between $\delta^{13}\text{C}$ of DOC and DIC (Figure 4.30), although clusters A2 and B1 occupy a narrow range. The total range of $\delta^{13}\text{C}$ for groundwater DOC in the study area is between -35.8 and -24.5 ‰ and the lowest $\delta^{13}\text{C}_{\text{DOC}}$ values are -35.4 and -35.1 ‰, which are for a duplicate sample in cluster A1. The most isotopically depleted $\delta^{13}\text{C}_{\text{DOC}}$ values occur primarily in Salina group groundwaters (Figure 4.30).

$\delta^{13}\text{C}_{\text{CH}_4}$ isotopic compositions were obtained where the methane concentration in groundwater was high enough ($>30 \mu\text{mol/L}$) to allow measurement of the isotopic composition and this limited the determination to 16 samples. Figure 4.31 displays the spatial distribution and sample ID's of groundwater samples analyzed for $\delta^{13}\text{C}_{\text{CH}_4}$ in the study area. With two exceptions, samples with isotopic signatures indicative of biogenic methane production (-50 to -80‰) are primarily located in the southwestern study area.

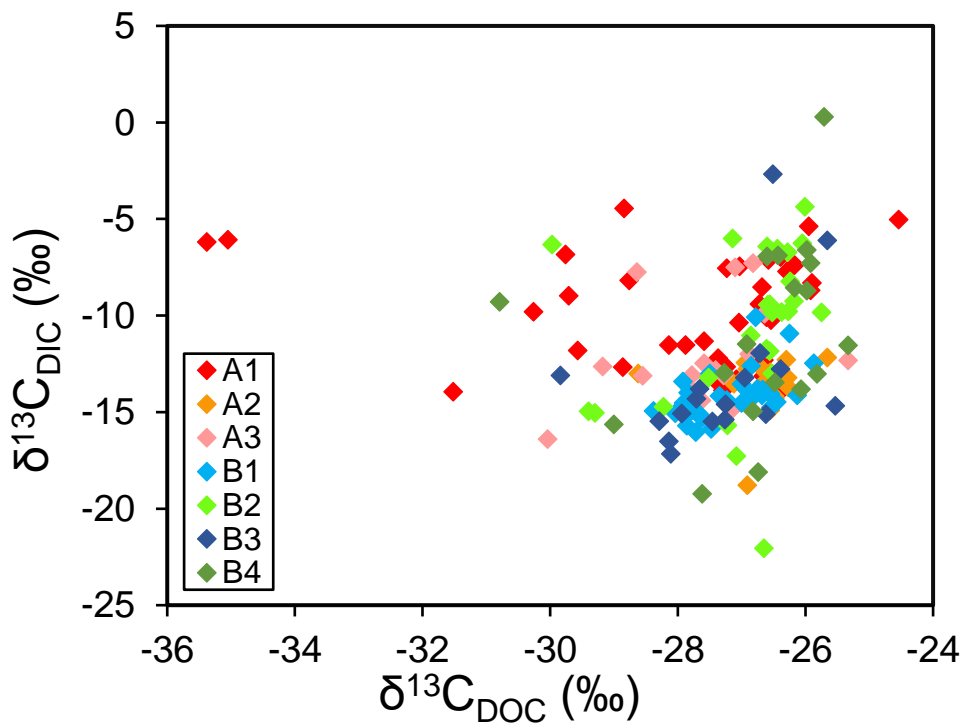


Figure 4.28: $\delta^{13}\text{C}_{\text{DOC}}$ (x-axis) and $\delta^{13}\text{C}_{\text{DIC}}$ (y-axis) isotopic signatures (‰) for all groundwater samples organized by cluster.

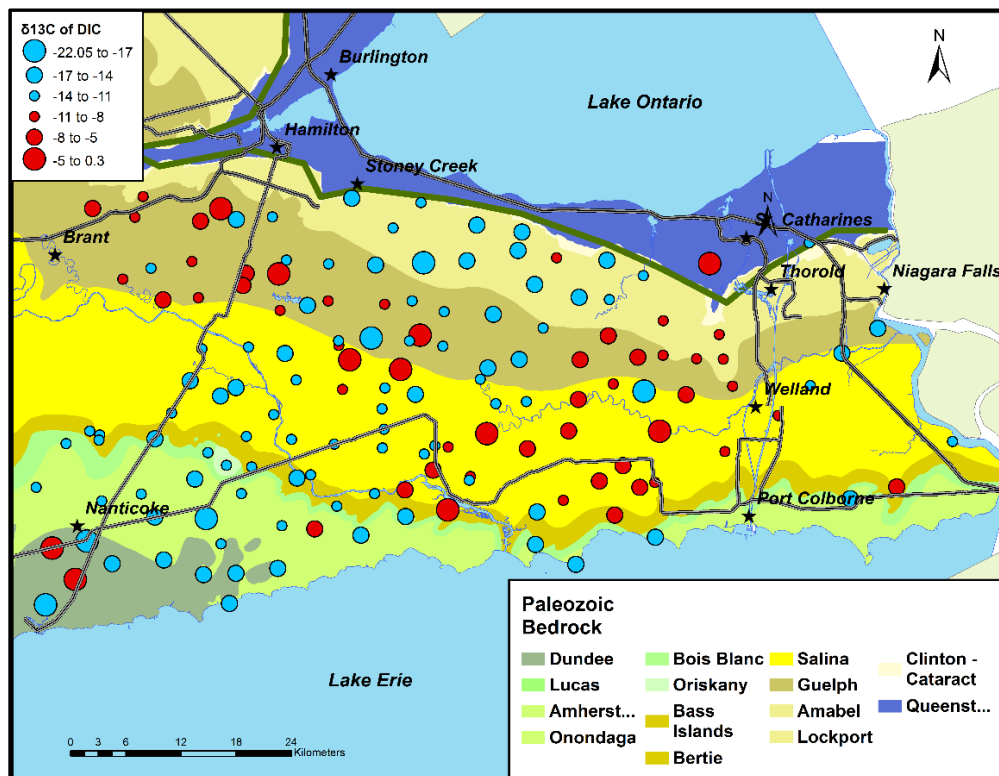
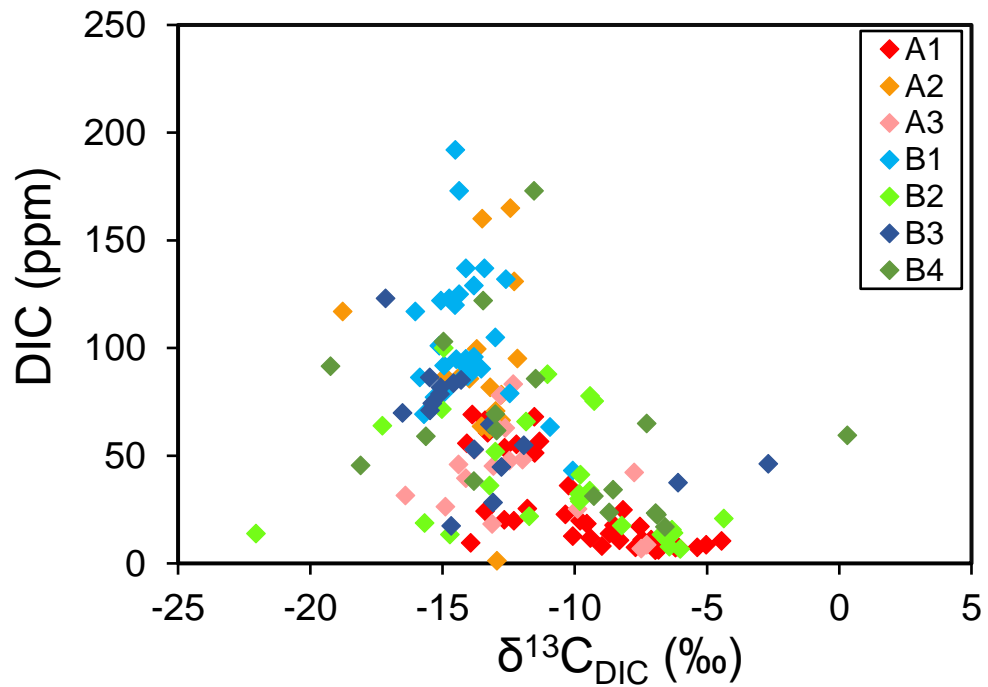


Figure 4.29: (a) Concentration of dissolved inorganic carbon (DIC) (ppm) (y-axis) compared with $\delta^{13}\text{C}$ of DIC (‰) (y-axis). (b) Spatial distribution of $\delta^{13}\text{C}$ of DIC (‰) isotopic signatures from groundwater samples in the study area.

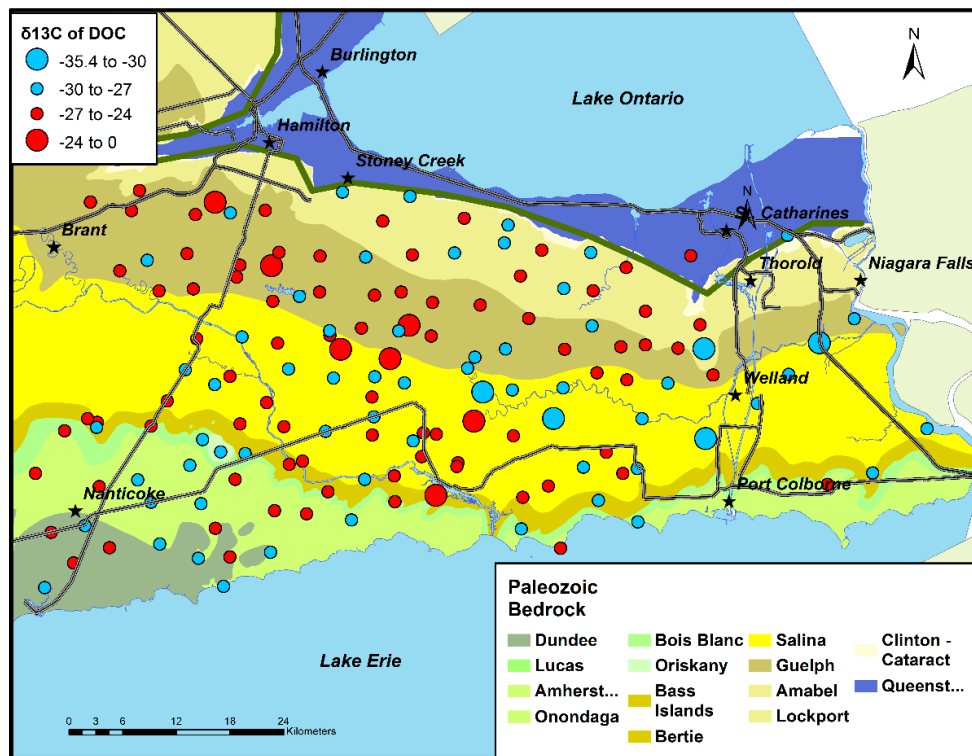
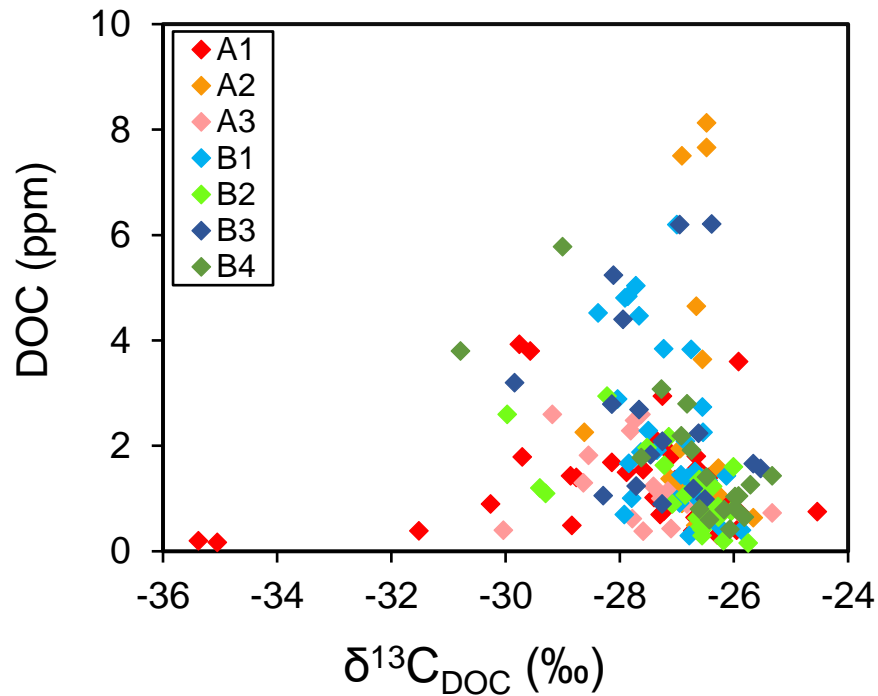


Figure 4.30: (a) Concentration of dissolved organic carbon (DOC) (ppm) (y-axis) compared with $\delta^{13}\text{C}$ of DOC (‰) (y-axis). (b) Spatial distribution of $\delta^{13}\text{C}$ of DOC (‰) isotopic signatures from groundwater samples in the study area.

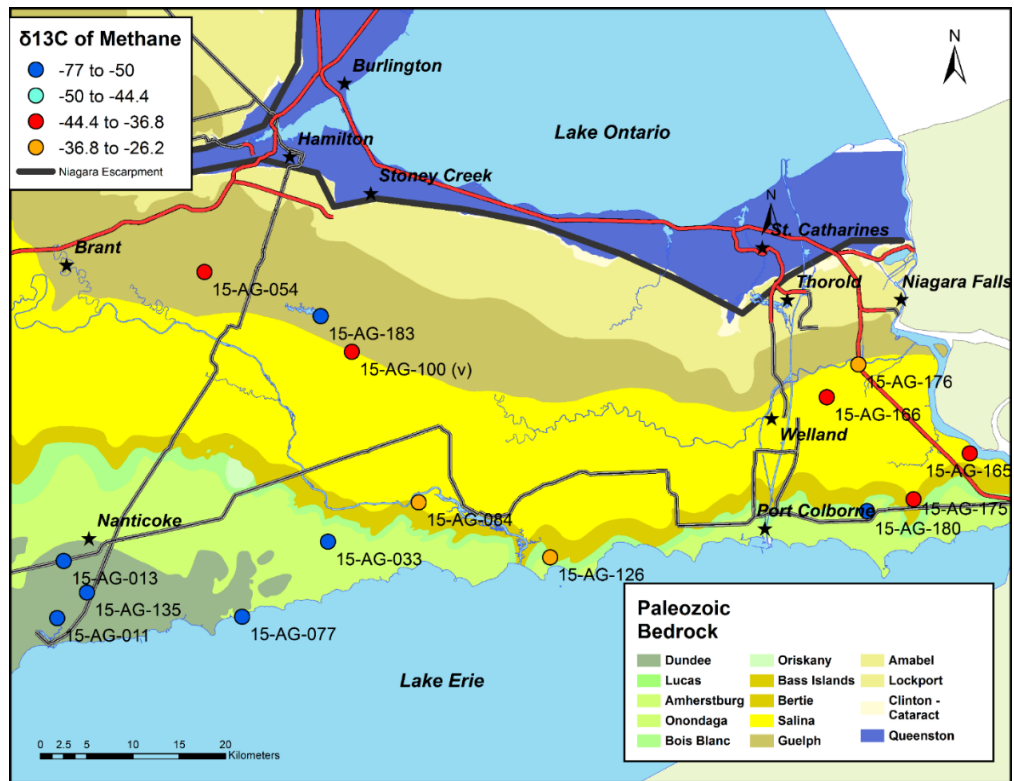


Figure 4.31: Spatial locations and sample ID's of wells sampled for $\delta^{13}\text{C}$ of methane (‰) overlain on the subcropping geology.

Figure 4.32 displays the relationship between $\delta^{13}\text{C}_{\text{CH}_4}$ and the concentrations of DOC (ppm) and HCO_3^- (ppm), respectively. Where either DOC or HCO_3^- have higher concentrations, $\delta^{13}\text{C}_{\text{CH}_4}$ is isotopically depleted. With the exception of two samples (from B2 and B4), samples from clusters B1, B2, B3 and B4 show $\delta^{13}\text{C}_{\text{CH}_4}$ signatures within the range of biogenic methane. $\delta^{13}\text{C}_{\text{CH}_4}$ values typical of local, deep-origin thermogenic methane (Barker and Fritz, 1981) are primarily confined to groundwaters from A1 and A3. The relationship between lab-derived methane concentrations and $\delta^{13}\text{C}_{\text{CH}_4}$ isotopic compositions is given in Figure 4.33. Where isotopically depleted values in the thermogenic and biogenic methane clusters exist, high concentrations of methane are present. This suggests partial oxidation of methane, which can reduce methane concentrations while enriching the $\delta^{13}\text{C}_{\text{CH}_4}$ value of the residual methane.

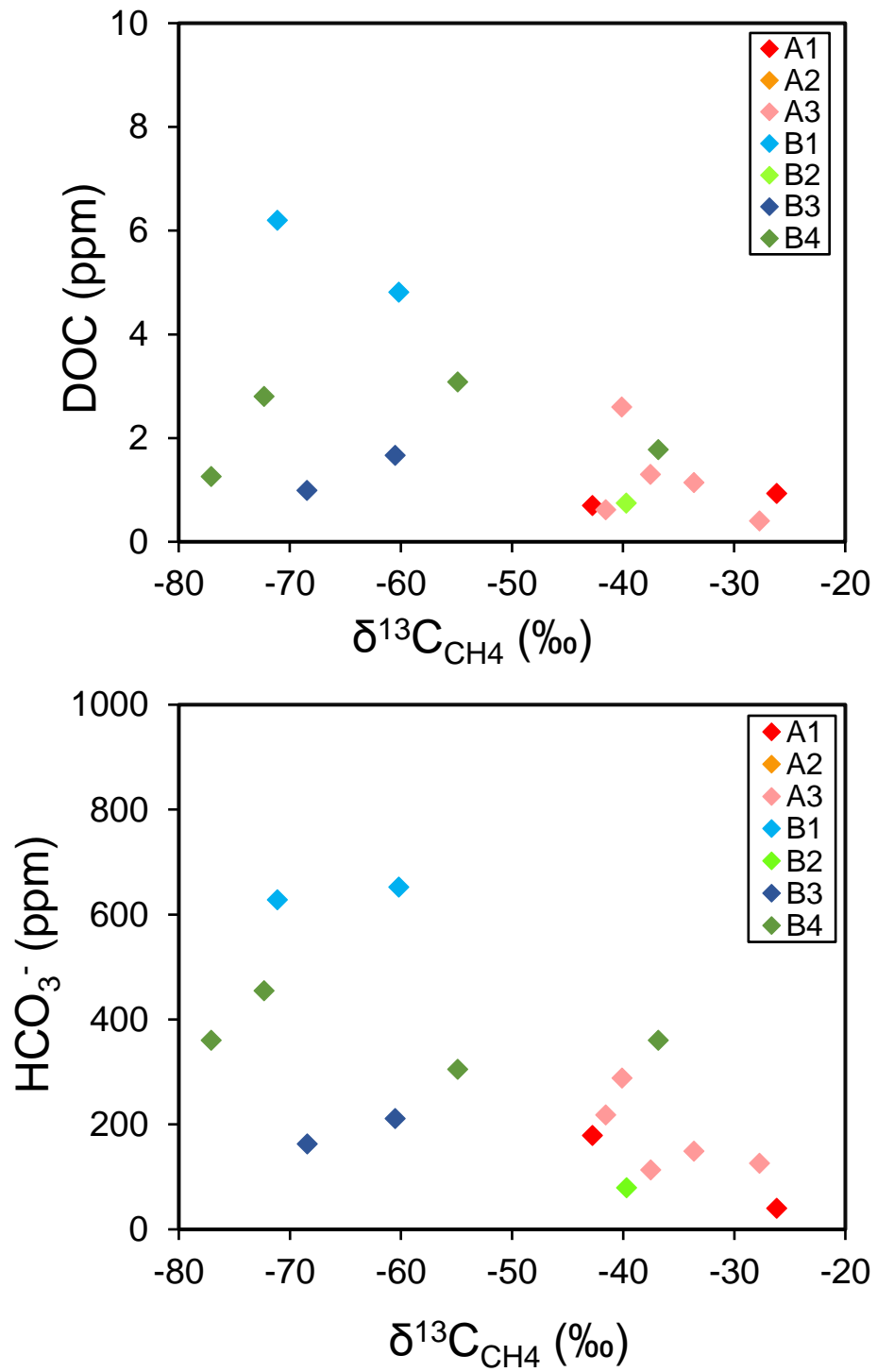


Figure 4.32: (a) concentration of $\delta^{13}\text{C}$ (‰) of methane (x-axis) vs. DOC (ppm) and (b) HCO_3^- (ppm).

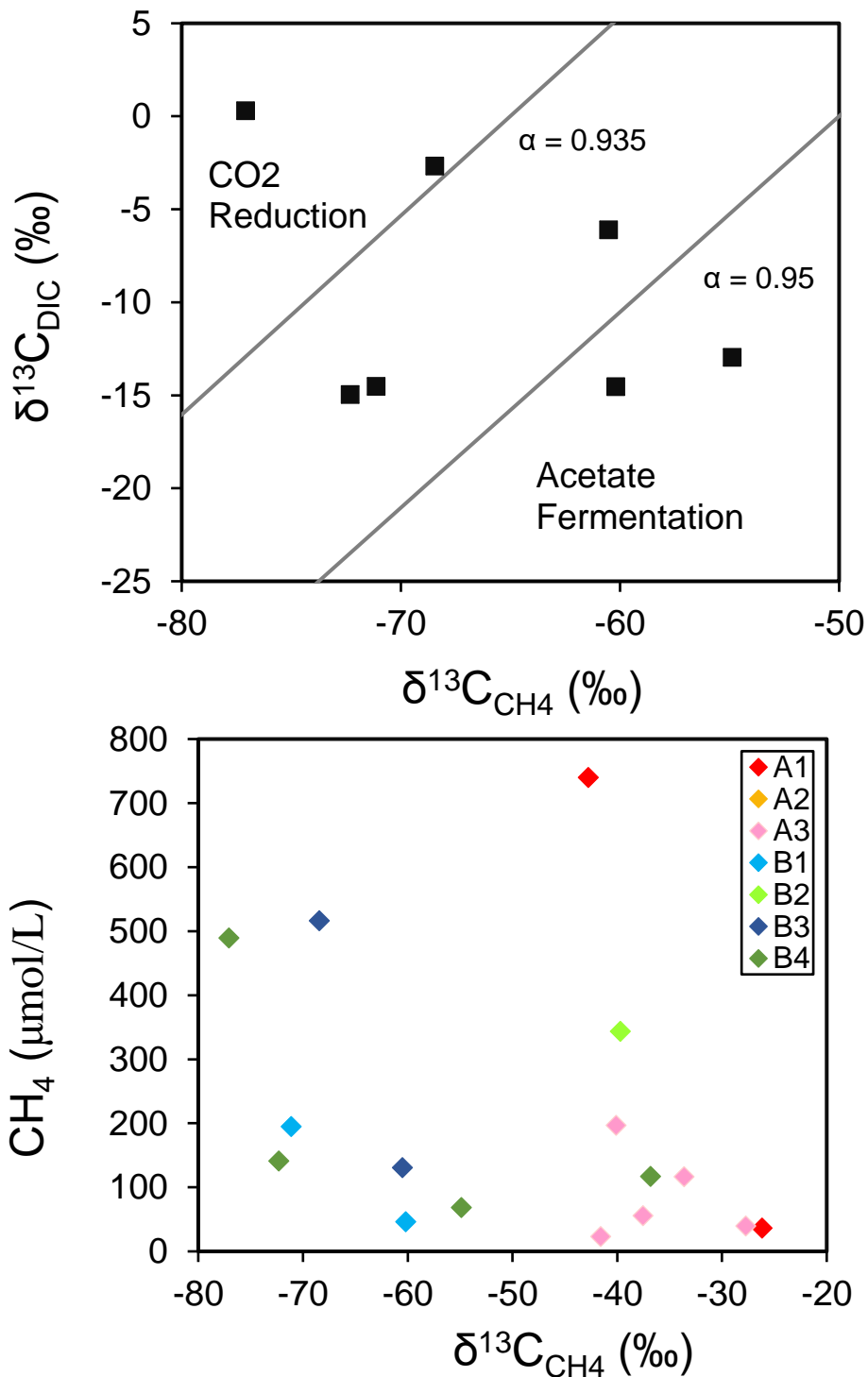


Figure 4.33: (a) $\delta^{13}\text{C}$ (‰) of methane (x-axis) vs. $\delta^{13}\text{C}$ of DIC (‰) (y-axis). The position of samples on the isotopic map define the methanogenic pathway for biogenically produced methane. (b) methane concentration ($\mu\text{mol/L}$) (y-axis) vs. $\delta^{13}\text{C}$ of methane (‰).

4.5 Dissolved Gasses

Methane concentrations were analyzed rigorously in the laboratory using a gas chromatograph at McMaster University (see methods), and in the field, 24 hours after sample collection following the protocols of Hamilton, 2015. A comparison between the two methods was completed to assess the reliability of the field method for determining gas contents of groundwater samples (Figure 4.34). As the low level methane sensor experienced mechanical failure during sampling, only high level methane measurements were used for comparison.

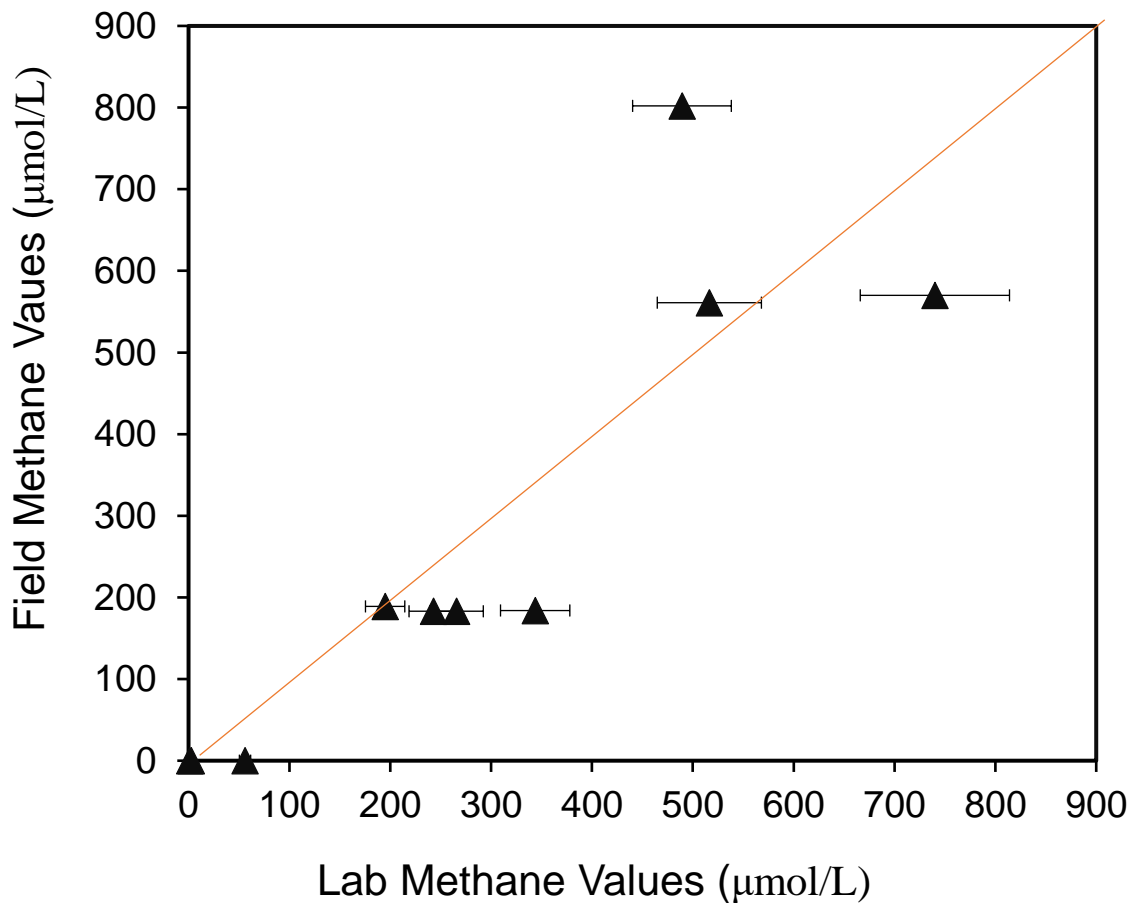


Figure 4.34: Comparison between laboratory and high-sensor field measurements of methane concentration from samples collected on the Niagara Peninsula.

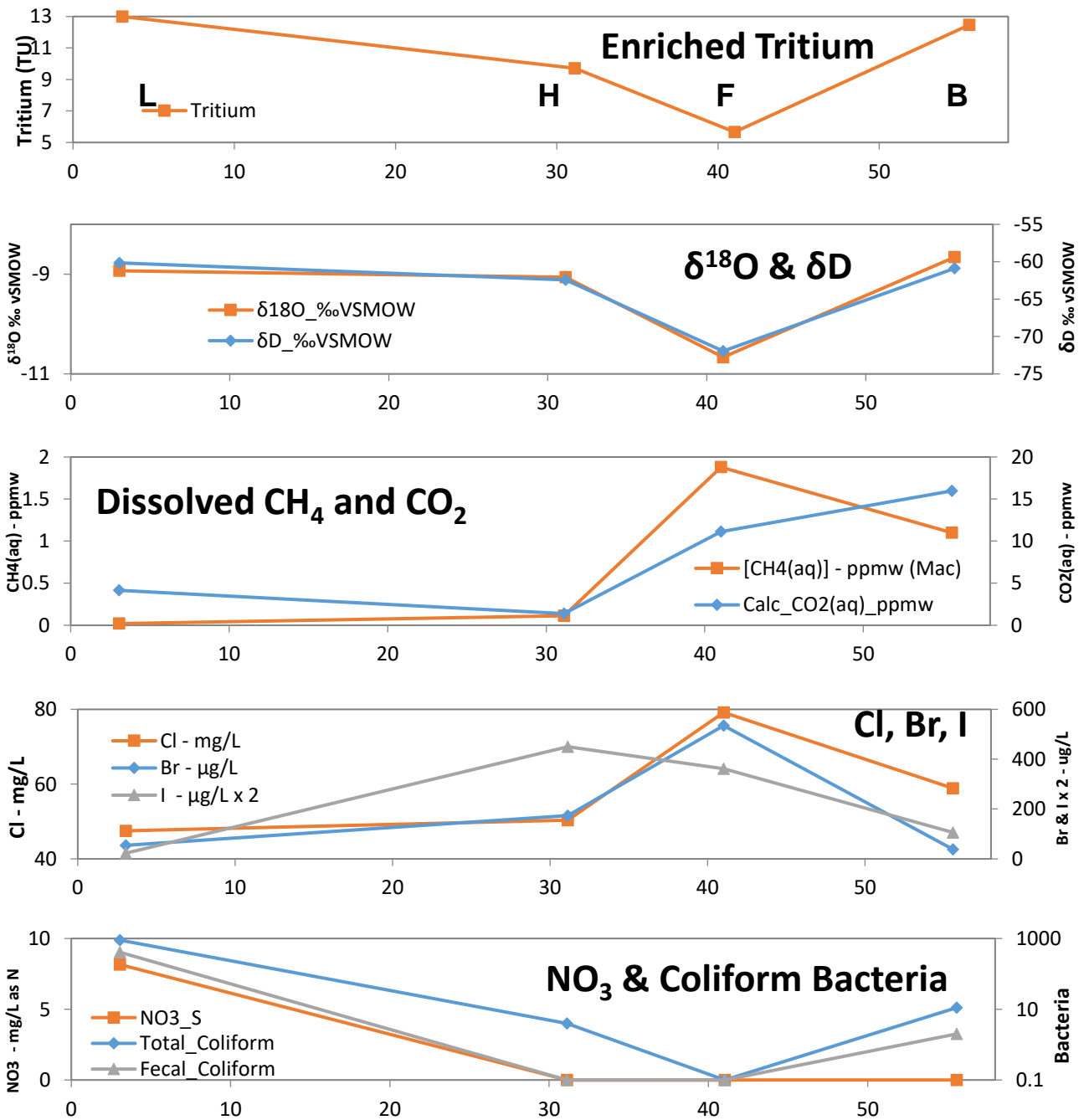
Differences between methods are suspected to be due to a time delay in measurement by the field instrument before registering the presence of gases, and the discrimination of free bubbles during sampling for the lab method. During the short time delay prior to measurement, small amounts of methane and other gasses in the headspace were able to escape through the top of the glass bottle. Laboratory methane measurements were used for this thesis in substitution for the field derived concentrations due to the time lapse in gas detection of the field instruments, and instrumental failure at low methane concentrations (< 1%) during the Niagara Peninsula sampling program.

4.6 Case Study: Norfolk Quarry Biogeochemistry

A local site where a change in the geochemical character of groundwater is visually evident was investigated to support the determination of biogeochemical reactions occurring in groundwater within the study area. A groundwater sampling transect was made along a 60 m-wide spring on the face of a flooded quarry. In the centre of the spring is a wide area where hydrogen sulfide-rich groundwater discharges and microbial mats have grown. On either side, the discharging groundwater clearly has different water chemistry because iron precipitate forms rather than the white microbial mat (Figure 4.35). Upon arriving at the site, hydrogen sulfide concentrations were measured in 12 approximately evenly spaced locations along the transect. Full sample suites and field measurements were taken at 4 sample locations chosen for comparison based on hydrogen sulfide measurements. The first location at the eastern side of the transect, site (L), was chosen due to the presence of iron-rich precipitate and a lack of hydrogen sulfide (apparent by the lack of smell). The remaining sites were chosen as follows; one site with a high hydrogen sulfide concentration (F; 'sulfur spring'), one site at the western edge of the transect (B), and one site between the sulfur spring and the iron spring (H). A full geochemical sample suite was collected at each of the four detailed sample sites, including geochemical data, dissolved gases, and isotopic data. $\delta^{13}\text{C}_{\text{CH}_4}$ was analyzed for two of the four

samples that had methane concentrations above detection limits for the isotopic analysis.

From Figure 4.35, it is observed that the left side of the transect (L), has a different geochemical signature than the right side (A) and waters at the centre (F and H) have a completely different character than those at either end. The hydrogen sulfide rich sample (F) is associated with low enriched tritium (older water), slightly depleted $\delta^{18}\text{O}$ and δD of H_2O (-10.7 ‰ and -72 ‰), relatively high CH_4 and CO_2 , high Cl^- and Br^- , an absence of NO_3^{2-} and coliform bacteria, high HCO_3^- , SO_4^{2-} and S^{2-} and low DOC. Sample F has highly enriched $\delta^{34}\text{S}$ of SO_4^{2-} (41.9 ‰) and slightly depleted $\delta^{34}\text{S}$ of S^{2-} (-3.1 ‰), enriched $\delta^{18}\text{O}$ of SO_4^{2-} (15.8 ‰) and enriched $\delta^{13}\text{C}$ of CH_4 (-36.8 ‰), suggesting the potential presence of thermogenic methane, and/or methane oxidation. In contrast, sample (L) located on the left side of the transect is associated with high tritium (13 TU), more enriched $\delta^{18}\text{O}$ and δD of water (-8.9 ‰ and -60.2 ‰ respectively), low amounts of dissolved gases, low concentrations of Cl^- , Br^- and I^- , high NO_3^{2-} concentrations and coliform bacterial counts, no detected H_2S , low concentrations of SO_4^{2-} , depleted $\delta^{34}\text{S}_{\text{SO}_4}$ (7.6 ‰) and $\delta^{18}\text{O}$ (4.76 ‰) and high DOC concentrations (6.21 mg/L). Samples (H) and (B) are generally intermediate in concentration and isotopic values between samples (L) and sample (F), suggesting (at least) two end-member water sources and that mixing contributes to the groundwater geochemical signature.



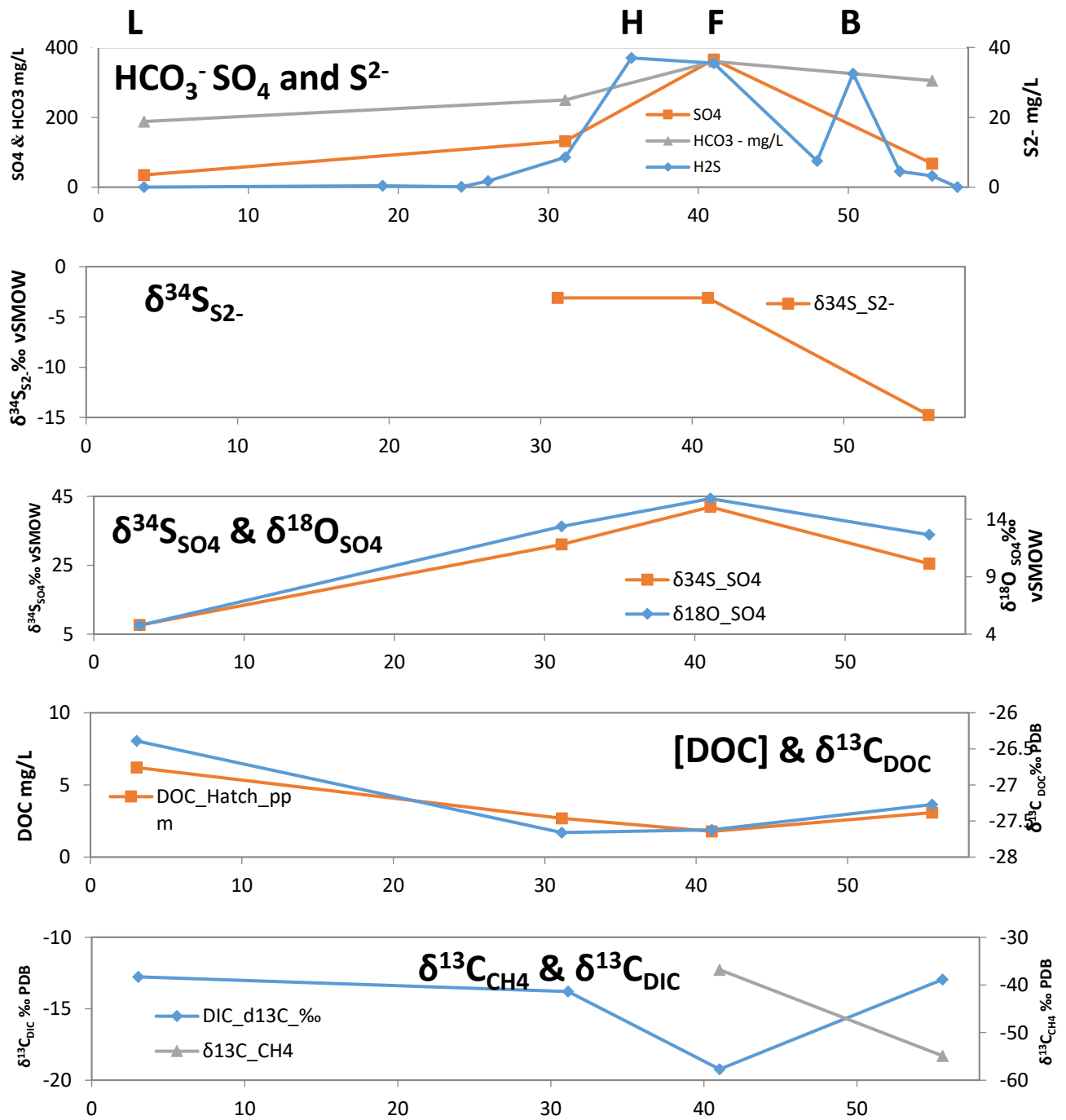


Figure 4.35: Changes in concentrations and isotopic values of geochemical parameters across a transect of groundwater from exposed bedrock at the Norfolk Quarry, near Port Dover, Ontario.

Chapter 5: Discussion

Groundwater chemistry on the Niagara Peninsula is controlled by anthropogenic influences, local hydrogeological conditions, water-rock interaction and localized geochemical cycling of redox-sensitive parameters. As shown in the results, elevated Ca^{2+} and HCO_3^- concentrations in clusters B1 and B3 (Table 4.3) implies carbonate dissolution is the dominant process controlling groundwater chemistry in the southern and northern Niagara Peninsula where samples in these groups are primarily located. A correlation between drift thickness and groundwater chemical differences signifies the importance of significant recharge areas, regional groundwater flow patterns and residence time on the geochemical evolution of groundwater. Where drift is thin (<5 m) or bedrock is exposed at surface, clusters B1 and B3 are dominant (Figure 5.1) and the water type has a Ca- HCO_3 geochemical facies, indicative of recent recharge interacting with local carbonate rocks. Where Quaternary sediment cover is thicker, as in the case of the Salina bedrock trough and the Erigan, Chippawa-Niagara Falls and Crystal Beach buried bedrock channels (Figures 2.2, 2.9 and 2.10), longer residence times, confined aquifer conditions and closed-system carbonate and evaporitic environments lead to the mineralization of groundwater over time resulting in groundwaters with higher conductivities (A1 and A3) (Table 4.3, Figure 5.1). Bedrock mineralogy can control groundwater chemistry where carbonate or evaporite dissolution is present and secondary minerals such as pyrite and fluorite are available for water-rock interaction. Anthropogenic sources of contamination and bedrock mineralogical heterogeneity result in geochemical distinctions and local-scale variations in microbial biodiversity between samples within similar hydrogeological and geological conditions, as demonstrated the Norfolk Quarry Case Study discussed in the previous chapter, and by the local variability of clusters in the study area, discussed further below.

Multivariate statistical techniques and the use of geochemical facies determined using Piper Plots were employed as methods of chemical grouping of samples. HCA has a distinct advantage over traditional water classification techniques due to its flexibility in the use of chosen parameters for comparing data. Whereas water-type determination methods, including piper plots, only consider the proportions of major cations and anions present in a geochemical sample, HCA can consider significantly more parameters and their concentrations. These extra capabilities are important for understanding geochemical processes and reactions. The combined use of HCA and traditional geochemical classification methods (i.e. piper plots, water-type determination) allows for large, inclusive 'geochemical zones' to be differentiated, within which major geochemical processes, including water-rock interaction, biogeochemical cycling, and the impact of meteoric recharge can be assessed for their contributions to the geochemical signature of a groundwater sample. Within geochemical zones, local variations in groundwater chemistry between clusters is the result of variations in the presence of nutrients for reaction resulting from surficial anthropogenic influences, including septic systems and road salt, and migrated fluids from depth along abandoned well casings. Differentiation in sediment cover thicknesses as well as faulting, fracturing and karst presence results in the introduction of nutrients in one location versus another. As illustrated in the Norfolk Quarry case study, sulfide production can be very localized and this explains the variations observed in the greater Niagara Peninsula.

Groundwater samples are grouped into three geochemical zones; the Escarpment Zone, the Salina Zone and the Guelph Zone, defined using the results of HCA, Cl/Br ratios and isotopic signatures (Figure 5.1). Geological controls on groundwater chemistry in the study area are defined initially for context, followed by the delineation of the specific processes controlling groundwater chemistry in each geochemical zone.

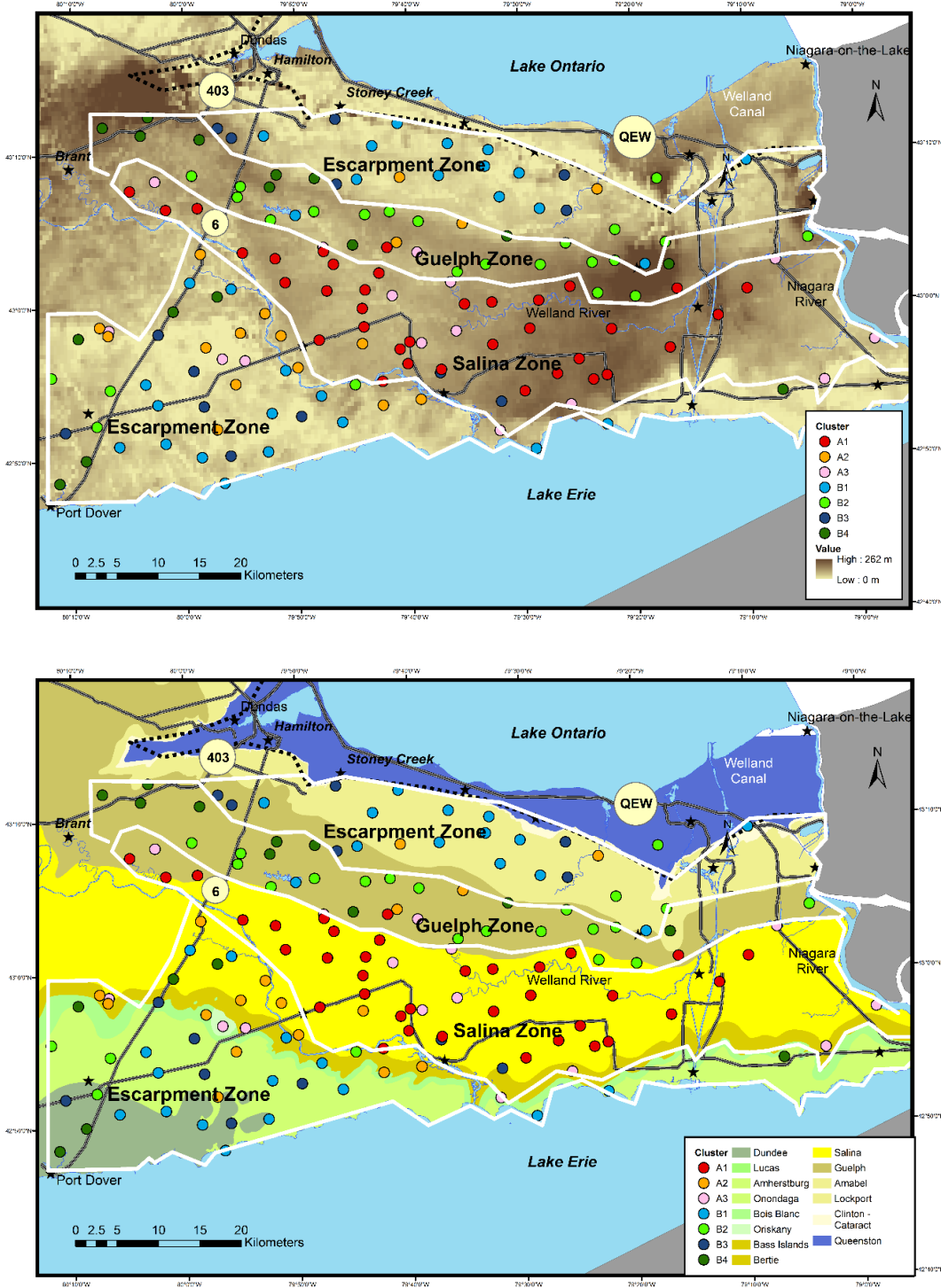


Figure 5.1: Geochemical Zones defined using results of HCA overlain on (a) drift thickness and (b) the Paleozoic Geology. Three Geochemical Zones were defined; the Escarpment Zone, Guelph Zone and Salina Zone.

5.1 Geological Context of the Niagara Geochemical Anomaly

An initial comparison of bedrock groundwater chemistry on the Niagara Peninsula was completed during the course of an undergraduate thesis by Matheson (2012). He suggested that corroding ‘century’ abandoned gas wells were a primary source for the differentiation between groundwater chemical concentrations on the Niagara Peninsula and elsewhere in southern Ontario. This was based on the hypothesis that corrosion of abandoned gas wells at various depths may result in the influx of brackish, highly mineralized groundwater from deeper formations to fresher shallow aquifers.

Limitations in sample density, isotopic characterization, and hydrogeological data restricted the interpretation of Matheson’s study and this was partly the justification for the collection of additional data and initiating this current study. The investigation of the ‘leaking gas well’ hypothesis was a primary component of this study, and is supported by geochemical evidence described below, including the introduction of a reduced carbon source for sulfate reduction, high sulfate concentrations where a reasonable sulfide source is not available, and $\delta^{13}\text{C}$ isotopic signatures within the thermogenic methane range described in other studies conducted on the north shore of Lake Erie near the study area (Barker and Fritz, 1981). Cl/Br ratios reflective of Appalachian Basin Brines (ABB) in Devonian carbonate formations provide additional evidence for the vertical migration of fluids, as the ABB signatures originates from halite precipitation during the upper Silurian.

Groundwaters obtained on the Niagara Peninsula tend to be highly mineralized compared to elsewhere in southern Ontario, with elevated concentrations of sulfate, calcium, magnesium, potassium, sodium, bromide, chloride, nickel, strontium, lithium and dissolved organic carbon (Table 4.1). Bicarbonate displays a bimodal distribution on the Niagara Peninsula, with extremely high values (many > 300 mg/L) in the southwestern and northern peninsula and low

concentrations (<80 mg/L) in the central Salina Group. Figure 5.2 – 5.6 provides a comparison of the groundwater chemistry of major ions from bedrock formations on the Niagara Peninsula and elsewhere in southwestern Ontario.

To compare groundwater chemical compositions between the Niagara Peninsula and the host bedrock formations, geochemical transects from Lake Huron to the Niagara River were plotted for each of the three main bedrock sequences: the Silurian carbonates, Silurian evaporites and Devonian carbonates (Figures 5.7 – 5.9). The '0' point on the figure represents Canfield, ON, a hamlet located in the geographic centre of the Niagara Peninsula. The results of these plots show elevated average concentrations of sulfate, calcium and magnesium on the Niagara Peninsula for each of the three formations. A cross-sectional transect running north-south across the central Niagara Peninsula revealed elevated concentrations of the anomalously elevated parameters centered on the Salina Group, within the boundaries of the Salina bedrock trough.

The Niagara Peninsula is uniquely situated in southern Ontario because it lies in the Appalachian Basin, whereas the same formations elsewhere exist along the Algonquin Arch, or westwards, in the Michigan Basin. Divergence of groundwater chemistry between the Niagara Peninsula and elsewhere may therefore, be due to variations in bedrock mineralogy based on the geological setting. Most groundwater wells in Silurian – Devonian carbonates on the Niagara Peninsula are completed at depths of less than 50 m from ground surface (Table 4.3), with the deepest wells located in the central Niagara Peninsula under thick, relatively impermeable sediment cover (Hamilton et al., 2011). Elevated sulfate, calcium and magnesium concentrations west of the Algonquin Arch (Figures 5.7 – 5.9) in the Salina Group suggests bedrock mineralogy controls groundwater chemistry within this formation. The much higher average values for magnesium east of the Algonquin Arch on the Niagara Peninsula (Figure 5.3) is likely the result of dedolomitization.

Although water-rock interaction likely influences the geochemical character of bedrock groundwater, elevated concentrations of calcium, magnesium and sulfate in the Niagara Peninsula compared to elsewhere in southern Ontario shows that geochemistry is likely also controlled by differences in thicknesses of quaternary sediments, the presence of surficial and bedrock features and the degree of ‘openness’ of the system. The western Salina Group is capped by sands and gravels near Lake Huron in contrast to the clays present in Niagara and this may result in the presence of ‘closed-system’ conditions with lower bicarbonate concentrations on the Niagara Peninsula.

When geological and hydrogeological factors have been considered, remaining differences between the geochemical conditions on the peninsula and elsewhere in the same geological units may result from anthropogenic influences including additions of surface contaminants such as road salt, septic systems and agricultural fertilizers, and the potential impact of deep brines and methane inputs by the vertical migration of fluids through abandoned gas well casings (Matheson, 2012). Elevated sulfate, calcium and magnesium concentrations are not present in groundwater from the Silurian carbonates and Devonian carbonates bedrock formations west of the Algonquin Arch (Figures 5.2 - 5.4), suggesting differences in bedrock geology, hydrogeological conditions or the impact of anthropogenic sources on the Niagara Peninsula.

Geochemical characterization of grouped zones on the Niagara Peninsula and the proposed biogeochemical reactions and geological processes that control their respective groundwater chemistry is discussed in this chapter. Where the geochemical assemblage of a sample does not appear to result from geological and hydrogeological factors, further investigation of natural and anthropogenic influences on groundwater chemistry is discussed. These ‘outliers’ may assist in determining the mechanisms responsible for anomalous groundwater chemistry in parts of the Niagara Peninsula.

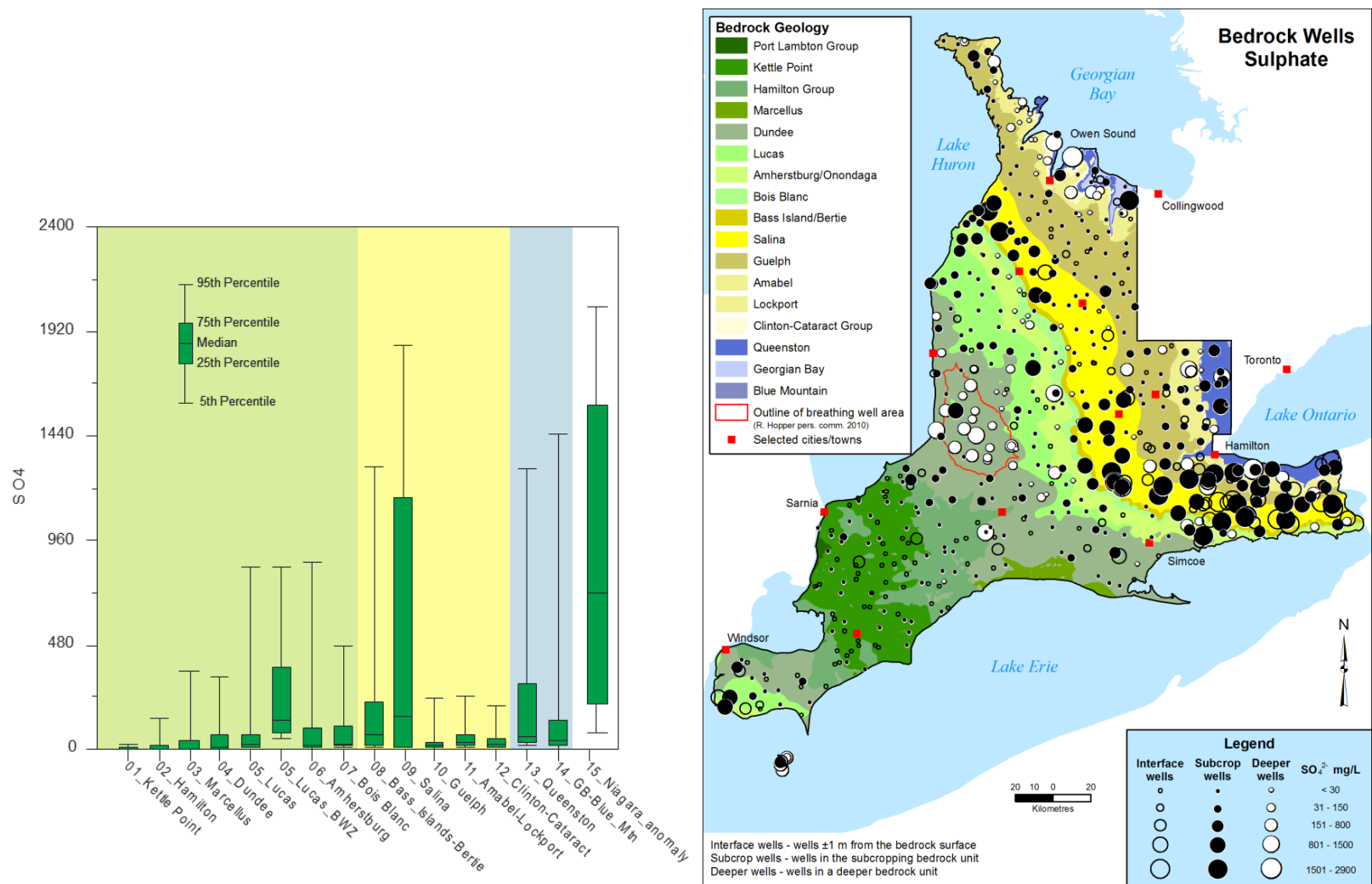


Figure 5.2: Comparison between Sulfate concentrations (mg/L) obtained from bedrock wells on the Niagara Peninsula and from bedrock formations in southern Ontario.

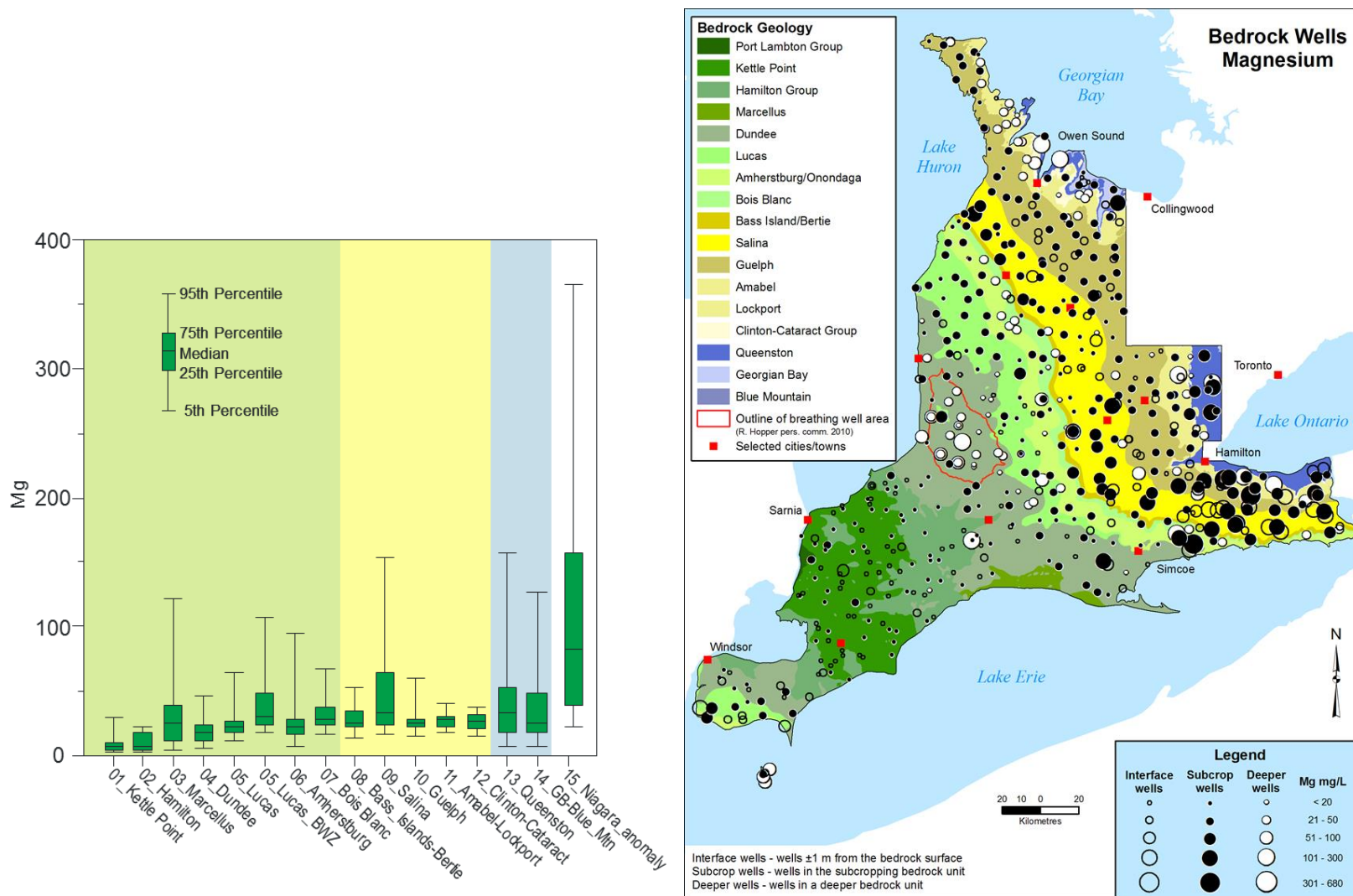


Figure 5.3: Comparison between Magnesium concentrations (mg/L) obtained from bedrock wells on the Niagara Peninsula and from bedrock formations in southern Ontario.

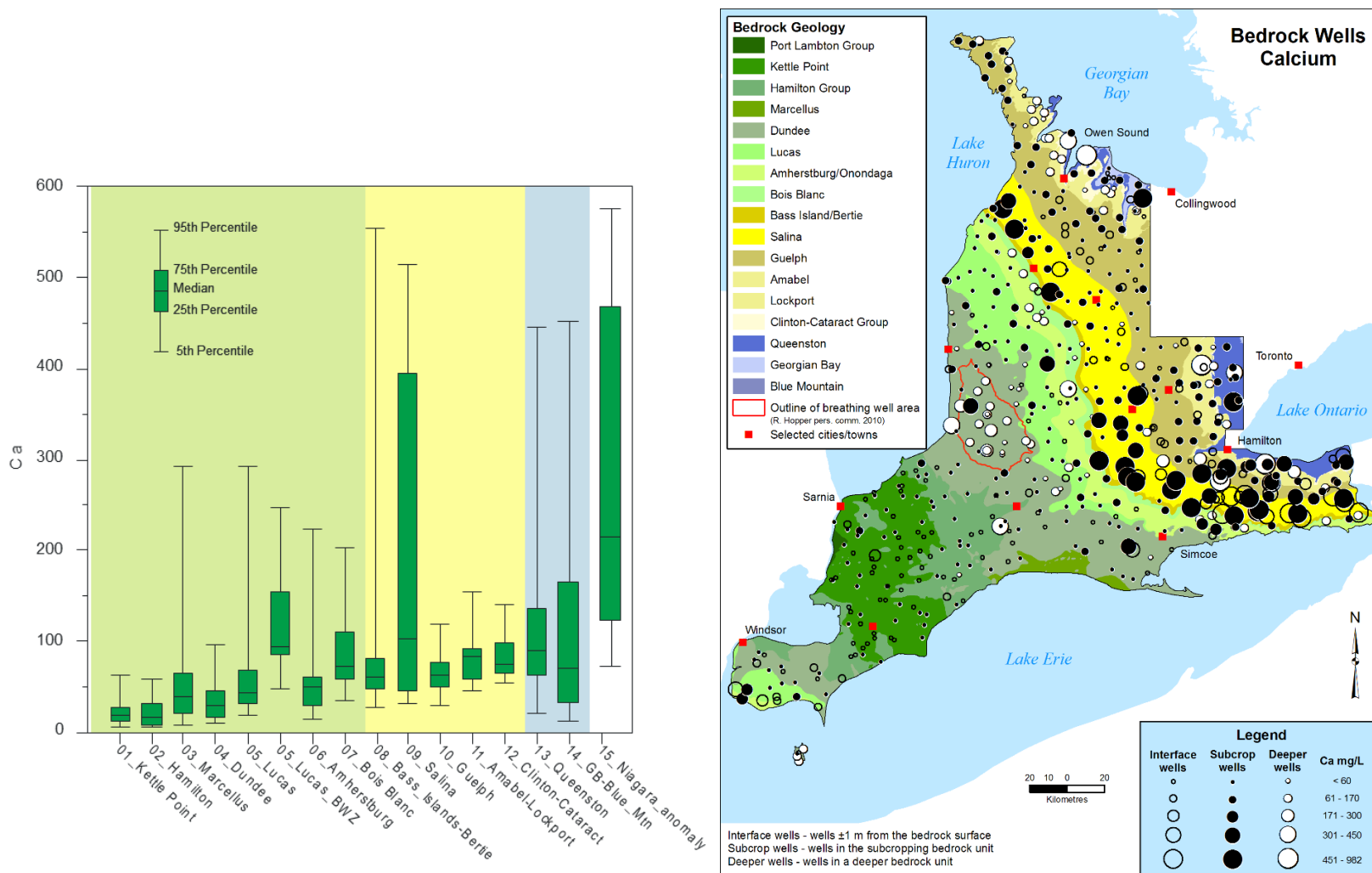


Figure 5.4: Comparison between Calcium concentrations (mg/L) obtained from bedrock wells on the Niagara Peninsula and from bedrock formations in southern Ontario.

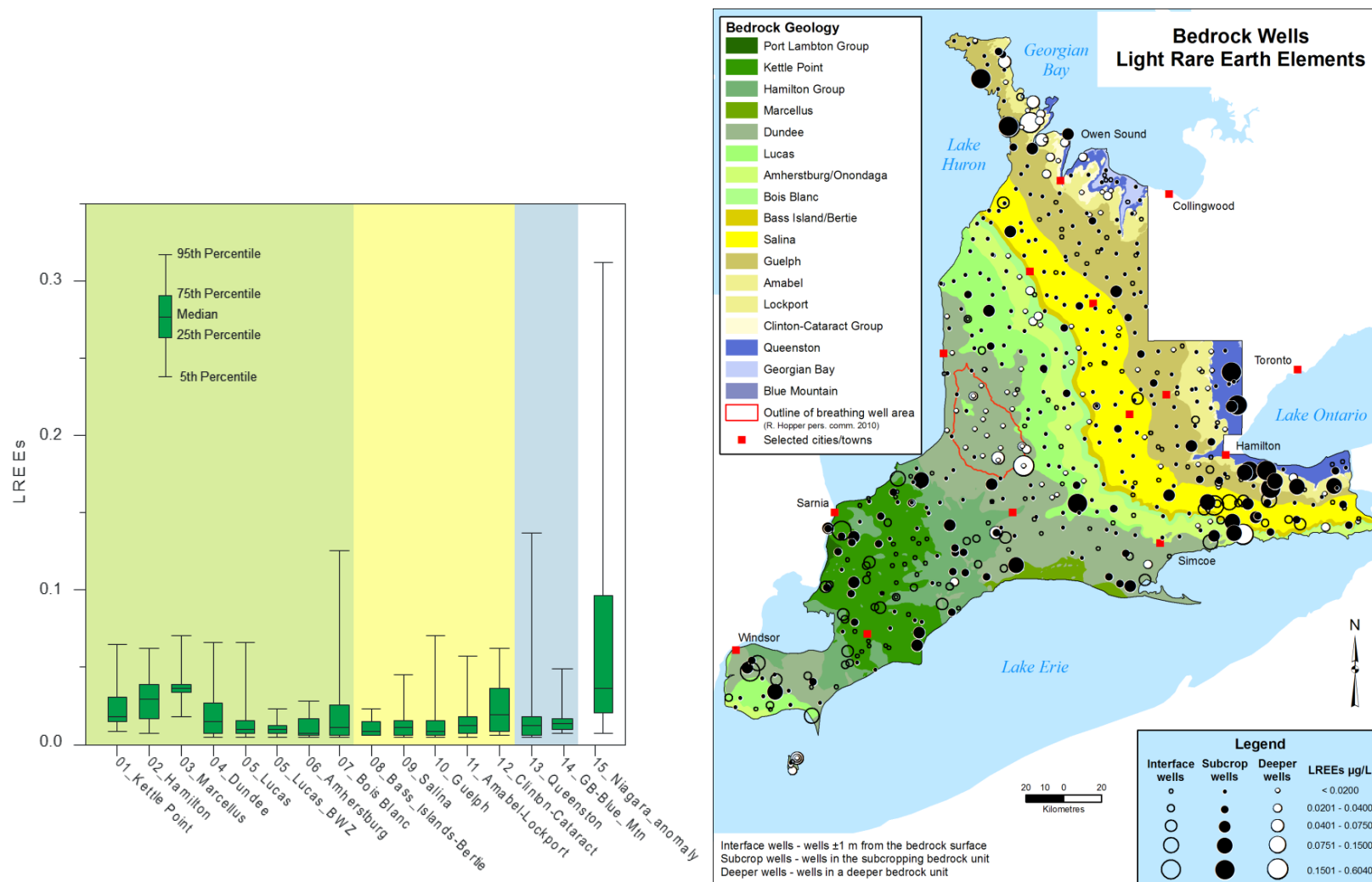


Figure 5.5: Comparison between Light Rare Earth Element concentrations ($\mu\text{g/L}$) obtained from bedrock wells on the Niagara Peninsula and from bedrock formations in southern Ontario.

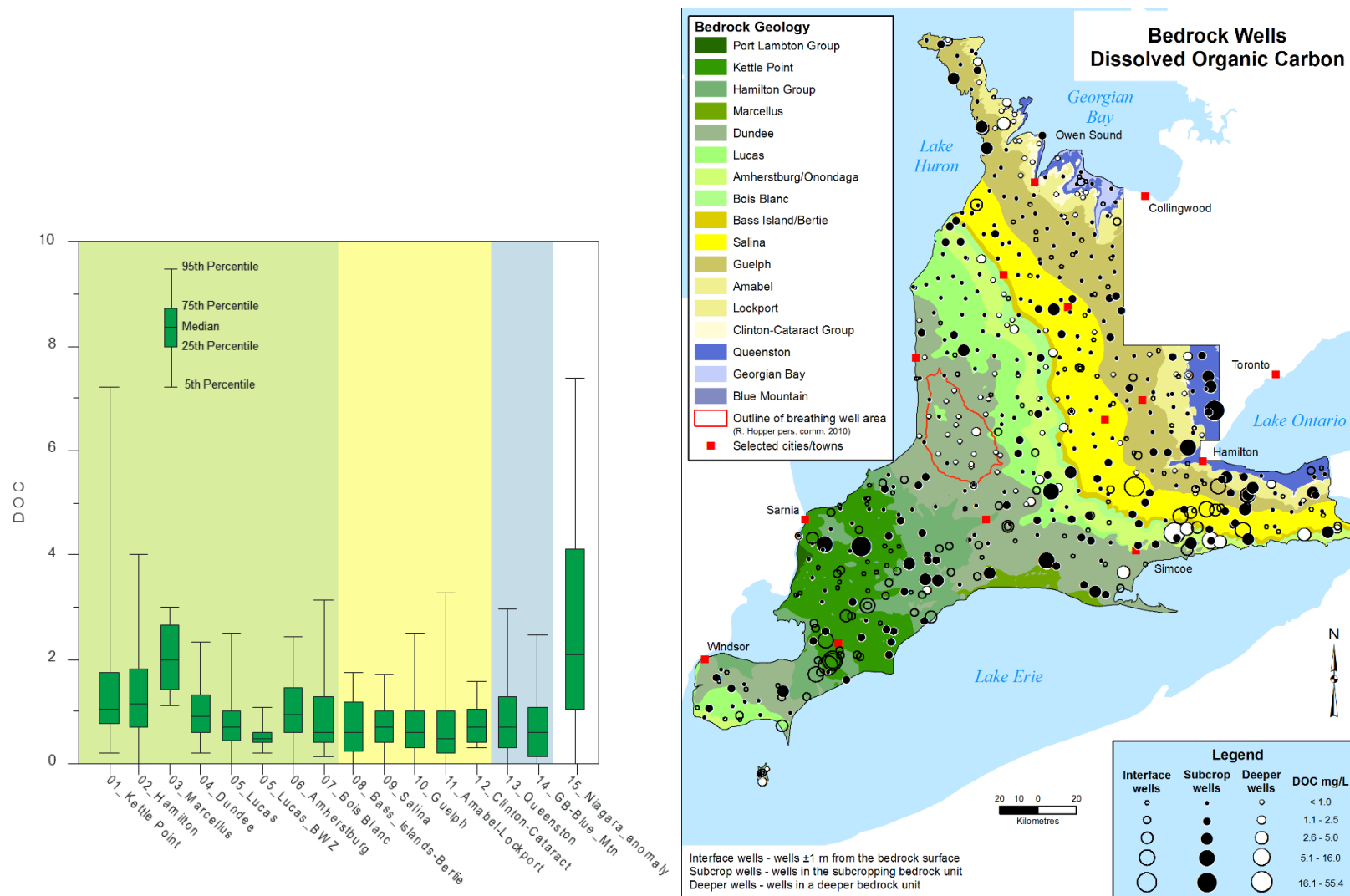


Figure 5.6: Comparison between Dissolved Organic Carbon concentrations (mg/L) obtained from bedrock wells on the Niagara Peninsula and from bedrock formations in southern Ontario.

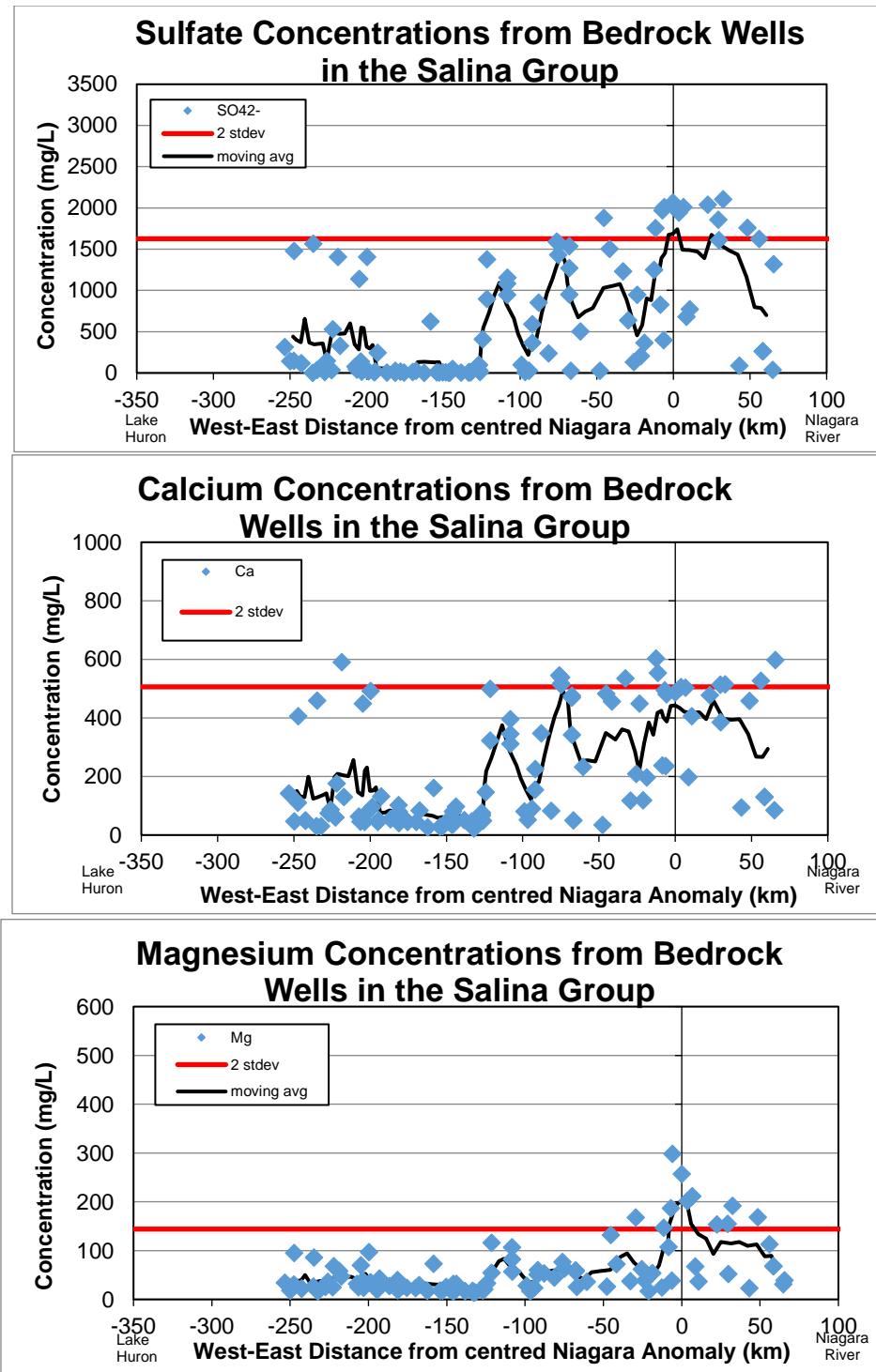


Figure 5.7: Longitudinal plots of SO_4^{2-} , Ca^{2+} and Mg^{2+} for the Salina Group transecting from Lake Huron in the west to the Niagara River in the east. The black line, centred on 0, indicates the centre on the Niagara Peninsula near Canfield, ON. The red line represents two standard deviations from the mean, excluding data from the Niagara Peninsula.

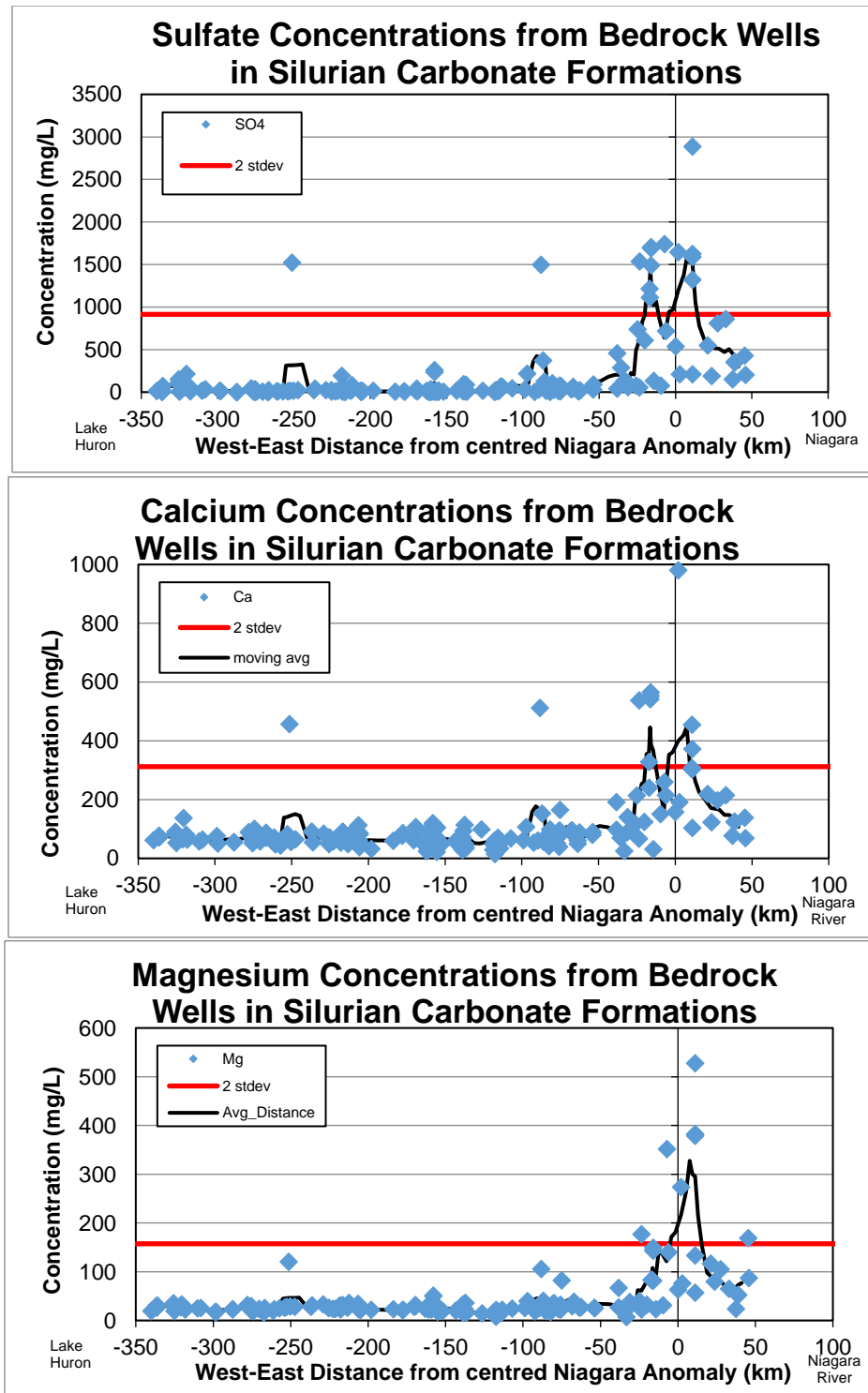


Figure 5.8: Longitudinal plots of SO₄²⁻, Ca²⁺ and Mg²⁺ for the Silurian carbonate units transecting from Lake Huron in the west to the Niagara River in the east. The black line, centred on 0, indicates the centre on the Niagara Peninsula near Canfield, ON. The red line represents two standard deviations from the mean, excluding data from the Niagara Peninsula.

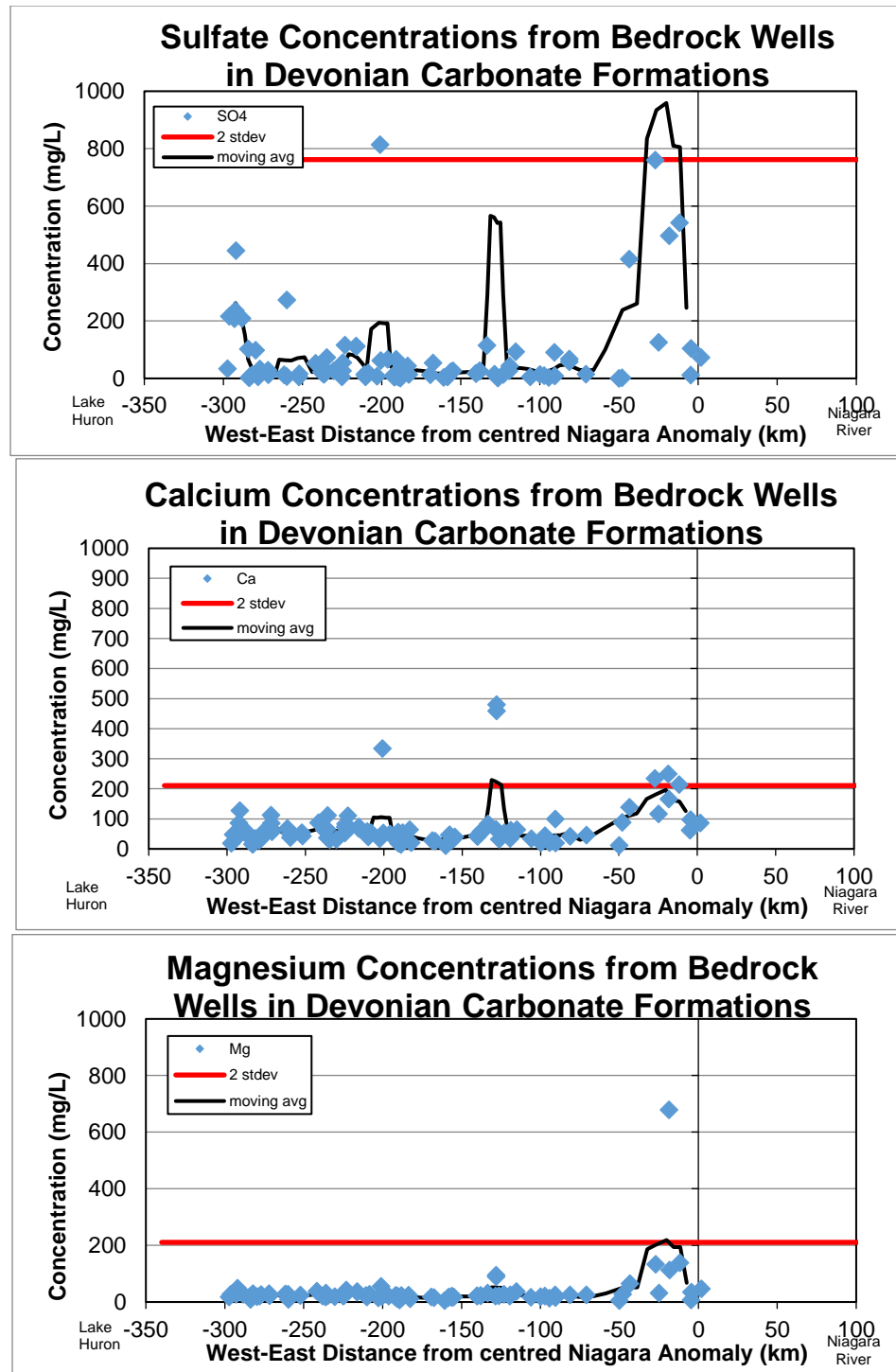


Figure 5.9: Longitudinal plots of SO₄²⁻, Ca²⁺ and Mg²⁺ for the Devonian carbonate units transecting from Lake Huron in the west to the Niagara River in the east. The black line, centred on 0, indicates the centre on the Niagara Peninsula near Canfield, ON. The red line represents two standard deviations from the mean, excluding data from the Niagara Peninsula.

5.2 Regional Hydrogeology of the Niagara Peninsula

The Niagara and Onondaga Escarpments are the primary regional bedrock recharge areas on the Niagara Peninsula (Figure 2.9). Topographic highs encourage recharge and these two escarpments represent the highest parts of the peninsula (Figure 5.10). Further, as Quaternary-aged sediments on the Niagara Peninsula are primarily composed of low-permeability silt and clay (Burt, 2015) recharge to bedrock aquifers is expected to be associated with regions where these sediments are thinnest and the most oxidized which also occurs along the escarpments. Thin drift thickness overlying the high permeability, 'glacial rubble' interface aquifer and exposed bedrock susceptible to recent and past karstification provides ample opportunity for recharge but also for surface contaminants, including road salt and septic waste to reach shallow bedrock aquifers (Brunton, 2013). Groundwater flow is hardly laminar in bedrock aquifers on the Niagara Peninsula, as the presence of karst landforms dominates groundwater movement where the potentiometric surface encourages groundwater flow (Worthington, 2002). Conduit flow can rapidly recharge rain and snow-melt where bedrock is exposed at surface.

Figure 5.1 displays the thickness of quaternary sediments overlain by clusters of groundwater samples colour-coded by geochemical zone. The lowest median drift thicknesses in the study area (Table 4.3) exists in cluster B1 (21.0 ft) and cluster B3 (25.0 ft), the locations for which are primarily along the Niagara and Onondaga Escarpments in areas of thin drift thickness. Several samples from B1 and B3 have drift thickness values <5 ft, suggesting locations are present where bedrock is exposed at the surface. Where drift thickness is thinnest the HCA clusters also indicate elevated concentrations of parameters reflective of surface contamination and modern precipitation, including road salt and septic influence (from Cl/Br ratios), elevated concentrations of HCO_3^- , and in some samples, elevated concentrations of NO_3^- and bacteria (Table 4.3). Elevated tritium and $\delta^{18}\text{O}_{\text{H}_2\text{O}}$ isotopic signatures in B1 and B3 are reflective of meteoric precipitation

and indicate modern recharge dominates groundwater chemistry along the two escarpments (Table 4.3, Figure 4.21, Figure 5.11).

Another recharge area on the Niagara Peninsula includes the medium-high permeability sediments in the Fonthill ice contact delta complex (NPCA, 2005). The Fonthill complex is the highest topographic point on the Niagara Peninsula, and provides groundwater recharge to the only cold-water creek (12 Mile Creek) within the Niagara regional boundaries. One sample (15-AG-181) obtained from the overburden aquifer at the highest point of the Fonthill ice contact delta complex, has surface influence (high NO_3^-) and a low electrical conductivity (789 $\mu\text{S}/\text{cm}$) in comparison to samples obtained from the surrounding Silurian bedrock (Figure 4.2). The Fonthill ice contact delta complex recharges bedrock aquifers, as demonstrated by the lower conductivities in bedrock surrounding the feature and in overburden-interface aquifer samples (east, 15-AG-168 = 364 $\mu\text{S}/\text{cm}$; west, 15-AG-114 = 481 $\mu\text{S}/\text{cm}$, northeast, 15-AG-172 = 716 $\mu\text{S}/\text{cm}$; northwest, 15-AG-134 = 416 $\mu\text{S}/\text{cm}$) (Figure 5.12). In contrast, the conductivity values are generally much higher in the highly mineralized Salina Group and the southern portion of the Guelph (Eramosa) Formation (Figure 5.12). Bicarbonate values are higher in samples influenced by the Fonthill complex than in surrounding background samples.

In contrast to the escarpments, the Salina trough and Guelph Formation are overlain by low permeability clay and silt sediments that restrict groundwater movement, as demonstrated by low tritium and isotopically depleted $\delta^{18}\text{O}_{\text{H}_2\text{O}}$ signatures (Figure 5.12). As diffusion is a slow process, recharge through the thick clays in the Salina trough is restricted and inputs of groundwater to the Salina Group and eastern Guelph Formation occurs due to lateral movement down-gradient from the regional recharge areas along the Niagara and Onondaga Escarpments. A potentiometric high exists in the western Guelph Formation near Ancaster, Ontario, with decreasing hydraulic head eastwards across much of the peninsula (Figures 2.9 and 5.11). As groundwater moves

down-gradient following recharge in the western Guelph Formation, geochemical evolution via carbonate dissolution and secondary mineral dissolution and oxidation occurs. Low tritium values indicate slow groundwater recharge through the low-permeability clay and silt sediments (Burt, 2015; Menzies and Taylor, 1998) confining the bedrock aquifer (Figure 5.12).

The Canfield groundwater catchment (Figure 2.8 and Figure 5.11) is mostly within the Salina trough. It is partially fed by the Hamilton catchment to the northwest (Matheson, 2012) and ultimately by recharge along the Niagara Escarpment. Low tritium, including many samples below detection (<0.8 TU), implies groundwater recharge occurred prior to 1952 in bedrock aquifers of the central to eastern Salina Group (Figure 5.11, Clark and Fritz, 1997). A positive relationship between conductivity values ($\mu\text{S}/\text{cm}$) and $\delta^{18}\text{O}_{\text{H}_2\text{O}}$ isotopic compositions (Figures 4.1, 4.17 and 4.19) of groundwater samples in the Salina Zone implies sluggish movement of groundwater in the region, which would allow more time for biogeochemical cycling and water-rock geochemical processes. Poor water quality and low population density resulting in low pumping rates limits groundwater removal from the bedrock aquifer, contributing to the maintenance of stagnant conditions in the regional hydrogeological system. Based on tritium data, a transition zone is apparent in the Guelph Formation between fresh, recently recharged groundwater along the Niagara Escarpment and old, mineralized groundwater in the Salina trough (Figure 5.11).

The presence of low tritium concentrations in the Erigan, Chippawa-Niagara Falls and Crystal Beach buried bedrock channels suggests little recharge from Lake Erie itself (Campbell and Burt, 2015). However, the potentiometric surfaces in these channels are below the water level of Lake Erie, even at the shore of the lake (Matheson, 2012). The potentiometric data suggest that the entire Wainfleet groundwater catchment (Figures 2.9 and 5.11) is being recharged from groundwater stored under Lake Erie and northward flow is indicated. In the central Wainfleet area, many groundwater samples show $\delta^{18}\text{O}_{\text{H}_2\text{O}}$ isotopic

signatures representative of mixing between Pleistocene-aged, glacially-influenced groundwater and more recent meteoric water ($\delta^{18}\text{O}_{\text{H}_2\text{O}} = -12$ to -17 ‰) (Figures 4.16 and 4.17, McIntosh and Walter, 2006). Drimmie et al., (1993) found isotopically depleted $\delta^{18}\text{O}_{\text{H}_2\text{O}}$ signatures indicative of Pleistocene recharge in groundwater under sediments of the Great Lakes including Lake Erie.

Accordingly, the low tritium and the Pleistocene-influenced $\delta^{18}\text{O}_{\text{H}_2\text{O}}$ signature in waters in the Wainfleet groundwater support the potentiometric data and indicate northward flow in the bedrock aquifer originating from beneath Lake Erie clays.

The Townline Tunnel is a car and rail tunnel under the Welland Canal at the eastern extremity of the Wainfleet watershed east of Welland, ON. It has been consistently dewatered since beginning operations in 1968 (Farvolden and Nunan, 1970). Pumping tests conducted at the Townline Tunnel caused a cone of depression resulting in a greater than expected water level drop of 4.5 m in a domestic well located 8 km west of the tunnel (Farvolden and Nunan, 1970). Influence from pumping appeared to be greater in wells located to the west of the pumping site, compared to wells located to the east or to the northwest, near the Fonthill ice contact delta complex (Farvolden and Nunan, 1970). The bedrock geology present at the site (Salina Group) described by Farvolden and Nunan (1970) was noted to be dolomite with interbedded shales, with cavities and fractures near the interface between bedrock and overlying low-permeability, clay-rich soils. The study did not mention the presence of anhydrite or gypsum, soluble calcium-sulfate minerals; they attributed the Ca-SO_4 geochemical facies present at the site to influence of the soils during recharge. Furthermore, the presence of a buried bedrock channel (now known as the Chippawa – Niagara Falls tunnel) underlying the Townline Tunnel area was not mentioned in the study. Recent investigation of the hydrogeological conditions of buried bedrock channels on the Niagara Peninsula (Campbell and Burt, 2015) showed lower water levels near the Townline Tunnel in the Chippawa-Niagara Falls channel

(Figure 5.13), confirming the presence of a regional cone of depression related to the tunnel dewatering. The cone of depression extends at least to the Wainfleet town centre (Figure 5.13), and the potentiometric and isotopic data just discussed suggests the influence may extend to the shore or even beneath Lake Erie. Tritium values below detection (<0.8) in all wells within the cone of depression in the Chippawa-Niagara Falls Channel indicates that if any younger waters had previously infiltrated along the Onondaga Escarpment, they have been replaced by or mixed with a larger component of Pleistocene waters from under Lake Erie.

The presence of gypsum in the down-cut bedrock (Salina Group) at the Townline Tunnel is clearly visible during field visits. Dissolution of gypsum due to long-term pumping has the potential to contribute to an enlargement of conduits and enhancement of permeability at the Townline Tunnel. To sustain water levels at the site, higher pumping rates may be required through time, resulting in increased risk of land collapse as the presence and size of solution-enhanced conduits increase during evaporite dissolution.

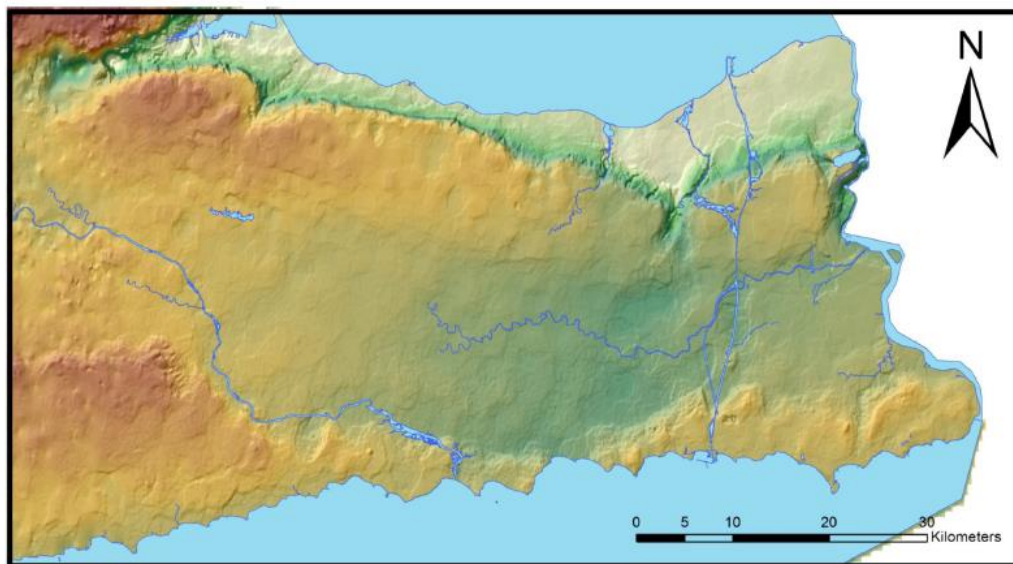


Figure 5.10: Bedrock topography on the Niagara Peninsula. Higher elevations are represented in red and yellow, and lower elevations are represented in green.

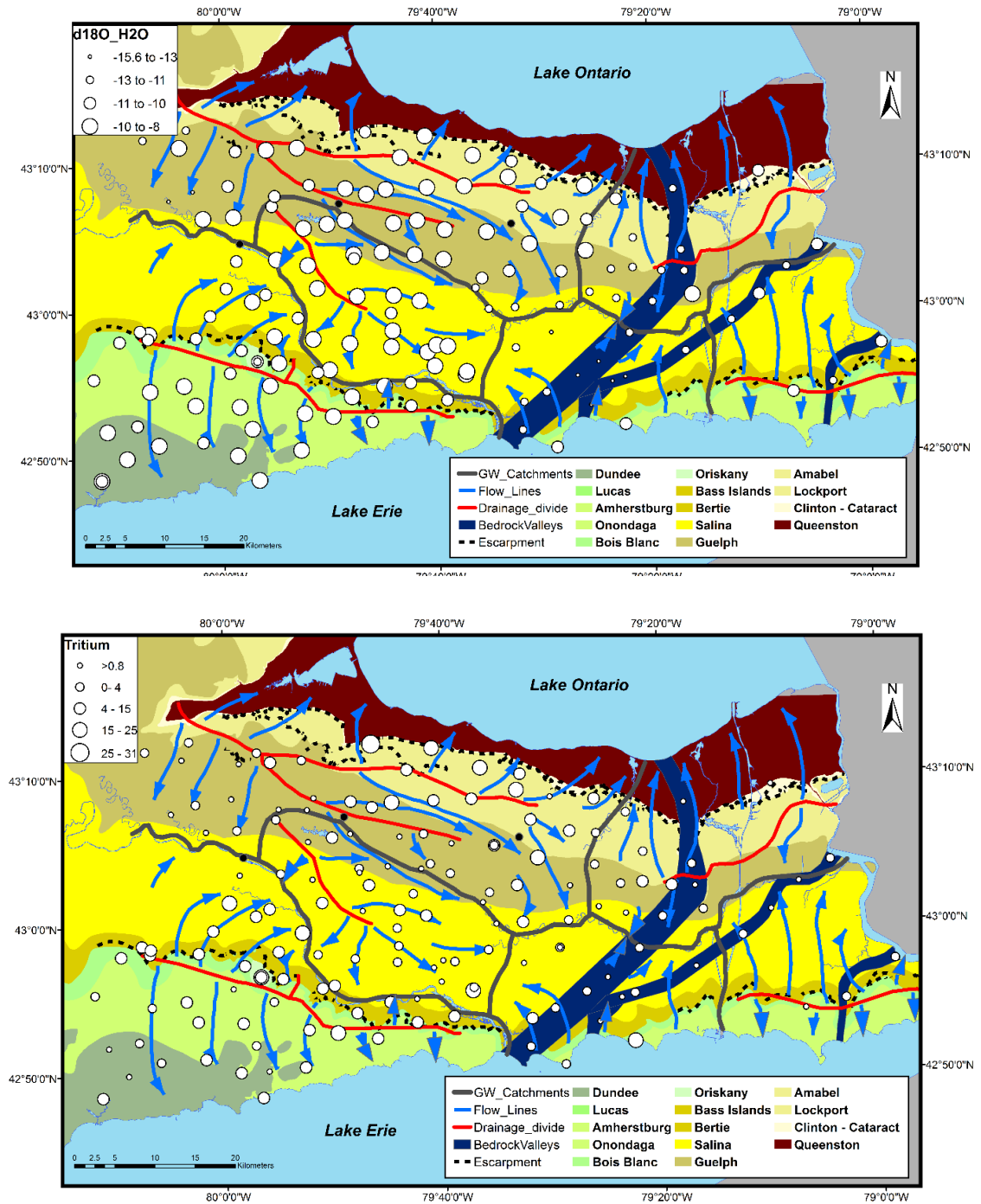


Figure 5.11: (a) Tritium and (b) $\delta^{18}\text{O}_{\text{H}_2\text{O}}$ isotopic signatures within groundwater catchments (Matheson, 2012) on the Niagara Peninsula. Buried bedrock valleys (Campbell and Burt, 2015) are shown in blue.

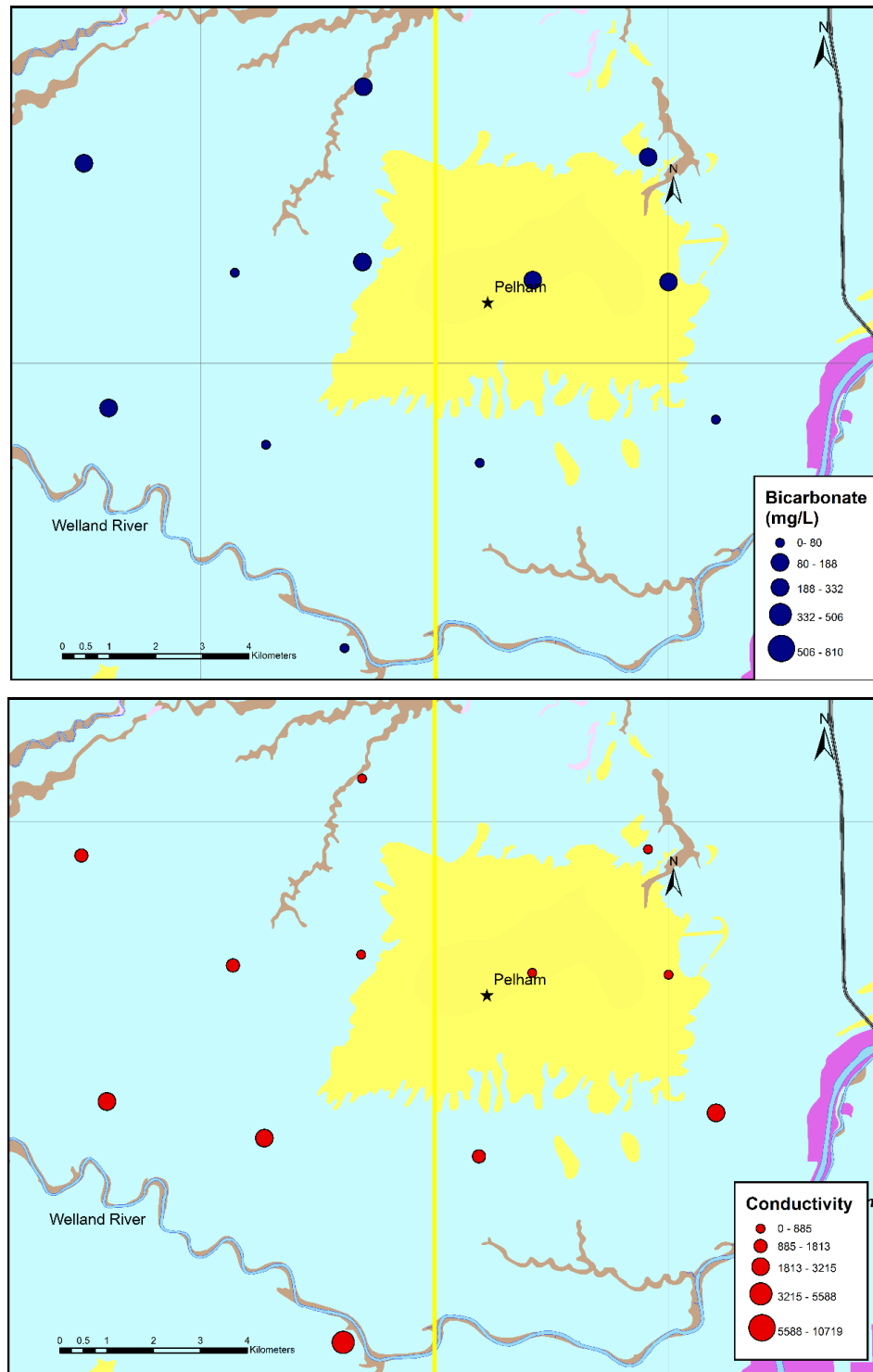


Figure 5.12: (a) Bicarbonate concentrations (mg/L) and (b) Conductivity ($\mu\text{S}/\text{cm}$) in wells located near the Fonthill ice contact delta complex.

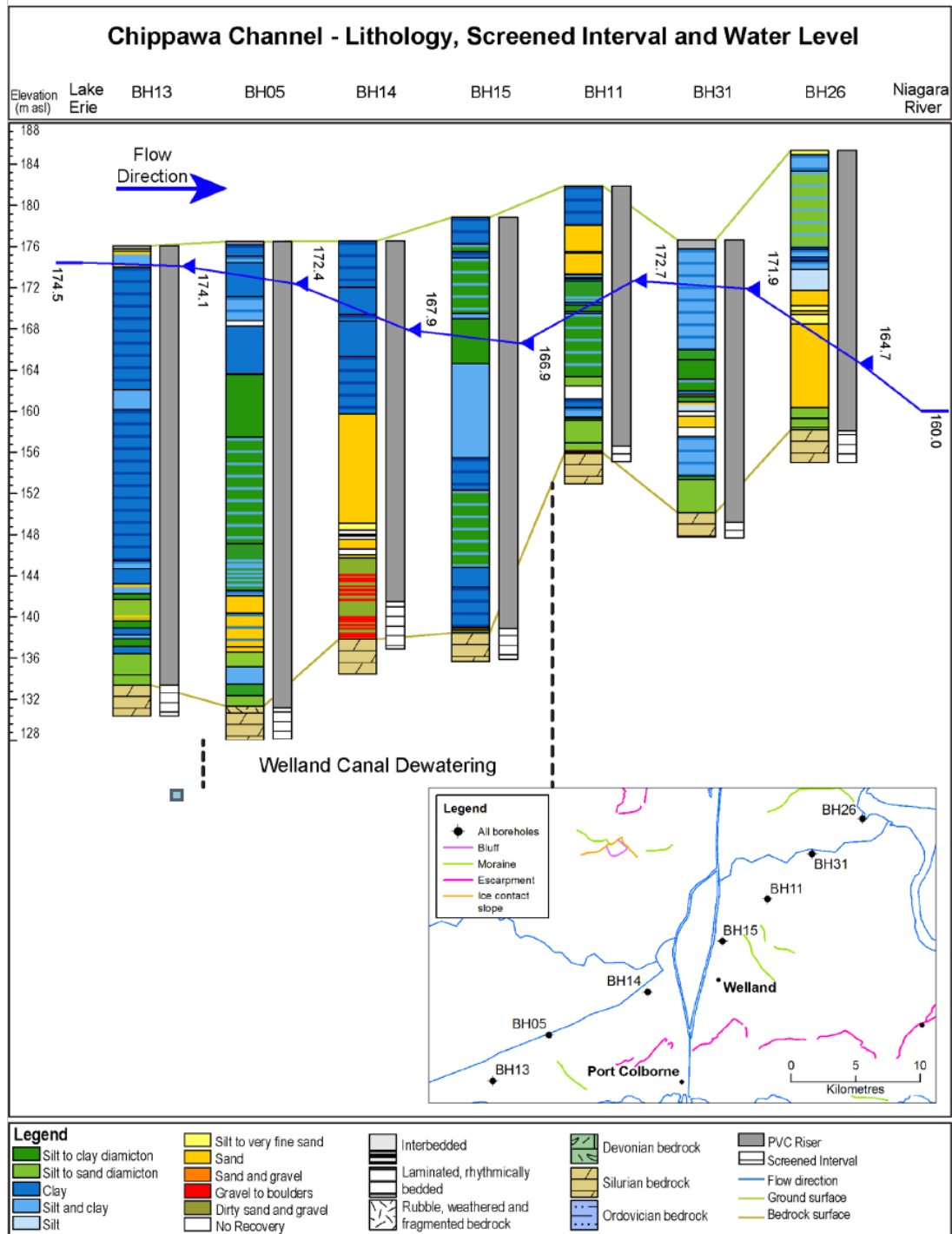


Figure 5.13: Water levels in the Chippawa (Niagara Falls) Channel from Lake Erie to the Niagara River. The cone of depression resulting from the dewatering of the Welland Townline Tunnel is visible in water level measurements taken along the tunnel in 2015 (Campbell and Burt, 2015).

5.3 Escarpment Zone Geochemical Grouping

The Escarpment Zone includes two east-west bands of samples at the northern and southern extents of the study area in close proximity to the crests of the Niagara and Onondaga Escarpments (Figure 5.1). The Escarpment Zone consists of groundwater samples primarily from clusters B1 and B3, with several from clusters A2, B2, and B4 (Figure 5.1). The two parts of this zone encompass (1) the City of Hamilton and the northern portion of the Region of Niagara and (2) Haldimand County, Norfolk County and the southern portion of the Region of Niagara. The northern Escarpment Zone entirely falls within the formational boundaries of the Lower Silurian Lockport Formation trending west-east from the City of Hamilton to the City of Niagara Falls. The southern Escarpment Zone includes groundwater samples obtained from western parts of the Silurian Salina Group and Bass Islands, Bertie Formations; and the lower Devonian Oriskany, Bois Blanc, Onondaga and Dundee Formations.

Groundwater samples obtained from the northern and southern portions of the Escarpment Zone display similar chemical assemblages represented by cluster groupings, water-type analysis, and isotopic composition. The similarity in chemistry between the two areas indicates that the presence of the two escarpments and their shallow carbonate host-rocks controls the geochemical composition of groundwater both north and south of the Salina trough and Guelph Formation. Large scale, comprehensive driving factors of groundwater chemical composition in the Escarpment Zone include carbonate bedrock mineralogy, open-system conditions due to thin sediment cover and modern groundwater recharge along the two bedrock topographic highs. With the exception of a number of samples obtained from the Bass Islands/Bertie Formation and the western Salina Group most waters from the Escarpment Zone are collected from non-evaporitic carbonate bedrock formations with localized influence from surface contamination and recent recharge. The zones also

contain a number of outliers identified by isotopically enriched $\delta^{34}\text{S}_{\text{SO}_4}$ signatures and Cl/Br Ratios that are discussed further below.

Escarpment Zone waters have Ca-HCO₃, Ca-SO₄, Mg-HCO₃ or Mg-SO₄ geochemical facies (Figure 4.6 – 4.11), and the majority have (1) high tritium values, (2) isotopically enriched $\delta^{18}\text{O}_{\text{H}_2\text{O}}$ and $\delta^2\text{H}_{\text{H}_2\text{O}}$ signatures and (3) isotopically depleted values of $\delta^{34}\text{S}_{\text{SO}_4}$, $\delta^{34}\text{S}_{\text{S}_2}$, $\delta^{13}\text{C}_{\text{DOC}}$, $\delta^{13}\text{C}_{\text{DIC}}$, and $\delta^{13}\text{C}_{\text{CH}_4}$ (Table 4.5, Figures 4.16, 4.17, 4.20, 4.21, 4.23, 4.24, 4.29, 4.31). Median HCO₃⁻ concentrations for groundwater in the escarpment areas are the highest in the study area (Figure 4.3), with values of 441 mg/L, 446 mg/L and 354 mg/L (Table 4.3), for clusters A2, B1 and B3 respectively. Median electrical conductivity for groups B1 and B3, which comprise the majority of the Escarpment Zone samples, are low (1466 $\mu\text{S}/\text{cm}$ and 1116 $\mu\text{S}/\text{cm}$, respectively, Table 4.3) in comparison to the rest of the study area. Low to moderate concentrations of hydrogen sulfide are found in nearly all samples from cluster B1, however, hydrogen sulfide is rarely detected in B3.

Many samples from the Escarpment Zone have groundwater composition indicative of surface influence, and in some cases, anthropogenic contamination, with elevated concentrations of HCO₃, DOC, NO₃⁻, and Coliform Bacteria (Figure 4.2, Table 4.3). Evidence for anthropogenic contamination of shallow bedrock aquifers underlying thin drift in the Escarpment Zone is clearly displayed from Cl/Br ratio mixing lines, as nearly all samples falling on the dilute groundwater - septic waste and dilute groundwater - halite (road salt) mixing lines are found in the Escarpment Zone (Figure 4.15). Median Cl/Br mass ratios of clusters B1 and B3 are 448 and 315 respectively; the highest in the study area (Table 4.3, Figure 4.15).

Samples from cluster A2 (Figure 5.1) are scattered across the western study area, with most its 18 locations present in the part of the southern Escarpment Zone study area underlain by the two Silurian evaporitic units (Salina Group and

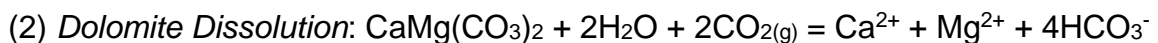
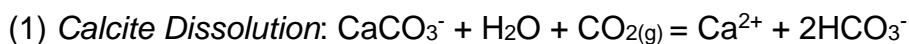
Bass Islands Formation). A2 is characterized by pH values <7, the highest Mg^{2+} concentrations of any of the groups, and elevated Ca, Fe, Sr and Si relative to other clusters (Table 4.3, Figures 4.9 – 4.10). The median conductivity value of 2700 $\mu S/cm$ for A2 is in the intermediate range relative to other clusters, as is the median tritium value of 4.74 TU (Table 4.3).

Interestingly, A2 is the only geochemical group in the study area with both elevated HCO_3^- (median value = 441 mg/L) and SO_4^{2-} (median value = 1810 mg/L) concentrations (Table 4.3). As discussed earlier in Chapter 4.2, the A2 Cluster has a mixed geochemical character. In the Devonian carbonate units in the southwestern part of the peninsula and in the Lower Silurian units in the northern Escarpment Zone, the mixed character of A2 is likely the result of a component of deeper, more brackish groundwater migrated to the Escarpment Zone shallow aquifer. A possible mechanism for the vertical migration of fluids could be through anthropogenically and naturally derived vertical conduits, including abandoned gas wells, vertical fractures and faults. A2 samples located in Devonian and Lower Silurian carbonates will be discussed as ‘outliers’ later in this chapter, and the source of the highly mineralized and mixed character of these samples determined.

5.3.1 Bedrock Geochemistry, Escarpment Zone

Ca- HCO_3 groundwater facies and elevated HCO_3^- concentrations in groundwater located in close proximity to the Niagara and Onondaga Escarpments is consistent with carbonate interaction as a controlling mechanism on groundwater chemistry. Mineral solubility is dependent on variations in the partial pressure of CO_2 , temperature, cation-exchange reactions and differences in the equilibrium constant between co-existing minerals (Freeze and Cherry, 1979). Environments with shallow sediments and exposed bedrock containing high dissolved CO_2 concentrations consistently replenished due to a connection with the atmosphere are described as open-system conditions (Appelo and Postma, 2005). These

geological conditions exist on the Escarpment Zone, as bedrock is exposed at surface or has sediment cover less than 10 m thick nearly everywhere in this zone. Fracturing and oxidation of clays has been noted up to 10 m below ground surface (Burt, 2016, P. Comm) in sediment cores obtained during recent drilling in the Escarpment Zone (Burt 2013, 2014, 2015). Clays on the Niagara Peninsula are swelling clays, which may undergo minor expansion in the presence of road salt. The mineralogical composition of the Devonian and Silurian bedrock in the Escarpment Zone consists of calcite (CaCO_3) and dolomite ($\text{CaMg}(\text{CO}_3)_2$), which undergo open-system dissolution in the presence of slightly acidic water (Equations 1 and 2);



Groundwater recharge on the Niagara Peninsula has a large winter snowmelt component (Matheson, 2012). Carbonate dissolution under open-system conditions and the addition of Ca^{2+} and HCO_3^- to saturation in near the ground surface, low-temperature waters, results in subsequent supersaturation and calcite precipitation under warmer conditions at greater depths below the ground surface (Clark, 2015). If early in the flow system, groundwater dissolves dolomite to equilibrium at temperatures greater than 10°C and later encounters calcite, dissolution of calcite will then occur because the equilibrium constant of dolomite is greater than that of calcite. Ca^{2+} and HCO_3^- will increase in solution and become supersaturated with respect to dolomite, but due to a slow dolomite precipitation reaction supersaturation will not result in significant precipitation of dolomite (Appelo and Postma, 2005).

Groundwater samples range from undersaturated to supersaturated for calcite and dolomite in the Escarpment Zone (Figure 4.12 – 4.14), with supersaturated samples predominantly found in B1 (12 of 30 samples for calcite, 8 of 30 samples for dolomite) and A2 (8 of 18 samples for calcite, 6 of 18 samples for

dolomite). All samples except one in A2 are at or above saturation with respect to calcite, and nearly half of samples are at equilibrium or supersaturated with respect to dolomite. As groundwater samples obtained from group A2 have a mixed geochemical character (see Chapter 4.2), supersaturation of calcite could be the result of the addition of Ca^{2+} and SO_4^{2-} from evaporite-impacted fluids from the Silurian Salina Group or Bass Islands Formation. Cluster B3 is undersaturated with respect to calcite and dolomite in the Escarpment Zone, representing recently recharged groundwater.

The input of isotopically enriched DIC from the dissolution of marine carbonates ($\delta^{13}\text{C} = \sim 0 \text{ ‰}$) will drive $\delta^{13}\text{C}$ isotopic compositions to more enriched values, however the degree of “openness” of the system determines the influence of carbonate dissolution on $\delta^{13}\text{C}_{\text{DIC}}$ values (Clark and Fritz, 1997). In open system conditions, infiltrating surface water and precipitation will hydrate and dissociate soil CO_2 , increasing concentrations of carbonate species in the DIC pool (Figure 4.29). The proportion of carbonate species represented by HCO_3^- and CO_3^{2-} is dependent on the pH of the groundwater system. Interaction between the atmosphere and soil CO_2 will drive $\delta^{13}\text{C}_{\text{DIC}}$ isotopic compositions to the $\delta^{13}\text{C}$ composition of DIC in equilibrium with soil CO_2 ($\delta^{13}\text{C} = \sim -14 \text{ ‰}$ at 25°C and neutral pH, Clark and Fritz, 1997). Most samples within the Escarpment Zone have isotopically depleted $\delta^{13}\text{C}_{\text{DIC}}$ isotopic compositions, near -14 ‰ (Figure 4.29). Open-system conditions yield higher $p\text{CO}_2$ and higher concentrations of DIC that has $\delta^{13}\text{C}_{\text{DIC}}$ closer to soil values than closed-system conditions (Figure 4.33). The extremely high bicarbonate values present in groundwater samples from the Escarpment Zone (Figure 4.2) may result from this process.

The Silurian Salina Group is characterized by argillaceous dolostones with high contents of anhydrite and gypsum. When in contact with groundwater (Armstrong and Carter, 2010) these contribute significant loadings of Ca^{2+} and SO_4^{2-} to bedrock groundwater (Eberts and George, 2000). Samples located in the western Salina Group largely consists of Ca-SO_4 waters (Figure 4.6), confirming

the influence of gypsum dissolution on groundwater chemistry in the area. The Ca-SO₄ geochemical facies is located further down the flow system from areas where Ca-HCO₃ waters dominate at the crest of the Onondaga Escarpment. This indicates greater interaction with evaporates during groundwater movement from the crest of the topographic high on the Onondaga Escarpment toward the Salina trough. Similarly, south of the crest of the Niagara Escarpment, groundwater transitions from Ca-HCO₃ to Ca-SO₄ geochemical facies to the south. A portion of the Escarpment Zone exists within the formational boundaries of the Salina Group near Caledonia, Ontario. This area lies south of the boundaries of the Salina bedrock trough, and exhibits chemistry reflective of mixing between groundwater recharged along the Onondaga Escarpment in Devonian carbonates and the evaporites present in the Salina Group and Bass Islands Formation.

5.3.2 Influence of Biogeochemical Cycling on Groundwater Chemistry

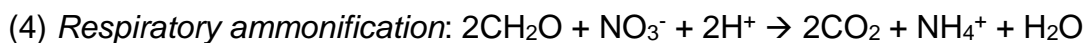
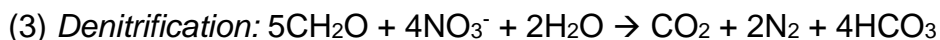
What follows is an interpretation of the Escarpment Zone groundwater chemistry from the perspective of biogeochemical cycling. With the exception of fecal and total coliform, no bacteriological data were collected as part of this study. However, the geochemical and isotopic data available can be used to make inferences about biogeochemical processes that may be occurring and these in turn may inform the discussion on the origin of the anomalous geochemical responses observed on the peninsula. First it is necessary to introduce several biogeochemical processes and concepts. This will be followed by a discussion of how the evidence supports the importance of such processes in modifying the groundwater chemical and isotopic signature in the Escarpment Zone and then the implications regarding sources of the anomalous solutes.

Geochemical reactions catalyzed by microbial populations can vary spatially based on the availability of electron acceptors and donors, redox conditions and

additions of organic and inorganic parameters from both anthropogenic and natural sources. Cl/Br ratios from the Niagara and Onondaga Escarpment areas show surface influences including those of septic, road salt and agricultural contaminants. Some samples also show the influence of deep sources, specifically mixing between shallow groundwaters and Appalachian Basin Brines (ABB) (Figures 4.15, 5.13, 5.14, 5.15; Table 4.3). Samples with Cl/Br ratios reflective of ABB signatures likely reflect the influence of upward migration of fluids originating in the lower Salina group through conduits that may include natural fractures and faults or abandoned gas well casings. Brine-impacted samples will be discussed later in this chapter as outliers, as these samples do not reflect the expected natural geochemical environments and common anthropogenic concerns resulting from the natural geological conditions of the shallow carbonate aquifers at the sites.

High localized concentrations of redox-sensitive nitrogen species (NO_3^- , NO_2^- , and $\text{NH}_3/\text{NH}_4^+$) may support the occurrence of nitrate reduction within the Escarpment Zone (Figure 5.16). The high Cl/Br ratios in many of these samples and a corresponding association with thin drift areas suggests the nitrogen compounds may have originated as NO_3^- from agricultural or septic sources and have subsequently been reduced. The metabolic pathway utilized during nitrate reduction depends on the presence of electron donors. Organic carbon is thermodynamically favored in nitrate reduction over most other electron donors including reduced sulphur compounds. Denitrification (Equation 3) and respiratory ammonification (Equation 4) are the two competing metabolic pathways responsible for nitrogen reduction using carbon as an electron donor. The metabolic pathway utilized for nitrogen reduction depends on the pH and temperature conditions of the groundwater, and the availability of carbon. Denitrification is the prominent nitrogen reduction pathway where the organic carbon electron donor is limited. Where the electron acceptor (e.g. NO_3^- , NO_2^-) is limited, respiratory ammonification (dissimilatory nitrate reduction to ammonium)

is the preferential pathway (Yoon et al., 2015). The presence of intermediate nitrogen species is a good indicator of nitrate reduction in groundwater systems; however, nitrate reduction commonly proceeds to the end product. An accompanying increase in pH and increased concentrations of carbonate species in groundwater will occur with complete nitrate reduction coupled to carbon oxidation.



The presence of intermediate nitrogen species, high $p\text{CO}_2$ and HCO_3^- concentrations, and isotopically depleted $\delta^{13}\text{C}_{\text{DIC}}$ signatures indicates that carbon oxidation is occurring in the Escarpment Zone, which may be related to nitrate reduction. Denitrification reactions add isotopically light organic carbon (average soil $\delta^{13}\text{C}_{\text{DOC}} = -25 \pm 2 \text{‰}$ in the study area from clusters) to the DIC reservoir, driving the $\delta^{13}\text{C}_{\text{DIC}}$ isotopic composition of the host groundwater to more depleted values. High DOC, DIC, NO_3^- , NO_2^- and NH_4^+ concentrations coupled with isotopically depleted $\delta^{13}\text{C}_{\text{DIC}}$ signatures and meteoric $\delta^{18}\text{O}_{\text{H}_2\text{O}}$ signatures in several localized regions attests to nitrate reduction as a mechanism controlling the geochemical evolution of groundwater in some samples in the Escarpment Zone.

Elevated hydrogen sulfide concentrations and elevated sulfate concentrations in many areas of the Escarpment Zone may suggest sulfur cycling as a dominant process occurring in bedrock aquifers in the region. Alternatively, where extremely elevated SO_4^{2-} concentrations are present, an exogenous sulfate source may be responsible for sulfur inputs in the shallow groundwater bedrock aquifers. Samples displaying evidence for an exogenous sulfate source are describe in more detail in the 'outliers' section. Most waters collected from the Escarpment Zone are from primarily non-evaporitic carbonate bedrock with the

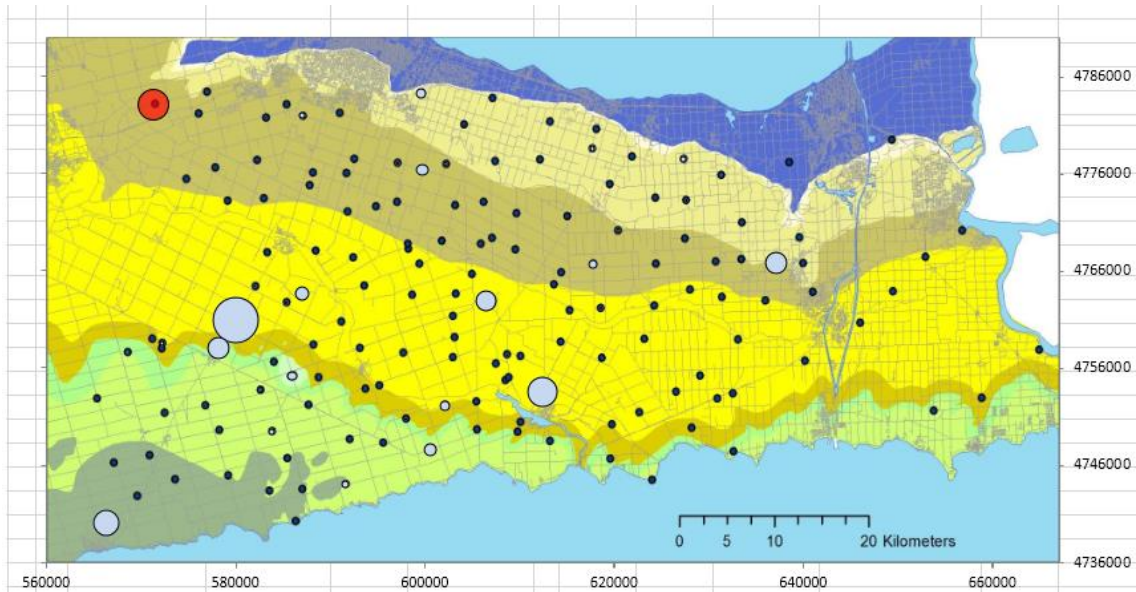
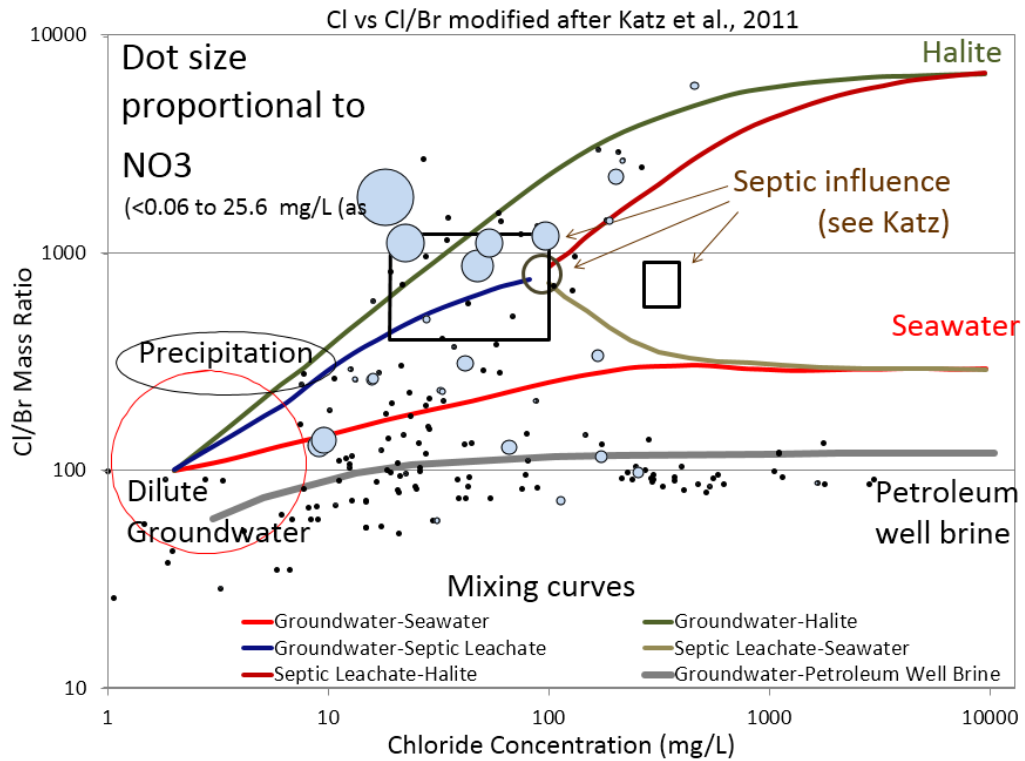


Figure 5.14: (a) Elevated Nitrate concentrations plotted on a chloride concentration vs. Cl/Br mass ratio chart. Elevated Nitrate concentrations are shown by the larger blue dots on figure (a). (b) Location of elevated Nitrate concentrations in Niagara.

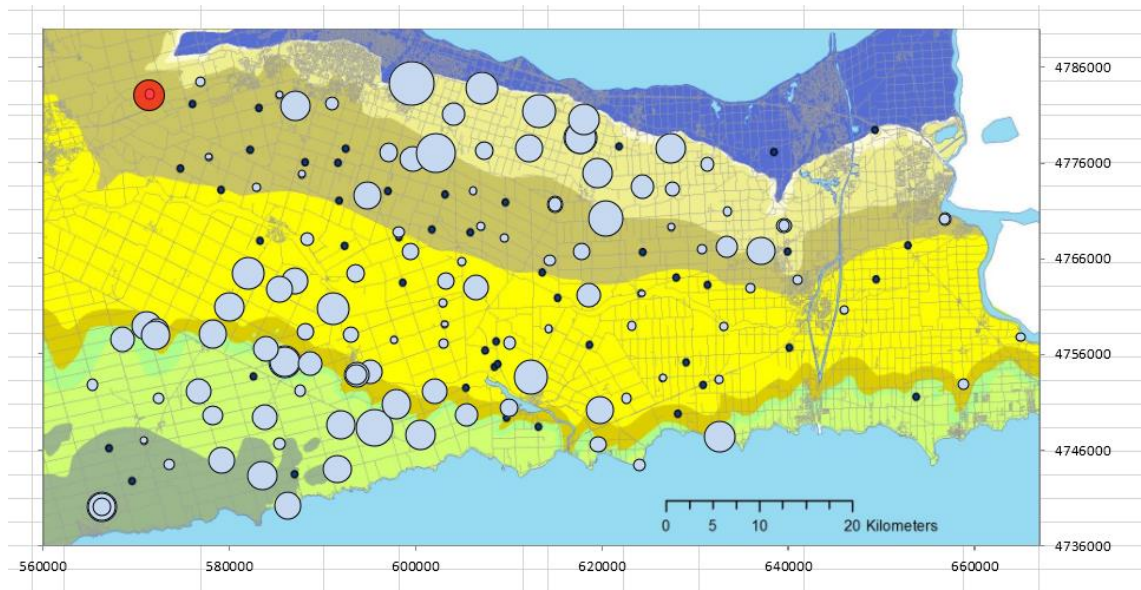
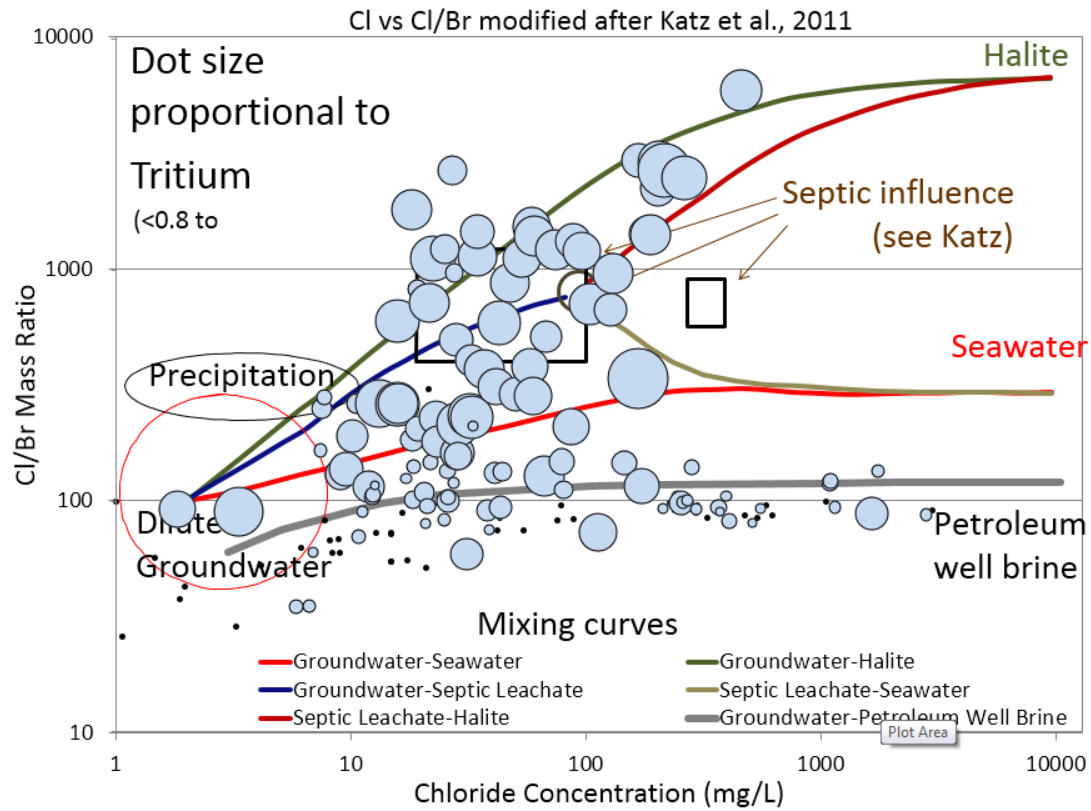


Figure 5.15: (a) Tritium values plotted on a chloride concentration vs. Cl/Br mass ratio chart. High Tritium is shown by the larger blue dots on figure (a). (b) Location of high Tritium in Niagara.

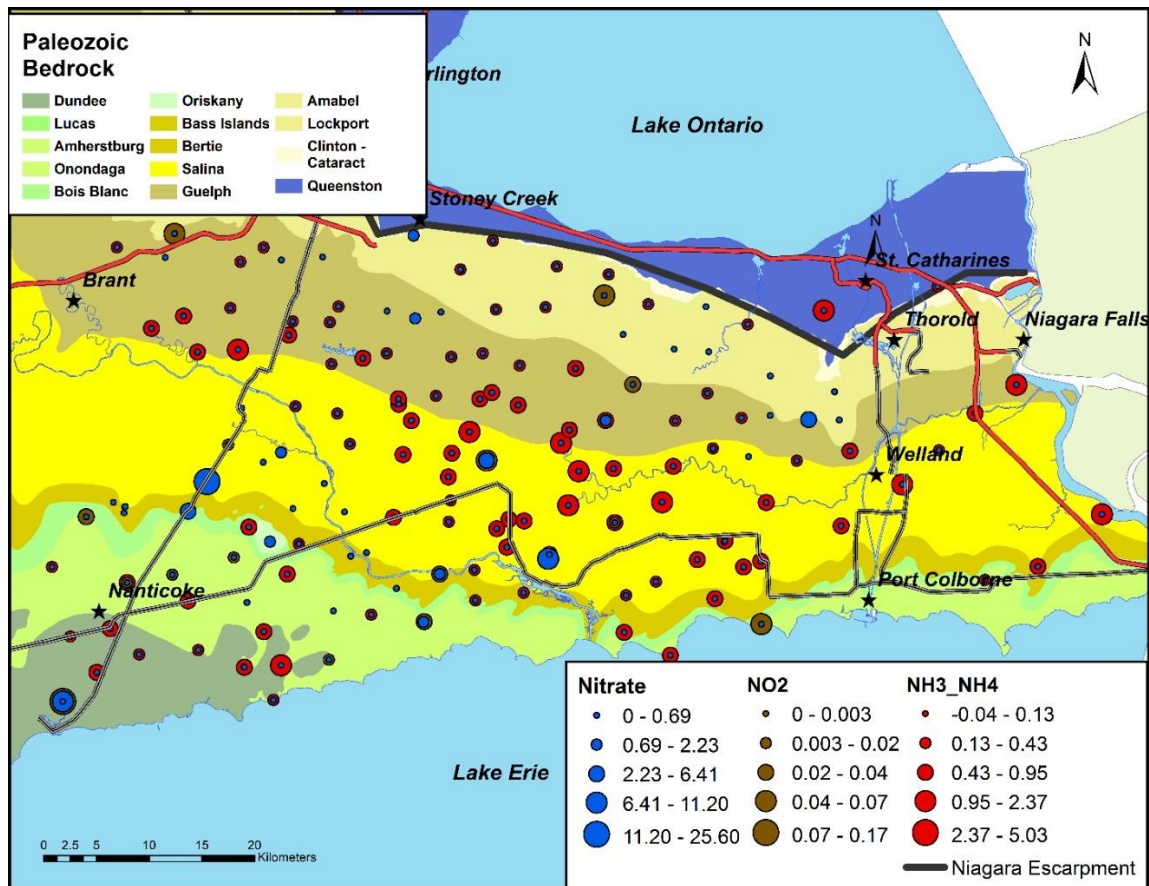


Figure 5.16: Nitrate, Nitrite and Ammonia concentrations (mg/L) on the Niagara Peninsula.

notable exception of those from the Salina Group and Bass Islands Formation. However, minor evaporitic sulfate sources exist in a much less significant extent in Devonian and Silurian carbonate units, particularly in the Dundee Formation, Eramosa Formation, and Goat Island and Gasport Members of the Lockport Group. Isotopic evidence for the oxidation of sulfide minerals, including pyrite, in southern Ontario shallow bedrock groundwater systems has been delineated by several researchers in recent years (Matheson, 2012; Freckelton, 2013; Skuce, 2014). Sulfide oxidation can be abiotic or biologically mediated, and can occur by several different pathways depending on the environmental conditions present. Biologically-mediated sulfide oxidation occurs primarily in unsaturated zone,

aerobic environments and proceeds at a faster rate than chemical oxidation pathways (Taylor et al., 1984).

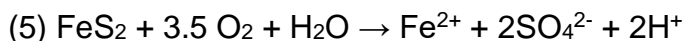
Biologically mediated reduced sulfur oxidation requires the transfer of 8 electrons through a series of intermediate reactionary steps. Intermediate sulfur species produced during the transfer of electrons from reduced aqueous and terrestrial sulfur species (ex. hydrogen sulfide, pyrite, sphalerite), to the most oxidized sulfur species, sulfate (SO_4^{2-}), include elemental sulfur (S^0), thiosulfate ($\text{S}_2\text{O}_3^{2-}$), tetrathionate ($\text{S}_4\text{O}_6^{2-}$) and sulfite (SO_3^{2-}). Pyrite and sphalerite are common constituents of sedimentary carbonate rocks and sediments, formed primarily in the depositional environment in the presence of organic matter. During oxidation of solid-phase sulfide, the $\delta^{34}\text{S}$ isotopic signature of sulfate does not show large variations from the precursor reduced sulfide isotopic composition; although depending on the oxidizing organism or material and pathway utilized an isotopic ^{34}S enrichment or depletion of a few permil has been reported (Fry et al., 1986). Values of $\delta^{34}\text{S}$ for sedimentary sulfides range from -24.2 to + 7.0 ‰ for marine carbonate formations located in the Findlay Arch District, Ohio (Carlson, 1994). Other studies of groundwater chemistry in southern Ontario have plotted maximum $\delta^{34}\text{S}_{\text{SO}_4}$ values representative of pyrite oxidation as high as +10 ‰ (Skuce, 2014; Matheson, 2012). Fractionations of -6 to -18 ‰ have been reported in the resulting sulfate for microbially-mediated oxidation of aqueous sulfide (Taylor et al., 1984).

The $\delta^{18}\text{O}_{\text{SO}_4}$ isotopic signature of sulfate resulting from pyrite (or sphalerite) oxidation is dependent on the interaction between $\delta^{18}\text{O}_{\text{SO}_4}$ and $\delta^{18}\text{O}_{\text{H}_2\text{O}}$ and the metabolic pathway taken during pyrite oxidation. Where sulfide oxidation occurs under aerobic conditions, a larger percentage of oxygen from the atmosphere (87.5 %) than water (12.5 %) is incorporated into the resulting sulfate (Taylor et al., 1984). With this in mind, the oxygen isotopic fractionation factor ($\delta^{18}\text{O}_{\text{SO}_4\text{-H}_2\text{O}}$) can indicate the redox reaction utilized for pyrite oxidation to sulfate. Where values are low ($\delta^{18}\text{O}_{\text{SO}_4\text{-H}_2\text{O}} = 1\text{-}4$), reaction occurs under saturated, anaerobic

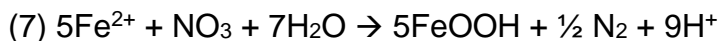
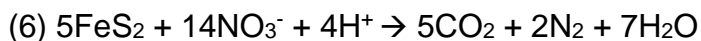
conditions, utilizing Fe^{3+} or NO_3^- as electron acceptors. Where values are higher ($\Delta^{18}\text{O}_{\text{SO}_4\text{-H}_2\text{O}} = 16\text{-}20$), pyrite oxidation occurs in the vadose zone, where conditions are unsaturated and the system is in connection with atmospheric oxygen (Equation 5). Most samples in the Escarpment Zones with $\delta^{34}\text{S}_{\text{SO}_4}$ signatures representative of sulfide oxidation ($\delta^{34}\text{S}_{\text{SO}_4} < 10\text{‰}$) have oxygen fractionation factors reflective of aerobic oxidation in connection with atmospheric oxygen ($\delta^{18}\text{O}_{\text{SO}_4} > 3\text{‰}$, Figure 5.17).

In the absence of oxygen as an electron acceptor, pyrite oxidation coupled to denitrification can occur producing high concentrations of dissolved SO_4^{2-} and Fe^{2+} and decreasing NO_3^- in the groundwater composition (Equations 6 to 8, Aravena and Robertson, 1998). Low concentrations of Fe^{2+} in groundwater may not suggest the absence of minor pyrite oxidation, as Fe^{2+} may be oxidized to Fe^{3+} and precipitated as amorphous ferric hydroxide ($\text{Fe}(\text{OH})_3$). Additionally, it is possible that the oxidation of organic matter and oxidation of pyrite coupled to nitrate reduction can happen simultaneously in some locations (Aravena and Robertson, 1998). The presence of a few isotopically depleted $\delta^{18}\text{O}_{\text{SO}_4}$ signatures ($\delta^{18}\text{O}_{\text{SO}_4} < 0\text{‰}$) with low SO_4^{2-} concentrations may suggest the presence of either abiotic or biologically-mediated pyrite oxidation in saturated conditions utilizing NO_3^- or Fe^{3+} as electron acceptors in parts of the Escarpment Zone (Figure 5.17).

Pyrite Oxidation using Oxygen as an Electron Donor:



Pyrite Oxidation using Nitrate as an Electron Donor:

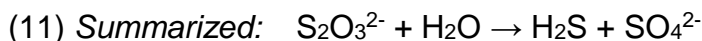


The $\delta^{34}\text{S}_{\text{SO}_4}$ and $\delta^{18}\text{O}_{\text{SO}_4}$ data suggests pyrite oxidation as a source of minor SO_4^{2-} in bedrock aquifers where isotopically depleted $\delta^{34}\text{S}_{\text{SO}_4}$ values are indicative of a terrestrial sedimentary sulfide source. Complete oxidation of pyrite using oxygen as an electron acceptor would result in significant acid production causing a decrease in pH to 2-3 in a non-buffered environment, however in carbonate terrains, influences of pyrite oxidation on pH is minimal for minor oxidation due to neutralization by carbonate species. Alternatively, the oxidation of aqueous sulfides could result in similar $\delta^{34}\text{S}_{\text{SO}_4}$ and $\delta^{18}\text{O}_{\text{SO}_4}$ isotopic signatures where SO_4^{2-} is in low concentrations. At high SO_4^{2-} an exogenous source of sulfate must be present, as substantial pyrite oxidation would result in a significant suppression of pH and elevated Fe^{2+} concentrations (>10 mg/L), which are not seen on the Niagara Peninsula.

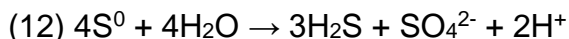
The multi-reaction transfer of electrons during sulfide oxidation to sulfate results in the production of several sulfur intermediate species, many of which are retained in the aquifer and available for further sulfur cycling. Light to bright yellow water, an indicator of colloidal (elemental) sulfur was noticed in several wells within the Escarpment Zone (Figure 5.18), providing further evidence for the presence of sulfur intermediates in the study area.

Disproportionation (simultaneous oxidation and reduction) of intermediate sulfur species can result in the production of both H_2S and SO_4^{2-} in groundwater (Equations 9 to 12; Canfield et al., 1998), as seen in many locations within the Escarpment Zone. Disproportionation of sulfur intermediaries results in the production of H_2S , CO_2 , and SO_4^{2-} , and a shift of the $\delta^{34}\text{S}_{\text{SO}_4}$ isotopic composition to more depleted values for sulfide (-6 to -30 ‰ depletion) and enriched values for SO_4^{2-} (~ 6 to 20 ‰ enrichment), the magnitude of depletion and enrichment depending on the intermediate sulfur species utilized and the microorganisms responsible for carrying out the reaction (Thamdrup et al., 1993, Canfield and Thamdrup, 1994, Canfield et al., 1998, Habicht et al., 1998).

Thiosulfate Disproportionation:



Elemental Sulfur Disproportionation:



Although disproportionation would explain the $\delta^{34}\text{S}_{\text{SO}_4}$ signatures ranging from 5 to 15 ‰ seen in the Escarpment Zone, disproportionation is usually endergonic ($\Delta G > 0$) at neutral pH (Thamdrup et al., 1993). Only in cases where all H_2S is removed from the system by reaction with MnO_2 , FeOOH or FeCO_3 can sulfur disproportionation be exergonic ($\Delta G < 0$) (Thamdrup et al., 1993). Sulfur disproportionation would therefore only be able to explain $\delta^{34}\text{S}_{\text{SO}_4}$ signatures between 5 and 15 ‰ where low SO_4^{2-} (<100 mg/L) and no H_2S is present. 15-AG-025 is the only sample within the study area that meets the above requirements, and has a $\delta^{34}\text{S}_{\text{SO}_4}$ value of 7.1 ‰, a $\delta^{18}\text{O}_{\text{SO}_4}$ value of 3.4 ‰, no H_2S and SO_4^{2-} of 72 mg/L.

In specific geochemical conditions, subsequent reduction of resulting sulfate later in the flow system may cause further enrichment of $\delta^{34}\text{S}_{\text{SO}_4}$ to values greater than 30 ‰, as seen in the southwestern and northeastern portions of the Escarpment Zone. Some samples enriched in $\delta^{34}\text{S}_{\text{SO}_4}$ within the Escarpment Zone will be discussed in more detail later in this chapter, as sequentially very specific redox conditions are required for pyrite oxidation, then sulfur disproportionation and finally subsequent sulfate reduction to occur. In cases where sulfate concentrations are high (<~300 mg/L) evaporite dissolution and subsequent sulfate reduction is more likely the source of enriched $\delta^{34}\text{S}_{\text{SO}_4}$ signatures.

Where deep brine Cl/Br Ratios correlate with isotopically enriched $^{34}\text{S}_{\text{SO}_4}$ signatures, and the samples are located south of the Salina Group, the impact of natural migration of deep fluids from the Salina Group is possible. Elevated

$\delta^{34}\text{S}_{\text{SO}_4}$ signatures within the Devonian evaporite range (15 to 23 ‰, Claypool et al., 1980) may be due to minor gypsum presence in Devonian carbonates. Elevated $\delta^{34}\text{S}_{\text{SO}_4}$ signatures within the Silurian evaporite isotopic range (24 to 32 ‰, Claypool et al., 1980) in the north-eastern Escarpment Zone may be the result of some gypsum presence in the Reformatory Quarry Member of the Eramosa Formation, as well as, to the north, the presence of gypsum in the Goat Island Formation and the lower Gasport Formation (Bolton and Liberty, 1955, F. Brunton, P. Comm, 2016).

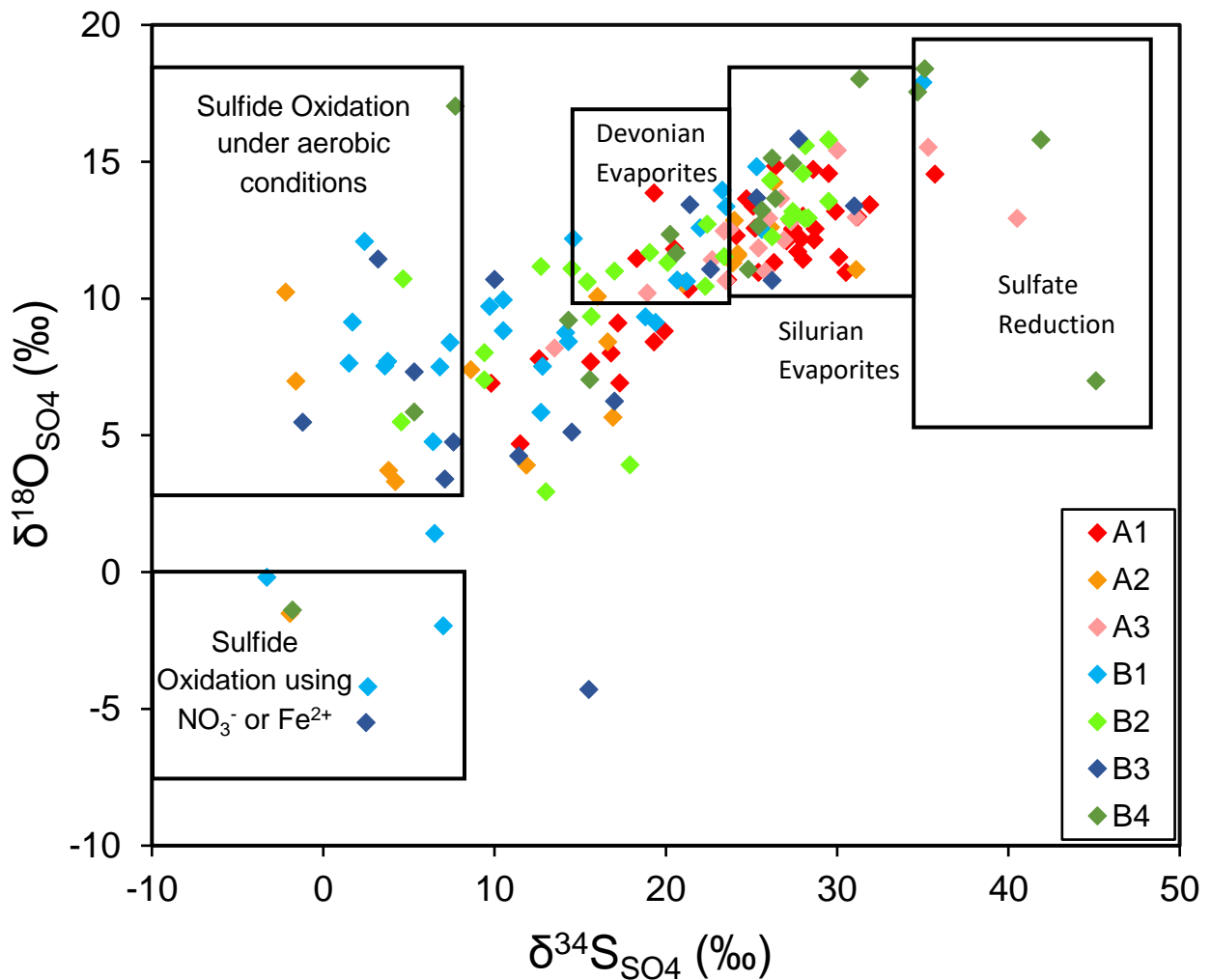


Figure 5.17: $\delta^{18}\text{O}_{\text{SO}_4}$ vs $\delta^{34}\text{S}_{\text{SO}_4}$ chart for samples from each cluster on the Niagara Peninsula. Sources of sulfate and their respective isotopic ranges are provided on the figure in boxes. Notes: (1) Samples located between 10 and 20 ‰ may contain mixed sources of sulfate, (2) Exogenous sulfate sources may account for the sulfate source of some of the depleted $\delta^{34}\text{S}_{\text{SO}_4}$.

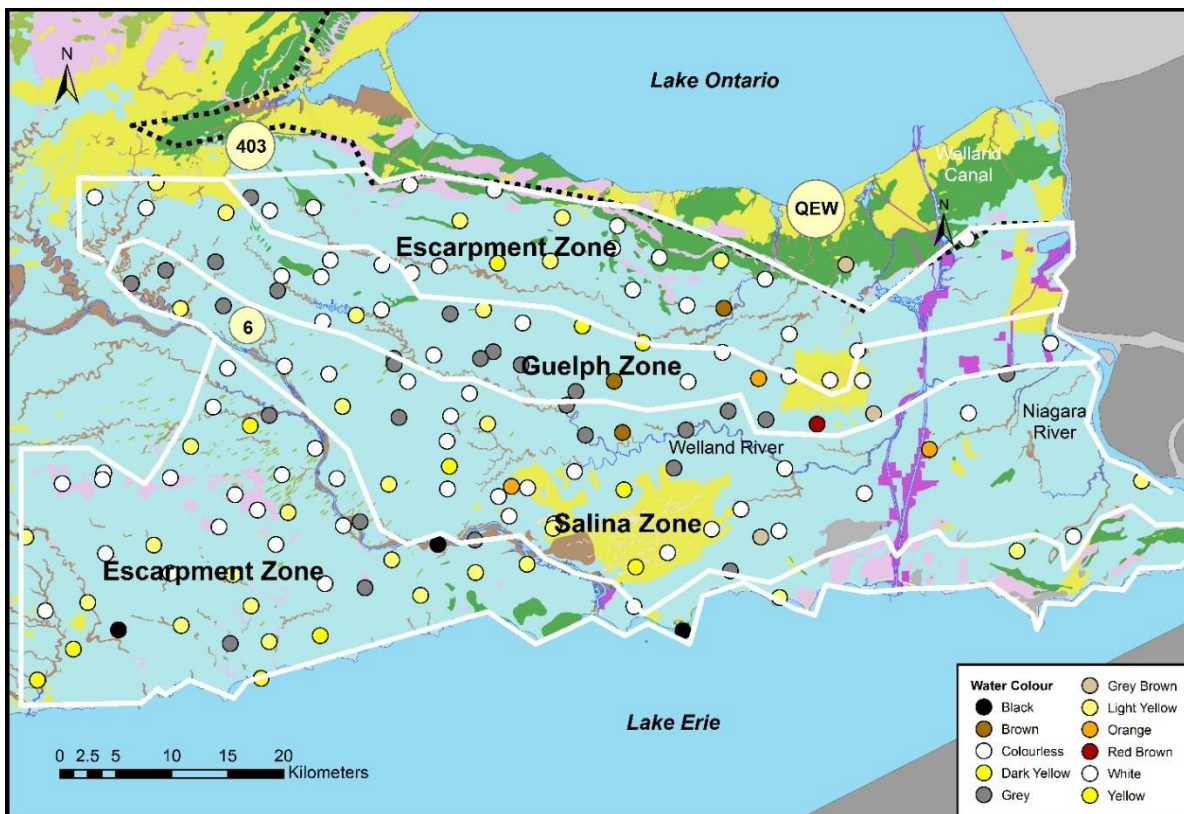
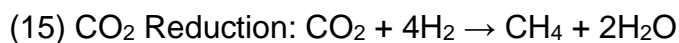


Figure 5.18: Water colour in Geochemical Zones on the Niagara Peninsula.

Elevated $\delta^{34}\text{S}_{\text{SO}_4}$ isotopic signatures in the western Escarpment Zone (Figure 4.24) obtained from the Salina Group are likely the result of evaporite dissolution as infiltrating groundwater moves into the evaporitic dolomite formation. $\delta^{34}\text{S}_{\text{SO}_4}$ signatures of samples obtained from the Salina Group fall within the range of Silurian marine evaporites in southern Ontario (+26 to +32 ‰; Figure 5.17), indicating gypsum dissolution is the dominant control on SO_4^{2-} concentrations in the Salina portion of the Escarpment Zone.

$\delta^{13}\text{C}_{\text{CH}_4}$ isotopic compositions representative of biogenic methanogenesis (-77 to -54 ‰) in the southern Escarpment Zone (Figures 4.31 - 4.33) correlating with high methane concentrations indicates methane production is occurring in shallow aquifers in part of the study area. The production of methane by

microbial metabolism can follow one of two metabolic pathways; CO₂ reduction or acetate fermentation (Figure 4.33, Equations 14 and 145).



Both methanogenic pathways cause a depletion in $\delta^{13}\text{C}$, as microbial populations favour the lighter isotope, ^{12}C , for metabolic reactions. Both the CO₂ reduction and acetate fermentation methanogenic pathways are utilized by microbial populations in the Escarpment Zones, as a wide range of fractionation factors ($\alpha^{13}\text{C}_{\text{CH}_4\text{-CO}_2}$) exist for samples with high, biogenic methane concentrations (Figure 4.33). Samples with biogenic methane $\delta^{13}\text{C}_{\text{CH}_4}$ signatures are discussed further in the ‘Outliers’ section. Two samples in the Escarpment Zone with elevated methane concentrations and $\delta^{13}\text{C}_{\text{CH}_4}$ signatures indicative of methanogenesis also have elevated SO₄²⁻ and H₂S concentrations. Thermodynamically, sulfate reduction proceeds prior to methanogenesis, removing sulfate from the aquifer prior to the production of significant methane concentrations. The presence of significant SO₄²⁻ concentrations in groundwater samples where elevated biogenic methane concentrations exist indicates mixing between two water sources, possibly by the upward migration of SO₄²⁻ through vertical conduits. These samples will be discussed further in the ‘Outliers’ section.

5.4 Salina Zone Geochemical Grouping

The Salina Zone is located in the central Niagara Peninsula, following the formational boundaries of the Silurian evaporitic and shale rich, dolomite Salina Group (Armstrong and Carter, 2010). The Salina Zone runs east-west through the Niagara Peninsula, transecting the communities of Chippawa (Niagara Falls), Welland, Wainfleet, Dunnville, Cansborough, Caistorville, Cayuga and Caledonia. The Salina Zone falls within the Salina bedrock trough, a bedrock depression running through the study area overlain by thick, impermeable clay

and silt sediments. Groundwater chemistry in the confined bedrock aquifer of the Salina Zone is highly mineralized, isotopically depleted in $\delta^{18}\text{O}_{\text{H}_2\text{O}}$ and has a consistent geochemical assemblage, subject to some variation due to local influences (Table 4.3, Figure 5.1, Figure 5.11). As discussed in the previous section, samples from the Salina Formation in the southwestern-most part of the study area are part of the Escarpment Zone.

The Salina Zone almost exclusively comprises A1 and A3 Group samples with geochemical facies Ca-SO₄ (Figure 4.6 and 5.1, Table 4.3). Major geochemical constituents of Group A1 and A3 samples include S²⁻, Ca²⁺, Mg²⁺, K⁺, Na⁺, SO₄²⁻, Cl⁻, Br⁻, Sr²⁺, NH₄⁺ and CH₄ (Table 4.3). A1 has the lowest HCO₃⁻ concentrations in the study area and the most elevated median SO₄²⁻ concentrations of any cluster (Table 4.3). A1 and A3 have fairly similar chemistry except A3 has a higher median HCO₃⁻ concentration (201 vs. 79 mg/L), a much higher S²⁻ concentration (5.25 vs. 0.11 mg/L) and SO₄²⁻, which is slightly lower (1830 vs. 2100 mg/L). Combined, these suggest A3 waters may be the product of sulfate reduction of waters with an initial chemical composition similar to those in group A1. Sulfate reduction coupled to carbon oxidation adds HCO₃⁻ to the DIC pool and reduces SO₄²⁻ to H₂S and, perhaps to Fe sulfides. A3 has the highest median concentration of H₂S in the study area (5.25 mg/L, Table 4.3), which supports the hypothesis of biologically mediated sulfate reduction in samples from this cluster. From a mass-balance perspective, the concentration of H₂S does not reflect the amount of sulfate reduced to sulfide. The reactivity of H₂S results in the precipitation of metallic sulfides, such as pyrite, where transitional metals are present.

Overwhelmingly, Cl-Br Ratios in the Salina bedrock trough display an ABB signature (Figure 5.19). Median Cl/Br mass ratios in Groups A1 (91.2) and A3 (95.6) fall well within the range of ABB signatures identified in shallow aquifers in the northwestern United States impacted by the vertical migration of fluids from the Silurian Salina Group. In the northeastern United States, the Silurian Salina

Group exists at depths up to 2.5 km (Llewellyn, 2014); however, on the Niagara Peninsula, the Silurian Salina Group is present as the subcropping unit. Halite precipitation during the Silurian resulted in higher Br⁻ concentrations and a distinct Cl/Br signature in residual fluids. In the Michigan Basin, halite is still present in the F, D, B and A-2 Units of the Silurian Salina Group (Armstrong and Carter, 2010), however in the Appalachian Basin, halite is not present due to dissolution through time. The presence of an ABB Cl/Br signature in the Salina Group within the Niagara Peninsula may suggest that migration of ABB fluids through faults, fractures and karst conduits from originally-halite bearing strata to subcropping anhydrite bearing units may have occurred sometime prior to the present, although in many parts of the Salina Group, migration is not required as the originally halite-bearing units are exposed in subcrop. Additionally, the presence of the Salina bedrock trough on the Niagara Peninsula may act as a basin for migrated fluids for two reasons, the first being that erosion of the upper, subcropping units of the Salina Group during the trough formation may have resulted in the exposure of deeper ABB-bearing units near the overburden-bedrock interface; the second that the bedrock depression in the Salina trough may encourage the lateral movement of fluids from deeper Salina units in the south towards the bedrock low. The lateral migration of fluids from the Salina group outside of the Salina trough could include a component of fluids vertically transported by faults or abandoned gas wells, prior to lateral migration towards the Salina bedrock low.

5.4.1 Bedrock Geochemistry, Salina Zone

The gypsiferous, shaley dolostones of the Salina Group contribute significant loadings of Ca²⁺ and SO₄²⁻ to bedrock aquifers and these solutes dominate groundwater chemistry (Eberts and George, 2000). The high solubility of gypsum in water allows for rapid dissolution of interstitial gypsum nodules when in contact with groundwater undersaturated in gypsum (Equation 16). Where gypsum dissolution has a strong influence on groundwater chemical composition, molar

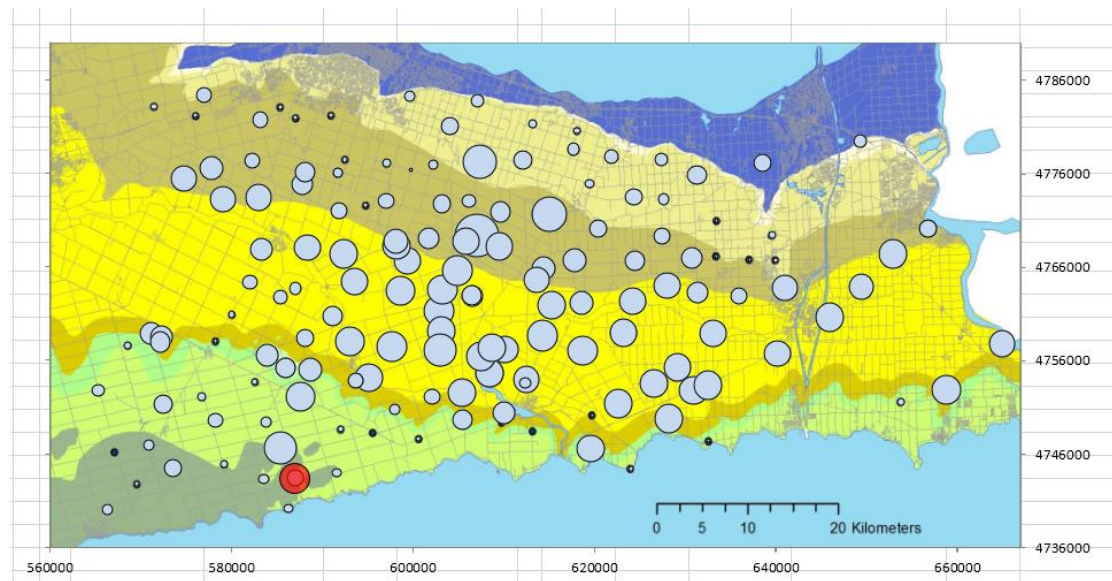
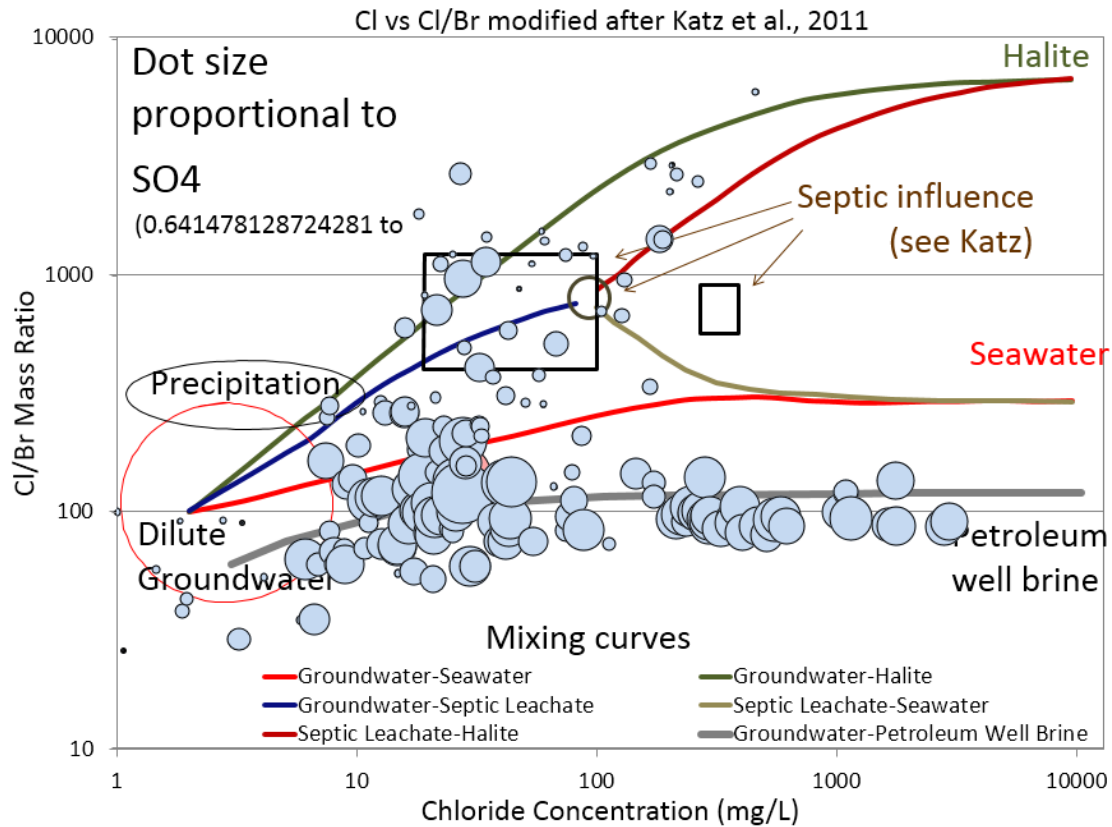


Figure 5.19: (a) SO_4^{2-} concentrations plotted on a chloride concentration vs. Cl/Br mass ratio chart. Elevated SO_4^{2-} concentrations shown by the larger blue dots in (a) fall primarily on the ABB mixing line. (b) Location of elevated SO_4^{2-} concentrations in Niagara.

concentrations of Ca^{2+} and SO_4^{2-} correlate across the concentration range up to saturation. Any deviation from a 1:1 correlation reflects the addition or removal of Ca^{2+} or SO_4^{2-} from other processes, which can include: dolomite dissolution, calcite precipitation, biologically mediated reactions and/or anthropogenic inputs. The removal of gypsum from the bedrock will proceed prior to the dissolution of carbonate minerals due to gypsum's higher solubility. Where Ca^{2+} and HCO_3^- are already found in groundwater at concentrations near saturation, dissolution of gypsum can result in calcite precipitation because of the common ion effect. This causes a disproportionate increase of SO_4^{2-} in solution (Equation 16). The corresponding removal of bicarbonate during calcite precipitation results in an undersaturation of dolomite and subsequent dolomite dissolution (Equation 17 and 18). Elevated Mg^{2+} contents in groundwater correlating with increased Ca^{2+} and SO_4^{2-} concentrations and low HCO_3^- concentrations is indicative of this dedolomitization process as a controlling mechanism on groundwater chemistry, and is apparent in the chemistry of groups A1 and A3 within the Salina Zone (Table 4.3).

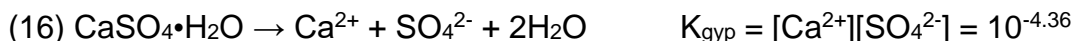
Incongruent dolomite dissolution with calcite precipitation generally proceeds in calcite-saturated, closed-system conditions because dolomite dissolution proceeds at a slow rate and would be limited by the addition of waters unsaturated with respect to calcite. In the Salina trough area of the Niagara Peninsula, the thick, low-permeability clay aquitard restricts rapid infiltration and recharge.

The importance of gypsum dissolution to the geochemical evolution of groundwater within the Salina Zone results from the rise in Ca^{2+} and Mg^{2+} , and the corresponding high hardness and low HCO_3^- concentrations (i.e. low alkalinity in low pH waters) (Equation 18, Figure 5.20). The impact of dedolomitization on the geochemical evolution of groundwater can be demonstrated using several additional lines of evidence, including $\text{Ca}^{2+}/\text{SO}_4^{2-}$ ratios and $\delta^{13}\text{C}_{\text{DIC}}$ and $\delta^{34}\text{S}_{\text{SO}_4}$

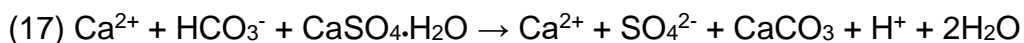
isotopic compositions. An anion excess on a Ca^{2+} vs. SO_4^{2-} chart (Figure 5.21) is resolved when Mg^{2+} concentrations are also considered (Figure 5.21). Whereas calcite precipitation has little influence on the residual $\delta^{13}\text{C}_{\text{DIC}}$ in groundwater, the addition of DIC from dolomite dissolution adds isotopically enriched carbonate with $\delta^{13}\text{C}_{\text{DIC}} = \sim 0 \text{ ‰}$ to the groundwater system, enriching the isotopic signature of the DIC pool (McIntosh and Walter, 2006; Figure 4.29). A1 has the lowest median isotopic composition for $\delta^{13}\text{C}_{\text{DIC}}$ of any group.

The use of $\delta^{34}\text{S}_{\text{SO}_4}$ in conjunction with $\delta^{13}\text{C}_{\text{DIC}}$ can affirm the influence of gypsum dissolution on groundwater evolution, as $\delta^{34}\text{S}_{\text{SO}_4}$ isotopic compositions from sulfate minerals are retained in groundwater after gypsum dissolution. Values of +25 to +32 ‰ for $\delta^{34}\text{S}$, and +12.5 to +15 ‰ for $\delta^{18}\text{O}$ were reported for marine evaporates of Silurian age within the study area (Fritz et al., 1988) and these show the same range as the observed values in groundwater (Figure 4.23, 4.24 and 5.17).

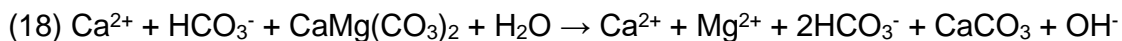
Gypsum Dissolution:



Dissolution of Gypsum and precipitation of Calcite:



Incongruent Dissolution of Dolomite:



Groundwater from the Salina Zone for clusters A1 and A3 plots along, or near, the 1:1 dissolution line for gypsum (Figure 5.21). Of the two clusters, A1 displays the most representative geochemical composition of groundwater influenced mostly by water-rock interaction in a gypsiferous aquifer. Isotopic and geochemical evidence suggest groundwaters of the A3 group have been subjected to biogeochemical cycling. Groundwater chemistry has evolved according to biogeochemical oxidation-reduction reactions that result in the

production of H_2S and increased HCO_3^- concentrations. $\delta^{34}\text{S}_{\text{SO}_4}$ and $\delta^{18}\text{O}_{\text{SO}_4}$ isotopic signatures remain distinctive of marine evaporites signatures from the area (Table 4.3).

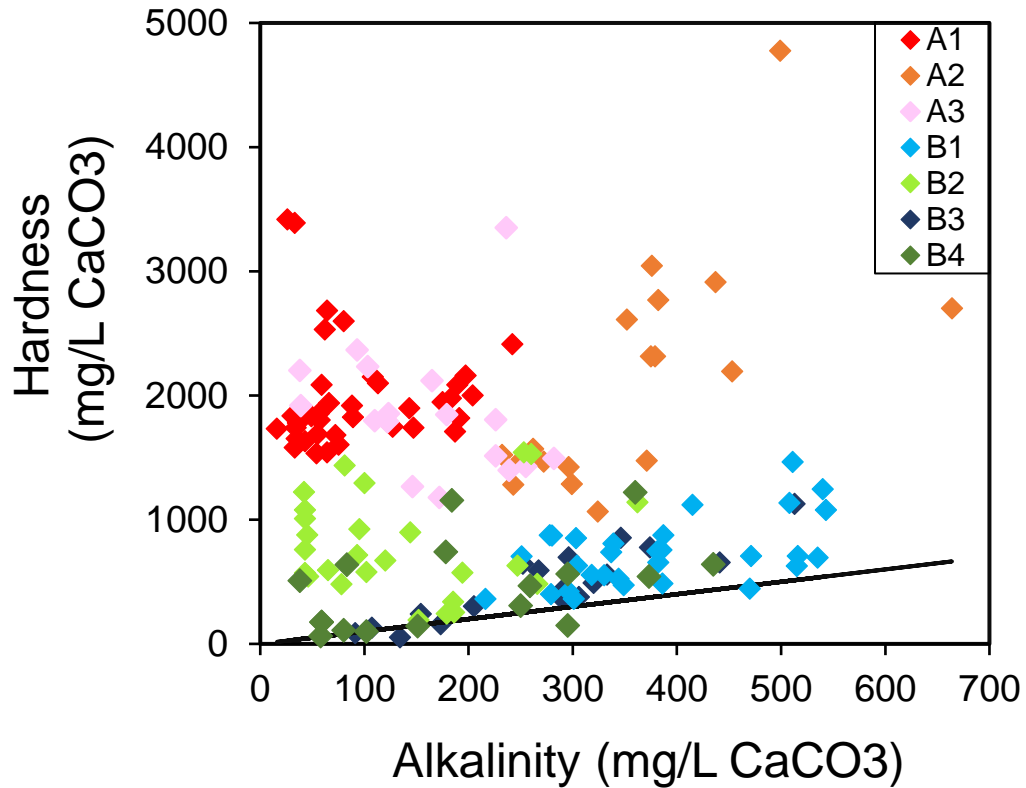


Figure 5.20: Hardness (mg/L CaCO_3^-) vs Alkalinity (mg/L CaCO_3). Notice the samples with the highest hardness values, in A1 and A3 have low alkalinity, indicative of dedolomitization. A2 has high alkalinity and hardness, suggesting mixed geochemical waters.

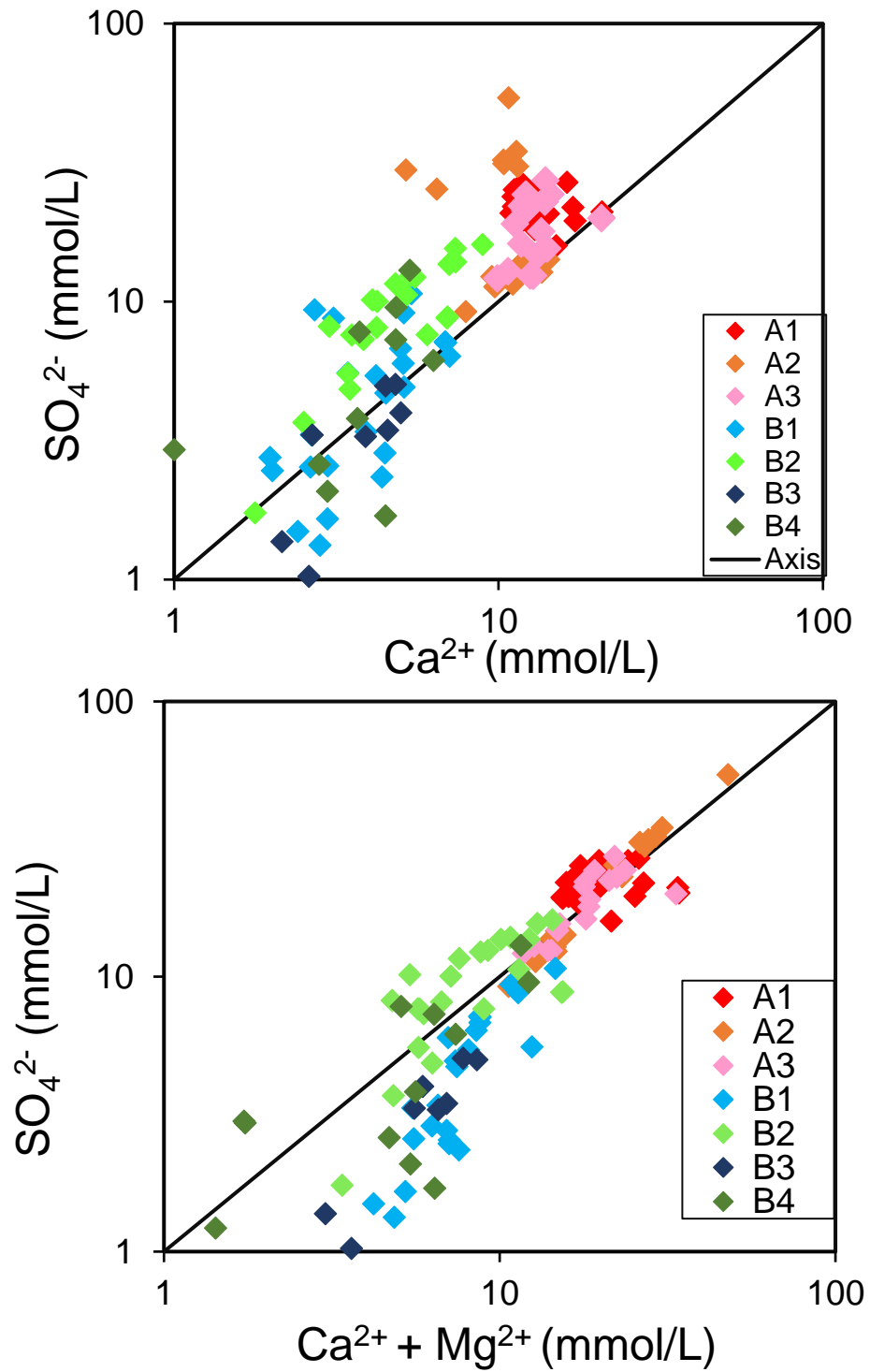
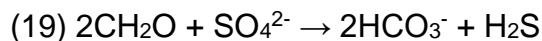


Figure 5.21: (a) Ca^{2+} (x-axis) vs. SO_4^{2-} (y-axis) chart, where the 1:1 line represents groundwaters impacted by gypsum dissolution. An anion excess on (a) indicates dedolomitization, which is balanced when Mg^{2+} is included on the x-axis (b).

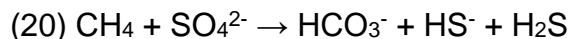
5.4.2 Influence of Biogeochemical Cycling on Groundwater Chemistry in the Salina Zone

Elevated sulfate concentrations originating from gypsum dissolution in a reducing, closed-system geochemical environment provides opportunity for microbial populations to utilize reduced carbon, if present, for metabolic reactions. In the absence of electron acceptors with higher thermodynamic favourability (i.e. NO_3^- , O_2), sulfate can be reduced in microbial metabolism (Equations 19 and 20). Sulfate reduction coupled to carbon oxidation can occur via one of two pathways; the oxidation of fixed, reduced, organic carbon compounds (DOC) that are present in the bedrock aquifer or overlying sediments (Equation 19 and 20), or the oxidation of methane introduced into the bedrock aquifer (Equation 21) from depth or created in a different part of the aquifer by methanogenesis.

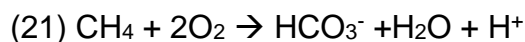
Sulfate Reduction coupled to the oxidation of Fixed Carbon:



Sulfate Reduction coupled to the oxidation of Reduced Carbon:



Methane Oxidation with Oxygen as an Electron Acceptor;



The metabolic preference for the lighter sulfur isotope (^{32}S) results in an isotopic enrichment in $\delta^{34}\text{S}_{\text{SO}_4}$ in the residual sulfur pool and an isotopic depletion in the resulting sulfide in $\delta^{34}\text{S}_{\text{S}_2}$ (Strebel et al., 2010). Isotopic enrichments for residual $\delta^{34}\text{S}_{\text{SO}_4}$ in groundwater of approximately 9 ‰ to 22 ‰ are common during bacterial sulfate reduction (Fritz et al., 1989). Enrichment factors for $\delta^{34}\text{S}$ are 2.5 to 4 times greater than $\delta^{18}\text{O}$ due to the moderating effect of $\delta^{18}\text{O}$ isotopic exchange between sulfate and water (Fritz et al., 1988). The presence of isotopically enriched $\delta^{34}\text{S}_{\text{SO}_4}$ signatures and anomalously high hydrogen sulfide

concentrations in several samples in the central peninsula indicates the occurrence of sulfate reduction in some samples within the Salina Zone (Figure 4.26, 4.27 and 5.22). As mentioned, cluster A3 displays higher median bicarbonate and hydrogen sulfide concentrations, and lower sulfate concentrations than A1 (Table 4.3) A black-dark grey colour was observed in several samples with isotopically elevated $\delta^{34}\text{S}_{\text{SO}_4}$ values, indicating corrosion of the well casing by H_2S .

The carbon source utilized during sulfate reduction in the Salina Zone needs to be understood to determine the carbon inputs and outputs in the bedrock aquifer. Organic carbon in primary aquifer sediments could be a fixed carbon source in the Salina Zone bedrock aquifer. Alternatively, methane in the bedrock aquifer, whether originating *in situ* biogenically or from external (deeper) sources, may contribute the carbon source for sulfate reduction. Methane created in aquifers by microbial methanogenesis has $\delta^{13}\text{C}_{\text{CH}_4}$ typically below -60 ‰ as a result of the preferential uptake of the lighter carbon isotope for metabolic processes during microbial methane production (Clark, 2015). In contrast, thermogenic methane created at depth in southern Ontario sedimentary bedrock formations has reported $\delta^{13}\text{C}_{\text{CH}_4}$ isotopic signatures of -44 to -36 ‰ (Barker and Fritz, 1981). Although the distinction between the isotopic compositions of thermogenic and biogenic methane seems clear, a positive shift in $\delta^{13}\text{C}_{\text{CH}_4}$ values during methane oxidation in the presence of oxygen (Equation 19) or SO_4^{2-} (Equation 18) may place the isotopic composition of partially oxidized, residual, microbial methane into the thermogenic range. In the Salina Zone $\delta^{13}\text{C}_{\text{CH}_4}$ ranges from -26 to -43 ‰ (Figure 4.31 - 4.33); well into the isotopic range for thermogenic methane previously reported in the area. Specific samples with enriched $\delta^{13}\text{C}_{\text{CH}_4}$ and their locations on the Niagara Peninsula is discussed further in the outlier's section. $\delta^{13}\text{C}_{\text{CH}_4}$ greater than -37 ‰ suggests reduction of sulfate by thermogenic methane in the Salina Zone may contribute to the geochemical evolution of groundwater in bedrock aquifers. The presence of abundant sulfate in the Salina

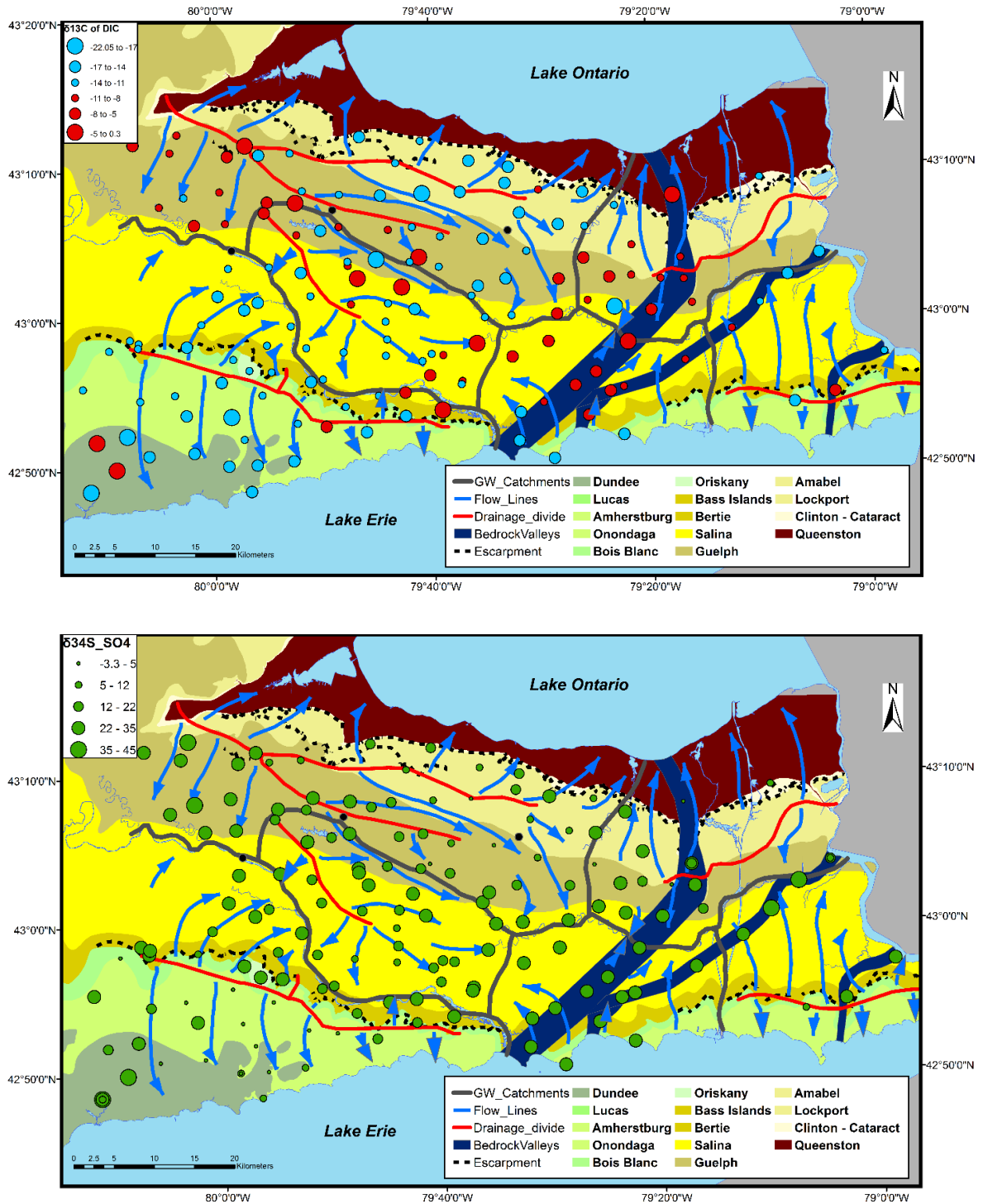


Figure 5:22: $\delta^{13}\text{C}_{\text{DIC}}$ and $\delta^{34}\text{S}_{\text{SO}_4}$ isotopic compositions overlain on the Paleozoic Geology, and groundwatersheds on the Niagara Peninsula. Buried bedrock channels present on the Peninsula are shown in dark blue, drainage divides are shown in red, and flow lines in light blue.

Zone ensures sulfate reduction can proceed if methane is available. The overwhelming presence of sulfate should limit methanogenesis, further minimizing its likelihood in the Salina Zone bedrock aquifer.

Another possibility is that biogenic methane is being transported along abandoned water or gas well casings vertically or by groundwater flow laterally, mixing with high-sulfate waters and subsequently being oxidized by sulfate to yield $\delta^{13}\text{C}_{\text{CH}_4}$ in the observed range. Samples containing $\delta^{13}\text{C}_{\text{CH}_4}$ between -26 and -43 ‰, show some evidence of sulfate reduction because part of the range of $\delta^{34}\text{S}_{\text{SO}_4}$ values (-27 to -35 ‰) is elevated above 32‰, suggesting residual enrichment. Samples measured for $\delta^{13}\text{C}_{\text{CH}_4}$ had the highest methane concentrations in the study area, as high concentrations were required for analytical analysis. The determination of $\delta\text{D}_{\text{CH}_4}$ in groundwater samples exhibiting high methane concentrations may aid in the differentiation of isotopic signatures of thermogenic methane and biogenic methane affected by oxidation. When plotted on a $\delta^{13}\text{C}_{\text{CH}_4}$ vs. $\delta\text{D}_{\text{CH}_4}$ chart, the location of samples may differentiate between thermogenic methane and oxidized biogenic methane produced using either the acetate fermentation or CO_2 reduction methanogenic pathways. To resolve the knowledge gaps regarding methane source, samples for $\delta\text{D}_{\text{CH}_4}$ will be obtained in the fall of 2016 as part of a follow-up project.

5.5 Guelph Zone Geochemical Grouping

The Guelph Zone is located within the subcropping formational boundaries of the Silurian Guelph and Eramosa Formations trending west-east in the north-central portion of the study area. The Guelph Formation is considered to be a major bedrock aquifer in southern Ontario due to its high permeability in the contact aquifer and well-developed, vuggy porosity. Major communities in the Guelph Zone include Ancaster, Binbrook, Smithville (southern portion), Pelham, Fonthill, Welland, and Niagara Falls. The Guelph Zone primarily encompasses samples from groups B2 and B4, with some samples classified to clusters B1 and B3.

Group B2 and B4 are present in a fairly even distribution across the formation, reflecting the bedrock compositional and geochemical processes occurring within this formation. At the southern mapped extent of the Guelph Formation, samples from clusters A1 and A3 are present. However, these may not actually be from the Guelph or Eramosa Formations. Paleozoic bedrock boundaries are currently being redefined (Burt, 2015; F. Brunton, P. Comm., 2016), and for the purposes of this thesis it is assumed those southernmost samples are within, or heavily influenced by the Salina Group evaporites.

The Guelph Zone contains the least mineralized, lowest conductivity groundwater on the Niagara Peninsula. Cluster B4 median values for Ca^{2+} , Mg^{2+} , K^+ , Cl^- , Br^- , SO_4^{2-} and electrical conductivity are among the lowest in the study area (Table 4.3). Yet this group has the highest fluoride concentrations, with a median of 1.28 mg/L, which is likely a result of the much lower Ca that would otherwise limit the solubility of fluorite (CaF_2). Low tritium and low median dissolved oxygen concentrations suggest that groundwater samples from Cluster B4 are not influenced by rapid local recharge. Cluster B2 is characterized by elevated Na^+ concentrations, the highest median pH of any cluster, and low DOC and HCO_3^- (Table 4.3). Cluster B2 has low tritium (median = 1.42 TU), indicating groundwater age is greater than 50 years for many samples, and low total coliform (median = 0). Overall, the groundwater composition of samples from the Guelph Zone is primarily Ca- SO_4 with some samples exhibiting Ca- HCO_3 , Mg- SO_4 , Ca-Cl and Mg- HCO_3 water facies (Figures 4.7 – 4.11, Table 4.4).

5.5.1 Bedrock Geochemistry and Biogeochemical Cycling in the Guelph Zone

Geochemical differences between clusters B2 and B4 illustrate the influences of water-rock interaction and biogeochemical cycling on groundwater evolution in the Guelph Zone bedrock aquifer. Both clusters mostly comprise dilute groundwater samples. Cluster B2 has somewhat elevated concentrations of Na^+ ,

S^{2-} and NH_4^+ , low concentrations of K^+ , HCO_3^- and DOC and the most alkaline pH values in the study area. Cross-formational, lateral, groundwater mixing between the Salina Group and the Guelph Formation likely contributes sulfate to the Guelph Zone bedrock aquifer within the boundaries of the Salina Trough. The Reformatory Quarry member of the Eramosa Formation contains gypsum nodules (F. Brunton, P.Comm., 2016), and may contribute sulfate to waters sampled from wells completed in that member. Local oxidation of sedimentary sulfides in the Eramosa Formation may contribute an additional source of sulfate to the bedrock aquifer. Samples classified as B2 generally occur downgradient of B4 samples within the southern Guelph Formation (see Figure 5.1). Cl/Br ratios of B2 samples fall mainly along the dilute groundwater or ABB mixing lines, suggesting little impact from surficial anthropogenic contamination. In most cases, the ABB Cl/Br character of B2 and B4 samples from the Salina trough bedrock low can be attributed to mixing between Salina Zone waters and Guelph Zone groundwater. The similarity between Guelph Zone waters and B4 waters of the southwestern Escarpment Zone may stem from similar lithology and, in the Guelph Zone, an influx of deeper sulfate bearing, $\delta^{34}S_{SO_4}$ -enriched fluids.

B4 has the highest F^- concentrations in the study area resulting from fluorite (CaF_2) in the Guelph Formation and Eramosa Formation. Fluorite deposits were found in the Beamsville and Vinemount Quarries from the Eramosa Formation with minor occurrences in the Guelph Formation. Fluorite occurs in the Eramosa member and Guelph Formation as an accessory mineral to minor lead and zinc Mississippi Valley-type (MVT) mineralization (Bailey et al., 2009, Farquhar et al., 1987).

Overall, groundwater chemistry in the Guelph Zone is representative of dilute, carbonate groundwater geochemistry typical in carbonate aquifers elsewhere in southern Ontario. Variations in groundwater chemistry may be the result of localized biogeochemical cycling and upward migration of deeper, higher TDS

fluids in some locations, however no dominant, formation-wide, redox reactions are apparent in this zone.

5.6 Exceptions and outliers within geochemical groupings

A number of samples show geochemical and isotopic compositions that are not reflective of the host bedrock mineralogy, the classified geochemical zone or local inputs of surface-sourced anthropogenic contaminants. The isotopic data are crucial to understanding the cause of these outliers and suggest that there are three dominant processes, (1) inputs of high concentrations of unusually $\delta^{34}\text{S}_{\text{SO}_4}$ -depleted exogenic sulfate likely as a result of upward movement of deeper fluids, (2) the input of thermogenic methane and related processes and (3) biogenic methane production in the shallow bedrock aquifer of the Dundee Formation. There are also a number of subprocesses related to geologic and hydrogeologic heterogeneity within the bedrock aquifer that act in concert with three dominant mechanisms to add additional variability to chemical and isotopic interpretation. Finally, there are several 'red herring' samples that appear to have anomalous chemistry but which result from heterogeneity in aquifer materials or character. These are discussed as 'Additional Outliers' and occur in the northern and southwestern Escarpment Zone.

5.6.1 Exogenic SO_4 -rich, $\delta^{34}\text{S}_{\text{SO}_4}$ -depleted fluids

Between the northern and southwestern Escarpment Zone, 14 samples have extremely high SO_4^{2-} concentrations (>1000 mg/L, averaging 2460 mg/L) correlating with depleted $\delta^{34}\text{S}_{\text{SO}_4}$ signatures (<15 ‰). A non-evaporitic source for these is indicated because Silurian and Devonian evaporites have $\delta^{34}\text{S}_{\text{SO}_4}$ values greater than 15 ‰ (Claypool et al., 1980). Six of the samples belong to cluster A2, characterized by a 'mixed' geochemical character, elevated SO_4^{2-} and HCO_3^- , and ABB Cl/Br Ratios. Although it would be reasonable to suggest sulfide oxidation as a mechanism for the production of depleted $\delta^{34}\text{S}_{\text{SO}_4}$ values where SO_4^{2-} is at low concentrations, pyrite oxidation cannot explain high SO_4^{2-}

concentrations in environments where massive quantities of pyrite are not present. The Niagara Peninsula may contain minor pyrite in glacial sediments and underlying bedrock formations, particularly where MVT mineralization has been documented, but extensive, regional deposits of pyrite or other massive sulfides have not been reported. Furthermore, major pyrite oxidation can occur only in unsaturated conditions in connection with oxygen, and would result in a significant pH suppression and the production of large amounts of Fe^{2+} and associated metals, including Zn, Ni, Cr, Cu, and Pb, which has not been reported in groundwaters on the Niagara Peninsula. The oxidation of aqueous sulfide to sulfate is also not possible as a widespread phenomenon in the Escarpment Zone, for similar reasons. Such a reaction requires oxidizing environments, and there would also be significant pH suppression, which is not seen. The source of elevated, $\delta^{34}\text{S}_{\text{SO}_4}$ -depleted SO_4^{2-} with must therefore be exogenic with respect to the aquifer. It has the $\delta^{34}\text{S}$ character of a terrestrial sulfate source (Matheson, 2012), which are the product of oxidation of terrestrial sulfides (Clark and Fritz, 1997) and can be retained in deep formations over time.

Thirteen of the 14 exogenic sulfate samples span the breadth of the Niagara Peninsula in a linear south-southwest to north-northeast trend (Figure 5.23). They are cross-formational with 2 occurring in the Lockport Group, 5 in the Guelph (or Eramosa) Formation, 4 in the Salina Group and 3 in the Onondaga Formation, including the one off-trend sample to the west (15-AG-006). The trend also crosses through the middle of three major groundwater flow systems (Fig. 2.9, 5.11, 5.23) with no apparent upgradient or downgradient response.

$\delta^{34}\text{S}_{\text{SO}_4}$ shows somewhat higher values in the Salina Group, and the closest two samples in the north bounding Guelph (Eramosa) Formation (average 12.3‰), than in the other exogenic sulfate samples (averaging 3.9‰). The elevated $\delta^{34}\text{S}_{\text{SO}_4}$ suggests a degree of mixing between the exogenic sulfate and the endogenic evaporitic sulfate that is ubiquitous in the Salina Group aquifer.

All exogenic sulfate samples are modern meteoric water with a very consistent $\delta^{18}\text{O}_{\text{H}_2\text{O}}$ of $-9.6 \pm 0.3\text{‰}$. All but one (see below) show depleted tritium from <0.8 to 5.3 TU indicating recharge rates in excess of a decade and usually much more. Most samples show detectable H_2S with high values in the southernmost mapped extent of the Guelph Formation (4 and 5.25 mg/L) and the three samples in the Onondaga Formation (3.5, 6.5 and 9 mg/L). The $\delta^{34}\text{S}_{\text{S}_2^-}$ in the elevated sulfide samples is depleted, averaging -13‰ , indicating some biogenic reduction of the sulfate is occurring.

Most of the exogenic sulfate samples have Cl/Br ratios that indicate ABB influence, with the notable exception of the most northerly sample (15-AG-048), on the Niagara Escarpment. This has a high ratio (1428) indicative of surface influence, most likely by road salt. This sample is also the only one that has elevated tritium (11.6 TU), which further suggests rapid connection with the surface environment. 15-AG-048 is completed in the Eramosa Formation, a metal-rich formation containing abundant reduced sulfides associated with MVT mineralization. This sample contains very high Fe (9.7 mg/L) and Zn (333 $\mu\text{g/L}$), two minerals indicative of reduced sulfide oxidation. This sample has lower pH (6.54) and higher CO_2 (1.9 ‰) than other samples from the Escarpment Zone. Pyrite and/or sphalerite oxidation likely contributes a large component of SO_4^{2-} to this sample, as demonstrated by elevated Fe, Zn, CO_2 , tritium and low H_2S . 15-AG-112 and 15-AG-050, located in close proximity to 15-AG-048, also have elevated concentrations of Fe (2.9 and 2.1 mg/L) and CO_2 (2.2 and 1.7%), however these samples have much higher SO_4^{2-} concentrations and ABB signatures. These samples may be partially influenced by pyrite and/or sphalerite oxidation with a larger component of an exogenic sulfate source.

The very high concentrations of the exogenous sulfate samples, the linear southwest-northeast incidence that crosses formations and flow systems, the ABB influence and the lack of possible surface sources of sulfate indicates that the source must be due to upward vertical migration of deeper, SO_4 -rich fluids. In

this area, the most plausible explanation for large-scale upward migration of fluids is as a result of corroded casings of legacy gas wells, which could provide a vertical pathway for fluid movement from depth. Gas wells in the area are drilled as deep as the Ordovician, but exogenous sulfate and a deep brine component could potentially come from any intervening formation (Skuce, 2014).

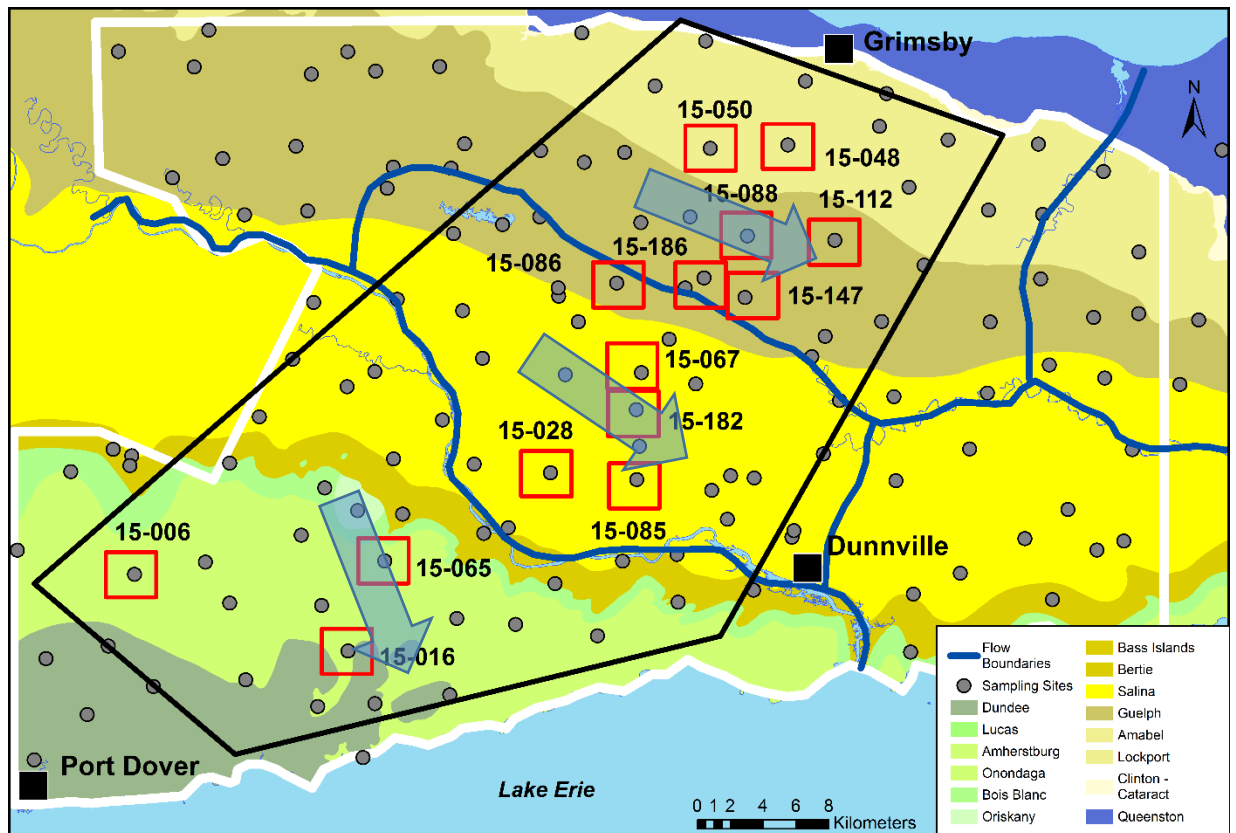


Figure 5.23: Locations of groundwater with exogenic sulfate (red squares) on the Niagara Peninsula. The polygon that defines the western part of the Niagara peninsula geochemical anomaly (Hamilton et al., 2011) is placed around samples. The exogenic samples form a northeast –southwest linear trend at the core of the anomaly. This trend is cross-formational and passes through the middle of three major groundwater flow systems, the boundaries of which are shown in blue (See Figure 2.9). Blue arrows indicate the dominant groundwater flow direction at the point where the exogenic sulfate trend crosses each flow system.

5.6.2 Exogenous Thermogenic Methane

5.6.2.1 Thermogenic gas

Six samples on the Niagara Peninsula have elevated methane concentrations with $\delta^{13}\text{C}$ signatures (-36 to -44‰) consistent with thermogenic methane (Barker and Fritz, 1981) (Figure 5.24). These samples occur in the Salina Trough, the Norfolk Quarry (discussed in section 5.6.5), and the Erigan, Chippawa-Niagara Falls, or Crystal Beach buried bedrock channels. They are samples 15-AG-054 (-40 ‰), 15-AG-100 (-42 ‰), 15-AG-166 (-43 ‰), 15-AG-165 (-40 ‰), 15-AG-010 (-37 ‰), and 15-AG-175 (-38 ‰).

5.6.2.2 Thermogenic gas and sulfate reduction

Three of the nine thermogenic samples on the Niagara Peninsula have enriched $\delta^{13}\text{C}_{\text{CH}_4}$ isotopic signatures, indicating partial oxidation of thermogenic methane that is interpreted here to be coupled to sulfate reduction (Figure 5.24). These samples include 15-AG-126 (-33 ‰), 15-AG-084 (-26 ‰) and 15-AG-176 (-28 ‰). All three have high H_2S concentrations (6.0, 34.8 and 2.0 mg/L respectively), indicative of sulfate reduction.

Several samples with available $\delta^{13}\text{C}_{\text{CH}_4}$ data, including 15-AG-010, 15-AG-100, and 15-AG-165, also show evidence of sulfate reduction, including isotopically enriched, residual $\delta^{34}\text{S}_{\text{SO}_4}$ signatures and elevated H_2S concentrations, which is expected with the introduction of a carbon source in the presence of gypsum-derived sulfate because sulfate reduction is thermodynamically favoured. The retention of the thermogenic methane signature is likely due to the oxidation of only a small component of methane introduced into the aquifer. High Iodide concentrations and low Cl/Br ratios representative of ABB signatures are present in all samples influenced by thermogenic methane, indicating a deeper source of dissolved solids. The thermogenic gas and deeper fluids in these waters implicates century gas wells, which are common throughout much of the peninsula. Sample 15-AG-100, a sulfur spring near Glanbrook, Hamilton, was reported to originate from a nearby abandoned gas well present to surface (City

of Hamilton, 2013). The exact location of the former well is uncertain because the casing has been removed.

5.6.2.3 Sulfate reduction with an unknown carbon source

Samples 15-AG-071 and 15-AG-151 have elevated H_2S (38.75 mg/L and 7.5 mg/L), enriched $\delta^{34}\text{S}_{\text{SO}_4}$ signatures (40.5 ‰ and 35 ‰, respectively), and depleted $\delta^{34}\text{S}_{\text{S}_2}$ values (-12.3 ‰ and -11.7 ‰) (Figure 5.24). Sample 15-AG-071 is from a well located in the Salina bedrock low, however the host bedrock formation is currently classified within the southern extent of the Silurian Guelph Formation. As formational boundaries are currently being redefined (F. Brunton, P. Comm., 2016), this sample is likely within, or heavily influenced by Salina Group evaporites. Sample 15-AG-151 is from a well in the Devonian Onondaga Formation, although the Devonian Bois Blanc Formation, Silurian Bertie Formation and Silurian Salina Group all subcrop within a 2 km transect south of the sample. The fractionation between $\delta^{34}\text{S}_{\text{SO}_4}$ and $\delta^{34}\text{S}_{\text{S}_2}$ in both samples is substantial (62.3 ‰ for 15-AG-071 and 46.7 ‰ for 15-AG-151) and indicative of bacterial sulfate reduction.

The carbon source utilized for sulfate reduction is not definitively clear for either sample. $\delta^{13}\text{C}_{\text{DIC}}$ signatures are -12.5 ‰ for 15-AG-071 and -15.1 ‰ for 15-AG-151. 15-AG-071 has low tritium (0.8 TU), low DOC (1.1 mg/L) and an elevated Cl concentration (512 mg/L) with an ABB Cl/Br Ratio, indicating little surface influence for this sample. It was collected near a sample with a thermogenic $\delta^{13}\text{C}_{\text{CH}_4}$. Thermogenic methane may therefore be the carbon source utilized for sulfate reduction. In contrast, 15-AG-151 has high tritium (15.1 TU), a Cl/Br ratio indicative of road salt or septic influence, and <1 m of sediment cover overlying unsaturated (static water level = 4.5 m) bedrock. 15-AG-151 was collected 300 m from the shore of Lake Erie along the Onondaga Escarpment. In this case, the organic carbon source cannot be determined.

5.6.3 Biogenic Methane

5.6.3.1 Endogenic Biogenic Methane

Samples 15-AG-013 and 15-AG-135 were collected from bedrock wells completed in the Devonian Dundee Formation (Figure 5.24). Sample 15-AG-013 has the lowest conductivity of any sample within the study area (264 $\mu\text{S}/\text{cm}$) and the SO_4^{2-} in the sample is less than 1 ppm, with a $\delta^{34}\text{S}_{\text{SO}_4}$ value of 15.5 ‰. The sample has no tritium, a Na- HCO_3 geochemical facies and the second highest CH_4 concentration in the study area (516 $\mu\text{mol}/\text{L}$). The CH_4 has a biogenic $\delta^{13}\text{C}_{\text{CH}_4}$ signature (-68 ‰). $\delta^{13}\text{C}_{\text{DIC}}$ is highly enriched with a value of -2.7 ‰, reflecting a residual enrichment of $\delta^{13}\text{C}$ in the DIC pool during methanogenesis. Similar to 15-AG-013, 15-AG-135 had elevated methane concentrations (490 $\mu\text{mol}/\text{L}$) and a biogenic methane isotopic signature (-77 ‰). It also has a low conductivity (697 $\mu\text{S}/\text{cm}$) and low SO_4^{2-} (89 mg/L) and H_2S^- of 8.1 mg/L, F^- of 3.16 mg/L and HCO_3^- of 360 mg/L. 15-AG-135 had a Na- HCO_3 geochemical facies and no tritium, similar to 15-AG-013, which was collected nearby and also from the Dundee Formation. Interestingly, 15-AG-135 has the highest reported values for both $\delta^{13}\text{C}_{\text{DIC}}$ (0.3 ‰) and $\delta^{34}\text{S}_{\text{SO}_4}$ (45 ‰), and a $\delta^{34}\text{S}_{\text{H}_2\text{S}}$ isotopic signature of 22.2 ‰.

The geochemical evolution of 15-AG-013 likely first involved minor pyrite oxidation (15-AG-013), subsequent sulfate reduction ($\text{H}_2\text{S} = 0.2$ mg/L) in the bituminous Dundee Formation followed by ion-exchange reactions replacing Na^+ (35 mg/L) for Ca^{2+} (11 mg/L) Biogenic methanogenesis then occurred, most likely in the shallow aquifer. The geochemical evolution of 15-AG-135 also included ion-exchange and then biogenic methanogenesis, however the presence of elevated SO_4^{2-} (>20 mg/L) indicates the addition of SO_4^{2-} by gypsum dissolution or mixing with a deeper, SO_4 -rich source following methane production.

15-AG-033 was collected from a well completed in the Devonian Onondaga Formation and has a $\delta^{13}\text{C}_{\text{CH}_4}$ value of -60 ‰ (Figure 5.24). Similar to 15-AG-013 and 15-AG-135, this sample has a low conductivity (297 $\mu\text{S}/\text{cm}$) and low SO_4^{2-}

(3.6 mg/L) concentration. This sample has H₂S of 0.65 mg/L, HCO₃⁻ of 211 mg/L and a Ca-HCO₃ geochemical facies. $\delta^{34}\text{S}_{\text{SO}_4}$ and $\delta^{34}\text{S}_{\text{S}_2}$, and $\delta^{13}\text{C}_{\text{DIC}}$ are 2.5 ‰, -15.4 ‰ and -6.1 ‰, respectively. Like sample 15-AG-013, the geochemical evolution of this sample first involved minor pyrite oxidation, followed by sulfate reduction and finally methanogenesis within the shallow aquifer.

5.6.3.2 Biogenic Methane with an Exogenic Sulfate Source

15-AG-180 was obtained from a bedrock well located on the Onondaga Formation in the eastern Peninsula (Figure 5.24). 15-AG-077 was collected from a well completed in the Dundee Formation. 15-AG-180 and 15-AG-077 both have elevated SO₄ (200 mg/L and 265 mg/L), depleted $\delta^{34}\text{S}_{\text{SO}_4}$, high H₂S (6.5 mg/L and 6.15 mg/L) and depleted $\delta^{13}\text{C}_{\text{CH}_4}$ values of -72 ‰ and -60 ‰. $\delta^{18}\text{O}_{\text{SO}_4}$ signatures are 17.0 ‰ and 9.7 ‰, respectively. The $\delta^{34}\text{S}_{\text{S}_2}$ signature was not measured for sample 15-AG-180, but has a value of -14 ‰ for 15-AG-077. In 15-AG-077 and possibly also 15-AG-180 the elevated SO₄²⁻, with depleted $\delta^{34}\text{S}_{\text{SO}_4}$ correlating with biogenic methane signatures and enriched $\delta^{18}\text{O}_{\text{SO}_4}$ signify a source of exogenic sulfate from depth. 15-AG-180 is less certain because its $\delta^{18}\text{O}_{\text{SO}_4}$ of 17‰ is very different than all other exogenous sulfate samples including 15-AG-077, which average 6.9 ± 3.5 .

In the case of 15-AG-077, the exogenic sulfate likely migrated in fluids from depth and mixed with groundwater containing biogenic methane. As in other exogenic sulfate cases the most likely vector is upward along corroded well casings. The tendency of biogenic methane to only form in sulfate-free environments and its short-lived nature in the presence of sulfate makes natural fractures much less likely. After mixing sulfate reduction would then have occurred, producing H₂S. This same sequence of processes is also demonstrated in 15-AG-180, by its similar geochemical and isotopic character, but the nature of the exogenic sulfate is different and there are no supporting $\delta^{34}\text{S}_{\text{S}_2}$ data.

5.6.4 Additional Outliers

Two sets of additional outliers appear to be related to natural dissolution of locally abundant evaporite minerals in the Silurian and Devonian carbonates of the northern and southern Escarpment Zones, respectively, as described in more detail below.

Sample 15-AG-098 from Cluster A2 in the Escarpment Zone, was obtained from a drilled well in the Lockport Group near the Niagara Escarpment. It has a Ca-Mg-SO₄ water facies, a SO₄²⁻ concentration of 1087 mg/L and an elevated Ca²⁺ concentration (391 mg/L). Hydrogen sulfide concentrations were below the detection limit (0.01) at this site. The conductivity of this sample (2076 µS/cm) is higher than the median conductivity for the Escarpment Zone, but compared with the entirety of the Niagara Peninsula, the conductivity is still relatively low. Isotopically enriched δ³⁴S and δ¹⁸O signatures (26.3 ‰ and 14.2 ‰) suggest the source of sulfate originates from the dissolution of Silurian evaporites. Gypsum presence has been noted in some locales within the Eramosa Formation, lower Goat Island Formation and Gasport Formation within the Lockport Group on the Niagara Peninsula (F. Brunton, P. Comm., 2016). Samples 15-AG-103 and 15-AG-133 have similar geochemical and isotopic signatures to 15-AG-098, suggesting the influence of upper Silurian gypsum dissolution in these samples as well.

Sample 15-AG-017, 15-AG-021 and 15-AG-012 are located within the Devonian Onondaga Formation. 15-AG-017 has a SO₄²⁻ concentration of 652 mg/L, a H₂S concentration of 0.02 mg/L and a HCO₃⁻ concentration of 472 mg/L. 15-AG-012 has an SO₄²⁻ concentration of 354 mg/L, a H₂S concentration of 4.2 mg/L and a HCO₃⁻ concentration of 324 mg/L. 15-AG-012 has a SO₄²⁻ concentration of 465 mg/L, a H₂S concentration of 3.5 mg/L and a HCO₃⁻ concentration of 472 mg/L. δ³⁴S_{SO4} and δ³⁴S_{S2-} values are 23.3 ‰ and below detection for 15-AG-017, 29.5 ‰ and -8.1 ‰ for 15-AG-021 and 27.4 ‰ and 6.55 ‰ for 15-AG-012. The

$\delta^{34}\text{S}_{\text{SO}_4}$ signatures are well within the range of Devonian evaporites (Claypool et al., 1980) where sulfate reduction has not notably occurred; as in 15-AG-017 where low H_2S concentrations were measured. Where sulfate reduction is apparent, as in 15-AG-021 and 15-AG-012, sulfate reduction may have enriched the residual $\delta^{34}\text{S}_{\text{SO}_4}$ of evaporite derived sulfate to slightly higher values. Alternatively, the source of sulfate could be from lower Silurian evaporites transported along vertical conduits.

5.6.5 Case study, Norfolk Quarry

Small-scale variations in groundwater chemistry at the Norfolk Quarry in the southwestern Escarpment Zone demonstrate the heterogeneity of microbial populations when responding to strong variations in groundwater chemistry. Sample F collected in the central section of the Norfolk Quarry transect (Figure 4.35) provides an excellent example of sulfate reduction induced by the presence of a reduced carbon source. Enriched $\delta^{34}\text{S}_{\text{SO}_4}$ (41.9 ‰) and $\delta^{13}\text{C}_{\text{CH}_4}$ (-36.8 ‰) and depleted $\delta^{34}\text{S}_{\text{S}_2}$ (-3.1 ‰) isotopic compositions indicate sulfate reduction coupled to methane oxidation and/or dissolved organic carbon oxidation is actively occurring prior to groundwater discharge in the quarry spring.

The enriched $\delta^{13}\text{C}_{\text{CH}_4}$ and high CH_4 concentrations suggest the methane source of sample F is thermogenic because, when methane is still present in high concentrations, the isotopic signature of the initial methane source would overprint any negative shift in $\delta^{13}\text{C}_{\text{CH}_4}$ values due to methane oxidation. Several ‘century’ gas wells located several hundred metres up-gradient of the quarry face (MNRF, 2016) may provide the source of thermogenic methane and possibly also the sulfate, dissolved in fluids from strata shallower than the methane source. An ABB Cl/Br Ratio from sample site F affirms a deeper origin of that groundwater composition relative to adjacent samples. This is also supported by

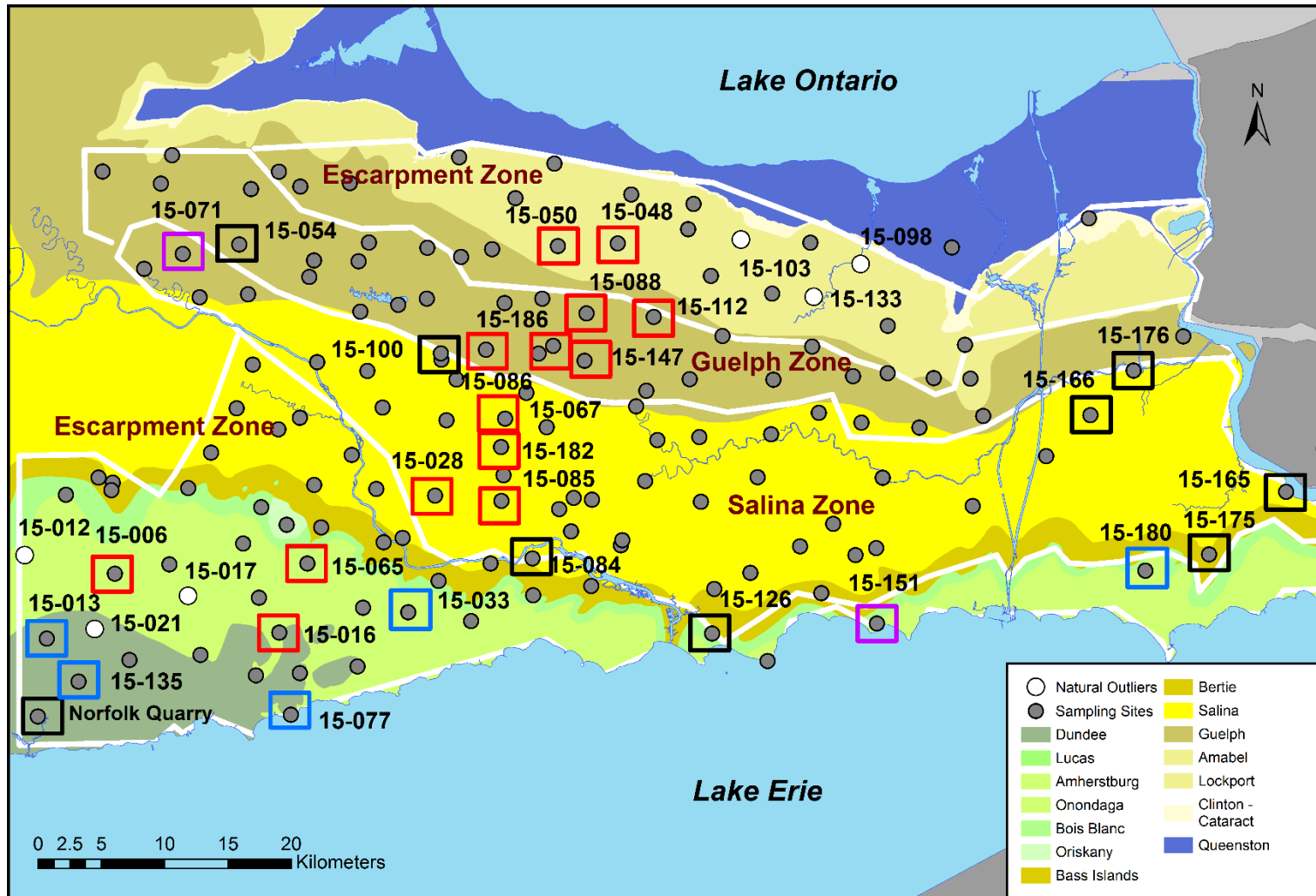


Figure 5.24: Location of exception and outliers within geochemical groupings. Outliers are labelled by their sample number. Red boxes represent samples with $\delta^{34}\text{S}_{\text{SO}_4}$ -depleted exogenic sulphate, purple boxes represent samples with evidence of sulfate reduction using an unknown carbon source, black boxes represent samples with evidence of exogenic thermogenic methane and green boxes represent samples with biogenic methane presence.

depressed tritium (5 TU) and $\delta^{18}\text{O}_{\text{H}_2\text{O}} / \delta\text{D}$ (-10.6 and -72.0 ‰), high iodine and non-detectable NO_3^- . In contrast, sample L located approximately 31 m to the east of sample F has elevated tritium of 13 TU, enriched $\delta^{18}\text{O}/\delta\text{D}$ (-8.9 and -60.2 ‰) of water, little methane, low I^- concentrations, a Cl/Br Ratio reflective of road salt and/or septic influence and high NO_3^- and DOC concentrations. A depleted $\delta^{34}\text{S}_{\text{SO}_4}$ (7.6 ‰) signature and low concentrations of SO_4^{2-} and non-detectable H_2S is indicative of minor pyrite oxidation.

The study of the Norfolk Quarry provides an analog to larger-scale variations in groundwater chemistry across the greater Niagara Peninsula. The geochemical heterogeneity here in the small-scale illustrates the importance of inputs and outputs of parameters and biogeochemical cycling on hydrogeochemical evolution. Site (F) is reflective of altered Salina Zone groundwater chemistry, with influence from sulfate reduction and deeper brines. There is also input of thermogenic methane, likely along the same vertical conduit(s) that carried sulfate-rich fluids but from deeper strata.

Chapter 6: Conclusions

Groundwater chemistry on the Niagara Peninsula has been identified as highly mineralized compared to other shallow waters collected from the same bedrock formations in southern Ontario. Geochemical and isotopic methods utilized as part of this study has discerned spatial variations in groundwater chemistry on the Niagara Peninsula related to bedrock lithology, hydrogeological conditions, local surficial anthropogenic inputs, mineralized, exogenic fluids and exogenic gases. Three geochemical zones have been delineated using the result of hierarchical cluster analysis (HCA) on groundwater geochemical parameters, including chloride/bromide (Cl/Br) ratios and separately using isotopic signatures. These geochemical zones include the Escarpment Zone, located on, or near the Niagara and Onondaga Escarpments, the Salina Zone, that encompasses the Salina bedrock trough and buried valley systems, and the Guelph Zone, spatially distributed east-west along the mapped extent of the Silurian Guelph and Eramosa Formations. The Escarpment Zone has thin to absent fractured clay sediments overlying carbonate bedrock, resulting in unconfined hydrogeological conditions dominated by recent recharge, as indicated by high tritium. Cl/Br ratio mixing lines provide evidence for anthropogenic contamination from surface as nearly all samples in the Escarpment Zone fall on the dilute groundwater - septic waste and dilute groundwater - halite (road salt) mixing lines. In contrast to the escarpment areas, the Guelph and Eramosa Formations and Salina Trough in the central Niagara Peninsula are overlain by thick (>10 m) low-permeability sediments that restrict groundwater movement to depth. Overall, the Salina Zone has consistent chemistry with elevated SO_4^{2-} concentrations and very high non-carbonate hardness reflective of the bedrock geology. Evidence for sulfate reduction is observed in many samples within the Salina Zone, particularly samples from Cluster A3 with elevated H_2S and HCO_3^- concentrations. The Guelph Zone contains the lowest Ca, Mg, K, Cl⁻, Br⁻, SO_4^{2-} and electrical

conductivity of the three zones and elevated F^- resulting from the dissolution of fluorite present in host bedrock formations.

Part of the Salina Zone near Lake Erie encompasses the Wainfleet groundwatershed catchment and the Erigan and Chippawa-Niagara Falls buried bedrock channels. These areas have potentiometric elevations that are below the level of Lake Erie. Within the Chippawa-Niagara Falls channel at the eastern extremity of the Wainfleet catchment, the Townline tunnel, a car and rail tunnel under the Welland Canal, has been consistently dewatered since 1968. A regional cone of depression extends from the tunnel to at least to the Wainfleet town centre and likely also to the shore of Lake Erie. Glacially-mixed, cold climate depleted $\delta^{18}O_{H_2O}$ and undetectable tritium suggest recharge to this site includes a large component of waters derived from under Lake Erie, apparently in response to the tunnel dewatering more than 25 km away. Near the tunnel itself, enhanced gypsum dissolution during groundwater flow may result in the solution enhancement of conduits in the parts of the aquifer influenced by the cone of depression. This suggests the need for continued temporal investigation to monitor changes in groundwater levels, pumping rates at the Townline Tunnel location and geochemical and isotopic composition of samples in the buried bedrock channels and Wainfleet.

Within the three geochemical zones, a significant number of outliers are present that do not display groundwater chemistry representative of the host geological and hydrogeological conditions. In some cases these are attributed to natural heterogeneity in the composition of aquifer materials and in particular to local accumulations of evaporitic sulfate minerals in Devonian and Silurian carbonate formations. Additional samples identified as outliers have biogenic methane ($\delta^{13}C_{CH_4}$ from -77 to -60‰) and result from reductive redox conditions conducive to methanogenesis in the absence of significant sulfate in an otherwise sulfate-rich bedrock aquifer. However, in other cases, these cannot be explained within

the context of aquifer materials or natural groundwater geochemical signatures in the host formations. Source differentiation of many of these samples indicate a component of fluids and gases of deeper origin including high concentrations of exogenic sulfate, Cl/Br ratios indicative of deeper, Appalachian Basin Brine and/or thermogenic methane

A significant number of samples with isotopically depleted $\delta^{34}\text{S}_{\text{SO}_4}$ (<15 ‰) signatures and elevated SO_4^{2-} concentrations (>1000 mg/L, average = 2460 mg/L) and low tritium (<5 m) were discovered in a linear northeast – southwest trend in the western peninsula. These 14 samples are cross-formational and transect the central parts of three major groundwater flow systems. This linear occurrence of exogenic sulfate must have appeared only in recent decades because a similar $\delta^{34}\text{S}_{\text{SO}_4}$ is not observed up or down-gradient in the same flow systems and because the tritium ages are in the order of decades. Such rapid temporal changes implicate anthropogenic activities and the most likely vector is via leakage of deeper fluids upward along corroded and abandoned gas well casings under the influence of upward potentiometric gradients regionally across the peninsula.

Nine samples were identified with elevated methane concentrations and $\delta^{13}\text{C}_{\text{CH}_4}$ above -44 ‰, which places them within or above the thermogenic methane isotopic range (Barker and Fritz, 1981). Six of these are collected from near the north shore of Lake Erie and have $\delta^{13}\text{C}_{\text{CH}_4}$ compositions between -36 ‰ to -44 ‰ that is interpreted here to represent thermogenic gas. These samples occur in the Salina Group, Salina Trough, or Erigan, Chippawa – Niagara Falls, or Crystal Beach buried bedrock channels. The three additional samples have elevated methane concentrations and $\delta^{13}\text{C}_{\text{CH}_4}$ signatures above -36 ‰, indicating partial methane oxidation of thermogenic methane coupled to sulfate reduction. As thermogenic methane is not produced within the shallow aquifer its presence indicates that vertical conduits must be present to allow upward migration of

methane from depth. Again, the most likely vectors are the corroded casings of abandoned gas wells that can be up to a century old and are present across much of the Peninsula, including near locations where thermogenic methane is present. Some of these gas wells are known to be artesian on the Niagara Peninsula (MNRF, 2016), and may add methane to shallow aquifers containing sulfate, resulting in sulfate reduction and the production of high concentrations of H₂S as seen across much of the Peninsula. The gas wells may also add sulfate-rich fluids from intermediate formations, that when mixed with the deeper-sourced methane would produce much the same effect.

A case study that involved sampling a 60 m-wide spring along a quarry face in the southwestern part of the peninsula illustrates the heterogeneity of geochemical parameters and microbial populations in a small-scale location where additions of thermogenic methane have altered groundwater chemistry. The quarry represents a microcosm of the peninsula writ-large, as the presence of groundwater of Salina Zone geochemical character with a thermogenic methane component within 10s of meters of the geochemical assemblage of the typical Escarpment Zone rock illustrates the potential impact of a vertical conduit on the groundwater chemical assemblage. A century gas well located 600 m, and another 750 m, from the quarry face are possible sources of the thermogenic methane and deeper fluids indicative of Salina Zone chemistry.

References

Alcalá, F. J., & Custodio, E. (2008). Using the Cl/Br ratio as a tracer to identify the origin of salinity in aquifers in Spain and Portugal. *Journal of Hydrology*, 359(1), 189-207.

Appelo, C. A. J., & Postma, D. (2005). *Geochemistry, groundwater and pollution*, 1993. Rotterdam: Balkema, 536.

Armstrong, D.K. (2007). Paleozoic geology of the southern Niagara Peninsula area; *in* Summary of Field Work and Other Activities 2007, Ontario Geological Survey, Open File Report 6213, p.15-1 to 15-8.

Armstrong, D.K. and Dodge, J.E.P. (2007). Paleozoic geology of southern Ontario; Ontario Geological Survey, Miscellaneous Release—Data 219.

Armstrong, D.K. and Carter, T.R. (2010). The subsurface Paleozoic stratigraphy of southern Ontario; Ontario Geological Survey, Special Volume 7, 301p.

Aravena, R., Wassenaar, L. I., & Barker, J. F. (1995). Distribution and isotopic characterization of methane in a confined aquifer in southern Ontario, Canada. *Journal of Hydrology*, 173(1), 51-70.

Aravena, R., & Robertson, W. D. (1998). Use of multiple isotope tracers to evaluate denitrification in ground water: study of nitrate from a large-flux septic system plume. *Ground Water*, 36(6), 975-982.

Ashley, R. P., & Lloyd, J. W. (1978). An example of the use of factor analysis and cluster analysis in groundwater chemistry interpretation. *Journal of Hydrology*, 39(3-4), 355-364.

Bailey, D. G., Hawkins, M., & Hiler, C. (2009). Minerals of The Silurian Lockport Group Central and Western New York State. *Rocks & Minerals*, 84(4), 326-337.

Barker, J. F., & Fritz, P. (1981). Carbon isotope fractionation during microbial methane oxidation. *Nature*, 293(5830), 289-291.

Barker, J. F., & Fritz, P. (1981). The occurrence and origin of methane in some groundwater systems. Natural Resource Council of Canada.

Bolton, A.E. & Liberty, B.E. (1955). Silurian stratigraphy of the Niagara Escarpment, Ontario. Michigan Geologic Field Trip Guidebook for 1955, 19-38.

Bolton, T. E. (1957). Silurian Stratigraphy and Palaeontology of the Niagara Escarpment in Ontario: Mines and Geology Branch: Bureau of Geology and Topography; Geological Survey; Memoir. Tafelbd. Cloutier.

Boyer, D.G. & Pasquarell, G.C. (1999). Agricultural land use impacts on bacterial water quality in a karst groundwater aquifer. Journal of the American Water Resources Association, 35(2), 291-300.

Brett, C.E., Tepper, D.H., Goodman, W.M., LoDuca, S.T. and Eckert, B.Y. (1995). Revised stratigraphy and correlations of the Niagaran provincial series (Medina, Clinton, and Lockport Groups) in the type area of western New York; United States Geological Survey, Bulletin 2086, 66p.

Brunton, F.R. (2008). Preliminary revisions to the Early Silurian stratigraphy of Niagara Escarpment: integration of sequence stratigraphy, sedimentology and hydrogeology to delineate hydrogeologic units; in Summary of Field Work and Other Activities, 2008, Ontario Geological Survey, Open File Report 6226, p.31-1 to 31-18.

Brunton, F. R., & Dodge, J. E. P. (2008). Karst of southern Ontario and Manitoulin Island. Ontario Geological Survey, Groundwater Resources Study, 5, 99.

Brunton, F. R. (2009). 25. Project Unit 08-004. Update of Revisions to the Early Silurian Stratigraphy of the Niagara Escarpment: Integration of Sequence Stratigraphy, Sedimentology and Hydrogeology to Delineate Hydrogeologic Units; in Summary of Field Work and Other Activities 2009, Ontario Geological Survey, Open File Report 6240, p.25--1 to 25--20.

Brunton, F.B. (2013). Karst and hazard lands mitigation: some guidelines for geological and geotechnical investigations in Ontario karst terrains; *in* Summary

of Field Work and Other Activities, 2013, Ontario Geological Survey, Open File Report 6290, p. 31-1 to 37-24.

Brunton, F. (2014) Personal communication, Ontario Geological Survey, Ministry of Northern Development and Mines.

Brunton, F. (2016) Personal communication, Ontario Geological Survey, Ministry of Northern Development and Mines.

Burnham, O.M. (2008). Trace element analysis of geological samples by inductively coupled plasma mass spectrometry (ICP-MS) at the Geoscience Laboratories: revised capabilities due to method improvements; *in* Summary of Field Work and Other Activities 2008, Ontario Geological Survey, Open File Report 6226, p.38-1 to 38-10.

Burnham, O.M., Schroeder, J., and Hamilton, S.M. (2012). Assessing laboratories capabilities for water analysis: results of a round-robin study; *in* Summary of Field Work and Other Activities 2012, Ontario Geological Survey, Open File Report 6280, p. 38-1 to 38-22.

Burt, A.K. (2013). The Niagara Peninsula study: a new three-dimensional Quaternary geology mapping project; *in* Summary of Field Work and Other Activities 2013, Open File Report 6290, p.38-1 to 38-21.

Burt, A.K. (2014). Penetrating Niagara with three-dimensional mapping; *in* Summary of Field Work and Other Activities 2014, Open File Report 6300, p.32-1 to 32-18.

Burt, A.K. (2015). Quaternary stratigraphy of the Niagara Peninsula revealed with three-dimensional mapping; *in* Summary of Field Work and Other Activities 2015, Open File Report 6313, p. 35-1 to 35-17.

Burt (2016). Personal Communication, presentation to the Ministry of the Environment and Climate Change. Ontario Geological Survey, Ministry of Northern Development and Mines.

Campbell, J.D. and Burt, A.K. (2015). Filling groundwater data gaps in the Niagara Region to assist Decision-Making Processes: *in* Summary of Field Work and Other Activities 2015, Open File Report 6313, p. 36-1 to 36-8.

Canfield, D. E., & Thamdrup, B. (1994). The production of (34) S-depleted sulfide during bacterial disproportionation of elemental sulfur. *Science*, 266(5193), 1973.

Canfield, D. E., Thamdrup, B., & Fleischer, S. (1998). Isotope fractionation and sulfur metabolism by pure and enrichment cultures of elemental sulfur-disproportionating bacteria. *Limnology and Oceanography*, 43(2), 253-264.

Carlson, E. H. (1994). Geologic, fluid inclusion, and isotopic studies of the Findlay Arch District, northwestern Ohio. *Economic Geology*, 89(1), 67-90.

Chapman, E. C., Capo, R. C., Stewart, B. W., Hedin, R. S., Weaver, T. J., & Edenborn, H. M. (2013). Strontium isotope quantification of siderite, brine and acid mine drainage contributions to abandoned gas well discharges in the Appalachian Plateau. *Applied geochemistry*, 31, 109-118.

City of Hamilton (2013). File no. 22.12.1, Glanbrook Landfill Sulphur Spring (FW99). Correspondence with the Ministry of Natural Resources and Forestry.

Clark, I. D., & Fritz, P. (1997). *Environmental isotopes in hydrogeology*. CRC press.

Clark, I. (2015) *Groundwater, Geochemistry and Isotopes*. CRC Press.

Clark, I. D., Ilin, D., Jackson, R. E., Jensen, M., Kennell, L., Mohammadzadeh, H., ... & Raven, K. G. (2015). Paleozoic-aged microbial methane in an Ordovician shale and carbonate aquiclude of the Michigan Basin, southwestern Ontario. *Organic Geochemistry*, 83, 118-126.

Claypool, G. E., Holser, W. T., Kaplan, I. R., Sakai, H., & Zak, I. (1980). The age curves of sulfur and oxygen isotopes in marine sulfate and their mutual interpretation. *Chemical Geology*, 28, 199-260.

Clayton, R. N., Friedman, I., Graf, D. L., Mayeda, T. K., Meents, W. F., & Shimp, N. F. (1966). The origin of saline formation waters: 1. Isotopic composition. *Journal of Geophysical Research*, 71(16), 3869-3882.

Cloutier, V., Lefebvre, R., Therrien, R., & Savard, M. M. (2008). Multivariate statistical analysis of geochemical data as indicative of the hydrogeochemical evolution of groundwater in a sedimentary rock aquifer system. *Journal of Hydrology*, 353(3), 294-313.

Craig, H. (1961). Isotopic variations in meteoric waters. *Science*, 133(3465), 1702-1703.

Cole, J., Coniglio, M., & Gautrey, S. (2009). The role of buried bedrock valleys on the development of karstic aquifers in flat-lying carbonate bedrock: insights from Guelph, Ontario, Canada. *Hydrogeology journal*, 17(6), 1411-1425.

Colgrove, L. M., Hamilton, S. M., and Longstaffe, F.J. (2014). Patterns and controls of shallow groundwater chemistry in eastern Ontario; in Summary of Field Work and Other Activities 2014, Ontario Geological Survey, Open File Report 6300, p.34-1 to 34-10.

Davis, S. N., Whittemore, D. O., & Fabryka-Martin, J. (1998). Uses of chloride/bromide ratios in studies of potable water. *Ground Water*, 36(2), 338-350.

Desaulniers, D. E., Cherry, J. A., & Fritz, P. (1981). Origin, age and movement of pore water in argillaceous Quaternary deposits at four sites in southwestern Ontario. *Journal of Hydrology*, 50, 231-257.

Dollar, P. S., Frape, S. K., & McNuff, R. H. (1991). Geochemistry of formation waters, southwestern Ontario, Canada and southern Michigan, USA: Implications for origin and evolution. Queen's Printer for Ontario.

Drimmie, R.J., Frape, S.K., Thomas, R.L. (1993) Stable isotope signature of meltwater in the sediments of Lake Erie and Lake Ontario. Proceedings of the International Symposium on Isotope Techniques in Studying Past and Current Environmental Changes in the Hydrosphere and the Atmosphere, IAEA-SM-329, IAEA, Vienna.

Eberts, S. M., & George, L. L. (2000). Regional ground-water flow and geochemistry in the Midwestern basins and arches aquifer system in parts of Indiana, Ohio, Michigan, and Illinois (Vol. 1423). US Geological Survey.

Farquhar, R. M., Haynes, S. J., Mostaghel, M. A., Tworo, A. G., Macqueen, R. W., & Fletcher, I. R. (1987). Lead isotope ratios in Niagara Escarpment rocks and galenas: implications for primary and secondary sulphide deposition. *Canadian Journal of Earth Sciences*, 24(8), 1625-1633.

Farvolden, R. N., & Nunan, J. P. (1970). Hydrogeologic aspects of dewatering at Welland. *Canadian Geotechnical Journal*, 7(2), 194-204.

Feenstra, B.H. (1981). Quaternary geology and industrial minerals of the Niagara–Welland area, southern Ontario; Ontario Geological Survey, Open File Report 5361, 260p.

Flint, J-J. and Lolcama, J. (1986). Buried ancestral drainage between lakes Erie and Ontario; *Geological Society of America Bulletin*, v.97, p.75-84.

Ford, D., & Williams, P. D. (2013). *Karst hydrogeology and geomorphology*. John Wiley & Sons.

Frape, S. K., Fritz, P., & McNutt, R. T. (1984). Water-rock interaction and chemistry of groundwaters from the Canadian Shield. *Geochimica et Cosmochimica Acta*, 48(8), 1617-1627.

Freckelton, C. N. and Hamilton, S. M. (2013). Ambient groundwater and geochemistry project of the Kingston-Peterborough Area; in *Summary of Field Work and Other Activities 2013*, Ontario Geological Survey, Open File Report 6290, p.39-1 to 39-5.

Freckelton, C. N. (2013). *A Physical and Geochemical Characterization of Southwestern Ontario's Breathing Well Region*, M.Sc. thesis, Western University, London, Ontario.

Freeze, R. A., & Cherry, J. A. (1979). *Groundwater* (No. 629.1 F7).

Friedman, I., & O'Neil, J. R. (1977). Data of geochemistry: Compilation of stable isotope fractionation factors of geochemical interest (Vol. 440). US Government Printing Office.

Fritz, P., Lapcevic, P. A., Miles, M., Frape, S. K., Lawson, D. E., & O'shea, K. J. (1988). Stable isotopes in sulphate minerals from the Salina formation in southwestern Ontario. *Canadian Journal of Earth Sciences*, 25(2), 195-205.

Fritz, P., Basharmal, G. M., Drimmie, R. J., Ibsen, J., & Qureshi, R. M. (1989). Oxygen isotope exchange between sulphate and water during bacterial reduction of sulphate. *Chemical Geology: Isotope Geoscience Section*, 79(2), 99-105.

Fritz, S. J. (1994). A survey of charge-balance errors on published analyses of potable ground and surface waters. *Ground Water*, 32(4), 539-546.

Fry, B., Cox, J., Gest, H., & Hayes, J. M. (1986). Discrimination between ^{34}S and ^{32}S during bacterial metabolism of inorganic sulfur compounds. *Journal of Bacteriology*, 165(1), 328-330.

Gao, C. Shirota, L., Kelly, R.I., Brunton, F.R. and Van Haaften, S. (2006). Bedrock topography and overburden thickness mapping, southern Ontario; Ontario Geological Survey, Miscellaneous Release – Data 207.

Gao, C. (2011). Buried bedrock valleys and glacial and subglacial meltwater erosion in southern Ontario, Canada. *Canadian Journal of Earth Sciences*, 48(5), 801-818.

Grasby, S. E., & Betcher, R. N. (2002). Regional hydrogeochemistry of the carbonate rock aquifer, southern Manitoba. *Canadian Journal of Earth Sciences*, 39(7), 1053-1063.

Güler, C., & Thyne, G. D. (2004). Delineation of hydrochemical facies distribution in a regional groundwater system by means of fuzzy c-means clustering. *Water Resources Research*, 40(12).

Habicht, K. S., Canfield, D. E., & Rethmeier, J. (1998). Sulfur isotope fractionation during bacterial reduction and disproportionation of thiosulfate and sulfite. *Geochimica et Cosmochimica Acta*, 62(15), 2585-2595.

Haeri-Ardakani, O. (2012). Geochemistry and Origin of Diagenetic Fluids and Paleohydrology of Paleozoic Carbonates in Southwestern Ontario, Canada.

Halton-Hamilton Source Protection (2015). Assessment report for the Hamilton region source protection area, version 2.7.

Hamilton, S.M., Brauneder, K. and Mellor, K.J. (2007). The Ambient Groundwater Geochemistry Project – southwestern Ontario. Summary of Field Work and Other Activities 2007, Ontario Geological Survey, Open File Report 6213 (20), 1-9.

Hamilton, S.M. and Brauneder, K. (2008). The Ambient Groundwater Geochemistry Project: Year 2. Summary of Field Work and Other Activities 2008, Ontario Geological Survey, Open File Report 6226 (34), 1-7.

Hamilton, S.M. and Freckelton, C.N. (2009). Ambient Groundwater Project: Grey–Bruce counties and area, 2009. Summary of Field Work and Other Activities, 2009, Ontario Geological Survey, Open File Report 6240 (27) 1-9.

Hamilton, S.M., Freckelton, C.N. and Mariotti, R. (2010). The Ambient Groundwater Geochemistry Program: Completion of sampling of southwestern Ontario; in Summary of Field Work and Other Activities 2010, Ontario Geological Survey, Open File Report 6260, p.34-1 to 34-4.

Hamilton, S.M. (2011). Ambient groundwater geochemistry data for southwestern Ontario, 2007–2010. Ontario Geological Survey, Miscellaneous Release—Data 283.

Hamilton, S.M., Matheson, E.J., Freckelton, C.N., Burke, H. (2011). Ambient Groundwater Geochemistry Program: The 2011 Aurora–Orillia Study Area and Selected Results for the Bruce and Niagara Peninsulas. Summary of Field Work and Other Activities, 2011, Ontario Geological Survey, Open File Report 6270 (32), 1-11

Hamilton, S.M. (2015). Ambient groundwater geochemistry data for southern Ontario, 2007–2014; Ontario Geological Survey, Miscellaneous Release—Data 283–Revised.

Hamilton, S.M. (2015). Personal Communication. Ontario Geological Survey, Ministry of Northern Development and Mines.

Hamilton, S. M., Grasby, S. E., McIntosh, J. C., & Osborn, S. G. (2015). The effect of long-term regional pumping on hydrochemistry and dissolved gas content in an undeveloped shale-gas-bearing aquifer in southwestern Ontario, Canada. *Hydrogeology Journal*, 23(4), 719-739.

Hargreaves, J.C. (2014). Summary of quality control data for the Geosciences Laboratories methods FEO-ION, GFA-PBG, IAW-200, ICW-100, IRC-100; *in* Summary of Field Work and Other Activities 2014, Ontario Geological Survey, Open File Report 6300, p. 39-1 to 39-4.

Haynes, S. J., Boland, R., & Hughes-Pearl, J. (1989). Depositional setting of gypsum deposits, southwestern Ontario; the Domtar Mine. *Economic Geology*, 84(4), 857-870.

Haynes, S. J., & Parkins, W. G. (1991). Stratigraphy of the Cayugan series: lithofacies of the Bertie and Bass Islands formations, Onondaga escarpment. Geoscience Research Grant Program, Summary of Research, 1992, 22-37.

Hautman, D.P. and Munch, D.J. (1997). Determination of inorganic anions in drinking water by ion chromatography, Revision 1.0. National Exposure Research Laboratory, Office of Research and Development, U.S. Environmental Protection Agency, Cincinnati, OH.

Hem, J. D. (1985). Study and interpretation of the chemical characteristics of natural water (Vol. 2254). Department of the Interior, US Geological Survey.

Hobbs, M.Y., S.K. Frape, O. Shouaker-Stash and L. Kennell, (2008). Phase I Regional Hydrogeochemistry Southern Ontario, OPG Report OPG 00216-REP-01300-00006-R00.

Husain, M., Cherry, J., Frape, S. (2004) The persistence of a large stagnation zone in a developed regional aquifer, southwestern Ontario. *Can Geotech*, 41, 943–958.

Jagger Hims Ltd. (2004). Provincial Groundwater Monitoring Network 2003 monitoring well installation program. Prepared for the Niagara Peninsula Conservation Authority.

Jagger Hims Ltd. (2009). Ambient groundwater quality, revised report, prepared for the Niagara Peninsula Conservation Authority; unpublished internal report, Niagara Peninsula Conservation Authority, 45p.

Jasechko, S., Gibson, J. J., & Edwards, T. W. (2014). Stable isotope mass balance of the Laurentian Great Lakes. *Journal of Great Lakes Research*, 40(2), 336.

Johnson, M.D., Armstrong, D.K., Sanford, B.V., Telford, P.G., and Rutka, M.A. (1992). Paleozoic and Mesozoic Geology of Ontario, Ontario Geological Survey, Special Volume 4, Part 2, p.907-1011.

Johnson, J. D., Graney, J. R., Capo, R. C., & Stewart, B. W. (2015). Identification and quantification of regional brine and road salt sources in watersheds along the New York/Pennsylvania border, USA. *Applied Geochemistry*, 60, 37-50.

IAEA (2001). GNIP Maps and Animations, International Atomic Energy Agency, Vienna. Accessible at <http://isohis.iaea.org>.

Isotopic Tracer Technologies (2015). Personal Communication, Quote for Analysis of $\delta^{18}\text{O}_{\text{H}_2\text{O}}$, $\delta^{18}\text{O}_{\text{H}_2\text{O}}$, Tritium, $\delta^{34}\text{S}_{\text{SO}_4}$, $\delta^{34}\text{S}_{\text{S}_2}$ and $\delta^{18}\text{O}_{\text{SO}_4}$.

Katz, B. G., Eberts, S. M., & Kauffman, L. J. (2011). Using Cl/Br ratios and other indicators to assess potential impacts on groundwater quality from septic systems: a review and examples from principal aquifers in the United States. *Journal of Hydrology*, 397(3), 151-166.

Kunert, M., Coniglio, M., & Jowett, E. C. (1998). Controls and age of cavernous porosity in Middle Silurian dolomite, southern Ontario. *Canadian Journal of Earth Sciences*, 35(9), 1044-1053.

Lake Erie Region Source Protection Committee (2015). Approved assessment report for the long point source protection area within the Lake Erie source protection region.

Lake Erie Region Source Protection Committee (2015). Approved source protection plan for the Grand River source protection area within the Lake Erie source protection region.

Llewellyn, G. T. (2014). Evidence and mechanisms for Appalachian Basin brine migration into shallow aquifers in NE Pennsylvania, USA. *Hydrogeology Journal*, 22(5), 1055-1066.

Longstaffe, F.J., Avalon, A., Hladyniuk, A., Hyodo, A., Macdonald, R., St Armour, A., Crowe, A., Huddart, P. (2011). The oxygen and hydrogen isotopic evolution of the Great Lakes. IAEA-CN-186-INV002.

Mahler, B. J., Personné, J. C., Lods, G. F., & Drogue, C. (2000). Transport of free and particulate-associated bacteria in karst. *Journal of Hydrology*, 238(3), 179-193.

Matheson, E. (2012). Analysis of anomalous groundwater geochemistry of the Niagara Peninsula, Ontario, Canada; unpublished BSc thesis, Queen's University, Kingston, Ontario, 164p.

McEwan, C.A., Hamilton, S.M., Slater, G.F., Campbell, J.D. (2015). Geochemical and isotopic sampling to delineate sources of highly mineralized groundwater on the Niagara Peninsula: *in* Summary of Field Work and Other Activities 2015, Open File Report 6313, p.37-1 to 37-8.

McIntosh, J. C., & Walter, L. M. (2006). Paleowaters in Silurian-Devonian carbonate aquifers: Geochemical evolution of groundwater in the Great Lakes region since the Late Pleistocene. *Geochimica et Cosmochimica Acta*, 70(10), 2454-2479

McIntosh, J. C., Grasby, S. E., Hamilton, S. M., & Osborn, S. G. (2014). Origin, distribution and hydrogeochemical controls on methane occurrences in shallow aquifers, southwestern Ontario, Canada. *Applied Geochemistry*, 50, 37-52.

Menzies, J. and Taylor, E.M. (1998). Urban geology of St. Catharines–Niagara Falls, Region Niagara; *in* Urban geology of Canadian cities, Geological Association of Canada, Special Paper 42, p.287-321.

MNRF (2016) Ontario Ministry of Natural Resources petroleum well data. http://www.ogsrlibrary.com/data_free_petroleum_ontario. Accessed 28 Nov 2016 (subscription required).

Mook, W. G., Gat, J. R., Meijer, H. A., Rozanski, K., & Froehlich, K. (2001). Environmental isotopes in the hydrological cycle: principles and applications.

Mullaney, J. R., Lorenz, D. L., & Arntson, A. D. (2009). Chloride in groundwater and surface water in areas underlain by the glacial aquifer system, northern United States. Reston, VA: US Geological Survey.

Novakowski, K. S., & Lapcevic, P. A. (1988). Regional hydrogeology of the Silurian and Ordovician sedimentary rock underlying Niagara Falls, Ontario, Canada. *Journal of Hydrology*, 104(1), 211-236.

NPCA (2011). Assessment Report: Niagara Peninsula Source Protection Area.

NPCA. (2013). Updated assessment report Niagara Peninsula source protection area. Approved by the Ontario Ministry of the Environment, Welland, Ontario.

NPCA (2014) Source protection plan for the Niagara Peninsula Source Protection Area. Approved by the Ontario Ministry of the Environment and Climate Change, Welland, Ontario.

O'Shea, K. J., Miles, M. C., Fritz, P., Frape, S. K., & Lawson, D. E. (1988). Oxygen-18 and carbon-13 in the carbonates of the Salina formation of southwestern Ontario. *Canadian Journal of Earth Sciences*, 25(2), 182-194.

Pamer, L. (2007). Major and trace element analysis of water samples by inductively coupled plasma atomic emission spectrometry (ICP-AES) at the Geosciences Laboratories: preliminary data; *in* Summary of Field Work and Other Activities 2007, Ontario Geological Survey, Open File Report 6213, p. 32-1 to 32-7.

Pamer, L. (2008). Trace concentration determination of total mercury in natural waters by atomic fluorescence spectroscopy at the geoscience laboratories; *in* Summary of Field Work and Other Activities 2008, Ontario Geological Survey, Open File Report 6226, p.40-1 to 40-4.

Pamer, L. (2011). Analysis of anions in waters by ion chromatography at the Geoscience Laboratories; *in* Summary of Field Work and Other Activities 2011, Ontario Geological Survey, Open File Report 6270, p. 34-1 to 34-5.

Pamer, L. (2016). Total Organic Carbon (TOC) Analysis at the Geoscience Laboratories (2015). Method Development Report, 2015, Geoscience Laboratories, Ministry of Northern Development and Mines, Sudbury, Ontario.

Sander (2014). Compilation of Henry's law constants (version 4.0) for water as solvent. *Atmospheric Chemistry and Physics*, 15, 4399 – 4981.

Sanford, B.V. (1969). Silurian of southwestern Ontario; Ontario Petroleum Institute, 8th Annual Conference Proceedings, Technical Paper No.5, p.1-44

Schot, P.P., van der Wal, J., 1992. Human impact on regional groundwater composition through intervention in natural flow patterns and changes in land use. *Journal of Hydrology* 134, 297–313.

Singer, S. N., Cheng, C. K., & Scafe, M. G. (2003). The hydrogeology of southern Ontario. Environmental Monitoring and Reporting Branch, Ministry of the Environment.

Skuce, M. E. (2013). Isotopic Fingerprinting of Shallow and Deep Groundwaters in Southwestern Ontario and its Applications to Abandoned Well Remediation. M.Sc. Thesis, Western University, London, Ontario.

Skuce, M., Potter, J., Longstaffe, F.J., Carter, T. (2014). The isotopic characterization of natural gas and water in Paleozoic bedrock formations in southwestern Ontario. Volume I. Water Geochemistry – Abandoned Works Program. University of Western Ontario and Ministry of Natural Resources and Forestry (Petroleum Operations Section).

Skuce, M., Longstaffe, F. J., Carter, T. R., & Potter, J. (2015). Isotopic fingerprinting of groundwaters in southwestern Ontario: Applications to abandoned well remediation. *Applied Geochemistry*, 58, 1-13.

Spencer, J. W. (1907). The Falls of Niagara, Their Evolution and Varying Relations to the Great Lakes: Characteristics of the Power, and the Effects of Its Diversion. SE Dawson.

Staddon, P. L. (2004). Carbon isotopes in functional soil ecology. *Trends in Ecology & Evolution*, 19(3), 148-154.

Strebel, O., Böttcher, J., & Fritz, P. (1990). Use of isotope fractionation of sulfate-sulfur and sulfate-oxygen to assess bacterial desulfurization in a sandy aquifer. *Journal of Hydrology*, 121(1-4), 155-172.

Steele, K. G., & Haynes, S. J. (2000). Mines and wines: Industrial minerals, geology and wineries of the Niagara region, field trip guidebook.

Taylor, B. E., Wheeler, M. C., & Nordstrom, D. K. (1984). Stable isotope geochemistry of acid mine drainage: Experimental oxidation of pyrite. *Geochimica et Cosmochimica Acta*, 48(12), 2669-2678.

Thamdrup, B., Finster, K., Hansen, J. W., & Bak, F. (1993). Bacterial disproportionation of elemental sulfur coupled to chemical reduction of iron or manganese. *Applied and environmental microbiology*, 59(1), 101-108.

Thomas, M. A. (2000). The effect of residential development on ground-water quality near Detroit, Michigan. *JAWRA Journal of the American Water Resources Association*, 36(5), 1023-1038.

Vengosh, A., & Pankratov, I. (1998). Chloride/bromide and chloride/fluoride ratios of domestic sewage effluents and associated contaminated ground water. *Ground Water*, 36(5), 815.

Warbick, J. (2015). Personal communication, Ministry of the Environment and Climate Change.

Warner, N. R., Jackson, R. B., Darrah, T. H., Osborn, S. G., Down, A., Zhao, K., ... & Vengosh, A. (2012). Geochemical evidence for possible natural migration of Marcellus Formation brine to shallow aquifers in Pennsylvania. *Proceedings of the National Academy of Sciences*, 109(30), 11961-11966.

Worthington, S. R. (2002). Test methods for characterizing contaminant transport in a glaciated carbonate aquifer. *Environmental Geology*, 42(5), 546-551.

Yoon, S., Cruz-García, C., Sanford, R., Ritalahti, K. M., & Löffler, F. E. (2015). Denitrification versus respiratory ammonification: environmental controls of two competing dissimilatory NO₃⁻/NO₂⁻ reduction pathways in *Shewanella loihica* strain PV-4. *The ISME journal*, 9(5), 1093-1104.

Zanini, L., Novakowski, K. S., Lapcevie, P., Bickerton, G. S., Voralek, J., & Talbot, C. (2000). Ground water flow in a fractured carbonate aquifer inferred from combined hydrogeological and geochemical measurements. *Ground water*, 38(3), 350-360.

Appendices

Appendix A: Field Parameters

Sample	Purging Vol	Alkalinity	T	DO	Cond	pH	ORP	H ₂ S
Unit	L	mg/L_ CaCO ₃	°C	% Saturation	µS/cm		mV	mg/L_ S ²⁻
15-AG-001	115	38	11.81	3.4	1380	7.74	-18.8	0
15-AG-002	180	83	13.19	56.6	1348	7.07	31.2	0
15-AG-003	300	102	9.86	0	388	7.58	-156.9	0.02
15-AG-004	180	283	10.73	0	989	6.68	2.2	0
15-AG-006	180	362	10.64	0	2095	6.79	-220.7	3.5
15-AG-007		154	10.01	7.1	587	7.02	-8.7	0
15-AG-008		205	11.06	0	714	7.02	-229.5	8.5
15-AG-009								
15-AG-010		295	10.19	0	1284	7	-298.4	35.5
15-AG-011		250	9.77	0	739	7.17	-222.8	3.25
15-AG-012	300	247	11.08	0	1195	6.76	-251	3.5
15-AG-013	200	134	10.7	0	264	7.57	-163	0.2
15-AG-014	200	282	11.2	0	2344	6.6	87.2	0
15-AG-015	245	471	9.84	0	1669	6.86	-75.2	0.08
15-AG-016	140	664	10.28	0	4674	6.79	-180.7	9
15-AG-017	150	387	10.54	0	1713	6.88	-92.4	0.02
15-AG-018	135	330	13.29	0	1464	6.85	-254.7	7
15-AG-019	135	333						7
15-AG-020	200	226	10.68	0	2404	7.01	-186.3	1.1
15-AG-021	250	266	11.8	0	1102	7.63	-267.8	4.2
15-AG-022	20	543	13.85	16.2	2105	7.35	-201.6	1.5
15-AG-023	260	296	11.39	0	1018	7.04	-13.5	0.1
15-AG-024	120	441	9.98	16.3	1299	6.8	83	0.02
15-AG-025	200	306	10.2	23.2	887	7	177.2	0
15-AG-026	140	250	10.61	0	2290	6.94	-87.7	0.39
15-AG-027	200	324	10.6	0	1804	6.95	-48.4	0.025
15-AG-028	130	113	10.66	1.5	3467	7.22	-8.5	0.03
15-AG-029	130	379	10.62	0	3416	6.77	-22.2	0.07
15-AG-030	240	280						0.03
15-AG-031	240	278	10.42	0	1515	7.18	-36.8	0.03
15-AG-033	260	173	10.8	0	297	7.69	-119.8	0.65
15-AG-034	0	435			1225	6.74	150.4	-0.01
15-AG-036	145	296	10.33	0	2261	6.5	-22.1	0.04
15-AG-037	140	187	10.45	0	2908	6.72	-68.2	0.36
15-AG-038	250	178	12.19	28.9	1560	7.16	122.2	0
15-AG-040	70	337	10.99	0	1379	6.97	94.4	-0.01
15-AG-041	200	127	10.53	0	3023	6.89	-39.7	-0.01

Sample	Purging Vol	Alkalinity	T	DO	Cond	pH	ORP	H ₂ S
Unit	L	mg/L CaCO ₃	°C	% Saturation	µS/cm		mV	mg/L S ²⁻
15-AG-042	135	143	10.19	0	3633	6.89	-266.2	6.5
15-AG-043	150	120	10.63	0	1496	7.24	-145.4	-0.01
15-AG-044	160	102	10.93	0	1382	7.31	-138.3	-0.01
15-AG-045	145	93	10.69	0	1680	7.4	-133.5	-0.01
15-AG-046	145	296	10.69	0	1545	6.65	74.4	0
15-AG-047	200	304	11.01	1.1	1687	6.64	-6.8	0
15-AG-048	160	511	10.36	0	2778	6.54	-73.7	0.02
15-AG-050	260	437	11.13	0	4410	6.67	-172	2
15-AG-051	140	259	11.22	34.2	976	6.81	86.1	0
15-AG-052	245	301	11.21	0	739	6.9	-101.8	-0.01
15-AG-053	180	320	9.9	4.3	2192	6.71	43.3	0
15-AG-054	200	65	10.32	0	1614	7.49	-162.3	0.04
15-AG-055	200	57	10.98	0	3836	6.98	-270.1	4
15-AG-056	210	55	10.44	0	3602	7.44	-247.4	3
15-AG-057	320	146						0
15-AG-058	200	54	10.86	0	2931	7.51	-131	-0.01
15-AG-059	214	89	12.16	1.3	3384	7.46	-187.8	0.12
15-AG-060	320	172	11.12	2.5	2317	6.82	94	0
15-AG-061	260	183	12.24	0	3239	7.02	-78.5	0.04
15-AG-062	0	386	10.94		1099	7.22	19.2	0.02
15-AG-063	280	299	10.55	0	2161	6.92	-42.1	0.09
15-AG-064	140	191	11.33	0	3032	7.01	-55.3	0.11
15-AG-065	140	453	10.71	0	3897	6.84	-180.9	6.5
15-AG-066	260	290	9.26	0	711	7.22	110.1	0
15-AG-067	180	197	10.65	0	3663	6.99	12.3	0.02
15-AG-068	50	382	12.54	69.2	1338	7.04	15.4	0
15-AG-069	170	43						0.215
15-AG-070	170	35	10.76	0	3221	7.77	-166.8	0.21
15-AG-071	280	226	10.11	0	3987	6.97	-290.6	38.75
15-AG-072	160	43	11.75	0	2335	8.02	-220.8	0.06
15-AG-073	140	151	10.78	0	529	8.1	-88.7	0.08
15-AG-074	270	45	10.35	0	2232	7.95	-150.4	0.02
15-AG-076	260	375	10.76	0	3759	6.7	94	0.02
15-AG-077	140	535	9.74	2	1468	7.19	-204.7	6.15
15-AG-078	190	516	9.79	0	1560	7.06	40.9	0.04
15-AG-080	100	415	10.1	1	2205	6.86	15.4	0.05
15-AG-081	71.361	204	13.15	12	3377	7.41	-107.9	0.1
15-AG-082	260	58	10.54	0	500	8.07	-158.7	-0.01

Sample	Purging Vol	Alkalinity	T	DO	Cond	pH	ORP	H ₂ S
Unit	L	mg/L CaCO ₃	°C	% Saturation	µS/cm		mV	mg/L S ²⁻
15-AG-083	170	303			1623	6.74	-24	-0.01
15-AG-084	140	33	11.02	0	3180	7.83	-263.7	2
15-AG-085	200	352	11.87	0	4284	6.63	-79.1	-0.01
15-AG-086	270	184	10.86	0	2480	6.98	-247.3	4
15-AG-087	200	88	10.99	0	4357	7.38	-159.5	-0.01
15-AG-088	170	95	10.58	0	2176	7.28	-151.8	-0.01
15-AG-090	140	81	10.91	0	3505	7.35	-213.5	0.16
15-AG-091	150	110	14.57	0	3214	6.97	-189.4	1.7
15-AG-093	2200	108	11.05	0	6458	7.33	-215.6	1.5
15-AG-094	1037.4	123	11.46	0	4217	7.18	-311.8	17.5
15-AG-095	783	34	11.59	0	3412	8.17	-193.6	-0.01
15-AG-096	140	381	10.59	0	1398	6.64	-199	0.12
15-AG-097	280	318	11.56	0	1140	6.78	-201.5	-0.01
15-AG-098	280	243	11.53	0	2076	6.8	-279.2	-0.01
15-AG-099	140	374						0.24
15-AG-100	20	179	10.12	0	3758	6.85	-319.7	30
15-AG-101	200	339	11.08	0	1582	6.95	-10.3	0.03
15-AG-102	180	344	9.83	0	1196	6.94	-28.9	0.09
15-AG-103	260	251	11.2	0	1476	7	7.3	0.05
15-AG-104	420	385	11.09	0	1803	6.86	-93	0.08
15-AG-105	280	100	11.11	0	3177	7.4	-86.1	0.02
15-AG-106	260	43	11.12	0	2060	7.76	-109.2	0.02
15-AG-107	380	78	11.9	0	1566	8.11	-159.5	0.03
15-AG-108	200	508	11.75	0	2073	6.92	-14.7	0.05
15-AG-109	150	376						0.03
15-AG-110	140	290	10.98	0	1116	7.03	173.5	0
15-AG-111	225	194	11.94	0	1137	7.32	-106.3	0.05
15-AG-112	150	382	11.16	0	4043	6.67	21.3	0.03
15-AG-113	200	346	10.52	78.2	1663	7.07	136.2	0
15-AG-114	220	179	10.45	0	481	7.57	-95.4	0.03
15-AG-116	280	42	11.11	0	2496	7.83	-183.9	0.25
15-AG-117	260	75	11.08	27.6	2574	7.62	-188.4	5.5
15-AG-118	220	279	10.71	0	885	6.95	26.7	0.02
15-AG-120	240	371	12.02	0	2422	6.72	-33.1	0.02
15-AG-121	300	39	11	0	3957	7.51	-154.1	1.7
15-AG-122	260	189	10.98	0	3426	7.19	-88.3	0.2
15-AG-123	280	267	11.14	35.4	1319	7.52	-65.7	-0.01
15-AG-124	290	40	11.31	0	3979	8.06	-208.9	0

Sample	Purging Vol	Alkalinity	T	DO	Cond	pH	ORP	H ₂ S
Unit	L	mg/L CaCO ₃	°C	% Saturation	µS/cm		mV	mg/L S ²⁻
15-AG-125	260	36	11.17	0	3803	7.51	-134	-0.01
15-AG-126	270	122	11.32	0	3192	7.17	-217.1	6
15-AG-127	450	56	11.28	0	3659	7.68	-165.6	0.16
15-AG-128	425	49	11.29	0	3988	7.9	-172.3	0.36
15-AG-130	1697	144	10.87	0	2252	7.66	-220.5	1.6
15-AG-131	1360	43	11.18	0	2263	7.73	-254.3	-0.01
15-AG-132	260	107	11.23	0	321	8.21	-177.3	0
15-AG-133	480	252	11.05	2.2	1151	6.96	134.3	0
15-AG-134	270	152	12.19	0	416	7.71	-136	-0.01
15-AG-135	560	295	11.83	0	697	7.72	-264	8.125
15-AG-136	250	72	11.58	0.2	3060	7.42	-70.1	-0.01
15-AG-136	250	72	11.58	0.2	3060	7.42	-70.1	-0.01
15-AG-137	1000	64	10.96	0	8031	7.87	-269.7	30
15-AG-138	20	272	11.03	5.5	2338	7	3.2	0.28
15-AG-139	2000	33		0				-0.01
15-AG-140		262	15.02	0	2522	6.95	-24.2	0.05
15-AG-141	1620	66	10.88	0	3949	7.34	-61.9	0.02
15-AG-143	280	31	10.78	0	3867	7.83	-69.6	-0.01
15-AG-144	1630	255	10.37	2.4	2241	6.82	-256	0
15-AG-145	280	360	10.72	0	2060	6.74	-63.6	-0.01
15-AG-146	2000	26	11.52	8.52	10706	7.39	-56.2	-0.01
15-AG-147	240	165	11.06	0	4235	6.89	-162.4	5.25
15-AG-148	300	16	11.33	1.9	3476	7.7	-128.9	0.25
15-AG-149	1630	239						0
15-AG-150	300	470	11.21	0	1003	7.13	-250.4	8.375
15-AG-151	300	349	10.17	0	1303	6.91	-294	7.5
15-AG-152	260	232	11.21	0	2879	6.94	2.4	0.06
15-AG-153	275	513	11.94	0	2422	7.12	-215.6	41.25
15-AG-165	406	236	11.72	0	7842	7.27	-277.7	37.5
15-AG-166	200	147	12.96	0	2543	7.57	-190.8	2.5
15-AG-167	200	59	12.6	0	4648	7.17	114.5	-0.01
15-AG-168	1781	80	11.84	0	363	8.23	-102.6	0.06
15-AG-170	300	62	11.7	0	5541	7.47	-39.6	-0.01
15-AG-171	240	46	14.45	0	1885	7.68	-92.2	0.02
15-AG-172	639	185	11.31	0	720	7.87	-55.2	-0.01
15-AG-173	170	186	10.7	0	515	8.05	-65.1	-0.01
15-AG-174	420	43	11.7	0	1294	7.96	-74.9	0.03
15-AG-175	1216	93	11.49	0	3742	7.26	-242.7	8

Sample	Purging Vol	Alkalinity	T	DO	Cond	pH	ORP	H ₂ S
Unit	L	mg/L CaCO ₃	°C	% Saturation	µS/cm		mV	mg/L S ²⁻
15-AG-176	878	103	11.12	0	4506	7.23	-268.2	33.75
15-AG-177	339	253	12.27	0	4595	6.98	-11.8	-0.01
15-AG-178	450	540	11.82	0	3144	6.99	2.8	0.04
15-AG-179	339	260						-0.01
15-AG-180	70	373	14.35	0	994	7.18	-208.7	6.5
15-AG-181	2382	216	12.55	90.9	789	7.46	40.9	-0.01
15-AG-182	337	242	10.43	0	3456	6.85	28.1	0.03
15-AG-183	300	515	10.54	0	1226	6.76	-118.3	0.1
15-AG-184	255	64	12.29	0	2659	7.74	-106.1	0.23
15-AG-185	500	175	10.92	0	2866	6.96	55.5	0
15-AG-186	86	499	10.94		6543	6.83	98.9	0
15-AG-187	1000	59	10.55	0	677	8.28	26.3	0.03
15-AG-188	347	80	14.31	0	6271	7.61	-86.2	5.5
15-AG-190	1000	38	10.54	0	4984	7.79	-210.7	6.25
15-AG-191	1142	91	9.86	0	330	8.42	98.8	0.06
15-AG-192	1000	59						0.03

Appendix B: Station Locations and Geologic Units

Sample	Easting	Northing	DEM	Aquifer type	Subcropping unit	Representative unit	Drift Thickness
			mASL				ft
15-AG-001	583565	4781660	230.1	Bedrock	Guelph	Guelph	77.0
15-AG-002	576977	4784402	229.6	Bedrock	Guelph	Amabel-Lockport	150.0
15-AG-003	575575	4782352	219.7	Bedrock	Guelph	Guelph	82.0
15-AG-004	568212	4757925	227.2	Bedrock	Onondaga	Onondaga	21.0
15-AG-005							
15-AG-006	572072	4751020	215.2	Bedrock	Onondaga	Onondaga	24.0
15-AG-007	566319	4740465		Bedrock	Dundee		
15-AG-008	566170	4740146		Bedrock	Dundee		
15-AG-009							
15-AG-010	566288	4739963		Bedrock	Dundee		
15-AG-011	566555	4739705		Bedrock	Dundee		
15-AG-012	564867	4752721	220.0	Bedrock	Onondaga	Amherstburg-Onondaga	30.0
15-AG-013	567116	4746058	211.6	Bedrock	Dundee	Dundee	56.0
15-AG-014	572351	4758107	215.1	Bedrock	Bertie	Bass Islands-Bertie	13.0

Sample	Easting	Northing	DEM	Aquifer type	Subcropping unit	Representative unit	Drift Thickness
			mASL				ft
15-AG-015	576957	4752338	211.7	Bedrock	Onondaga	Bass Islands-Bertie	10.0
15-AG-016	585891	4746294	195.9	Bedrock	Onondaga	Amherstburg-Onondaga	19.0
15-AG-017	577732	4749753	205.2	Bedrock	Onondaga	Amherstburg-Onondaga	23.0
15-AG-018	583253	4743674	185.5	Bedrock	Onondaga	Amherstburg-Onondaga	25.0
15-AG-019	583346	4743773	185.5	Bedrock	Onondaga	Amherstburg-Onondaga	25.0
15-AG-020	588224	4755378	197.0	Overburden	Bertie	Bass Islands-Bertie	10.0
15-AG-021	570828	4746834	200.8	Bedrock	Dundee	Dundee	47.0
15-AG-022	573375	4744015	205.9	Bedrock	Dundee	Dundee	40.0
15-AG-023	579389	4745389	196.0	Bedrock	Onondaga	Dundee	22.0
15-AG-024	584208	4749575	204.0	Bedrock	Onondaga	Onondaga	10.0
15-AG-025	577976	4757863	216.3	Bedrock	Bois Blanc	Bertie	15.0
15-AG-026	584048	4756670	223.5	Bedrock	Bois Blanc	Bertie	0.0
15-AG-027	588017	4758692	199.9	Bedrock	Salina	Salina	35.0
15-AG-028	597677	4757120	199.7	Bedrock	Salina	Salina	65.0
15-AG-029	595202	4753699	187.9	Bedrock	Salina	Salina	40.0
15-AG-030	593909	4753321	185.0	Bedrock	Bertie	Bertie	17.0
15-AG-031	593340	4753990	185.0	Bedrock	Bertie	Bertie	17.0
15-AG-032							
15-AG-033	595997	4747824	203.9	Bedrock	Onondaga	Bois Blanc	9.0
15-AG-034	579657	4760457	211.3	Overburden	Salina	Salina	57.0
15-AG-035							
15-AG-036	582807	4767968	202.0	Overburden	Salina	Overburden	42.0
15-AG-037	587990	4767747	204.9	Bedrock	Salina	Salina	33.0
15-AG-038	584845	4762921	200.3	Overburden	Salina	Salina	45.0
15-AG-039							
15-AG-040	587179	4764096	191.1	Overburden	Salina	Salina	20.0
15-AG-041	592778	4767610	205.6	Overburden	Salina	Salina	55.0
15-AG-042	598157	4768228	190.0	Bedrock	Salina	Salina	53.0
15-AG-043	592025	4771766	204.0	Bedrock	Guelph	Guelph	60.0
15-AG-044	596812	4772622	195.1	Bedrock	Guelph	Guelph	56.0
15-AG-045	603659	4772359	204.4	Bedrock	Guelph	Guelph	73.0
15-AG-046	599220	4783935	187.0	Bedrock	Lockport	Lockport	12.0
15-AG-047	602577	4777210	202.5	Bedrock	Guelph	Guelph	23.0
15-AG-048	612528	4777872	200.0	Bedrock	Lockport	Lockport	23.0
15-AG-049							
15-AG-050	607038	4776789	200.0	Bedrock	Lockport	Lockport	30.0
15-AG-051	597269	4776645	210.4	Bedrock	Guelph	Guelph	40.0
15-AG-052	590617	4781907	225.0	Bedrock	Guelph	Guelph	18.0

Sample	Easting	Northing	DEM	Aquifer type	Subcropping unit	Representative unit	Drift Thickness
			mASL				ft
15-AG-053	586990	4782157	237.0	Overburden	Guelph	Overburden	100.0
15-AG-054	582395	4777427	215.0	Bedrock	Guelph	Guelph	68.0
15-AG-055	574625	4775701	195.1	Bedrock	Guelph	Guelph	77.0
15-AG-056	583035	4773049	210.2	Bedrock	Guelph	Guelph	63.0
15-AG-057	606786	4763294	190.0	Bedrock	Salina	Salina	62.0
15-AG-058	578823	4772787	204.5	Bedrock	Salina	Salina	78.0
15-AG-059	598288	4763788	190.4	Bedrock	Salina	Salina	56.0
15-AG-060	606815	4763295	190.0	Bedrock	Salina	Salina	62.0
15-AG-061	607940	4756283	181.7	Bedrock	Salina	Salina	56.0
15-AG-062	591826	4748399	200.0	Bedrock	Onondaga	Onondaga	10.0
15-AG-063	590953	4760463	191.0	Bedrock	Salina	Salina	48.0
15-AG-064	593398	4764430	201.0	Bedrock	Salina	Salina	90.0
15-AG-065	587798	4751777	209.6	Bedrock	Onondaga	Onondaga	16.0
15-AG-066	582562	4753762	215.0	Bedrock	Onondaga	Onondaga	2.0
15-AG-067	603418	4763121	187.6	Bedrock	Salina	Salina	41.0
15-AG-068	598131	4750583	195.2	Bedrock	Bertie	Bertie	34.0
15-AG-069	608356	4754620	180.0	Bedrock	Salina	Salina	87.0
15-AG-070	608624	4754937	180.0	Bedrock	Salina	Salina	87.0
15-AG-071	578090	4776116	206.7	Bedrock	Guelph	Guelph	72.0
15-AG-072	588218	4774636	215.5	Overburden	Guelph	Guelph	87.0
15-AG-073	592251	4777644	213.0	Overburden	Guelph	Guelph	53.0
15-AG-074	587682	4776362	210.5	Bedrock	Guelph	Guelph	83.0
15-AG-075							
15-AG-076	593074	4758409	194.9	Bedrock	Salina	Salina	49.0
15-AG-077	586299	4740229	176.7	Bedrock	Dundee	Dundee	12.5
15-AG-078	591365	4743624	195.8	Bedrock	Onondaga	Onondaga	8.0
15-AG-079							
15-AG-080	603833	4780748	201.2	Bedrock	Lockport	Amabel-Lockport	16.0
15-AG-081	603406	4759319	186.5	Bedrock	Salina	Salina	48.0
15-AG-082	571023	4783579	224.9	Bedrock	Guelph	Guelph	147.0
15-AG-083	581944	4764695	198.3	Bedrock	Salina	Salina	4.0
15-AG-084	605575	4752260	180.1	Bedrock	Salina	Salina	66.0
15-AG-085	603356	4757020	189.7	Bedrock	Salina	Salina	44.0
15-AG-086	601663	4768807	192.5	Bedrock	Guelph	Guelph	77.0
15-AG-087	605830	4768515	190.0	Bedrock	Guelph	Guelph	44.0
15-AG-088	609198	4771446	202.1	Bedrock	Guelph	Guelph	75.0
15-AG-089							
15-AG-090	614402	4765707	183.0	Overburden	Guelph	Guelph	56.0

Sample	Easting	Northing	DEM mASL	Aquifer type	Subcropping unit	Representative unit	Drift Thickness ft
15-AG-091	609714	4756679	180.5	Bedrock	Salina	Salina	59.0
15-AG-092							
15-AG-093	618951	4761639	178.2	Bedrock	Salina	Salina	102.0
15-AG-094	613806	4764873	180.5	Bedrock	Guelph	Guelph	78.0
15-AG-095	618896	4756569	178.5	Bedrock	Salina	Salina	93.0
15-AG-096	617314	4778368	192.4	Bedrock	Lockport	Lockport	10.0
15-AG-097	619200	4774676	195.3	Bedrock	Lockport	Lockport	43.0
15-AG-098	631702	4775828	172.5	Bedrock	Lockport	Lockport	32.0
15-AG-099	617999	4778716	192.4	Bedrock	Lockport	Lockport	10.0
15-AG-100	598402	4768240	187.5	Bedrock	Salina	Salina	16.4
15-AG-101	607122	4784071	200.0	Bedrock	Lockport	Lockport	43.0
15-AG-102	618102	4780593	191.9	Bedrock	Lockport	Lockport	5.0
15-AG-103	622296	4778160	205.0	Bedrock	Lockport	Lockport	39.0
15-AG-104	613551	4781349	192.5	Bedrock	Lockport	Amabel-Lockport	17.0
15-AG-105	617957	4766954	185.0	Bedrock	Guelph	Guelph	97.0
15-AG-106	624849	4766271	186.2	Bedrock	Guelph	Guelph	98.0
15-AG-107	627193	4768844	185.0	Bedrock	Guelph	Guelph	81.0
15-AG-108	624188	4773554	190.0	Bedrock	Lockport	Lockport	24.0
15-AG-109	614876	4771843	190.9	Bedrock	Guelph	Guelph	21.0
15-AG-110	599913	4776572	202.3	Bedrock	Guelph	Guelph	30.0
15-AG-111	606548	4772698	205.5	Bedrock	Guelph	Guelph	60.0
15-AG-112	614763	4771390	190.9	Bedrock	Guelph	Guelph	21.0
15-AG-113	627357	4777865	188.2	Bedrock	Lockport	Clinton-Cataract	4.0
15-AG-114	633519	4767297	189.2	Bedrock	Guelph	Guelph	111.0
15-AG-115							
15-AG-116	630993	4763603	181.7	Bedrock	Salina	Salina	140.0
15-AG-117	628437	4763601	181.0	Bedrock	Salina	Salina	140.0
15-AG-118	600270	4747628	191.0	Bedrock	Onondaga	Bois Blanc	10.0
15-AG-119							
15-AG-120	605169	4749624	190.3	Bedrock	Bois Blanc	Bois Blanc	40.0
15-AG-121	628094	4749432	175.4	Bedrock	Bertie	Bertie	140.0
15-AG-122	609069	4757279	181.0	Bedrock	Salina	Salina	51.0
15-AG-123	612578	4753905	180.2	Bedrock	Salina	Salina	88.0
15-AG-124	631231	4752572	175.6	Bedrock	Salina	Salina	145.0
15-AG-125	626277	4753641	177.2	Bedrock	Salina	Salina	146.0
15-AG-126	619443	4746670	177.7	Bedrock	Bois Blanc	Bois Blanc	144.7
15-AG-127	633297	4758950	177.1	Bedrock	Salina	Salina	157.3
15-AG-128	632241	4753458	178.0	Bedrock	Salina	Salina	148.1

Sample	Easting	Northing	DEM mASL	Aquifer type	Subcropping unit	Representative unit	Drift Thickness ft
15-AG-129							
15-AG-130	602473	4752186	181.2	Bedrock	Salina	Salina	61.0
15-AG-131	631093	4766566	185.0	Bedrock	Guelph	Guelph	119.8
15-AG-132	620024	4750501	177.2	Bedrock	Salina	Salina	128.0
15-AG-133	627725	4772805	184.7	Bedrock	Lockport	Lockport	27.0
15-AG-134	633373	4770907	175.1	Bedrock	Lockport	Lockport	62.0
15-AG-135	569569	4742808	205.1	Bedrock	Dundee	Dundee	58.0
15-AG-136	612953	4753594	180.5	Bedrock	Salina	Salina	63.0
15-AG-136	612489	4753801	180.5	Bedrock	Salina	Salina	63.0
15-AG-137	615704	4762089	175.0	Bedrock	Salina	Salina	64.0
15-AG-138	572606	4758134	210.0	Bedrock	Bertie	Bertie	19.7
15-AG-139	622705	4758670	177.9	Bedrock	Salina	Salina	133.0
15-AG-140	571379	4759247	214.2	Bedrock	Bertie	Bertie	23.0
15-AG-141	624002	4762579	174.9	Bedrock	Salina	Salina	105.0
15-AG-142							
15-AG-143	629346	4755411	175.5	Bedrock	Salina	Salina	111.0
15-AG-144	585637	4755272	215.2	Bedrock	Oriskany	Bertie	2.0
15-AG-145	620619	4770046	180.2	Bedrock	Guelph	Guelph	23.0
15-AG-146	622979	4758589	177.9	Bedrock	Salina	Salina	133.0
15-AG-147	609175	4767759	190.1	Bedrock	Guelph	Guelph	48.0
15-AG-148	622297	4751623	177.6	Bedrock	Salina	Salina	117.5
15-AG-149	585938	4754704	215.2	Bedrock	Oriskany	Bertie	2.0
15-AG-150	623927	4744701	187.2	Bedrock	Onondaga	Onondaga	24.0
15-AG-151	632627	4747024	179.9	Bedrock	Onondaga	Bois Blanc	2.0
15-AG-152	609631	4749986	181.8	Bedrock	Bertie	Bertie	57.0
15-AG-153	587169	4743464		Bedrock	Dundee	Dundee	25.0
15-AG-165	664816	4757921	176.0	Bedrock	Salina	Salina	39.7
15-AG-166	649430	4763707	182.2	Bedrock	Salina	Salina	85.3
15-AG-167	646213	4760634	180.0	Bedrock	Salina	Salina	132.4
15-AG-168	639632	4766521	199.3	Bedrock	Lockport	Lockport	212.4
15-AG-169							
15-AG-170	639967	4756815	176.4	Bedrock	Salina	Salina	127.0
15-AG-171	638961	4776890	113.0	Bedrock	Queenston	Queenston	168.0
15-AG-172	639329	4769707	159.8	Bedrock	Lockport	Lockport	77.4
15-AG-173	639849	4769769	159.8	Overburden	Lockport	Overburden	77.4
15-AG-174	636192	4763322	182.4	Bedrock	Salina	Salina	180.4
15-AG-175	658716	4753202	179.7	Bedrock	Bertie	Bertie	98.8
15-AG-176	653085	4767170	176.4	Bedrock	Salina	Salina	86.9

Sample	Easting	Northing	DEM mASL	Aquifer type	Subcropping unit	Representative unit	Drift Thickness ft
15-AG-177	656547	4769592	179.4	Bedrock	Guelph	Guelph	89.1
15-AG-178	649018	4779213	120.4	Bedrock	Clinton-Cataract	Clinton-Cataract	145.2
15-AG-179	657176	4770399	179.4	Bedrock	Guelph	Guelph	89.1
15-AG-180	653639	4751561	186.5	Bedrock	Onondaga	Onondaga	6.6
15-AG-181	637335	4766496	236.6	Overburden	Guelph	Overburden	352.0
15-AG-182	602596	4761536	189.9	Bedrock	Salina	Salina	54.1
15-AG-183	594841	4772831	201.3	Overburden	Guelph	Guelph	51.0
15-AG-184	641055	4764287	187.6	Bedrock	Guelph	Guelph	133.7
15-AG-185	599800	4766754	190.4	Bedrock	Salina	Salina	63.5
15-AG-186	607079	4769023	194.5	Bedrock	Guelph	Guelph	41.0
15-AG-187	592102	4775663	225.1	Bedrock	Guelph	Guelph	130.2
15-AG-188	605253	4765821	189.5	Bedrock	Salina	Salina	49.2
15-AG-189							
15-AG-190	614745	4759048	179.9	Bedrock	Salina	Salina	75.3
15-AG-191	585725	4783164	248.6	Bedrock	Guelph	Guelph	105.8
15-AG-192	591658	4776011	225.1	Bedrock	Guelph	Guelph	130.2

Appendix C: Station and Well Information

Sample	Station	MOE Well No.	Well Type	Year Drilled	Well Depth	Static Water Level	Depth to Bedrock
					ft	ft	Ft
15-AG-001	10-AG-118	6802243	Drilled	1957	91	75.00	77
15-AG-002	10-AG-071	6807287	Drilled	1969	180		150
15-AG-003	15-AG-003	6813591	Drilled	2001	135	30.00	82
15-AG-004	15-AG-004	2602367	Drilled	1989	90	50.53	21
15-AG-005	15_Field_SRM						
15-AG-006	15-AG-006	2601134	Drilled	1952	75	50.00	24
15-AG-007	07-AG-054		Spring				
15-AG-008	07-AG-053		Spring				263
15-AG-009	15_Field_SRM						
15-AG-010	07-AG-053		Spring				263
15-AG-011	07-AG-053		Spring				263
15-AG-012	14-AG-048	4408162	Drilled	2004	62	45.11	30
15-AG-013	10-AG-113	4403393	Drilled	1974	66	0.62	56
15-AG-014	10-AG-240	2601231	Drilled	1967	24		13
15-AG-015	10-AG-058	2601479	Drilled	1971	85		10
15-AG-016	10-AG-036	2601055	Drilled	1962	36		19
15-AG-017	10-AG-037	2602473	Drilled	1992	63		23
15-AG-018	10-AG-024		Drilled	1970	25		25
15-AG-019	10-AG-024		Drilled	1970	25		25
15-AG-020	10-AG-005	2602426	Drilled	1991	67		
15-AG-021	15-AG-021	2602669	Drilled	2002	66	51.51	47
15-AG-022	15-AG-022		Drilled	1990	150	32.00	40
15-AG-023	15-AG-023	2601528	Drilled	1972	57	35.48	22
15-AG-024	15-AG-024	2601062	Drilled	1964	58	20.00	10
15-AG-025	15-AG-025	2602510	Drilled	1996	48	35.00	15
15-AG-026	15-AG-026	2601270	Drilled	1968	73	9.00	0

Sample	Station	MOE Well No.	Well Type	Year Drilled	Well Depth	Static Water Level	Depth to Bedrock
					ft	ft	Ft
15-AG-027	15-AG-027	2602111	Drilled	1983	38	12.00	35
15-AG-028	15-AG-028	2600281	Drilled	1966	70	48.00	65
15-AG-029	10-AG-003	2600338	Drilled	1962	60		40
15-AG-030	15-AG-031		Drilled	2008	33	29.00	17
15-AG-031	15-AG-031		Drilled	2008	33	29.00	17
15-AG-032	15_Field_SRM						
15-AG-033	10-AG-022		Drilled	2001	35		9
15-AG-034	10-AG-050	2602148	Drilled	1984	57		
15-AG-035	15_Field_SRM						
15-AG-036	15-AG-036	2601478	Drilled	1971	52	28.00	42
15-AG-037	15-AG-037	2602264	Drilled	1987	42	32.00	33
15-AG-038	10-AG-048	2601553	Drilled	1972	43		
15-AG-039	15_Field_SRM						
15-AG-040	10-AG-047	2601599	Drilled	1973	27		
15-AG-041	15-AG-041	2600637	Drilled	1956	68	37.50	55
15-AG-042	15-AG-042	2601294	Drilled	1968	53	11.00	53
15-AG-043	15-AG-043	6812169	Drilled	1991	64	25.00	60
15-AG-044	15-AG-044	6809559	Drilled	1976	58	12.00	56
15-AG-045	15-AG-045	3801839	Drilled	1968	76	20.00	73
15-AG-046	15-AG-046	6807439	Drilled	1968	38	9.00	12
15-AG-047	15-AG-047	6801108	Drilled	1953	25	10.00	23
15-AG-048	15-AG-048	3802618	Drilled	1977	48	11.65	23
15-AG-049	15_Field_SRM						
15-AG-050	15-AG-050	3802053	Drilled	1970	32	20.00	30
15-AG-051	15-AG-051	6801446	Drilled	1967	63	30.00	40
15-AG-052	15-AG-052	6803472	Drilled	1955	22	0.00	18
15-AG-053	15-AG-053	6808604	Bored	1973	50	25.00	
15-AG-054	15-AG-054	6808311	Drilled	1971	72	28.90	68
15-AG-055	15-AG-055	1306520	Drilled	2005	101.7	8.20	77
15-AG-056	15-AG-056	2600728	Drilled	1963	78	59.65	63
15-AG-057	15-AG-060		Drilled	1915	80	24.00	62
15-AG-058	15-AG-058	1301426	Drilled	1969	80	39.00	78
15-AG-059	15-AG-059	2601876	Drilled	1977	90	25.69	56
15-AG-060	15-AG-060		Drilled	1915	80	24.00	62
15-AG-061	10-AG-001	2601544	Drilled	1972	75		56
15-AG-062	15-AG-062		Drilled	1995	50	20.00	10
15-AG-063	15-AG-063	2601847	Drilled	1976	52	25.00	48

Sample	Station	MOE Well No.	Well Type	Year Drilled	Well Depth	Static Water Level	Depth to Bedrock
					ft	ft	ft
15-AG-064	10-AG-046	2602153	Drilled	1984	91		90
15-AG-065	15-AG-065	2601336	Drilled	1969	32	16.00	16
15-AG-066	15-AG-066		Drilled	1940	27.5	9.02	2
15-AG-067	10-AG-043	2601680	Drilled	1974	43		41
15-AG-068	15-AG-068	2601389	Drilled	1970	65	50.00	34
15-AG-069	15-AG-070	2600072	Drilled	1966	92	15.00	87
15-AG-070	15-AG-070	2600072	Drilled	1966	92	15.00	87
15-AG-071	10-AG-057	1302401	Drilled	1976	80	3.66	72
15-AG-072	10-AG-055	6809287	Drilled	1975	91	12.19	
15-AG-073	10-AG-062	6803986	Drilled	1965	52		
15-AG-074	10-AG-063	6810806	Drilled	1976	95	25.26	83
15-AG-075	15_Field_SRM						
15-AG-076	15-AG-076	2602355	Drilled	1989	58	49.00	49
15-AG-077	15-AG-077	2602525	Drilled	1997	27	15.00	13
15-AG-078	15-AG-078		Drilled	1930	32	8.33	8
15-AG-079	15_Field_SRM						
15-AG-080	10-AG-086	6807521	Drilled	1970	25		16
15-AG-081	15-AG-081		Drilled	1975	51.3	18.44	48
15-AG-082	10-AG-073		Drilled	2007	150	56.73	147
15-AG-083	10-AG-051	2600427	Drilled	1958	28	3.05	4
15-AG-084	15-AG-084	2602322	Drilled	1989	77	14.00	66
15-AG-085	15-AG-085		Drilled	1985	46	65.81	44
15-AG-086	15-AG-086	6808880	Drilled	1974	77	19.00	77
15-AG-087	15-AG-087	3800032	Drilled	1948	45	20.00	44
15-AG-088	15-AG-088	3800093	Drilled	1952	85	24.00	75
15-AG-089	15_Field_SRM						
15-AG-090	10-AG-011	3802783	Drilled	1979	55	6.49	
15-AG-091	15-AG-091	2600063	Drilled	1957	61	10.00	59
15-AG-092	15_Field_SRM						
15-AG-093	15-AG-093	3800417	Drilled	1958	115	11.81	102
15-AG-094	15-AG-094		Drilled	1960	84.3	16.73	78
15-AG-095	15-AG-095	2601660	Drilled	1973	96	10.30	93
15-AG-096	15-AG-096	3802119	Drilled	1971	28	12.00	10
15-AG-097	15-AG-097	3803382	Drilled	1990	47	24.28	43
15-AG-098	15-AG-098	3801841	Drilled	1968	56	26.00	32
15-AG-099	15-AG-096	3802119	Drilled	1971	28	12.00	10
15-AG-100	15-AG-100		Spring			0.00	

Sample	Station	MOE Well No.	Well Type	Year Drilled	Well Depth	Static Water Levels	Depth to Bedrock
					ft	ft	ft
15-AG-101	15-AG-101	6804729	Drilled	1963	51	36.00	43
15-AG-102	15-AG-102	3802317	Drilled	1973	26	10.00	5
15-AG-103	15-AG-103	3803710	Drilled	1995	60	38.00	39
15-AG-104	10-AG-088	3804235	Drilled	2005	32		17
15-AG-105	15-AG-105	3800458	Drilled	1952	102	20.00	97
15-AG-106	15-AG-106	3802004	Drilled	1970	102	38.00	98
15-AG-107	15-AG-107	3802366	Drilled	1974	82	29.00	81
15-AG-108	15-AG-108	3800388	Drilled	1959	42	15.00	24
15-AG-109	10-AG-098	3802411	Drilled	1974	28		21
15-AG-110	10-AG-061	6809873	Drilled	1978	32	12.63	30
15-AG-111	10-AG-038		Drilled	1995	64		60
15-AG-112	10-AG-098	3802411	Drilled	1974	28		21
15-AG-113	10-AG-067	3800286	Drilled	1965	43	4.66	4
15-AG-114	15-AG-114	6602764	Drilled	1973	120	45.00	111
15-AG-115	15_Field_SRM						
15-AG-116	15-AG-116	3801852	Drilled	1969	150	34.00	140
15-AG-117	10-AG-033	3802704	Drilled	1978	163		140
15-AG-118	10-AG-064	2601819	Drilled	1976	58		10
15-AG-119	15_Field_SRM						
15-AG-120	15-AG-120	7209783	Drilled	2013	55	40.00	40
15-AG-121	15-AG-121	7226390	Drilled	2014	150	9.32	140
15-AG-122	10-AG-002	2602375	Drilled	1990	55		51
15-AG-123	10-AG-007	2600206	Drilled	1948	90		88
15-AG-124	10-AG-054	6602189	Drilled	1951	148	18.37	145
15-AG-125	15-AG-125	7226316	Monitoring	2014	155.3	15.88	146
15-AG-126	15-AG-126	7233499	Monitoring	2014	152.2	9.02	145
15-AG-127	15-AG-127	7226393	Monitoring	2014	167.5	13.30	157
15-AG-128	15-AG-128	7226315	Monitoring	2014	158.8	15.91	148
15-AG-129	15_Field_SRM						
15-AG-130	15-AG-130	2600867	Drilled	1948	62	14.67	61
15-AG-131	15-AG-131	7226317	Monitoring	2014	133.4	31.30	120
15-AG-132	15-AG-132	2600250	Drilled	1948	131	32.84	128
15-AG-133	15-AG-133	3803575	Drilled	1992	62	24.48	27
15-AG-134	15-AG-134	6601462	Drilled	1966	67	20.00	62
15-AG-135	15-AG-135	4407915	Drilled	2002	135	60.99	58
15-AG-136	15-AG-136		Drilled	2004	76	13.00	63
15-AG-136	15-AG-136		Drilled	2004	76	13.00	63
15-AG-137	15-AG-137	3800006	Drilled	1964	65	6.37	64

Sample	Station	MOE Well No.	Well Type	Year Drilled	Well Depth	Static Water Level	Depth to Bedrock
					ft	ft	ft
15-AG-138	15-AG-138		Spring			0.00	
15-AG-139	15-AG-146	6604700	Drilled	2002	134	10.00	133
15-AG-140	15-AG-140		Spring			0.00	
15-AG-141	15-AG-141		Drilled		111.5	11.68	105
15-AG-142	15_Field_SRM						
15-AG-143	10-AG-034	6603341	Drilled	1979	125		111
15-AG-144	15-AG-144		Drilled	2002	85	69.65	2
15-AG-145	15-AG-145	3803953	Drilled	2001	35	4.41	23
15-AG-146	15-AG-146	6604700	Drilled	2002	134	10.00	133
15-AG-147	15-AG-147	3803824	Drilled	1998	66	35.00	48
15-AG-148	15-AG-148	2602302	Drilled	1988	127	21.19	118
15-AG-149	15-AG-144		Drilled	2002	85	69.65	2
15-AG-150	15-AG-150		Drilled	1970	67.2	34.58	24
15-AG-151	15-AG-151	6603884	Drilled	1989	33	15.35	2
15-AG-152	15-AG-152	2600124	Drilled	1964	66	23.00	57
15-AG-153	15-AG-153		Drilled	1940	45	27.00	25
15-AG-165	15-AG-165	7228874	Monitoring	2014	45.2	10.07	40
15-AG-166	15-AG-166	7226394	Monitoring	2014	95.0	31.76	85
15-AG-167	15-AG-167	7226392	Monitoring	2014	141.7	43.27	132
15-AG-168	15-AG-168	7226393	Monitoring	2014	223.3	69.16	212
15-AG-169	15_Field_SRM						
15-AG-170	15-AG-170	7226391	Monitoring	2014	138.0	31.30	127
15-AG-171	15-AG-171	7233498	Monitoring	2014	174.9	52.82	168
15-AG-172	15-AG-172	6604857	Monitoring	2004	86.6	3.71	77
15-AG-173	15-AG-173	6604857	Monitoring	2004	29.5	4.76	77
15-AG-174	15-AG-174	7226389	Monitoring	2014	190.3	33.36	180
15-AG-175	15-AG-175	7228875	Monitoring	2014	109.8	5.01	99
15-AG-176	15-AG-176	7231244	Monitoring	2014	94.7	19.13	87
15-AG-177	15-AG-177	7228877	Monitoring	2014	99.5	70.21	89
15-AG-178	15-AG-178	7226318	Monitoring	2015	155.0	39.37	145
15-AG-179	15-AG-177	7228877	Monitoring	2014	99.5	70.21	89
15-AG-180	15-AG-180	7140781	Monitoring	2003	16.1	7.87	7
15-AG-181	15-AG-181	6601550	Monitoring	1966	147.5	117.03	352
15-AG-182	15-AG-182	7140790	Monitoring	2003	65.7	20.18	54
15-AG-183	15-AG-183	6809537	Monitoring	1973	50.5	29.00	51
15-AG-184	15-AG-184	7228876	Monitoring	2014	140.0	53.69	134
15-AG-185	15-AG-185		Monitoring	2015	70.2	28.38	63
15-AG-186	15-AG-186		Monitoring	1998	46.3	42.93	41

Sample	Station	MOE Well No.	Well Type	Year Drilled	Well Depth ft	Static Water Levels ft	Depth to Bedrock ft
15-AG-187	15-AG-187		Monitoring	2015	138.5	72.41	130
15-AG-188	15-AG-188		Monitoring	2015	57.0	28.25	49
15-AG-189	15_Field_SRM						
15-AG-190	15-AG-190		Monitoring	2015	82.4	15.72	75
15-AG-191	15-AG-191		Monitoring	2015	112.7	16.63	106
15-AG-192	15-AG-187		Monitoring	2015	138.5	72.41	130

Appendix D: Major Ion Chemistry

Sample	Ca ²⁺ mg/L	Mg ²⁺ mg/L	K ⁺ mg/L	Na ⁺ mg/L	HCO ₃ ⁻ mg/L	SO ₄ ²⁻ mg/L	Cl ⁻ mg/L	F ⁻ mg/L
15-AG-001	149	33	5.6	109	46	748	3	1.2
15-AG-002	193	38	5.6	49	101	700	11	2.1
15-AG-003	23	10	6.3	39	125	93	4	2.3
15-AG-004	<0.2	<0.5	5.1	218	345	170	35	1.0
15-AG-005	156	48	4.7	8		400	5	1.4
15-AG-006	209	150	9.3	74	441	1016	22	1.4
15-AG-007	67	17	7.0	18	188	35	48	0.2
15-AG-008	86	21	6.9	25	250	132	50	0.4
15-AG-009	10	3	4.8	5		60	203	7.4
15-AG-010	147	47	8.6	45	360	365	79	1.3
15-AG-011	86	22	9.7	29	305	67	59	1.3
15-AG-012	140	68	6.5	15	301	465	8	2.0
15-AG-013	12	6	4.4	35	163	1	1	0.3
15-AG-014	530	41	6.0	9	344	1411	31	1.5
15-AG-015	81	123	6.5	78	574	237	168	1.9
15-AG-016	208	532	11.2	269	810	2858	26	0.6
15-AG-017	200	91	9.1	46	472	652	29	0.4
15-AG-018	106	70	9.6	88	402	319	127	0.4
15-AG-019	107	71	9.6	88	406	319	131	0.5
15-AG-020	566	24	6.9	11	276	1493	24	0.3
15-AG-021	101	56	7.0	55	324	354	33	1.4
15-AG-022	109	197	9.3	121	662	898	12	1.4
15-AG-023	97	44	9.3	50	361	143	88	0.3
15-AG-024	156	65	8.3	42	538	315	28	0.3
15-AG-025	108	26	11.9	31	373	73	54	0.2
15-AG-026	500	55	9.4	10	305	1404	28	0.8
15-AG-027	317	66	6.9	27	395	884	18	0.6

Sample	Ca ²⁺	Mg ²⁺	K ⁺	Na ⁺	HCO ₃ ⁻	SO ₄ ²⁻	Cl ⁻	F ⁻
	mg/L	mg/L	mg/L	mg/L	mg/L	mg/L	mg/L	mg/L
15-AG-028	460	231	7.4	158	138	2470	17	0.8
15-AG-029	478	273	8.7	77	462	2212	12	0.6
15-AG-030	275	45	6.4	19	341	688	23	0.1
15-AG-031	275	45	6.8	19	339	683	27	0.0
15-AG-032	<0.2	<0.5	4.4	<0.8		<0.5	3	0.5
15-AG-033	54	6	4.6	2	211	4	3	0.1
15-AG-034	180	47	8.3	13	530	163	18	1.3
15-AG-035	155	48	4.9	7		415	6	0.2
15-AG-036	468	62	7.7	16	361	1311	13	0.6
15-AG-037	497	114	10.6	90	228	1973	28	0.3
15-AG-038	253	26	7.9	48	217	591	87	2.4
15-AG-039	9	5	6.4	197		63	210	0.5
15-AG-040	205	55	6.1	27	411	474	42	0.5
15-AG-041	478	135	7.0	121	155	2283	6	0.6
15-AG-042	523	144	13.1	168	174	2123	294	0.7
15-AG-043	169	61	7.2	69	146	776	25	1.1
15-AG-044	142	55	5.2	77	125	730	9	1.2
15-AG-045	169	71	5.9	103	113	962	8	1.3
15-AG-046	182	58	7.0	69	361	332	167	0.2
15-AG-047	179	44	5.3	102	371	274	216	0.3
15-AG-048	216	225	7.0	91	623	1026	183	0.3
15-AG-049	11	3	4.6	5		56	207	7.6
15-AG-050	415	457	8.2	130	533	3101	28	0.3
15-AG-051	112	46	6.6	17	316	249	13	1.1
15-AG-052	67	47	5.3	12	367	66	19	0.2
15-AG-053	152	27	5.5	210	390	82	459	0.1
15-AG-054	154	51	6.8	100	79	703	75	1.4
15-AG-055	493	139	13.0	207	69	1918	329	0.7
15-AG-056	485	116	14.8	190	67	1893	260	0.6
15-AG-057	428	48	31.4	25	178	1236	9	0.4
15-AG-058	462	92	6.8	114	66	1860	43	0.4
15-AG-059	456	167	8.5	144	108	2281	17	0.5
15-AG-060	397	45	33.6	23	210	1164	10	0.4
15-AG-061	478	191	7.4	125	223	2530	19	0.7
15-AG-062	113	49	4.7	36	471	128	61	0.5
15-AG-063	443	44	6.1	19	365	1111	29	0.4
15-AG-064	492	143	7.9	116	233	2065	19	0.2
15-AG-065	259	377	12.5	132	552	2438	21	0.7

Sample	Ca ²⁺	Mg ²⁺	K ⁺	Na ⁺	HCO ₃ ⁻	SO ₄ ²⁻	Cl ⁻	F ⁻
	mg/L	mg/L	mg/L	mg/L	mg/L	mg/L	mg/L	mg/L
15-AG-066	104	25	8.0	11	354	99	17	0.2
15-AG-067	476	236	9.3	135	240	2429	44	0.6
15-AG-068	157	64	5.5	26	466	327	37	0.1
15-AG-069	457	119	6.6	159	52	2147	15	0.8
15-AG-070	462	121	7.1	163	43	2140	15	0.7
15-AG-071	471	153	13.8	200	276	1552	512	0.7
15-AG-072	283	73	6.0	135	52	1311	39	0.7
15-AG-073	25	19	4.2	43	184	117	1	1.1
15-AG-074	221	79	5.4	145	55	1178	54	0.6
15-AG-075	155	49	3.9	8		378	6	1.3
15-AG-076	491	265	7.5	90	457	2369	21	0.7
15-AG-077	79	121	10.5	63	652	265	58	0.9
15-AG-078	106	108	7.0	61	629	244	113	0.4
15-AG-079	9	5	5.8	191		58	214	2.5
15-AG-080	205	148	6.0	56	506	876	68	0.5
15-AG-081	472	200	7.7	98	249	2252	13	0.5
15-AG-082	15	6	3.9	67	71	146	6	2.1
15-AG-083	283	35	5.5	14	369	611	16	0.4
15-AG-084	446	114	6.2	168	40	2111	9	0.7
15-AG-085	459	357	8.5	139	429	2950	19	0.8
15-AG-086	214	151	7.2	131	224	1245	78	0.9
15-AG-087	438	200	8.7	294	107	2000	470	0.6
15-AG-088	216	93	5.2	131	115	1195	8	0.8
15-AG-089	10	3	4.5	5		57	213	2.5
15-AG-090	358	132	9.0	231	99	1542	368	0.6
15-AG-091	473	150	6.7	112	134	2122	18	0.7
15-AG-092	<0.2	<0.5	4.0	<0.8		<0.5	0	0.0
15-AG-093	603	157	21.5	659	131	1528	1641	0.3
15-AG-094	451	177	18.8	330	150	1832	622	0.5
15-AG-095	449	151	8.8	252	41	2429	88	0.6
15-AG-096	180	72	5.5	28	465	451	32	0.2
15-AG-097	119	62	5.2	42	388	247	74	0.4
15-AG-098	391	74	6.5	75	296	1087	80	0.2
15-AG-099	193	72	5.9	29	456	484	33	0.2
15-AG-100	543	119	9.4	194	218	1720	408	0.6
15-AG-101	168	94	7.4	31	413	520	43	0.1
15-AG-102	119	55	6.5	37	419	159	104	0.1
15-AG-103	204	47	5.6	41	306	576	8	0.2

Sample	Ca ²⁺	Mg ²⁺	K ⁺	Na ⁺	HCO ₃ ⁻	SO ₄ ²⁻	Cl ⁻	F ⁻
	mg/L	mg/L	mg/L	mg/L	mg/L	mg/L	mg/L	mg/L
15-AG-104	175	77	5.6	61	469	225	263	0.0
15-AG-105	295	136	7.5	208	122	1495	255	0.5
15-AG-106	193	67	5.3	163	52	1115	17	0.9
15-AG-107	121	43	4.5	144	95	784	7	1.4
15-AG-108	124	201	7.2	64	619	838	10	0.1
15-AG-109	455	464	8.6	168	458	3338	44	0.1
15-AG-110	125	29	6.7	78	354	77	202	0.5
15-AG-111	138	56	4.9	55	237	529	11	0.9
15-AG-112	416	421	9.8	153	466	3014	41	0.1
15-AG-113	180	99	4.8	64	422	478	188	0.4
15-AG-114	45	32	4.1	13	218	65	25	0.7
15-AG-115	154	48	4.3	7		377	6	1.3
15-AG-116	282	126	7.1	165	51	1314	237	0.7
15-AG-117	476	101	7.3	106	91	1876	42	1.1
15-AG-118	88	44	8.0	24	340	93	66	0.4
15-AG-119	9	5	5.5	192		58	214	2.4
15-AG-120	382	127	6.7	41	452	1184	33	0.3
15-AG-121	486	171	7.6	268	48	2333	289	0.8
15-AG-122	501	203	6.3	132	230	2228	22	1.0
15-AG-123	200	22	44.1	9	326	383	22	0.1
15-AG-124	470	173	8.2	272	49	2317	228	1.2
15-AG-125	476	143	11.0	268	44	2183	214	1.2
15-AG-126	485	141	9.7	125	149	2036	38	0.9
15-AG-127	512	140	11.2	177	68	1996	271	1.2
15-AG-128	475	157	9.4	280	60	2241	246	1.2
15-AG-129	10	3	4.0	5		57	203	6.9
15-AG-130	242	71	15.7	89	176	732	173	0.8
15-AG-131	296	82	5.8	115	52	1334	7	1.7
15-AG-132	36	9	6.8	7	130	56	2	0.3
15-AG-133	191	41	4.4	8	307	392	8	0.3
15-AG-134	26	31	4.3	11	185	64	1	1.1
15-AG-135	29	19	5.9	83	360	90	15	3.2
15-AG-136	484	114	5.5	138	88	1990	21	1.3
15-AG-136	484	114	5.5	138	88	1990	21	1.3
15-AG-137	680	240	18.9	798	78	2097	1783	1.0
15-AG-138	545	25	5.2	11	332	1229	34	0.5
15-AG-139	835	317	21.7	1133	40	2022	2949	0.9
15-AG-140	573	33	5.4	7	319	1361	22	0.4

Sample	Ca ²⁺	Mg ²⁺	K ⁺	Na ⁺	HCO ₃ ⁻	SO ₄ ²⁻	Cl ⁻	F ⁻
	mg/L	mg/L	mg/L	mg/L	mg/L	mg/L	mg/L	mg/L
15-AG-141	497	169	9.4	232	80	1972	372	1.2
15-AG-142	0	0	3.2	<0.8		<0.5	0	0.0
15-AG-143	494	147	10.4	226	38	2068	298	1.1
15-AG-144	513	36	6.4	8	311	1193	16	0.4
15-AG-145	194	179	6.2	34	439	916	13	1.1
15-AG-146	843	319	22.0	1139	32	1931	2814	0.9
15-AG-147	491	217	11.5	242	201	2144	295	1.2
15-AG-148	445	151	7.5	223	20	2295	30	1.4
15-AG-149	502	35	6.9	8	291	1195	16	0.4
15-AG-150	56	74	6.2	38	573	90	12	1.0
15-AG-151	112	46	7.2	55	426	51	204	0.5
15-AG-152	524	52	7.2	77	283	1351	146	0.4
15-AG-153	206	149	8.4	128	625	786	173	0.4
15-AG-165	832	310	14.2	538	288	1917	1756	0.7
15-AG-166	520	108	4.2	80	179	1746	20	1.0
15-AG-167	531	185	10.7	332	72	2280	397	0.8
15-AG-168	30	8	0.7	32	98	84	1	2.2
15-AG-169	11	3	0.8	5		33	130	1.2
15-AG-170	691	196	10.3	375	76	1878	1045	0.9
15-AG-171	164	32	12.1	213	56	975	21	0.4
15-AG-172	71	39	1.6	17	226	167	26	0.6
15-AG-173	48	33	1.4	7	227	67	11	0.5
15-AG-174	149	49	1.8	74	52	732	25	1.3
15-AG-175	580	223	8.0	115	113	2340	283	1.6
15-AG-176	557	205	11.0	274	126	2198	585	1.5
15-AG-177	279	206	12.5	393	308	845	1100	0.8
15-AG-178	138	220	12.5	234	658	533	537	0.3
15-AG-179	278	203	12.4	415	317	840	1094	0.8
15-AG-180	119	60	3.1	19	455	200	21	1.3
15-AG-181	93	32	1.4	20	263	62	97	0.1
15-AG-182	540	259	7.7	95	295	2533	11	1.0
15-AG-183	154	59	1.9	33	628	77	60	1.0
15-AG-184	468	91	4.1	87	78	1849	7	1.1
15-AG-185	572	126	4.3	71	213	1989	26	1.0
15-AG-186	431	902	9.4	290	608	5203	28	2.2
15-AG-187	40	18	1.2	70	72	286	2	1.2
15-AG-188	651	237	16.5	637	98	2586	1147	0.9
15-AG-189	9	6	2.3	205		59	209	2.3

Sample	Ca ²⁺	Mg ²⁺	K ⁺	Na ⁺	HCO ₃ ⁻	SO ₄ ²⁻	Cl ⁻	F ⁻
	mg/L	mg/L	mg/L	mg/L	mg/L	mg/L	mg/L	mg/L
15-AG-190	559	196	8.4	451	46	2624	555	1.4
15-AG-191	19	9	0.8	30	111	75	3	0.5
15-AG-192	40	18	1.2	70	72	282	2	1.2

Appendix E: Bacterial and Nitrogen Parameters

Sample	NO ₃ ⁻	NO ₂ ⁻	NH ₃ NH ₄ ⁺	TKN	Organic N	Total Coliforms	Fecal Coliforms
	mg/L as N	mg/L as N	mg/L as N	mg/L as N	mg/L as N	Count	Count
15-AG-001	0.048	<0.003	0.16	0.18	<0.05	0	0
15-AG-002	0.058	0.064	0.09	0.13	<0.05	17	10
15-AG-003	<0.006	<0.003	0.04	0.11	0.07	0	0
15-AG-004	0.024	<0.003	<0.04	0.3	0.27	0	0
15-AG-005	3.16	<0.003	<0.04	0.63	0.6	0	0
15-AG-006	0.012	<0.003	0.92	1.14	0.22	36	0
15-AG-007	8.16	0.174	<0.04	0.28	0.26	900	409
15-AG-008	<0.006	<0.003	0.13	0.35	0.22	4	0
15-AG-009	0.187	<0.003	4.55	4.58	<0.05	0	0
15-AG-010	<0.006	<0.003	0.44	0.56	0.12	0	0
15-AG-011	<0.006	<0.003	0.51	0.77	0.26	11	2
15-AG-012	<0.006	<0.003	0.29	0.24	<0.05	0	0
15-AG-013	<0.006	<0.003	0.16	0.27	0.11	0	0
15-AG-014	0.344	<0.003	<0.04	<0.05	<0.05	27	0
15-AG-015	0.113	0.009	0.37	0.32	<0.05	36	0
15-AG-016	<0.006	<0.003	0.44	0.53	0.09	0	0
15-AG-017	<0.006	<0.003	0.48	0.58	0.1	0	0
15-AG-018	<0.006	<0.003	0.49	0.77	0.28	1	1
15-AG-019	<0.006	<0.003	0.54	0.75	0.21	0	0
15-AG-020	<0.006	<0.003	0.22	0.3	0.08	0	0
15-AG-021	0.009	<0.003	0.59	0.73	0.14	0	0
15-AG-022	<0.006	<0.003	0.36	0.41	0.05	6	0
15-AG-023	<0.006	<0.003	0.22	0.45	0.23		
15-AG-024	0.518	<0.003	<0.04	0.3	0.3		
15-AG-025	6.23	0.003	0.04	<0.05	<0.05	29	1
15-AG-026	0.008	<0.003	0.45	0.53	0.08	0	0
15-AG-027	<0.006	<0.003	0.13	0.14	<0.05	0	0
15-AG-028	0.039	<0.003	0.51	0.54	<0.05	1	0

Sample	NO ₃ ⁻	NO ₂ ⁻	NH ₃ NH ₄ ⁺	TKN	Organic N	Total Coliforms	Fecal Coliforms
	mg/L as N	mg/L as N	mg/L as N	mg/L as N	mg/L as N	Count	Count
15-AG-029	<0.006	<0.003	<0.04	<0.05	<0.05	0	0
15-AG-030	<0.006	<0.003	<0.04	0.07	0.05	1	0
15-AG-031	<0.006	<0.003	0.05	<0.05	<0.05	0	0
15-AG-032	<0.006	<0.003	<0.04	<0.05	<0.05	0	0
15-AG-033	<0.006	<0.003	0.22	0.56	0.34	0	0
15-AG-034	25.6	<0.003	0.37	0.5	0.13	39	0
15-AG-035	0.102	<0.003	0.04	<0.05	<0.05	0	0
15-AG-036	<0.006	<0.003	0.04	<0.05	<0.05	0	0
15-AG-037	<0.006	<0.003	0.43	0.7	0.27	940	560
15-AG-038	0.229	<0.003	<0.04	0.24	0.22	1020	237
15-AG-039	0.008	<0.003	<0.04	<0.05	<0.05	0	0
15-AG-040	2.23	<0.003	0.18	0.25	0.07	0	0
15-AG-041	<0.006	<0.003	0.35	0.37	<0.05	0	0
15-AG-042	<0.006	<0.003	0.95	1.8	0.85	0	0
15-AG-043	<0.006	<0.003	0.29	0.32	<0.05	0	0
15-AG-044	<0.006	<0.003	0.27	0.26	<0.05	0	0
15-AG-045	<0.006	<0.003	0.26	0.33	0.07	0	0
15-AG-046	1.21	0.003	0.12	0.13	<0.05	7	0
15-AG-047	0.267	<0.003	<0.04	<0.05	<0.05	21	0
15-AG-048	<0.006	<0.003	0.21	0.18	<0.05	8	0
15-AG-049	0.198	<0.003	5.03	4.96	<0.05	0	0
15-AG-050	<0.006	<0.003	0.29	0.41	0.12	0	0
15-AG-051	0.165	<0.003	<0.04	<0.05	<0.05	2	0
15-AG-052	<0.006	<0.003	0.1	0.11	<0.05	0	0
15-AG-053	0.559	<0.003	<0.04	<0.05	<0.05	49	1
15-AG-054	<0.006	<0.003	0.19	0.24	0.05	1	0
15-AG-055	<0.006	<0.003	0.54	1.45	0.91	0	0
15-AG-056	<0.006	<0.003	1.23	1.8	0.57	1	1
15-AG-057	4.32	0.091	0.08	0.39	0.31	197	216
15-AG-058	0.009	<0.003	0.46	0.52	0.06	0	0
15-AG-059	<0.006	<0.003	0.8	0.83	<0.05	0	0
15-AG-060	5.37	0.067	<0.04	<0.05	<0.05	205	217
15-AG-061	<0.006	<0.003	0.5	0.47	<0.05	0	0
15-AG-062	0.009	<0.003	0.06	<0.05	<0.05	0	0
15-AG-063	<0.006	<0.003	<0.04	0.06	0.05	1	0
15-AG-064	<0.006	<0.003	0.35	0.51	0.16	49	0
15-AG-065	<0.006	<0.003	0.8	1	0.2	0	0

Sample	NO ₃ ⁻	NO ₂ ⁻	NH ₃ NH ₄ ⁺	TKN	Organic N	Total Coliforms	Fecal Coliforms
	mg/L as N	mg/L as N	mg/L as N	mg/L as N	mg/L as N	Count	Count
15-AG-066	0.068	0.009	<0.04	0.19	0.18	1	0
15-AG-067	<0.006	<0.003	0.45	0.55	0.1	1	0
15-AG-068	0.154	<0.003	<0.04	<0.05	<0.05	0	0
15-AG-069	<0.006	<0.003	0.54	0.65	0.11	0	0
15-AG-070	<0.006	<0.003	0.54	0.7	0.16	55	0
15-AG-071	<0.006	<0.003	0.94	0.89	<0.05	0	0
15-AG-072	<0.006	<0.003	0.45	0.46	<0.05	80	0
15-AG-073	<0.006	<0.003	0.2	0.18	<0.05	0	0
15-AG-074	<0.006	<0.003	0.39	0.41	<0.05	0	0
15-AG-075	3.15	0.004	0.07	0.06	<0.05	0	0
15-AG-076	<0.006	<0.003	0.05	0.08	<0.05	1	0
15-AG-077	<0.006	<0.003	0.19	0.6	0.41	51	1
15-AG-078	0.692	0.02	0.07	<0.05	<0.05	17	1
15-AG-079	0.2	<0.003	0.06	<0.05	<0.05	0	0
15-AG-080	0.007	<0.003	0.37	0.66	0.29	39	0
15-AG-081	0.008	<0.003	0.42	0.62	0.2	7	1
15-AG-082	<0.006	<0.003	0.16	0.14	<0.05	0	0
15-AG-083	0.098	0.013	<0.04	0.05	0.11	0	0
15-AG-084	<0.006	<0.003	0.31	0.43	0.12	0	0
15-AG-085	<0.006	<0.003	0.22	0.27	0.05	36	0
15-AG-086	<0.006	<0.003	0.35	0.5	0.15	0	0
15-AG-087	0.006	<0.003	0.76	1.15	0.39	8	3
15-AG-088	<0.006	<0.003	0.36	0.48	0.12	2	0
15-AG-089	5.02	<0.003	4.91	5.06	0.15	0	0
15-AG-090	<0.006	<0.003	0.73	1.35	0.62	0	0
15-AG-091	<0.006	<0.003	0.49	0.64	0.15	0	0
15-AG-092	0.098	<0.003	0.06	<0.05	<0.05	0	0
15-AG-093	0.144	<0.003	0.85	0.84	<0.05	200	99
15-AG-094	<0.006	<0.003	1.52	1.65	0.13	340	40
15-AG-095	<0.006	0.018	0.46	0.47	<0.05	14	1
15-AG-096	0.425	0.066	0.09	0.07	<0.05	48	33
15-AG-097	<0.006	<0.003	0.13	0.08	<0.05	0	0
15-AG-098	0.046	<0.003	0.14	0.3	0.16	0	0
15-AG-099	0.39	0.074	<0.04	0.09	0.06	50	37
15-AG-100	<0.006	<0.003	0.68	1.08	0.4	2	0
15-AG-101	<0.006	<0.003	0.27	0.35	0.08	12	0
15-AG-102	<0.006	<0.003	0.21	0.33	0.12	4	1

Sample	NO ₃ ⁻	NO ₂ ⁻	NH ₃ NH ₄ ⁺	TKN	Organic N	Total Coliforms	Fecal Coliforms
	mg/L as N	mg/L as N	mg/L as N	mg/L as N	mg/L as N	Count	Count
15-AG-103	<0.006	<0.003	0.19	0.26	0.07	2	0
15-AG-104	<0.006	<0.003	0.21	0.22	<0.05	0	0
15-AG-105	1.03	0.018	0.51	0.7	0.19	89	80
15-AG-106	<0.006	<0.003	0.21	0.28	0.07	68	7
15-AG-107	<0.006	<0.003	0.19	0.28	0.09	0	0
15-AG-108	0.019	<0.003	0.04	0.11	0.07	0	0
15-AG-109	0.011	<0.003	0.67	0.7	<0.05	16	0
15-AG-110	2.04	<0.003	<0.04	<0.05	<0.05	33	0
15-AG-111	<0.006	<0.003	0.27	0.23	<0.05	0	0
15-AG-112	0.028	<0.003	0.61	0.9	0.29	20	0
15-AG-113	0.478	<0.003	<0.04	<0.05	<0.05	44	0
15-AG-114	<0.006	<0.003	<0.04	<0.05	<0.05	0	0
15-AG-115	3.13	<0.003	<0.04	<0.05	<0.05	0	0
15-AG-116	<0.006	<0.003	0.12	0.1	<0.05	68	21
15-AG-117	<0.006	<0.003	0.27	0.32	0.05	0	0
15-AG-118	1.96	0.04	0.27	0.34	0.07		137
15-AG-119	0.199	<0.003	<0.04	<0.05	<0.05	0	0
15-AG-120	<0.006	<0.003	0.24	0.28	<0.05	0	0
15-AG-121	<0.006	<0.003	0.57	1.6	1.03	0	0
15-AG-122	0.078	<0.003	0.65	0.71	0.06	5	0
15-AG-123	11.2	<0.003	<0.04	<0.05	<0.05	88	77
15-AG-124	<0.006	<0.003	0.55	0.35	<0.05	8	0
15-AG-125	<0.006	<0.003	0.6	0.9	0.3	0	0
15-AG-126	<0.006	<0.003	0.65	0.73	0.08	1	0
15-AG-127	<0.006	<0.003	0.67	0.87	0.2	59	0
15-AG-128	<0.006	<0.003	0.69	0.83	0.14	53	0
15-AG-129	0.192	<0.003	3.64	3.69	0.05	0	0
15-AG-130	1.44	0.03	0.19	0.27	0.08	0	0
15-AG-131	<0.006	<0.003	0.23	0.3	0.07	10	4
15-AG-132	0.017	<0.003	0.15	0.15	<0.05	1	0
15-AG-133	0.11	<0.003	<0.04	0.08	0.08	1	0
15-AG-134	<0.006	<0.003	0.09	0.06	<0.05	1	1
15-AG-135	<0.006	<0.003	0.45	0.81	0.36	8	0
15-AG-136	<0.006	<0.003	0.52	0.54	<0.05	0	0
15-AG-136	<0.006	<0.003	0.52	0.54	<0.05	0	0
15-AG-137	<0.006	<0.003	2.04	2.1	0.06	2	0
15-AG-138	<0.006	<0.003	<0.04	0.16	0.16	1	0

Sample	NO ₃ ⁻	NO ₂ ⁻	NH ₃ NH ₄ ⁺	TKN	Organic N	Total Coliforms	Fecal Coliforms
	mg/L as N	mg/L as N	mg/L as N	mg/L as N	mg/L as N	Count	Count
15-AG-139	<0.006	<0.003	2.29	2.6	0.31	1	0
15-AG-140	<0.006	<0.003	0.06	0.12	0.06	22	19
15-AG-141	<0.006	<0.003	0.95	1.3	0.35	52	1
15-AG-142	<0.006	<0.003	<0.04	<0.05	<0.05	0	0
15-AG-143	<0.006	<0.003	0.63	0.75	0.12	0	0
15-AG-144	1.09	<0.003	0.08	0	<0.05	1	0
15-AG-145	0.27	0.028	<0.04	0.08	0.06	86	0
15-AG-146	<0.006	<0.003	2.37	3.7	1.05	2	0
15-AG-147	<0.006	<0.003	0.48	0.56	0.08	103	0
15-AG-148	<0.006	<0.003	0.4	0.44	<0.05	0	0
15-AG-149	1.1	<0.003	<0.04	0	<0.05	1	0
15-AG-150	0.021	<0.003	0.48	0.51	<0.05	440	11
15-AG-151	0.043	0.049	0.24	0.5	0.26	620	49
15-AG-152	0.032	<0.003	0.42	0.7	0.28		
15-AG-153	<0.006	<0.003	1.29	1.28	<0.05	25	19
15-AG-165	<0.006	<0.003	1.86	2.2	0.34	0	0
15-AG-166	<0.006	<0.003	0.18	0.24	0.06	2	0
15-AG-167	0.006	<0.003	1.21	1.6	0.34	5	0
15-AG-168	<0.006	<0.003	<0.04	<0.05	<0.05	0	0
15-AG-169	<0.006	<0.003	0.13	0.16	<0.05	0	0
15-AG-170	<0.006	<0.003	0.64	1.55	0.91	0	0
15-AG-171	<0.006	<0.003	1.13	1.16	<0.05	1	0
15-AG-172	<0.006	<0.003	0.09	0.11	<0.05	0	0
15-AG-173	<0.006	<0.003	0.06	<0.05	<0.05	0	0
15-AG-174	<0.006	<0.003	0.16	0.15	<0.05	1	0
15-AG-175	<0.006	<0.003	0.79	0.71	<0.05	0	0
15-AG-176	<0.006	<0.003	0.87	1.4	0.53	0	0
15-AG-177	<0.006	<0.003	1.07	1.9	0.83	0	0
15-AG-178	0.026	<0.003	0.33	0.95	0.62	0	0
15-AG-179	<0.006	<0.003	1.17	1.75	0.58	0	0
15-AG-180	<0.006	<0.003	0.3	0.56	0.26	0	0
15-AG-181	6.41	0.014	<0.04	0.14	0.14	0	0
15-AG-182	<0.006	<0.003	0.46	0.56	0.1	0	0
15-AG-183	<0.006	<0.003	0.92	1.17	0.25	0	0
15-AG-184	<0.006	<0.003	0.48	0.49	<0.05	200	0
15-AG-185	<0.006	<0.003	0.62	0.68	0.06	3	0
15-AG-186	<0.006	<0.003	0.54	0.64	0.1	400	0

Sample	NO ₃ ⁻	NO ₂ ⁻	NH ₃ NH ₄ ⁺	TKN	Organic N	Total Coliforms	Fecal Coliforms
	mg/L as N	mg/L as N	mg/L as N	mg/L as N	mg/L as N	Count	Count
15-AG-187	<0.006	<0.003	0.18	0.18	<0.05	2	0
15-AG-188	<0.006	<0.003	1.26	2.6	1.34	20	0
15-AG-189	0.176	<0.003	0.09	0.06	<0.05	0	0
15-AG-190	<0.006	<0.003	1.1	1.18	0.08	27	0
15-AG-191	<0.006	0.01	0.17	0.18	<0.05	0	0
15-AG-192	<0.006	<0.003	0.19	0.2	<0.05	20	1

Appendix F: Dissolved Gasses and Carbon Species

Sample	Field CH ₄	Field CO ₂	Lab CH ₄ - M	Lab CH ₄	Dissolved Organic Carbon
	ppmw	ppmw	μmol/L	ppmw	mg/L
15-AG-001	0	0	0.67	0.01	1.05
15-AG-002	0	2.76	3.17	0.05	1.04
15-AG-003	0	0	0.50	0.01	0.79
15-AG-004	0	25.96			2.19
15-AG-005					0.51
15-AG-006	0	37.47	6.16	0.10	1.07
15-AG-007	0	4.14	1.21	0.02	6.21
15-AG-008	0	1.39	7.08	0.11	2.69
15-AG-009					0.92
15-AG-010	0.27	11.11	117.11	1.88	1.78
15-AG-011	0.17	15.98	68.65	1.10	3.08
15-AG-012	0	18.99	23.79	0.38	0.41
15-AG-013	9.00	0.68	516.39	8.28	0.99
15-AG-014	0	34.61	0.16	0.00	0.73
15-AG-015	0	37.27			2.29
15-AG-016	0	102.50	2.95	0.05	4.65
15-AG-017	0	35.28	2.36	0.04	1.92
15-AG-018	0.16	31.28	4.89	0.08	4.47
15-AG-019	0	29.29	6.20	0.10	4.4
15-AG-020	0	15.64	4.79	0.08	2.29
15-AG-021	0	10.15	9.42	0.15	0.9
15-AG-022	0	28.37	22.22	0.36	1.43
15-AG-023	0	30.77	7.97	0.13	4.52
15-AG-024	0	78.27	0.66	0.01	5.24
15-AG-025	0	44.00	0.16	0.00	2.24

Sample	Field CH ₄	Field CO ₂	Lab CH ₄ - M	Lab CH ₄	Dissolved Organic Carbon
	ppmw	ppmw	µmol/L	ppmw	mg/L
15-AG-026	0	37.27	1.20	0.02	2.26
15-AG-027	0	51.25	0.34	0.01	0.91
15-AG-028	0.14	9.32	0.71	0.01	1.55
15-AG-029	0	62.44	0.23	0.00	1.58
15-AG-030	0	25.12	0.26	0.00	1.39
15-AG-031	0	22.11	0.33	0.01	1.51
15-AG-032					0.06
15-AG-033	0.42	4.55	130.99	2.10	1.665
15-AG-034	0	107.65	0.07	0.00	1.43
15-AG-035					0.42
15-AG-036	0	58.67			0.64
15-AG-037	0	23.41	8.20	0.13	1.69
15-AG-038	0	16.72	0.12	0.00	5.78
15-AG-039					14.52
15-AG-040	0	46.14	0.44	0.01	1.34
15-AG-041	0	9.76	1.17	0.02	1.4
15-AG-042	0	5.85	14.41	0.23	0.57
15-AG-043	0	5.35	2.58	0.04	0.65
15-AG-044	0	2.67	3.73	0.06	0.81
15-AG-045	0	2.67	0.85	0.01	1.23
15-AG-046	0	37.17	0.48	0.01	1.24
15-AG-047	0	43.35	0.14	0.00	1.01
15-AG-048	0	91.37	0.42	0.01	3.84
15-AG-049					0.9
15-AG-050	0	52.02	12.62	0.20	7.5
15-AG-051	0	22.83	0.09	0.00	0.65
15-AG-052	0	18.80	0.25	0.00	0.4
15-AG-053	0	33.29	0.06	0.00	1.055
15-AG-054	2.96	0.67	343.71	5.51	0.74
15-AG-055	0	6.02	7.11	0.11	0.39
15-AG-056	0	1.34	3.44	0.06	0.66
15-AG-057	0	13.46	0.11	0.00	2.48
15-AG-058	0	0.67	0.43	0.01	0.75
15-AG-059	0	4.04	0.87	0.01	1.21
15-AG-060	0	13.46	0.09	0.00	2.6
15-AG-061	0	16.05	1.21	0.02	1.82
15-AG-062	0	41.35	2.14	0.03	1.45
15-AG-063	0	40.02	0.15	0.00	1.01

Sample	Field CH ₄	Field CO ₂	Lab CH ₄ - M	Lab CH ₄	Dissolved Organic Carbon
	ppmw	ppmw	µmol/L	ppmw	mg/L
15-AG-064	0	19.34	0.97	0.02	2.945
15-AG-065	0	67.16	9.63	0.15	1.39
15-AG-066	0	18.80	0.24	0.00	2.79
15-AG-067	0	21.49	0.79	0.01	2.01
15-AG-068	0	41.64	1.05	0.02	1.03
15-AG-069	0	0.67	1.13	0.02	1.36
15-AG-070	0	0.67	1.24	0.02	1.2
15-AG-071	0.23	14.14	13.40	0.21	0.38
15-AG-072	0	0	0.93	0.01	0.835
15-AG-073	0	0.67	0.46	0.01	0.42
15-AG-074	0	0	1.13	0.02	0.76
15-AG-075					0.39
15-AG-076	0	76.72	0.43	0.01	1.24
15-AG-077	0.55	49.04	46.17	0.74	4.81
15-AG-078	0	62.57	0.52	0.01	5.04
15-AG-079					14.38
15-AG-080	0	72.69	1.32	0.02	3.83
15-AG-081	0	16.84	2.19	0.04	2.12
15-AG-082	0	0	1.06	0.02	0.82
15-AG-083	0	39.60	1.45	0.02	1.88
15-AG-084	0.41	0	36.53	0.59	0.93
15-AG-085	0	68.09	0.48	0.01	1.95
15-AG-086	0.23	12.33	13.82	0.22	1.92
15-AG-087	0	3.89	1.03	0.02	1.02
15-AG-088	0	3.25	0.47	0.01	1.36
15-AG-089					0.88
15-AG-090	0	3.25	3.23	0.05	1.63
15-AG-091	0	8.70	1.42	0.02	1.46
15-AG-092					0.13
15-AG-093	0	4.06	1.92	0.03	1.43
15-AG-094	0	1.35	0.05	0.00	1.82
15-AG-095	0	0	1.10	0.02	0.71
15-AG-096	0	49.68	0.32	0.01	1.9
15-AG-097	0	23.82	0.30	0.00	2.74
15-AG-098	0	27.91	0.18	0.00	0.49
15-AG-099	0	54.45	0.41	0.01	1.83
15-AG-100	0.44	28.58	23.14	0.37	0.62
15-AG-101	0	47.38	0.18	0.00	0.98

Sample	Field CH ₄	Field CO ₂	Lab CH ₄ - M	Lab CH ₄	Dissolved Organic Carbon
	ppmw	ppmw	µmol/L	ppmw	mg/L
15-AG-102	0	46.08	2.29	0.04	1.67
15-AG-103	0	27.91	0.20	0.00	0.46
15-AG-104	0	54.52	0.34	0.01	2.26
15-AG-105	0	4.69	0.91	0.01	2.945
15-AG-106	0	0.67	0.49	0.01	1.32
15-AG-107	0	0	0.63	0.01	2.17
15-AG-108	0	72.31	0.10	0.00	2.09
15-AG-109	0	75.03	0.26	0.00	7.66
15-AG-110	0	27.71	0.13	0.00	0.9
15-AG-111	0	12.17	0.71	0.01	1.24
15-AG-112	0	59.48	0.29	0.00	8.13
15-AG-113	0	27.71	0.10	0.00	2.09
15-AG-114	0	3.89	0.16	0.00	0.47
15-AG-115					0.46
15-AG-116	0	0	14.38	0.23	0.63
15-AG-117	0	2.97	3.54	0.06	0.645
15-AG-118	0	63.81	0.30	0.00	4.84
15-AG-119					9.39
15-AG-120	0	128.94	1.29	0.02	3.64
15-AG-121	0	0.75	5.26	0.08	0.43
15-AG-122	0	42.76	2.22	0.04	1.58
15-AG-123	0	17.10	0.21	0.00	6.2
15-AG-124	0	0.66	3.50	0.06	0.31
15-AG-125	0	0.65	6.01	0.10	3.93
15-AG-126	0.80	11.49	116.46	1.87	1.14
15-AG-127	0	3.38	0.77	0.01	0.49
15-AG-128	0	1.48	7.86	0.13	1.79
15-AG-129					0.97
15-AG-130	0	0.65	4.06	0.07	1.965
15-AG-131	0	2.02	0.64	0.01	0.85
15-AG-132	0	0	0.09	0.00	1.57
15-AG-133	0	37.17	0.21	0.00	1.19
15-AG-134	0	4.05	0.21	0.00	0.16
15-AG-135	11.86	0	489.25	7.85	1.26
15-AG-136	0	3.24	0.22	0.00	1.13
15-AG-136	0	3.24	1.42	0.02	1.13
15-AG-137	0	8.43	0.87	0.01	0.39
15-AG-138	0	26.29	1.04	0.02	1.38

00Sample	Field CH ₄	Field CO ₂	Lab CH ₄ - M	Lab CH ₄	Dissolved Organic Carbon
	ppmw	ppmw	µmol/L	ppmw	mg/L
15-AG-139	0	0	2.54	0.04	0.17
15-AG-140	0	36.40	5.22	0.08	1.07
15-AG-141	0	4.15	0.77	0.01	0.76
15-AG-142					0.06
15-AG-143	0	0	2.02	0.03	0.4
15-AG-144	0	31.12	0.07	0.00	1.23
15-AG-145	0	41.07	0.09	0.00	1.41
15-AG-146	0	0	2.74	0.04	0.2
15-AG-147	0.62	13.69	0.87	0.01	1.01
15-AG-148	0	0	2.34	0.04	0.74
15-AG-149	0	28.35	0.11	0.00	1
15-AG-150	1.85	37.25	0.06	0.00	0.915
15-AG-151	1.68	27.34	0.12	0.00	2.89
15-AG-152	0	34.17	1.10	0.02	
15-AG-153	0.25	83.58	25.27	0.41	3.35
15-AG-165	0.16	11.20	196.85	3.16	2.6
15-AG-166	9.14	10.54	740.01	11.87	0.7
15-AG-167			2.54	0.04	1.4
15-AG-168	0	0.66	0.31	0.01	3.8
15-AG-169					0.9
15-AG-170	0	1.97	5.13	0.08	0.9
15-AG-171			1.10	0.02	1.6
15-AG-172	0	6.02	0.14	0.00	0.2
15-AG-173	0	4.68	0.13	0.00	0.3
15-AG-174	0	0	0.90	0.01	2.6
15-AG-175			56.01	0.90	1.3
15-AG-176	0.38	0	39.86	0.64	0.4
15-AG-177	0	30.41	0.68	0.01	1.2
15-AG-178	0	62.81	0.29	0.00	0.7
15-AG-179	0	26.44	0.72	0.01	1.1
15-AG-180	1.06	29.57	141.38	2.27	2.8
15-AG-181	0	7.88	0.31	0.01	0.3
15-AG-182	0	42.05	0.57	0.01	1.8
15-AG-183	3.03	132.95	194.94	3.13	6.2
15-AG-184	0.22	0	13.87	0.22	3.6
15-AG-185	0	21.25	1.23	0.02	1.5
15-AG-186	0	85.02	0.16	0.00	1.1
15-AG-187	0	0	0.52	0.01	0.6

Sample	Field CH ₄	Field CO ₂	Lab CH ₄ - M	Lab CH ₄	Dissolved Organic Carbon
	ppmw	ppmw	µmol/L	ppmw	mg/L
15-AG-188	0	0.61	1.77	0.03	3.8
15-AG-189					
15-AG-190	0	0	2.73	0.04	0.9
15-AG-191	0	0	0.94	0.02	3.2
15-AG-192	0	0	0.60	0.01	0.8

Appendix G: Minor Constituents – B, PO₄, Si, Sr, B, Fe and I

Sample	Br	PO ₄	Si	Sr	B	Fe	I
	ppm	ppm	ppm	ppm	ppb	ppb	ppb
15-AG-001	0.11	<0.04	3.6	11.0	315	<15	85
15-AG-002	0.15	<0.04	4.2	6.9	455	<15	55
15-AG-003	0.08	<0.04	3.2	0.6	311	<15	41
15-AG-004	0.02	<0.04	2.9	0.0	29	<15	6
15-AG-005	0.02	<0.04	4.6	12.6	68	<15	4
15-AG-006	0.15	<0.04	4.9	9.4	761	410	53
15-AG-007	0.05	<0.04	2.3	0.6	37	<15	11
15-AG-008	0.17	<0.04	2.2	2.6	118	<15	225
15-AG-009	0.42	<0.04	2.1	0.1	17	66	176
15-AG-010	0.53	<0.04	3.4	9.4	407	<15	181
15-AG-011	0.04	<0.04	2.1	1.3	90	<15	53
15-AG-012	0.03	<0.04	5.4	7.7	366	202	49
15-AG-013	0.04	<0.04	5.4	0.7	277	<15	27
15-AG-014	0.53	<0.04	5.3	14.1	144	<15	7
15-AG-015	0.06	<0.04	4.9	2.0	70	1017	21
15-AG-016	0.19	<0.04	7.0	6.6	241	981	51
15-AG-017	0.18	<0.04	4.8	6.9	779	2533	15
15-AG-018	0.19	<0.04	4.9	1.7	282	72	182
15-AG-019	0.14	<0.04	4.9	1.8	280	<15	130
15-AG-020	0.13	<0.04	3.7	20.1	167	<15	31
15-AG-021	0.16	<0.04	5.8	6.7	773	106	98
15-AG-022	0.12	<0.04	7.2	9.5	415	239	48
15-AG-023	0.07	<0.04	3.9	1.3	48	578	29
15-AG-024	0.06	<0.04	6.5	1.5	37	<15	9
15-AG-025	0.05	<0.04	4.6	10.1	24	<15	7
15-AG-026	0.18	<0.04	3.8	12.9	466	210	11
15-AG-027	0.10	<0.04	7.9	16.4	136	1165	12
15-AG-028	0.14	0.00	7.1	10.9	1016	1070	46

Sample	Br	PO4	Si	Sr	B	Fe	I
	ppm	ppm	ppm	ppm	ppb	ppb	ppb
15-AG-029	0.10	<0.04	7.1	10.9	315	316	22
15-AG-030	0.10	<0.04	4.5	10.1	130	1315	13
15-AG-031	<0.02	<0.04	4.3	10.1	130	1316	15
15-AG-032	<0.02	<0.04	0.3	<0.005	<10	<15	4
15-AG-033	0.04	<0.04	2.1	0.3	22	<15	12
15-AG-034	<0.02	<0.04	4.2	1.9	37	<15	9
15-AG-035	0.05	<0.04	4.5	12.5	61	<15	2
15-AG-036	0.17	<0.04	6.1	11.9	245	2058	8
15-AG-037	0.03	<0.04	8.2	11.7	865	1009	38
15-AG-038	0.41	<0.04	3.5	9.0	42	<15	6
15-AG-039	0.14	<0.04	3.4	0.5	1755	510	38
15-AG-040	0.13	<0.04	5.4	3.0	104	279	10
15-AG-041	0.10	0.00	7.9	11.5	661	419	38
15-AG-042	3.29	<0.04	5.9	11.8	1596	90	160
15-AG-043	0.29	<0.04	7.8	15.0	456	1348	38
15-AG-044	0.13	<0.04	5.2	15.3	372	556	57
15-AG-045	0.14	<0.04	4.6	10.2	250	622	52
15-AG-046	0.49	<0.04	4.9	3.7	111	<15	26
15-AG-047	0.08	<0.04	5.4	1.4	63	71	13
15-AG-048	0.13	<0.04	4.6	0.9	45	7807	14
15-AG-049	0.50	<0.04	1.8	0.1	13	76	147
15-AG-050	0.14	<0.04	7.7	5.3	94	2114	31
15-AG-051	0.04	<0.04	4.8	17.9	161	<15	5
15-AG-052	0.02	<0.04	11.8	0.6	75	1004	6
15-AG-053	0.08	<0.04	4.8	1.2	57	<15	14
15-AG-054	0.91	<0.04	3.4	10.3	329	184	100
15-AG-055	3.85	<0.04	3.4	11.1	1065	6996	100
15-AG-056	2.63	<0.04	3.4	10.7	3107	253	101
15-AG-057	0.07	0.29	4.8	8.7	294	<15	6
15-AG-058	0.51	<0.04	4.5	10.7	1581	480	32
15-AG-059	0.19	<0.04	5.8	10.2	1467	4324	45
15-AG-060	0.07	<0.04	5.0	8.0	268	<15	7
15-AG-061	0.19	0.00	9.7	11.2	943	1874	104
15-AG-062	0.04	<0.04	6.3	1.0	20	642	12
15-AG-063	0.13	<0.04	4.9	8.0	125	1416	8
15-AG-064	0.09	<0.04	5.9	10.5	812	1509	37
15-AG-065	0.22	<0.04	4.0	12.5	507	192	76
15-AG-066	0.06	<0.04	2.5	0.3	26	<15	2

Sample	Br	PO4	Si	Sr	B	Fe	I
	ppm	ppm	ppm	ppm	ppb	ppb	ppb
15-AG-067	0.46	<0.04	7.1	10.3	1401	1513	40
15-AG-068	0.10	<0.04	3.1	26.6	45	1637	9
15-AG-069	0.20	<0.04	4.9	10.2	884	952	96
15-AG-070	0.20	<0.04	5.1	10.3	889	489	96
15-AG-071	6.43	<0.04	3.5	11.9	820	<15	153
15-AG-072	0.52	<0.04	4.0	10.3	430	266	76
15-AG-073	0.03	<0.04	4.7	20.6	284	<15	22
15-AG-074	0.72	<0.04	4.2	12.8	361	347	127
15-AG-075	<0.02	<0.04	4.2	12.3	59	<15	5
15-AG-076	0.19	<0.04	6.8	10.7	422	1345	14
15-AG-077	0.15	<0.04	5.6	1.8	120	348	69
15-AG-078	1.55	<0.04	5.1	1.2	26	91	60
15-AG-079	0.49	<0.04	3.1	0.5	1719	461	38
15-AG-080	0.13	<0.04	5.6	2.1	64	1798	18
15-AG-081	0.11	<0.04	7.1	10.7	785	9513	30
15-AG-082	0.17	<0.04	3.2	0.6	483	<15	112
15-AG-083	0.03	<0.04	4.4	3.1	46	160	8
15-AG-084	0.15	<0.04	3.8	10.1	482	2099	0
15-AG-085	0.13	<0.04	8.8	11.3	657	2197	36
15-AG-086	0.81	<0.04	6.8	12.1	467	<15	100
15-AG-087	5.40	<0.04	5.2	12.4	541	2476	124
15-AG-088	0.12	<0.04	4.7	12.3	253	927	54
15-AG-089	0.49	<0.04	1.8	0.1	<10	<15	159
15-AG-090	3.90	<0.04	5.1	12.4	935	798	111
15-AG-091	0.18	0.09	6.7	10.8	1148	<15	68
15-AG-092	<0.02	<0.04	<0.065	<0.005	<10	<15	3
15-AG-093	18.56	0.26	4.8	11.1	812	260	247
15-AG-094	7.14	1.42	4.7	11.6	1365	<15	281
15-AG-095	1.04	<0.04	3.4	9.8	2004	222	125
15-AG-096	0.14	<0.04	5.0	2.2	95	67	6
15-AG-097	0.06	<0.04	5.4	1.4	50	1576	15
15-AG-098	0.71	<0.04	6.3	3.9	361	440	13
15-AG-099	0.14	<0.04	5.1	2.5	98	<15	8
15-AG-100	4.99	<0.04	5.2	12.8	659	<15	650
15-AG-101	0.07	<0.04	6.0	3.7	198	735	16
15-AG-102	0.15	<0.04	5.3	0.8	49	79	11
15-AG-103	0.09	<0.04	5.1	8.0	337	241	18
15-AG-104	0.11	<0.04	5.3	1.3	28	2880	29

Sample	Br	PO4	Si	Sr	B	Fe	I
	ppm	ppm	ppm	ppm	ppb	ppb	ppb
15-AG-105	2.60	<0.04	4.5	10.2	462	1497	106
15-AG-106	0.31	<0.04	3.2	11.4	392	411	106
15-AG-107	0.11	<0.04	3.2	3.1	315	211	67
15-AG-108	0.05	<0.04	6.8	2.1	127	234	8
15-AG-109	0.33	<0.04	6.8	9.1	124	2946	23
15-AG-110	0.09	<0.04	5.2	0.8	83	<15	14
15-AG-111	0.12	<0.04	5.6	4.1	194	1343	25
15-AG-112	0.31	<0.04	6.4	8.2	114	2156	26
15-AG-113	0.13	<0.04	4.6	0.8	32	<15	10
15-AG-114	0.02	<0.04	7.3	0.4	35	131	7
15-AG-115	<0.02	<0.04	4.2	12.2	50	<15	2
15-AG-116	2.60	<0.04	4.3	14.0	933	403	211
15-AG-117	0.55	<0.04	3.6	9.2	531	235	80
15-AG-118	0.52	<0.04	2.7	1.1	40	90	11
15-AG-119	0.49	<0.04	3.0	0.5	1728	486	36
15-AG-120	0.08	0.11	4.7	40.6	212	1693	17
15-AG-121	3.10	<0.04	4.2	10.3	2161	<15	181
15-AG-122	0.23	<0.04	9.2	11.3	1031	2017	46
15-AG-123	0.02	0.66	5.7	1.1	86	<15	0
15-AG-124	2.33	<0.04	3.3	10.5	2765	2293	161
15-AG-125	2.30	<0.04	4.0	10.6	2360	739	130
15-AG-126	0.42	<0.04	6.8	10.5	2655	<15	226
15-AG-127	2.67	<0.04	4.7	10.9	1690	373	73
15-AG-128	2.33	<0.04	3.9	10.3	3200	96	155
15-AG-129	0.48	<0.04	1.8	0.1	12	103	155
15-AG-130	1.49	<0.04	4.1	22.4	840	303	72
15-AG-131	0.19	0.08	3.1	9.6	614	189	94
15-AG-132	0.02	<0.04	1.1	0.6	190	<15	14
15-AG-133	0.03	<0.04	5.1	7.1	52	<15	6
15-AG-134	<0.02	<0.04	6.6	1.9	81	85	7
15-AG-135	0.27	<0.04	2.9	3.8	774	<15	203
15-AG-136	0.26	<0.04	6.8	10.8	639	1123	78
15-AG-136	0.26	<0.04	6.8	10.8	639	1123	78
15-AG-137	20.46	<0.04	3.8	14.2	3044	231	420
15-AG-138	0.03	0.17	3.4	18.1	190	68	14
15-AG-139	32.33	0.15	3.4	18.3	4709	542	506
15-AG-140	0.03	<0.04	5.1	18.8	227	1065	33
15-AG-141	4.14	<0.04	5.6	11.4	896	1373	113

Sample	Br	PO4	Si	Sr	B	Fe	I
	ppm	ppm	ppm	ppm	ppb	ppb	ppb
15-AG-142	<0.02	<0.04	<0.065	<0.005	<10	<15	3
15-AG-143	3.10	<0.04	3.5	10.9	2159	261	111
15-AG-144	0.06	0.11	2.2	16.4	257	<15	5
15-AG-145	0.05	0.15	6.4	12.6	97	<15	8
15-AG-146	32.28	<0.04	3.3	18.4	4738	609	515
15-AG-147	3.21	<0.04	4.1	11.4	675	<15	124
15-AG-148	0.50	<0.04	2.8	9.6	1471	800	102
15-AG-149	0.06	0.05	2.2	16.2	252	<15	5
15-AG-150	0.12	<0.04	6.2	11.8	312	676	88
15-AG-151	0.07	<0.04	3.7	2.4	81	218	178
15-AG-152	1.00	<0.04	7.0	8.8	606	546	42
15-AG-153	1.30	0.08	5.5	5.3	1786	<15	25
15-AG-165	13.05	<0.04	7.9	17.4	6142	<15	346
15-AG-166	0.25	<0.04	8.6	11.3	466	685	67
15-AG-167	3.77	<0.04	4.9	11.0	4147	359	150
15-AG-168	<0.02	<0.04	4.5	0.6	301	115	10
15-AG-169	0.19	0.37	2.0	0.1	12	96	42
15-AG-170	10.45	<0.04	6.1	15.0	1577	1418	240
15-AG-171	0.40	<0.04	4.2	4.8	1504	245	182
15-AG-172	0.25	<0.04	8.0	1.1	90	342	12
15-AG-173	0.04	<0.04	7.1	0.7	55	199	7
15-AG-174	0.30	<0.04	5.6	7.5	523	193	56
15-AG-175	2.01	<0.04	6.8	11.4	3008	<15	454
15-AG-176	6.11	<0.04	8.6	11.0	938	<15	239
15-AG-177	9.00	<0.04	14.7	7.3	670	1415	124
15-AG-178	6.29	<0.04	14.9	4.5	439	2406	70
15-AG-179	9.14	<0.04	14.5	7.3	652	1415	124
15-AG-180	0.07	<0.04	4.4	5.9	695	<15	262
15-AG-181	0.08	<0.04	7.0	0.2	50	176	8
15-AG-182	0.10	<0.04	9.5	11.0	1243	1810	23
15-AG-183	0.21	<0.04	10.1	51.5	107	2267	285
15-AG-184	0.05	<0.04	4.2	8.6	702	394	40
15-AG-185	0.26	<0.04	11.2	11.4	644	1492	25
15-AG-186	0.23	<0.04	9.7	10.2	550	390	19
15-AG-187	0.05	<0.04	4.1	16.3	414	<15	47
15-AG-188	12.20	<0.04	7.9	13.4	2590	213	243
15-AG-189	0.47	<0.04	3.7	0.6	1915	571	39
15-AG-190	5.97	<0.04	3.9	10.9	2194	<15	158

Sample	Br	PO4	Si	Sr	B	Fe	I
	ppm	ppm	ppm	ppm	ppb	ppb	ppb
15-AG-191	0.03	<0.04	5.3	12.4	234	<15	11
15-AG-192	0.05	<0.04	4.1	16.4	419	<15	47

Appendix H: Trace Constituents – Ag, Al, As, Ba, Be, Bi, Cd

Sample	Ag	Al	As	Ba	Be	Bi	Cd
	µg/L	µg/L	µg/L	µg/L	µg/L	µg/L	µg/L
15-AG-001	0.01	<5	2.94	9.5	<0.01	<0.05	0.10
15-AG-002	0.007	<5	0.67	11.7	<0.01	<0.05	0.04
15-AG-003	<0.005	<5	5.77	6.1	<0.01	<0.05	0.09
15-AG-004	<0.005	<5	0.11	0.1	<0.01	<0.05	0.02
15-AG-005	0.01	<5	0.1	34.1	<0.01	<0.05	0.04
15-AG-006	0.008	<5	0.12	17.9	0.013	<0.05	<0.01
15-AG-007	<0.005	10	0.37	27.7	<0.01	<0.05	<0.01
15-AG-008	0.006	6	0.25	22.6	<0.01	<0.05	0.02
15-AG-009	<0.005	51	0.44	15.2	<0.01	<0.05	0.01
15-AG-010	0.009	<5	0.28	25.8	0.011	<0.05	<0.01
15-AG-011	<0.005	<5	0.15	30.7	<0.01	<0.05	<0.01
15-AG-012	0.007	<5	0.05	30.6	0.014	<0.05	<0.01
15-AG-013	<0.005	<5	0.08	27.2	<0.01	<0.05	0.07
15-AG-014	0.012	<5	0.23	4.7	<0.01	<0.05	0.02
15-AG-015	<0.005	<5	0.28	83.4	<0.01	<0.05	0.01
15-AG-016	0.006	<5	0.18	20.6	<0.01	<0.05	<0.01
15-AG-017	0.009	<5	0.13	102.8	<0.01	<0.05	<0.01
15-AG-018	<0.005	<5	0.4	49.2	<0.01	<0.05	<0.01
15-AG-019	<0.005	<5	0.43	49.6	<0.01	<0.05	<0.01
15-AG-020	0.017	<5	0.23	33.4	<0.01	<0.05	<0.01
15-AG-021	0.006	<5	0.14	199.7	<0.01	<0.05	<0.01
15-AG-022	0.009	<5	0.26	33.6	<0.01	<0.05	<0.01
15-AG-023	<0.005	<5	0.29	53.7	<0.01	<0.05	<0.01
15-AG-024	<0.005	<5	0.36	70.3	<0.01	<0.05	0.01
15-AG-025	0.009	<5	0.33	87.9	<0.01	<0.05	0.03
15-AG-026	0.011	<5	0.26	2.5	<0.01	<0.05	<0.01
15-AG-027	0.014	<5	2.7	13.6	<0.01	<0.05	0.01
15-AG-028	0.01	6	10.18	5	<0.01	<0.05	0.03
15-AG-029	0.01	<5	0.47	6.8	<0.01	<0.05	0.02
15-AG-030	0.01	<5	2.14	29.9	<0.01	<0.05	<0.01
15-AG-031	0.01	<5	2.15	30.2	<0.01	<0.05	<0.01

Sample	Ag	Al	As	Ba	Be	Bi	Cd
	µg/L	µg/L	µg/L	µg/L	µg/L	µg/L	µg/L
15-AG-032	<0.005	<5	<0.03	<0.02	<0.01	<0.05	<0.01
15-AG-033	<0.005	<5	0.1	17	0.012	<0.05	<0.01
15-AG-034	<0.005	<5	0.34	130	<0.01	<0.05	<0.01
15-AG-035	0.012	<5	0.14	35.5	0.011	<0.05	0.05
15-AG-036	0.011	<5	1.93	9.8	<0.01	<0.05	0.02
15-AG-037	0.008	<5	3.59	8.4	0.01	<0.05	0.03
15-AG-038	0.008	14	0.83	92.2	<0.01	<0.05	0.03
15-AG-039	0.006	12	<0.03	33.3	0.013	<0.05	0.10
15-AG-040	<0.005	<5	1.12	53.4	<0.01	<0.05	0.02
15-AG-041	0.011	<5	0.37	2	<0.01	<0.05	0.01
15-AG-042	0.01	<5	1.95	2.7	<0.01	<0.05	<0.01
15-AG-043	0.0135	<5	0.37	5.4	<0.01	<0.05	<0.01
15-AG-044	0.011	<5	1.02	5.1	<0.01	<0.05	0.04
15-AG-045	0.008	48	0.58	12.2	<0.01	<0.05	0.02
15-AG-046	0.006	<5	0.83	38	<0.01	<0.05	0.02
15-AG-047	<0.005	<5	1.17	52.3	0.012	<0.05	0.03
15-AG-048	<0.005	<5	12.63	45.7	<0.01	<0.05	0.02
15-AG-049	<0.005	48.5	0.47	15	0.012	<0.05	0.02
15-AG-050	0.008	<5	0.32	29	0.012	<0.05	<0.01
15-AG-051	0.019	<5	0.13	26.9	<0.01	<0.05	0.02
15-AG-052	<0.005	<5	1.45	79.2	<0.01	<0.05	<0.01
15-AG-053	<0.005	<5	1.66	110	<0.01	<0.05	0.01
15-AG-054	0.011	<5	0.55	11.4	<0.01	<0.05	0.02
15-AG-055	0.011	<5	1.64	4.9	<0.01	<0.05	<0.01
15-AG-056	0.01	<5	1.19	3.5	<0.01	<0.05	<0.01
15-AG-057	0.009	<5	2.01	32.5	<0.01	<0.05	0.06
15-AG-058	0.014	<5	0.52	3.7	<0.01	<0.05	0.02
15-AG-059	0.011	<5	0.27	2.2	<0.01	<0.05	0.03
15-AG-060	0.009	9	1.81	34.2	<0.01	<0.05	0.07
15-AG-061	0.009	<5	0.49	2.7	0.015	<0.05	<0.01
15-AG-062	<0.005	<5	0.53	61.4	<0.01	<0.05	<0.01
15-AG-063	0.009	<5	0.65	22.2	<0.01	<0.05	<0.01
15-AG-064	0.01	<5	3.07	16.1	<0.01	<0.05	0.02
15-AG-065	0.012	<5	0.15	5.3	0.016	<0.05	<0.01
15-AG-066	<0.005	<5	0.24	53.3	<0.01	<0.05	0.01
15-AG-067	0.015	<5	1.04	8.5	<0.01	<0.05	0.02
15-AG-068	0.025	<5	0.11	50.4	<0.01	<0.05	0.02
15-AG-069	0.011	<5	0.12	4.5	<0.01	<0.05	0.01

Sample	Ag	Al	As	Ba	Be	Bi	Cd
	µg/L	µg/L	µg/L	µg/L	µg/L	µg/L	µg/L
15-AG-070	0.01	<5	0.12	4.1	0.027	<0.05	0.02
15-AG-071	0.013	70	2.59	7.6	0.012	<0.05	<0.01
15-AG-072	0.013	<5	0.5	7.2	<0.01	<0.05	0.02
15-AG-073	0.021	<5	8.81	43.3	<0.01	<0.05	0.02
15-AG-074	0.013	<5	0.34	5.1	<0.01	<0.05	0.02
15-AG-075	0.009	137	0.15	44.1	<0.01	<0.05	0.05
15-AG-076	0.013	<5	3.13	8.9	0.011	<0.05	0.03
15-AG-077	<0.005	6	0.23	44.6	<0.01	<0.05	<0.01
15-AG-078	<0.005	<5	0.5	70.5	<0.01	<0.05	0.03
15-AG-079	<0.005	16	<0.03	33	<0.01	<0.05	0.09
15-AG-080	<0.005	<5	0.89	67.5	0.011	<0.05	0.01
15-AG-081	0.011	<5	0.45	5.8	<0.01	<0.05	<0.01
15-AG-082	<0.005	<5	5.86	12.1	<0.01	<0.05	0.11
15-AG-083	<0.005	<5	0.47	47.4	<0.01	<0.05	<0.01
15-AG-084	0.011	<5	0.13	3.2	<0.01	<0.05	<0.01
15-AG-085	0.012	<5	2.99	4.6	<0.01	<0.05	0.02
15-AG-086	0.012	<5	0.3	8.6	<0.01	<0.05	<0.01
15-AG-087	0.015	<5	2.15	5.5	<0.01	<0.05	<0.01
15-AG-088	0.012	<5	0.85	7.6	<0.01	<0.05	0.04
15-AG-089	<0.005	51	0.47	13.3	0.018	<0.05	<0.01
15-AG-090	0.012	<5	1.26	25.5	<0.01	<0.05	0.01
15-AG-091	0.011	<5	0.24	3.7	<0.01	<0.05	<0.01
15-AG-092	<0.005	<5	<0.03	<0.02	<0.01	<0.05	<0.01
15-AG-093	0.011	<5	9.05	89.7	<0.01	<0.05	0.03
15-AG-094	0.012	8	2.79	29.9	<0.01	<0.05	<0.01
15-AG-095	0.011	<5	1.06	4.2	<0.01	<0.05	0.04
15-AG-096	<0.005	<5	0.27	27.8	<0.01	<0.05	0.03
15-AG-097	<0.005	<5	1.75	222.3	<0.01	<0.05	<0.01
15-AG-098	<0.005	<5	0.48	7.5	<0.01	<0.05	<0.01
15-AG-099	<0.005	<5	0.3	25.7	0.012	<0.05	0.03
15-AG-100	0.015	<5	1.4	3.7	0.012	<0.05	<0.01
15-AG-101	<0.005	<5	1.94	11.9	0.02	<0.05	<0.01
15-AG-102	<0.005	<5	0.41	53.4	<0.01	<0.05	<0.01
15-AG-103	0.006	<5	0.45	7.8	<0.01	<0.05	<0.01
15-AG-104	<0.005	<5	0.99	461	0.014	<0.05	<0.01
15-AG-105	0.006	6	2.21	25.4	<0.01	<0.05	0.01
15-AG-106	<0.005	<5	1.04	5.3	<0.01	<0.05	0.06
15-AG-107	<0.005	<5	0.99	4.8	<0.01	<0.05	0.06

Sample	Ag	Al	As	Ba	Be	Bi	Cd
	µg/L	µg/L	µg/L	µg/L	µg/L	µg/L	µg/L
15-AG-108	<0.005	<5	0.91	13.3	<0.01	<0.05	0.03
15-AG-109	0.0075	11.5	0.92	64.3	0.016	<0.05	0.02
15-AG-110	<0.005	<5	1.08	82.4	<0.01	<0.05	0.02
15-AG-111	<0.005	<5	1.86	27.4	<0.01	<0.05	0.02
15-AG-112	<0.005	10	0.92	64.6	0.014	<0.05	0.03
15-AG-113	<0.005	<5	0.49	12.9	<0.01	<0.05	0.21
15-AG-114	<0.005	<5	7.01	35	<0.01	<0.05	<0.01
15-AG-115	0.012	<5	0.15	40.6	<0.01	<0.05	0.04
15-AG-116	0.013	<5	0.35	7.2	<0.01	<0.05	<0.01
15-AG-117	0.008	<5	0.12	6	<0.01	<0.05	<0.01
15-AG-118	<0.005	10	2.81	66.4	<0.01	<0.05	0.03
15-AG-119	<0.005	13	<0.03	34.5	0.013	<0.05	0.09
15-AG-120	0.035	<5	1.57	59.2	<0.01	<0.05	0.01
15-AG-121	0.008	<5	0.6	2.7	<0.01	<0.05	<0.01
15-AG-122	0.009	<5	0.19	3.1	<0.01	<0.05	<0.01
15-AG-123	<0.005	17	1.26	69.9	<0.01	<0.05	0.07
15-AG-124	0.009	<5	1.06	4.7	0.013	<0.05	<0.01
15-AG-125	0.009	<5	3.59	7.5	<0.01	<0.05	0.03
15-AG-126	0.01	<5	0.31	4.5	<0.01	<0.05	<0.01
15-AG-127	0.01	<5	3	4.9	<0.01	<0.05	0.01
15-AG-128	0.009	<5	1.9	6.4	<0.01	<0.05	0.02
15-AG-129	<0.005	49	0.42	16.9	<0.01	<0.05	<0.01
15-AG-130	0.019	<5	1.64	153.5	<0.01	<0.05	0.03
15-AG-131	0.009	<5	0.32	5.6	<0.01	<0.05	0.13
15-AG-132	<0.005	<5	0.07	6.2	<0.01	<0.05	0.02
15-AG-133	0.008	<5	0.39	27.1	<0.01	<0.05	0.09
15-AG-134	<0.005	<5	7.62	35	<0.01	<0.05	0.01
15-AG-135	<0.005	<5	0.1	16.5	<0.01	<0.05	<0.01
15-AG-136	0.009	<5	0.35	2.8	<0.01	<0.05	<0.01
15-AG-136	0.009	<5	0.35	2.8	<0.01	<0.05	<0.01
15-AG-137	0.01	<5	9.79	4.6	<0.01	<0.05	<0.01
15-AG-138	0.016	<5	0.51	18.3	<0.01	<0.05	<0.01
15-AG-139	0.013	<5	19.65	3.7	<0.01	<0.05	0.03
15-AG-140	0.016	<5	0.96	3.6	<0.01	<0.05	<0.01
15-AG-141	0.01	<5	2.8	4	<0.01	<0.05	0.01
15-AG-142	<0.005	<5	0.04	0	<0.01	<0.05	<0.01
15-AG-143	0.0095	<5	1.53	3.6	<0.01	<0.05	0.03
15-AG-144	0.016	<5	0.39	7.9	<0.01	<0.05	<0.01

Sample	Ag	Al	As	Ba	Be	Bi	Cd
	µg/L	µg/L	µg/L	µg/L	µg/L	µg/L	µg/L
15-AG-145	0.01	<5	0.62	20.1	<0.01	<0.05	0.05
15-AG-146	0.012	<5	19.63	3.9	<0.01	<0.05	0.03
15-AG-147	0.01	<5	1.3	3	0.011	<0.05	<0.01
15-AG-148	0.007	<5	0.35	3.2	<0.01	<0.05	<0.01
15-AG-149	0.016	<5	0.26	8.4	<0.01	<0.05	0.01
15-AG-150	0.009	<5	0.47	83.2	<0.01	<0.05	<0.01
15-AG-151	<0.005	<5	0.71	261.2	<0.01	<0.05	<0.01
15-AG-152	0.006	<5	1.18	13.9	<0.01	<0.05	<0.01
15-AG-153	0.008	<5	0.47	138.6	<0.01	<0.05	<0.01
15-AG-165	0.013	<5	5.5	17.9	<0.01	<0.05	0.01
15-AG-166	0.018	<5	0.91	8.7	<0.01	<0.05	<0.01
15-AG-167	0.011	<5	1.57	5.7	<0.01	<0.05	0.01
15-AG-168	0.0145	<5	8.47	40.6	<0.01	<0.05	0.02
15-AG-169	<0.005	51	0.49	15	<0.01	<0.05	<0.01
15-AG-170	0.025	<5	3.95	5.7	<0.01	<0.05	0.02
15-AG-171	0.006	<5	3.8	8.9	0.011	<0.05	0.10
15-AG-172	<0.005	<5	4.15	17.7	<0.01	<0.05	<0.01
15-AG-173	<0.005	<5	10.08	30	<0.01	<0.05	<0.01
15-AG-174	0.01	<5	7.22	20.6	<0.01	<0.05	0.11
15-AG-175	0.012	<5	1.19	4.6	<0.01	<0.05	<0.01
15-AG-176	0.019	<5	2.14	5.3	<0.01	<0.05	<0.01
15-AG-177	0.009	<5	8.9	12.7	<0.01	<0.05	0.01
15-AG-178	<0.005	<5	14.54	12.1	<0.01	<0.05	0.02
15-AG-179	0.008	<5	8.97	12.4	<0.01	<0.05	0.01
15-AG-180	0.007	<5	0.21	7.9	<0.01	<0.05	<0.01
15-AG-181	<0.005	<5	0.49	167.5	<0.01	<0.05	<0.01
15-AG-182	0.012	<5	0.92	1.7	<0.01	<0.05	<0.01
15-AG-183	0.054	<5	1.51	256.7	<0.01	<0.05	<0.01
15-AG-184	0.01	<5	2.4	8.6	<0.01	<0.05	0.09
15-AG-185	0.009	<5	2.65	4.4	<0.01	<0.05	<0.01
15-AG-186	0.005	<5	2.17	2.1	<0.01	<0.05	0.03
15-AG-187	0.013	<5	4.32	11.7	<0.01	<0.05	0.06
15-AG-188	0.006	90	3.61	11.1	0.016	<0.05	0.02
15-AG-189	<0.005	13	<0.03	31.7	<0.01	<0.05	0.09
15-AG-190	0.005	<5	1.45	5.1	<0.01	<0.05	<0.01
15-AG-191	0.009	19	9.22	35	<0.01	<0.05	0.01
15-AG-192	0.013	<5	4.15	11	<0.01	<0.05	0.06

Appendix I: Trace Constituents – Ce, Co, Cr, Cs, Cu, Dy, Er

Sample	Ce	Co	Cr	Cs	Cu	Dy	Er
	µg/L	µg/L	µg/L	µg/L	µg/L	µg/L	µg/L
15-AG-001	<0.002	0.04	<0.02	0.01	0.84	<0.001	<0.001
15-AG-002	<0.002	<0.005	<0.02	0.01	1.58	<0.001	<0.001
15-AG-003	0.00	0.26	<0.02	0.01	0.66	<0.001	<0.001
15-AG-004	<0.002	0.02	0.03	0.01	15.50	<0.001	0.00
15-AG-005	<0.002	<0.005	0.08	0.00	1.84	<0.001	<0.001
15-AG-006	0.03	<0.005	0.02	0.03	1.27	0.01	0.01
15-AG-007	0.04	0.39	0.06	0.01	2.38	0.01	0.01
15-AG-008	0.01	<0.005	0.09	0.02	0.50	0.00	0.00
15-AG-009	0.27	0.04	0.23	0.00	16.74	0.02	0.01
15-AG-010	<0.002	<0.005	0.03	0.05	0.54	0.00	0.00
15-AG-011	0.01	<0.005	0.05	0.03	0.26	0.00	0.00
15-AG-012	<0.002	<0.005	<0.02	0.03	0.73	<0.001	<0.001
15-AG-013	0.00	0.05	<0.02	0.01	0.45	0.00	<0.001
15-AG-014	0.00	<0.005	<0.02	0.01	4.24	0.00	<0.001
15-AG-015	0.00	0.05	0.03	0.01	1.28	0.00	0.00
15-AG-016	0.01	<0.005	0.11	0.05	2.71	0.00	0.00
15-AG-017	0.00	<0.005	0.03	0.05	1.82	0.00	<0.001
15-AG-018	0.03	<0.005	0.16	0.00	0.61	0.03	0.02
15-AG-019	0.03	<0.005	0.16	0.01	0.73	0.02	0.02
15-AG-020	0.01	<0.005	0.05	0.01	2.39	0.00	0.00
15-AG-021	0.01	<0.005	0.02	0.00	0.84	0.00	0.00
15-AG-022	0.01	<0.005	0.05	0.00	1.14	0.00	0.00
15-AG-023	0.06	<0.005	0.11	0.00	0.57	0.02	0.01
15-AG-024	0.01	<0.005	0.11	0.00	3.98	0.01	0.01
15-AG-025	<0.002	0.03	0.06	0.01	2.74	0.00	0.00
15-AG-026	<0.002	<0.005	<0.02	0.03	2.40	<0.001	<0.001
15-AG-027	0.01	<0.005	<0.02	0.01	1.34	<0.001	<0.001
15-AG-028	0.02	<0.005	0.12	0.01	4.25	0.00	0.00
15-AG-029	0.06	2.44	0.03	0.00	3.90	0.00	0.00
15-AG-030	0.01	<0.005	<0.02	0.00	1.22	0.00	0.00
15-AG-031	0.01	<0.005	0.03	0.00	1.21	0.00	0.00
15-AG-032	<0.002	<0.005	<0.02	0.00	0.48	<0.001	<0.001
15-AG-033	0.00	<0.005	0.04	0.00	<0.2	0.00	0.00
15-AG-034	0.01	0.48	0.02	0.00	4.47	0.01	0.01
15-AG-035	<0.002	<0.005	0.08	0.00	2.30	<0.001	<0.001
15-AG-036	0.02	<0.005	<0.02	0.00	2.14	<0.001	0.00
15-AG-037	0.02	<0.005	0.04	0.01	3.68	0.00	0.00

Sample	Ce	Co	Cr	Cs	Cu	Dy	Er
	µg/L	µg/L	µg/L	µg/L	µg/L	µg/L	µg/L
15-AG-038	0.06	0.32	0.09	0.01	6.26	0.01	0.00
15-AG-039	0.02	0.08	0.26	0.03	2.99	0.00	0.00
15-AG-040	0.01	0.38	0.03	0.00	20.79	0.00	0.00
15-AG-041	0.01	<0.005	<0.02	0.02	3.58	<0.001	<0.001
15-AG-042	<0.002	<0.005	0.04	0.02	3.53	<0.001	<0.001
15-AG-043	0.00	<0.005	0.18	0.00	4.92	<0.001	<0.001
15-AG-044	<0.002	0.01	0.12	0.01	1.12	<0.001	<0.001
15-AG-045	<0.002	<0.005	0.10	0.01	2.29	<0.001	<0.001
15-AG-046	<0.002	<0.005	0.02	0.02	1.91	0.00	0.00
15-AG-047	0.00	<0.005	0.04	0.01	1.55	0.01	0.01
15-AG-048	0.20	3.94	0.11	0.01	1.85	0.02	0.02
15-AG-049	0.25	0.06	0.22	0.01	16.88	0.02	0.01
15-AG-050	0.02	<0.005	0.18	0.01	4.98	0.00	0.00
15-AG-051	0.00	0.01	<0.02	0.00	18.98	<0.001	<0.001
15-AG-052	0.00	<0.005	<0.02	0.01	0.34	<0.001	<0.001
15-AG-053	0.00	<0.005	0.04	0.00	5.15	0.02	0.01
15-AG-054	<0.002	0.08	<0.02	0.01	1.29	<0.001	<0.001
15-AG-055	0.00	<0.005	0.69	0.03	2.73	<0.001	<0.001
15-AG-056	0.01	<0.005	0.02	0.05	3.88	<0.001	<0.001
15-AG-057	0.01	0.08	0.06	0.01	4.83	0.00	0.00
15-AG-058	0.00	<0.005	0.02	0.02	4.33	<0.001	<0.001
15-AG-059	0.00	<0.005	0.05	0.02	3.64	<0.001	0.00
15-AG-060	0.01	0.12	0.07	0.01	4.56	0.00	0.00
15-AG-061	0.01	<0.005	0.02	0.02	3.44	<0.001	0.00
15-AG-062	0.03	<0.005	<0.02	0.00	0.65	0.00	0.00
15-AG-063	0.01	0.40	<0.02	0.00	2.84	0.00	0.00
15-AG-064	0.04	<0.005	0.05	0.02	4.49	0.01	0.00
15-AG-065	0.00	<0.005	<0.02	0.08	4.21	0.00	0.00
15-AG-066	<0.002	0.22	<0.02	0.02	4.37	<0.001	<0.001
15-AG-067	0.02	<0.005	<0.02	0.03	5.32	0.00	0.00
15-AG-068	0.00	0.01	0.67	0.01	0.97	0.00	0.00
15-AG-069	0.00	<0.005	<0.02	0.02	3.77	<0.001	<0.001
15-AG-070	0.00	<0.005	<0.02	0.02	4.18	<0.001	<0.001
15-AG-071	0.01	<0.005	0.18	0.03	3.99	0.00	<0.001
15-AG-072	<0.002	<0.005	<0.02	0.01	2.40	<0.001	<0.001
15-AG-073	<0.002	0.04	<0.02	0.01	0.68	<0.001	<0.001
15-AG-074	0.00	0.01	<0.02	0.01	1.93	<0.001	<0.001
15-AG-075	<0.002	<0.005	0.35	<0.0005	2.38	0.00	<0.001

Sample	Ce	Co	Cr	Cs	Cu	Dy	Er
	µg/L	µg/L	µg/L	µg/L	µg/L	µg/L	µg/L
15-AG-076	0.04	3.79	0.02	0.01	5.11	0.01	0.00
15-AG-077	0.02	0.03	0.09	0.01	0.75	0.01	0.01
15-AG-078	0.02	0.31	0.05	0.00	1.61	0.01	0.01
15-AG-079	0.02	0.07	0.25	0.03	2.47	0.00	0.00
15-AG-080	0.12	0.01	0.09	0.01	2.16	0.02	0.01
15-AG-081	<0.002	<0.005	0.04	0.01	3.45	<0.001	<0.001
15-AG-082	<0.002	0.21	<0.02	0.00	0.47	<0.001	<0.001
15-AG-083	0.03	<0.005	0.03	0.00	2.13	0.00	0.00
15-AG-084	<0.002	<0.005	<0.02	0.00	3.26	<0.001	<0.001
15-AG-085	0.01	<0.005	0.02	0.02	5.83	0.00	0.00
15-AG-086	<0.002	<0.005	0.03	0.01	2.62	<0.001	<0.001
15-AG-087	<0.002	<0.005	0.02	0.01	3.98	<0.001	<0.001
15-AG-088	0.00	<0.005	<0.02	0.02	2.23	<0.001	<0.001
15-AG-089	0.23	0.05	0.23	0.01	17.38	0.02	0.01
15-AG-090	0.03	<0.005	0.03	0.00	3.09	0.00	0.00
15-AG-091	0.00	<0.005	0.04	0.03	4.91	<0.001	<0.001
15-AG-092	<0.002	<0.005	<0.02	<0.0005	<0.2	<0.001	<0.001
15-AG-093	0.01	<0.005	0.21	0.04	3.85	<0.001	<0.001
15-AG-094	0.02	<0.005	0.66	0.04	4.50	0.00	0.00
15-AG-095	0.00	<0.005	0.04	0.03	6.67	<0.001	<0.001
15-AG-096	0.02	<0.005	0.02	0.01	1.84	0.00	0.00
15-AG-097	0.03	0.08	0.05	0.00	0.73	0.01	0.01
15-AG-098	<0.002	<0.005	<0.02	0.02	2.86	<0.001	<0.001
15-AG-099	0.02	<0.005	<0.02	0.01	1.78	0.00	0.00
15-AG-100	0.00	<0.005	<0.02	0.04	4.56	<0.001	<0.001
15-AG-101	0.01	<0.005	<0.02	0.01	1.56	0.00	0.00
15-AG-102	0.01	<0.005	<0.02	0.01	0.82	0.01	0.01
15-AG-103	<0.002	<0.005	<0.02	0.02	1.31	<0.001	<0.001
15-AG-104	0.05	<0.005	0.04	0.01	0.89	0.01	0.01
15-AG-105	0.02	0.06	0.08	0.00	3.22	0.00	0.00
15-AG-106	<0.002	<0.005	<0.02	0.01	1.96	<0.001	<0.001
15-AG-107	<0.002	0.05	<0.02	0.00	1.43	<0.001	<0.001
15-AG-108	0.01	0.77	<0.02	0.00	6.66	0.00	0.00
15-AG-109	0.21	0.05	0.21	0.02	5.95	0.03	0.02
15-AG-110	<0.002	0.18	0.07	0.00	6.64	<0.001	0.00
15-AG-111	0.00	0.01	0.03	0.01	1.06	<0.001	0.00
15-AG-112	0.20	0.01	0.22	0.02	6.09	0.03	0.02
15-AG-113	0.00	<0.005	<0.02	0.01	6.56	0.00	0.00

Sample	Ce	Co	Cr	Cs	Cu	Dy	Er
	µg/L	µg/L	µg/L	µg/L	µg/L	µg/L	µg/L
15-AG-114	<0.002	0.01	<0.02	0.00	0.49	<0.001	<0.001
15-AG-115	<0.002	<0.005	0.08	0.00	2.53	<0.001	0.00
15-AG-116	0.01	<0.005	<0.02	0.00	2.64	0.00	<0.001
15-AG-117	<0.002	<0.005	0.02	0.01	4.27	<0.001	<0.001
15-AG-118	0.08	0.02	0.15	0.01	7.74	0.01	0.01
15-AG-119	0.02	0.07	0.52	0.03	2.60	0.00	0.00
15-AG-120	0.02	<0.005	0.04	0.02	1.87	0.00	0.00
15-AG-121	0.01	<0.005	0.13	0.03	5.25	<0.001	<0.001
15-AG-122	0.01	<0.005	0.07	0.01	2.50	<0.001	<0.001
15-AG-123	0.01	0.14	0.20	0.02	4.19	0.00	0.00
15-AG-124	0.00	<0.005	0.03	0.03	3.02	<0.001	<0.001
15-AG-125	0.03	<0.005	0.23	0.03	2.51	0.01	0.00
15-AG-126	0.01	<0.005	0.10	0.04	2.88	0.00	<0.001
15-AG-127	0.01	<0.005	0.06	0.03	2.65	0.00	0.00
15-AG-128	0.01	<0.005	0.12	0.02	2.76	0.00	0.00
15-AG-129	0.29	0.05	0.24	0.00	18.25	0.02	0.01
15-AG-130	<0.002	1.79	0.15	0.01	1.35	<0.001	<0.001
15-AG-131	0.00	<0.005	0.06	0.02	1.80	<0.001	<0.001
15-AG-132	<0.002	0.02	<0.02	0.00	0.54	<0.001	<0.001
15-AG-133	0.00	0.20	<0.02	0.01	2.47	<0.001	0.00
15-AG-134	<0.002	0.01	0.02	0.00	5.52	<0.001	<0.001
15-AG-135	0.00	0.01	0.21	0.06	0.20	<0.001	<0.001
15-AG-136	0.01	<0.005	0.02	0.02	2.47	<0.001	0.00
15-AG-136	0.01	<0.005	0.02	0.02	2.47	<0.001	0.00
15-AG-137	0.00	<0.005	0.18	0.02	3.21	<0.001	<0.001
15-AG-138	0.01	<0.005	0.04	0.02	2.36	0.00	<0.001
15-AG-139	0.00	<0.005	0.06	0.04	3.41	<0.001	0.00
15-AG-140	0.01	<0.005	<0.02	0.01	2.25	<0.001	<0.001
15-AG-141	0.00	<0.005	<0.02	0.02	2.61	<0.001	<0.001
15-AG-142	<0.002	<0.005	<0.02	<0.0005	<0.2	<0.001	<0.001
15-AG-143	0.01	<0.005	<0.02	0.04	2.89	0.00	<0.001
15-AG-144	0.00	<0.005	0.02	0.01	2.62	<0.001	0.00
15-AG-145	0.01	0.80	0.02	0.01	2.43	0.00	0.00
15-AG-146	0.00	<0.005	0.05	0.04	3.38	<0.001	0.00
15-AG-147	0.00	<0.005	<0.02	0.04	3.27	<0.001	<0.001
15-AG-148	0.00	<0.005	<0.02	0.02	2.74	<0.001	<0.001
15-AG-149	0.00	<0.005	0.02	0.02	2.63	0.00	0.00
15-AG-150	0.02	0.04	1.58	0.01	0.20	0.00	0.00

Sample	Ce	Co	Cr	Cs	Cu	Dy	Er
	µg/L	µg/L	µg/L	µg/L	µg/L	µg/L	µg/L
15-AG-151	0.00	0.01	0.05	0.02	0.26	0.00	0.00
15-AG-152	0.01	0.07	0.07	0.03	3.61	0.00	0.00
15-AG-153	0.06	<0.005	0.63	0.04	1.28	0.02	0.01
15-AG-165	0.02	<0.005	0.19	0.05	3.17	0.00	0.00
15-AG-166	0.01	<0.005	0.08	0.01	2.49	0.00	0.00
15-AG-167	0.02	<0.005	0.22	0.06	3.03	0.00	0.00
15-AG-168	0.00	0.01	0.15	0.00	0.33	0.00	0.00
15-AG-169	0.26	0.05	0.24	0.00	17.16	0.02	0.01
15-AG-170	0.02	<0.005	0.05	0.04	2.59	0.00	0.00
15-AG-171	0.01	<0.005	0.46	0.09	2.34	0.00	<0.001
15-AG-172	0.00	<0.005	0.05	0.00	0.48	<0.001	<0.001
15-AG-173	<0.002	0.01	<0.02	0.00	0.28	0.00	0.00
15-AG-174	0.00	0.06	0.09	0.01	0.81	0.00	0.00
15-AG-175	0.01	<0.005	0.05	0.03	2.70	0.00	0.00
15-AG-176	0.01	<0.005	0.09	0.03	2.47	0.00	0.00
15-AG-177	0.01	0.01	0.19	0.02	1.12	0.00	0.00
15-AG-178	0.01	<0.005	0.08	0.04	0.73	0.01	0.01
15-AG-179	0.01	<0.005	0.98	0.02	1.03	0.00	<0.001
15-AG-180	0.01	<0.005	0.27	0.04	0.37	0.00	0.00
15-AG-181	<0.002	0.04	4.42	0.00	0.26	0.00	0.00
15-AG-182	0.02	<0.005	0.13	0.04	2.59	0.00	0.00
15-AG-183	0.00	0.20	0.10	0.01	0.41	0.00	<0.001
15-AG-184	0.01	0.01	0.34	0.01	2.26	0.00	<0.001
15-AG-185	0.02	0.16	0.15	0.01	2.54	0.00	0.00
15-AG-186	0.12	5.35	0.02	0.01	5.42	0.01	0.01
15-AG-187	<0.002	0.07	0.23	0.01	0.50	<0.001	<0.001
15-AG-188	0.21	<0.005	0.23	0.02	3.32	0.02	0.01
15-AG-189	0.02	0.07	0.22	0.02	2.70	0.00	0.00
15-AG-190	0.01	<0.005	0.10	0.04	3.36	0.00	0.00
15-AG-191	0.00	0.03	<0.02	0.00	0.36	<0.001	<0.001
15-AG-192	<0.002	0.07	0.23	0.01	0.51	<0.001	<0.001

Appendix J: Trace Constituents – Eu, Ga, Gd, Hf, Hg, Ho, La

Sample	Eu	Ga	Gd	Hf	Hg	Ho	La
	µg/L	µg/L	µg/L	µg/L	ng/L	µg/L	µg/L
15-AG-001	<0.0004	0.02	<0.001	<0.004	23.20	<0.0001	<0.001
15-AG-002	<0.0004	0.00	<0.001	<0.004	25.25	<0.0001	<0.001

Sample	Eu	Ga	Gd	Hf	Hg	Ho	La
	µg/L	µg/L	µg/L	µg/L	ng/L	µg/L	µg/L
15-AG-003	<0.0004	0.02	<0.001	<0.004	22.80	<0.0001	0.00
15-AG-004	<0.0004	0.00	0.00	<0.004	4.60	0.00	0.00
15-AG-005	<0.0004	0.00	<0.001	<0.004	<1.5	0.00	0.00
15-AG-006	0.00	0.01	0.01	<0.004	3.10	0.00	0.02
15-AG-007	0.00	0.01	0.01	<0.004	36.20	0.00	0.03
15-AG-008	0.00	0.02	0.00	<0.004	52.20	0.00	0.01
15-AG-009	0.01	0.02	0.03	<0.004	0.00	0.00	0.22
15-AG-010	<0.0004	0.03	0.00	<0.004	22.40	0.00	0.00
15-AG-011	<0.0004	0.01	0.00	<0.004	26.30	0.00	0.01
15-AG-012	<0.0004	0.01	0.00	<0.004	2.80	0.00	0.00
15-AG-013	<0.0004	0.01	0.00	<0.004	20.30	0.00	0.00
15-AG-014	<0.0004	0.01	<0.001	<0.004	13.00	0.00	0.00
15-AG-015	<0.0004	0.01	0.00	<0.004	<1.5	0.00	0.00
15-AG-016	<0.0004	0.02	0.00	0.02	17.80	0.00	0.01
15-AG-017	<0.0004	0.01	0.00	<0.004	6.00	0.00	0.00
15-AG-018	0.00	0.01	0.02	0.01	10.50	0.01	0.03
15-AG-019	0.00	0.01	0.02	0.01	37.30	0.01	0.03
15-AG-020	<0.0004	0.01	0.00	0.01	15.90	0.00	0.01
15-AG-021	<0.0004	0.01	0.01	<0.004	15.30	0.00	0.01
15-AG-022	<0.0004	0.01	0.00	<0.004	12.10	0.00	0.01
15-AG-023	0.00	0.02	0.01	0.01	8.00	0.00	0.06
15-AG-024	0.00	0.00	0.01	<0.004	6.00	0.00	0.02
15-AG-025	<0.0004	0.00	0.00	<0.004	21.60	0.00	0.00
15-AG-026	<0.0004	0.01	<0.001	<0.004	13.30	<0.0001	0.00
15-AG-027	<0.0004	0.01	0.00	<0.004	2.70	<0.0001	0.00
15-AG-028	<0.0004	0.01	0.00	<0.004	<1.5	0.00	0.01
15-AG-029	<0.0004	0.02	0.00	<0.004	<1.5	0.00	0.03
15-AG-030	<0.0004	0.01	0.00	<0.004	<1.5	0.00	0.01
15-AG-031	0.00	0.01	0.00	<0.004	0.10	0.00	0.01
15-AG-032	<0.0004	<0.002	0.00	<0.004	<1.5	<0.0001	<0.001
15-AG-033	<0.0004	0.01	0.00	<0.004	6.40	0.00	0.00
15-AG-034	<0.0004	0.03	0.00	<0.004	4.40	0.00	0.01
15-AG-035	<0.0004	0.00	0.00	<0.004	<1.5	0.00	0.00
15-AG-036	0.00	0.01	0.00	<0.004	<1.5	0.00	0.01
15-AG-037	<0.0004	0.01	0.01	<0.004	5.00	0.00	0.01
15-AG-038	<0.0004	0.01	0.01	<0.004	7.70	0.00	0.03
15-AG-039	<0.0004	1.81	0.01	<0.004	4.40	0.00	0.01
15-AG-040	<0.0004	0.01	0.00	<0.004	10.90	0.00	0.01

Sample	Eu	Ga	Gd	Hf	Hg	Ho	La
	µg/L	µg/L	µg/L	µg/L	ng/L	µg/L	µg/L
15-AG-041	<0.0004	0.01	0.00	<0.004	<1.5	0.00	0.01
15-AG-042	0.00	0.01	<0.001	<0.004	<1.5	0.00	0.00
15-AG-043	<0.0004	0.01	<0.001	<0.004	3.00	0.00	0.00
15-AG-044	<0.0004	0.01	<0.001	<0.004	<1.5	<0.0001	<0.001
15-AG-045	<0.0004	0.01	0.00	<0.004	<1.5	0.00	<0.001
15-AG-046	<0.0004	0.01	<0.001	<0.004	12.90	0.00	0.00
15-AG-047	0.00	0.01	0.02	<0.004	87.60	0.00	0.00
15-AG-048	0.01	0.04	0.03	0.01	36.30	0.01	0.14
15-AG-049	0.01	0.02	0.03	<0.004	0.00	0.00	0.20
15-AG-050	<0.0004	0.01	0.00	0.01	5.90	0.00	0.02
15-AG-051	<0.0004	0.01	0.00	<0.004	4.10	0.00	0.00
15-AG-052	<0.0004	0.00	0.00	<0.004	14.50	0.00	0.00
15-AG-053	0.01	0.01	0.03	<0.004	6.40	0.00	0.01
15-AG-054	<0.0004	0.01	0.00	<0.004	5.30	<0.0001	0.00
15-AG-055	0.00	0.03	<0.001	<0.004	15.20	0.00	0.00
15-AG-056	0.00	0.01	0.00	<0.004	10.70	0.00	0.01
15-AG-057	<0.0004	0.01	0.00	<0.004	49.45	0.00	0.01
15-AG-058	<0.0004	0.01	<0.001	<0.004	7.10	<0.0001	0.00
15-AG-059	<0.0004	0.01	<0.001	<0.004	2.50	0.00	0.00
15-AG-060	<0.0004	0.01	0.00	<0.004	14.60	0.00	0.01
15-AG-061	<0.0004	0.01	0.00	<0.004	<1.5	0.00	0.01
15-AG-062	<0.0004	0.01	0.00	<0.004	6.40	0.00	0.02
15-AG-063	0.00	0.01	0.00	<0.004	9.00	0.00	0.01
15-AG-064	0.00	0.01	0.00	<0.004	3.70	0.00	0.03
15-AG-065	<0.0004	0.00	0.00	<0.004	<1.5	0.00	0.01
15-AG-066	<0.0004	0.00	0.00	<0.004	7.10	0.00	0.00
15-AG-067	0.00	0.01	0.00	<0.004	7.70	0.00	0.01
15-AG-068	0.00	0.01	<0.001	<0.004	5.50	0.00	0.01
15-AG-069	<0.0004	0.01	<0.001	<0.004	2.20	0.00	0.00
15-AG-070	<0.0004	0.01	<0.001	<0.004	10.10	0.00	0.00
15-AG-071	<0.0004	0.01	0.00	<0.004	<1.5	0.00	0.01
15-AG-072	<0.0004	0.01	<0.001	<0.004	3.60	<0.0001	<0.001
15-AG-073	<0.0004	0.00	<0.001	<0.004	9.80	<0.0001	<0.001
15-AG-074	0.00	0.01	<0.001	<0.004	3.50	0.00	0.00
15-AG-075	<0.0004	0.01	0.00	<0.004	<1.5	0.00	0.00
15-AG-076	<0.0004	0.01	0.00	<0.004	5.70	0.00	0.02
15-AG-077	0.00	0.01	0.01	0.01	3.90	0.00	0.01
15-AG-078	0.00	0.02	0.01	<0.004	<1.5	0.00	0.02

Sample	Eu	Ga	Gd	Hf	Hg	Ho	La
	µg/L	µg/L	µg/L	µg/L	ng/L	µg/L	µg/L
15-AG-079	<0.0004	1.80	0.00	<0.004	2.50	0.00	0.01
15-AG-080	0.01	0.01	0.02	0.01	3.60	0.00	0.09
15-AG-081	0.00	0.02	<0.001	<0.004	9.10	<0.0001	<0.001
15-AG-082	<0.0004	0.02	<0.001	<0.004	21.50	<0.0001	<0.001
15-AG-083	<0.0004	0.00	0.00	<0.004	8.00	0.00	0.02
15-AG-084	<0.0004	0.01	<0.001	<0.004	9.40	<0.0001	0.00
15-AG-085	<0.0004	0.01	0.00	<0.004	<1.5	0.00	0.01
15-AG-086	<0.0004	0.00	<0.001	<0.004	2.70	0.00	<0.001
15-AG-087	<0.0004	0.01	<0.001	<0.004	<1.5	<0.0001	0.00
15-AG-088	0.00	0.01	<0.001	<0.004	<1.5	0.00	0.00
15-AG-089	0.01	0.02	0.02	<0.004	0.00	0.00	0.19
15-AG-090	0.00	0.01	0.00	<0.004	6.70	0.00	0.03
15-AG-091	0.00	0.01	<0.001	<0.004	2.20	<0.0001	0.00
15-AG-092	<0.0004	<0.002	<0.001	<0.004	<1.5	<0.0001	<0.001
15-AG-093	<0.0004	0.04	0.00	<0.004	4.60	<0.0001	0.01
15-AG-094	0.00	0.01	0.00	<0.004	<1.5	0.00	0.02
15-AG-095	<0.0004	0.01	<0.001	<0.004	<1.5	0.00	0.00
15-AG-096	0.00	0.00	0.01	<0.004	<1.5	0.00	0.02
15-AG-097	<0.0004	0.01	0.01	0.01	3.90	0.00	0.02
15-AG-098	<0.0004	0.01	<0.001	<0.004	<1.5	<0.0001	<0.001
15-AG-099	<0.0004	0.01	0.01	<0.004	1.50	0.00	0.02
15-AG-100	<0.0004	0.01	<0.001	<0.004	<1.5	<0.0001	0.00
15-AG-101	0.00	0.01	0.00	<0.004	<1.5	0.00	0.01
15-AG-102	0.00	0.01	0.00	<0.004	2.30	0.00	0.00
15-AG-103	<0.0004	0.01	<0.001	<0.004	3.60	<0.0001	<0.001
15-AG-104	<0.0004	0.02	0.01	0.01	2.50	0.00	0.04
15-AG-105	<0.0004	0.02	0.00	<0.004	3.90	0.00	0.01
15-AG-106	<0.0004	0.02	<0.001	<0.004	13.00	<0.0001	0.00
15-AG-107	<0.0004	0.02	<0.001	<0.004	6.50	<0.0001	<0.001
15-AG-108	<0.0004	0.01	0.00	<0.004	<1.5	0.00	0.01
15-AG-109	0.01	0.03	0.03	0.02	2.10	0.01	0.16
15-AG-110	<0.0004	0.01	0.00	<0.004	2.80	0.00	0.00
15-AG-111	<0.0004	0.00	<0.001	<0.004	1.60	<0.0001	0.00
15-AG-112	0.01	0.02	0.04	0.01	<1.5	0.01	0.14
15-AG-113	0.00	0.01	0.00	<0.004	2.20	0.00	0.00
15-AG-114	<0.0004	0.00	<0.001	<0.004	4.60	<0.0001	<0.001
15-AG-115	<0.0004	<0.002	<0.001	<0.004	<1.5	0.00	0.00
15-AG-116	0.00	0.01	0.00	<0.004	7.50	<0.0001	0.00

Sample	Eu	Ga	Gd	Hf	Hg	Ho	La
	µg/L	µg/L	µg/L	µg/L	ng/L	µg/L	µg/L
15-AG-117	<0.0004	0.01	<0.001	<0.004	4.10	0.00	0.00
15-AG-118	0.00	0.02	0.02	<0.004	5.50	0.00	0.06
15-AG-119	<0.0004	1.78	0.00	<0.004	3.80	0.00	0.01
15-AG-120	<0.0004	0.01	0.00	0.00	2.70	0.00	0.01
15-AG-121	<0.0004	0.01	0.00	<0.004	<1.5	0.00	0.01
15-AG-122	0.00	0.01	<0.001	<0.004	3.40	0.00	0.01
15-AG-123	0.00	0.01	0.00	<0.004	1.70	0.00	0.01
15-AG-124	<0.0004	0.01	<0.001	<0.004	<1.5	0.00	0.00
15-AG-125	0.00	0.01	0.01	<0.004	10.10	0.00	0.02
15-AG-126	<0.0004	0.01	0.00	<0.004	<1.5	0.00	0.01
15-AG-127	0.00	0.01	0.00	<0.004	1.50	0.00	0.01
15-AG-128	0.00	0.01	<0.001	<0.004	7.80	0.00	0.00
15-AG-129	0.01	0.02	0.03	<0.004	0.00	0.00	0.24
15-AG-130	<0.0004	0.01	0.00	<0.004	4.30	<0.0001	0.00
15-AG-131	<0.0004	0.01	<0.001	<0.004	<1.5	0.00	0.00
15-AG-132	<0.0004	0.01	<0.001	<0.004	1.70	<0.0001	<0.001
15-AG-133	<0.0004	0.01	0.00	<0.004	<1.5	0.00	0.00
15-AG-134	0.00	0.00	<0.001	<0.004	<1.5	<0.0001	0.00
15-AG-135	<0.0004	0.01	<0.001	<0.004	<1.5	0.00	0.00
15-AG-136	<0.0004	0.01	<0.001	<0.004	1.70	0.00	0.00
15-AG-136	<0.0004	0.01	<0.001	<0.004	1.70	0.00	0.00
15-AG-137	<0.0004	0.03	<0.001	<0.004	<1.5	0.00	0.00
15-AG-138	<0.0004	0.01	0.00	<0.004	3.70	0.00	0.01
15-AG-139	<0.0004	0.05	<0.001	<0.004	6.40	0.00	0.00
15-AG-140	<0.0004	0.01	0.00	<0.004	2.80	0.00	0.01
15-AG-141	0.00	0.01	<0.001	<0.004	2.00	0.00	0.00
15-AG-142	<0.0004	<0.002	<0.001	<0.004	<1.5	<0.0001	<0.001
15-AG-143	<0.0004	0.01	0.00	<0.004	1.40	0.00	0.01
15-AG-144	0.00	0.00	<0.001	<0.004	13.40	0.00	0.01
15-AG-145	0.00	0.01	0.00	<0.004	1.80	0.00	0.01
15-AG-146	0.00	0.05	0.00	<0.004	3.50	<0.0001	0.00
15-AG-147	<0.0004	0.01	<0.001	<0.004	<1.5	0.00	0.00
15-AG-148	<0.0004	0.01	<0.001	<0.004	12.70	0.00	0.00
15-AG-149	<0.0004	0.00	<0.001	<0.004	2.70	0.00	0.01
15-AG-150	0.00	0.01	0.00	<0.004	3.10	0.00	0.01
15-AG-151	<0.0004	0.01	0.01	0.01	7.90	0.00	0.01
15-AG-152	0.00	0.01	0.00	<0.004	5.40	0.00	0.00
15-AG-153	0.00	0.01	0.02	0.01	<1.5	0.00	0.05

Sample	Eu	Ga	Gd	Hf	Hg	Ho	La
	µg/L	µg/L	µg/L	µg/L	ng/L	µg/L	µg/L
15-AG-165	0.00	0.01	0.00	0.01	<1.5	0.00	0.01
15-AG-166	<0.0004	0.00	0.00	<0.004	3.90	0.00	0.01
15-AG-167	0.00	0.01	0.00	<0.004	14.80	0.00	0.02
15-AG-168	<0.0004	0.01	0.00	<0.004	4.50	0.00	0.00
15-AG-169	0.01	0.01	0.03	<0.004	0.00	0.00	0.21
15-AG-170	<0.0004	0.01	0.00	<0.004	12.20	0.00	0.01
15-AG-171	<0.0004	0.01	<0.001	<0.004	50.60	0.00	0.00
15-AG-172	<0.0004	0.01	<0.001	<0.004	2.70	0.00	0.00
15-AG-173	<0.0004	0.00	0.00	<0.004	23.80	0.00	<0.001
15-AG-174	<0.0004	0.01	<0.001	<0.004	12.30	0.00	0.00
15-AG-175	<0.0004	0.01	0.01	<0.004	7.90	0.00	0.01
15-AG-176	<0.0004	0.01	0.00	<0.004	1.50	0.00	0.01
15-AG-177	<0.0004	0.01	0.00	<0.004	25.90	0.00	0.00
15-AG-178	<0.0004	0.01	0.00	<0.004	18.30	0.00	0.01
15-AG-179	<0.0004	0.01	0.00	<0.004	8.60	0.00	0.00
15-AG-180	<0.0004	0.01	0.00	0.01	3.90	0.00	0.01
15-AG-181	<0.0004	<0.002	0.00	<0.004	22.70	0.00	0.01
15-AG-182	0.00	0.00	0.00	<0.004	17.60	0.00	0.01
15-AG-183	<0.0004	0.02	0.00	0.01	13.40	0.00	0.00
15-AG-184	<0.0004	0.01	0.00	<0.004	6.40	0.00	0.00
15-AG-185	0.00	0.01	0.00	<0.004	19.50	0.00	0.01
15-AG-186	0.00	0.01	0.01	<0.004	17.60	0.00	0.09
15-AG-187	<0.0004	0.02	<0.001	<0.004	<1.5	<0.0001	<0.001
15-AG-188	0.00	0.04	0.03	0.00	15.30	0.00	0.09
15-AG-189	<0.0004	0.80	0.00	<0.004	20.80	0.00	0.01
15-AG-190	<0.0004	0.01	0.00	<0.004	6.40	0.00	0.01
15-AG-191	<0.0004	0.02	<0.001	<0.004	13.40	<0.0001	0.00
15-AG-192	<0.0004	0.02	<0.001	<0.004	2.85	<0.0001	<0.001

Appendix K: Trace Constituents – Li, Lu, Mn, Mo, Nb, Nd, Ni

Sample	Li	Lu	Mn	Mo	Nb	Nd	Ni
	µg/L	µg/L	µg/L	µg/L	µg/L	µg/L	µg/L
15-AG-001	4.02	<0.0001	25.50	40.80	<0.001	0.00	<0.1
15-AG-002	4.12	<0.0001	5.00	12.50	<0.001	0.00	<0.1
15-AG-003	5.32	0.00	6.00	28.96	<0.001	<0.003	0.33
15-AG-004	10.48	0.00	<5	7.78	<0.001	0.01	1.20

Sample	Li	Lu	Mn	Mo	Nb	Nd	Ni
	µg/L	µg/L	µg/L	µg/L	µg/L	µg/L	µg/L
15-AG-005	4.18	<0.0001	<5	3.59	<0.001	<0.003	<0.1
15-AG-006	117.40	0.00	37.00	0.49	0.00	0.02	<0.1
15-AG-007	2.70	0.00	15.00	1.19	0.00	0.05	4.47
15-AG-008	21.77	0.00	11.00	0.13	0.00	0.01	0.77
15-AG-009	0.51	0.00	<5	0.22	0.00	0.21	0.37
15-AG-010	79.80	0.00	6.00	0.07	0.00	0.01	<0.1
15-AG-011	9.76	0.00	30.50	0.10	0.00	0.01	0.69
15-AG-012	54.00	<0.0001	8.00	0.25	<0.001	<0.003	<0.1
15-AG-013	5.13	0.00	<5	11.06	0.00	<0.003	<0.1
15-AG-014	25.78	<0.0001	13.00	2.27	0.00	0.00	<0.1
15-AG-015	66.70	0.00	43.00	1.50	0.00	0.01	1.16
15-AG-016	149.10	0.00	333.00	0.32	0.00	0.01	0.43
15-AG-017	96.00	0.00	72.00	0.52	0.00	0.00	0.40
15-AG-018	128.30	0.00	143.00	0.05	0.01	0.04	1.05
15-AG-019	126.90	0.01	141.00	0.03	0.01	0.05	0.84
15-AG-020	19.05	0.00	11.00	0.02	0.00	0.01	<0.1
15-AG-021	73.50	0.00	64.00	0.02	0.00	0.01	0.88
15-AG-022	102.00	0.00	71.00	0.47	0.00	0.01	0.36
15-AG-023	27.35	0.00	180.00	2.60	0.01	0.07	0.48
15-AG-024	7.61	0.00	<5	0.69	0.00	0.03	2.18
15-AG-025	4.24	0.00	<5	1.63	<0.001	0.01	1.66
15-AG-026	30.70	0.00	10.00	0.03	0.00	<0.003	<0.1
15-AG-027	44.50	0.00	18.00	3.03	0.00	0.00	0.67
15-AG-028	95.60	0.00	70.00	7.81	0.00	0.01	0.49
15-AG-029	103.80	0.00	414.00	4.01	0.00	0.01	3.08
15-AG-030	29.38	0.00	45.00	0.93	0.00	0.01	0.46
15-AG-031	31.22	0.00	45.00	0.97	0.00	0.01	0.50
15-AG-032	<0.01	0.00	5.00	<0.01	<0.001	<0.003	<0.1
15-AG-033	2.59	0.00	15.00	1.88	<0.001	0.01	0.72
15-AG-034	6.94	0.00	519.00	0.48	0.00	0.01	3.70
15-AG-035	4.90	<0.0001	<5	3.33	0.00	<0.003	0.63
15-AG-036	64.30	<0.0001	40.00	1.54	0.00	0.01	<0.1
15-AG-037	67.80	0.00	108.00	4.53	0.00	0.02	0.76
15-AG-038	5.97	0.00	16.00	1.99	0.00	0.03	2.74
15-AG-039	60.40	0.00	36163.00	8.06	0.00	0.02	0.13
15-AG-040	30.61	0.00	44.00	0.92	0.00	0.01	1.47
15-AG-041	55.90	<0.0001	72.00	2.28	0.00	0.01	<0.1
15-AG-042	209.20	0.00	32.00	0.11	0.01	0.01	<0.1

Sample	Li	Lu	Mn	Mo	Nb	Nd	Ni
	µg/L	µg/L	µg/L	µg/L	µg/L	µg/L	µg/L
15-AG-043	35.20	<0.0001	25.00	0.90	0.00	0.00	0.41
15-AG-044	12.70	<0.0001	12.00	10.78	<0.001	0.01	607.00
15-AG-045	13.53	<0.0001	14.00	6.84	<0.001	0.00	0.31
15-AG-046	41.60	0.00	25.00	0.49	0.00	0.00	1.68
15-AG-047	15.83	0.00	14.00	1.88	0.00	0.02	2.01
15-AG-048	30.54	0.00	373.00	0.84	0.01	0.13	3.87
15-AG-049	0.44	0.00	5.00	0.26	0.00	0.18	0.49
15-AG-050	84.40	0.00	129.00	0.10	0.02	0.02	1.11
15-AG-051	14.15	0.00	<5	4.44	0.00	0.00	2.77
15-AG-052	28.86	0.00	15.00	1.07	<0.001	0.00	0.29
15-AG-053	8.41	0.00	<5	0.19	0.00	0.09	1.30
15-AG-054	22.37	<0.0001	<5	6.73	0.00	0.01	1.08
15-AG-055	137.40	<0.0001	351.00	0.85	0.01	0.01	<0.1
15-AG-056	197.20	<0.0001	13.00	0.16	0.01	0.01	0.32
15-AG-057	16.11	0.00	45.00	9.39	0.00	0.01	1.32
15-AG-058	47.60	<0.0001	83.00	4.92	0.00	0.00	0.52
15-AG-059	84.50	0.00	100.00	4.14	0.00	0.01	0.83
15-AG-060	15.52	0.00	35.00	8.57	0.00	0.01	2.47
15-AG-061	122.50	0.00	45.00	1.28	0.00	0.01	<0.1
15-AG-062	19.53	0.00	94.00	1.47	0.00	0.02	0.97
15-AG-063	30.26	0.00	55.00	2.04	0.00	0.00	1.49
15-AG-064	60.20	0.00	103.00	6.39	0.00	0.02	1.48
15-AG-065	215.70	0.00	16.00	0.04	<0.001	0.01	1.85
15-AG-066	5.72	0.00	10.00	1.12	0.00	<0.003	16.86
15-AG-067	122.40	0.00	99.50	2.41	0.00	0.01	2.63
15-AG-068	16.69	0.00	75.00	0.50	0.00	0.00	4.07
15-AG-069	47.00	<0.0001	83.00	2.39	0.00	0.01	2.32
15-AG-070	55.75	0.00	83.00	2.85	0.00	0.01	2.07
15-AG-071	198.50	<0.0001	26.00	0.21	0.01	0.01	1.47
15-AG-072	25.17	<0.0001	60.00	6.38	0.00	0.01	1.13
15-AG-073	8.95	0.00	<5	10.59	0.00	0.00	0.22
15-AG-074	17.71	0.00	49.00	6.11	0.00	0.02	1.35
15-AG-075	4.55	0.00	<5	3.47	0.00	0.00	1.18
15-AG-076	137.20	0.00	84.00	4.97	0.00	0.02	7.79
15-AG-077	56.80	0.00	30.00	0.74	0.00	0.02	1.36
15-AG-078	33.90	0.00	187.00	2.29	0.00	0.03	9.59
15-AG-079	55.70	0.00	35351.00	7.93	<0.001	0.02	0.17
15-AG-080	40.80	0.00	100.00	0.59	0.00	0.08	2.58

Sample	Li	Lu	Mn	Mo	Nb	Nd	Ni
	µg/L	µg/L	µg/L	µg/L	µg/L	µg/L	µg/L
15-AG-081	87.70	<0.0001	195.00	0.80	0.00	0.00	1.29
15-AG-082	4.05	0.00	12.00	51.60	<0.001	0.02	0.13
15-AG-083	16.20	0.00	13.00	1.06	0.00	0.02	1.07
15-AG-084	18.29	<0.0001	97.00	0.43	0.00	0.01	2.39
15-AG-085	162.80	<0.0001	139.00	5.51	0.00	0.01	3.16
15-AG-086	52.50	0.00	19.00	0.03	0.00	0.01	1.66
15-AG-087	138.10	<0.0001	86.50	1.00	0.00	0.01	3.51
15-AG-088	20.65	0.00	18.00	16.22	0.00	0.00	1.41
15-AG-089	0.46	0.00	5.00	0.23	0.01	0.18	0.60
15-AG-090	104.30	0.00	65.00	3.28	0.00	0.03	1.98
15-AG-091	71.30	<0.0001	27.00	0.05	0.00	0.01	2.07
15-AG-092	0.01	<0.0001	<5	<0.01	<0.001	<0.003	<0.1
15-AG-093	485.00	<0.0001	166.00	4.55	0.02	0.03	7.92
15-AG-094	221.00	0.00	83.00	0.37	0.01	0.03	2.50
15-AG-095	88.50	<0.0001	75.00	17.12	0.00	0.01	1.71
15-AG-096	30.60	0.00	45.00	0.23	0.00	0.02	2.02
15-AG-097	12.79	0.00	65.50	0.96	<0.001	0.02	1.71
15-AG-098	73.50	<0.0001	60.00	3.76	0.00	<0.003	1.25
15-AG-099	31.60	<0.0001	46.00	0.17	0.00	0.02	1.81
15-AG-100	234.00	<0.0001	24.00	0.14	0.01	0.01	0.50
15-AG-101	64.40	0.00	45.00	0.93	0.00	0.01	1.47
15-AG-102	41.20	0.00	34.00	0.04	<0.001	0.01	1.10
15-AG-103	35.60	<0.0001	23.00	1.40	0.00	<0.003	1.49
15-AG-104	9.82	0.00	418.00	0.09	0.00	0.05	2.49
15-AG-105	71.40	0.00	169.00	2.37	0.00	0.03	2.40
15-AG-106	16.13	<0.0001	14.00	41.90	<0.001	0.01	1.56
15-AG-107	7.35	<0.0001	17.00	28.64	<0.001	0.01	1.36
15-AG-108	134.50	0.00	96.00	3.29	<0.001	0.01	4.02
15-AG-109	125.30	0.00	326.00	1.58	0.02	0.18	3.73
15-AG-110	18.84	0.00	10.00	3.25	<0.001	0.00	3.64
15-AG-111	21.50	0.00	13.00	9.20	0.00	<0.003	1.38
15-AG-112	122.10	0.00	303.00	1.64	0.01	0.16	4.06
15-AG-113	28.10	0.00	<5	1.34	0.00	<0.003	5.56
15-AG-114	12.13	<0.0001	<5	1.55	<0.001	<0.003	0.59
15-AG-115	5.11	<0.0001	<5	3.65	<0.001	<0.003	1.94
15-AG-116	74.10	<0.0001	25.00	0.25	<0.001	0.03	2.14
15-AG-117	41.60	0.00	34.00	0.10	<0.001	<0.003	2.04
15-AG-118	11.46	0.00	39.50	6.19	0.01	0.08	0.83

Sample	Li	Lu	Mn	Mo	Nb	Nd	Ni
	µg/L	µg/L	µg/L	µg/L	µg/L	µg/L	µg/L
15-AG-119	58.70	<0.0001	35436.00	8.23	<0.001	0.01	0.20
15-AG-120	39.10	0.00	24.00	1.19	0.00	0.01	<0.1
15-AG-121	202.40	<0.0001	64.00	0.21	0.00	0.01	1.79
15-AG-122	104.40	<0.0001	60.00	0.36	0.00	0.01	<0.1
15-AG-123	7.91	0.00	<5	11.48	0.00	0.01	1.50
15-AG-124	134.00	0.00	73.00	1.84	0.00	0.01	<0.1
15-AG-125	115.60	0.00	157.00	9.86	0.01	0.02	<0.1
15-AG-126	144.30	0.00	71.00	0.22	0.00	0.01	<0.1
15-AG-127	184.20	0.00	65.00	3.06	0.00	0.01	<0.1
15-AG-128	149.60	0.00	66.00	7.07	0.01	0.01	<0.1
15-AG-129	0.49	0.00	<5	0.22	0.00	0.23	0.55
15-AG-130	104.40	<0.0001	66.00	7.56	0.00	0.01	2.07
15-AG-131	20.62	<0.0001	11.00	46.50	0.00	0.01	<0.1
15-AG-132	4.46	<0.0001	16.00	6.63	<0.001	<0.003	0.38
15-AG-133	16.78	0.00	13.00	2.26	<0.001	0.00	0.84
15-AG-134	10.90	<0.0001	<5	1.87	<0.001	<0.003	0.23
15-AG-135	222.40	<0.0001	69.00	0.04	0.00	0.02	0.47
15-AG-136	54.80	0.00	62.00	2.02	0.00	0.01	<0.1
15-AG-136	54.80	0.00	62.00	2.02	0.00	0.01	<0.1
15-AG-137	761.00	<0.0001	43.00	0.99	0.01	0.02	<0.1
15-AG-138	15.29	0.00	6.00	0.98	0.01	0.01	<0.1
15-AG-139	1044.00	0.00	117.00	11.11	0.03	0.03	<0.1
15-AG-140	20.22	0.00	19.50	1.03	0.01	0.00	<0.1
15-AG-141	140.60	<0.0001	49.00	1.28	0.01	0.01	<0.1
15-AG-142	0.03	<0.0001	<5	0.01	<0.001	<0.003	<0.1
15-AG-143	120.45	<0.0001	99.00	10.13	0.01	0.01	<0.1
15-AG-144	31.70	0.00	<5	2.78	0.01	0.01	0.89
15-AG-145	100.90	0.00	68.00	11.58	0.00	0.01	7.08
15-AG-146	1049.00	0.00	118.00	11.65	0.03	0.03	<0.1
15-AG-147	118.80	0.00	50.00	0.17	0.01	0.01	<0.1
15-AG-148	62.40	<0.0001	75.00	1.74	0.01	0.01	1.25
15-AG-149	28.93	<0.0001	<5	2.56	0.01	0.01	2.45
15-AG-150	73.30	0.00	63.50	0.52	0.00	0.01	0.70
15-AG-151	46.70	0.00	41.00	1.27	0.00	0.01	0.73
15-AG-152	84.20	0.00	34.00	0.52	0.01	0.01	0.91
15-AG-153	260.90	0.00	73.00	0.06	0.01	0.05	0.38
15-AG-165	508.00	0.00	20.50	0.21	0.05	0.02	<0.1
15-AG-166	31.80	0.00	50.00	1.16	0.01	0.01	<0.1

Sample	Li	Lu	Mn	Mo	Nb	Nd	Ni
	µg/L	µg/L	µg/L	µg/L	µg/L	µg/L	µg/L
15-AG-167	185.10	0.00	114.00	3.12	0.01	0.02	<0.1
15-AG-168	6.97	0.00	22.00	9.25	0.00	0.01	0.33
15-AG-169	0.48	0.00	5.00	0.22	0.00	0.20	0.46
15-AG-170	150.10	0.00	95.00	10.44	0.01	0.02	<0.1
15-AG-171	65.30	0.00	154.00	54.60	0.00	0.02	0.18
15-AG-172	19.48	<0.0001	19.00	1.43	<0.001	0.00	0.23
15-AG-173	14.93	0.00	6.00	2.73	<0.001	<0.003	0.67
15-AG-174	15.97	<0.0001	59.50	51.00	<0.001	0.01	0.34
15-AG-175	219.90	0.00	24.00	0.18	0.01	0.01	<0.1
15-AG-176	203.20	0.00	106.00	0.16	0.01	0.01	0.39
15-AG-177	343.50	0.00	39.00	3.51	0.01	0.01	0.99
15-AG-178	350.00	0.00	51.00	6.81	0.01	0.01	0.79
15-AG-179	321.00	0.00	37.00	3.69	0.01	0.01	1.28
15-AG-180	83.80	0.00	6.00	0.02	0.00	0.01	0.39
15-AG-181	10.09	0.00	12.00	0.35	0.00	0.00	38.86
15-AG-182	134.60	0.00	74.00	1.70	0.01	0.01	0.99
15-AG-183	16.59	0.00	460.00	0.77	0.01	0.02	0.48
15-AG-184	28.31	0.00	63.50	46.40	0.01	0.00	2.11
15-AG-185	73.20	0.00	104.00	2.90	0.01	0.01	<0.1
15-AG-186	172.60	0.00	163.00	6.30	0.01	0.04	7.96
15-AG-187	4.25	<0.0001	8.00	33.20	<0.001	<0.003	0.25
15-AG-188	439.00	0.00	193.00	2.50	0.02	0.11	0.28
15-AG-189	50.00	0.00	30724.00	7.76	<0.001	0.02	0.12
15-AG-190	226.60	0.00	58.00	0.91	0.00	0.01	<0.1
15-AG-191	3.32	<0.0001	16.00	5.74	<0.001	<0.003	0.13
15-AG-192	4.18	<0.0001	8.00	32.50	<0.001	<0.003	0.18

Appendix L: Trace Constituents – Pb, Pr, Rb, Sb, Sc, Se, Sm

Sample	Pb	Pr	Rb	Sb	Sc	Se	Sm
	µg/L	µg/L	µg/L	µg/L	µg/L	µg/L	µg/L
15-AG-001	0.01	<0.0004	0.82	<0.01	0.21	0.61	<0.001
15-AG-002	0.01	<0.0004	0.76	0.01	0.33	0.60	<0.001
15-AG-003	0.04	0.00	1.08	0.02	0.15	0.27	<0.001
15-AG-004	0.04	0.00	0.90	0.13	<0.1	0.56	0.00
15-AG-005	0.04	<0.0004	0.56	<0.01	0.37	<0.2	<0.001
15-AG-006	<0.002	0.00	4.39	<0.01	0.50	0.70	0.01
15-AG-007	0.08	0.01	0.55	0.14	0.30	0.50	0.01

Sample	Pb	Pr	Rb	Sb	Sc	Se	Sm
	µg/L	µg/L	µg/L	µg/L	µg/L	µg/L	µg/L
15-AG-008	0.08	0.00	1.63	0.03	0.31	0.75	0.00
15-AG-009	0.07	0.05	1.29	0.34	0.16	0.21	0.04
15-AG-010	0.01	<0.0004	4.24	0.01	0.31	1.99	0.00
15-AG-011	0.01	0.00	2.35	0.03	0.26	0.38	0.00
15-AG-012	0.01	<0.0004	3.55	<0.01	0.41	<0.2	<0.001
15-AG-013	0.00	<0.0004	0.45	<0.01	<0.1	<0.2	0.00
15-AG-014	0.03	0.00	1.84	0.03	0.26	0.49	<0.001
15-AG-015	0.01	0.00	1.56	0.03	0.35	2.02	0.00
15-AG-016	<0.002	0.00	5.08	<0.01	0.44	1.33	0.00
15-AG-017	<0.002	0.00	4.99	<0.01	0.32	1.01	0.00
15-AG-018	0.01	0.01	2.38	0.01	0.36	0.81	0.02
15-AG-019	0.01	0.01	2.43	0.01	0.39	0.83	0.02
15-AG-020	<0.002	0.00	2.76	<0.01	0.21	0.83	<0.001
15-AG-021	0.01	0.00	1.57	<0.01	0.13	0.38	0.00
15-AG-022	<0.002	0.00	1.87	<0.01	0.21	0.38	0.00
15-AG-023	0.01	0.01	1.58	0.01	0.33	0.29	0.01
15-AG-024	0.03	0.01	0.45	0.09	0.29	0.65	0.01
15-AG-025	0.16	0.00	1.70	0.06	0.30	0.66	0.00
15-AG-026	<0.002	<0.0004	5.73	<0.01	0.23	0.99	0.00
15-AG-027	0.01	0.00	1.91	<0.01	0.26	0.23	<0.001
15-AG-028	0.04	0.00	3.39	0.02	0.40	0.71	0.00
15-AG-029	0.01	0.00	1.12	0.02	0.57	0.62	0.00
15-AG-030	0.01	0.00	1.74	<0.01	0.35	0.24	0.00
15-AG-031	<0.002	0.00	1.79	<0.01	0.30	0.49	0.00
15-AG-032	0.01	<0.0004	0.01	<0.01	0.23	<0.2	0.00
15-AG-033	<0.002	0.00	0.61	<0.01	0.25	<0.2	0.00
15-AG-034	0.13	0.00	2.29	0.17	0.42	1.15	0.00
15-AG-035	0.04	0.00	0.54	<0.01	0.21	0.33	<0.001
15-AG-036	0.01	0.00	2.12	<0.01	0.25	0.33	0.00
15-AG-037	0.04	0.00	4.43	0.02	0.34	1.03	0.00
15-AG-038	0.06	0.01	1.88	0.39	0.26	0.36	0.01
15-AG-039	0.15	0.00	1.97	0.02	0.10	1.85	0.00
15-AG-040	0.06	0.00	1.04	0.03	0.35	0.59	0.00
15-AG-041	0.01	0.00	2.92	<0.01	0.34	0.42	0.00
15-AG-042	0.00	0.00	7.57	<0.01	0.47	0.14	<0.001
15-AG-043	0.24	0.00	2.07	<0.01	<0.1	1.26	<0.001
15-AG-044	0.01	<0.0004	1.26	<0.01	<0.1	0.61	0.00
15-AG-045	0.05	<0.0004	1.06	<0.01	0.14	0.73	<0.001
15-AG-046	0.55	0.00	2.98	0.03	0.37	1.68	0.00
15-AG-047	0.06	0.00	0.93	0.04	0.33	0.37	0.02

Sample	Pb	Pr	Rb	Sb	Sc	Se	Sm
	µg/L	µg/L	µg/L	µg/L	µg/L	µg/L	µg/L
15-AG-048	1.53	0.03	1.09	0.02	0.30	0.74	0.02
15-AG-049	0.12	0.05	1.25	0.34	0.24	0.59	0.03
15-AG-050	<0.002	0.00	2.25	<0.01	0.43	0.88	0.00
15-AG-051	0.19	0.00	1.91	0.25	<0.1	<0.2	<0.001
15-AG-052	0.00	0.00	0.81	<0.01	<0.1	<0.2	0.00
15-AG-053	0.05	0.01	0.62	0.02	0.27	0.34	0.03
15-AG-054	<0.002	0.00	1.80	<0.01	0.20	2.94	<0.001
15-AG-055	<0.002	<0.0004	7.36	<0.01	0.34	12.59	0.00
15-AG-056	0.03	0.00	10.53	<0.01	0.43	8.48	0.00
15-AG-057	0.05	0.00	2.63	0.68	<0.1	0.96	0.00
15-AG-058	<0.002	0.00	3.45	<0.01	0.36	2.19	<0.001
15-AG-059	<0.002	0.00	5.20	<0.01	0.24	1.42	<0.001
15-AG-060	0.05	0.00	2.69	0.70	<0.1	0.84	0.00
15-AG-061	<0.002	0.00	3.95	<0.01	0.26	0.97	0.00
15-AG-062	<0.002	0.00	0.98	<0.01	0.20	<0.2	0.00
15-AG-063	0.00	0.00	1.11	<0.01	0.27	0.90	0.00
15-AG-064	<0.002	0.00	4.31	<0.01	0.33	0.55	0.01
15-AG-065	<0.002	0.00	9.01	<0.01	0.18	1.09	<0.001
15-AG-066	0.02	<0.0004	3.21	0.30	0.19	0.85	0.00
15-AG-067	0.00	0.00	5.21	0.02	0.45	1.93	0.00
15-AG-068	0.02	0.00	2.51	0.03	0.13	0.83	0.00
15-AG-069	<0.002	0.00	3.17	0.01	0.31	1.14	<0.001
15-AG-070	<0.002	0.00	3.25	<0.01	0.35	1.31	0.00
15-AG-071	0.04	0.00	8.66	0.01	0.33	<0.2	0.00
15-AG-072	<0.002	0.00	1.69	0.01	<0.1	2.22	0.00
15-AG-073	<0.002	<0.0004	0.60	<0.01	<0.1	<0.2	<0.001
15-AG-074	<0.002	0.00	1.38	<0.01	<0.1	2.67	<0.001
15-AG-075	0.06	0.00	0.55	0.01	<0.1	0.36	0.00
15-AG-076	0.03	0.00	2.52	<0.01	0.29	0.91	0.00
15-AG-077	0.01	0.00	2.88	0.01	<0.1	0.75	0.01
15-AG-078	0.00	0.01	0.62	0.21	<0.1	<0.2	0.00
15-AG-079	0.10	0.00	1.95	0.02	<0.1	1.68	0.00
15-AG-080	0.50	0.02	2.30	0.02	<0.1	1.02	0.02
15-AG-081	<0.002	<0.0004	3.36	<0.01	<0.1	1.41	<0.001
15-AG-082	<0.002	<0.0004	0.35	<0.01	<0.1	0.68	<0.001
15-AG-083	0.56	0.00	1.12	0.06	<0.1	0.43	0.00
15-AG-084	<0.002	<0.0004	2.05	<0.01	0.16	1.30	0.00
15-AG-085	<0.002	0.00	3.23	<0.01	0.16	1.20	<0.001
15-AG-086	<0.002	0.00	2.51	<0.01	<0.1	2.98	0.00
15-AG-087	0.01	<0.0004	3.55	0.01	<0.1	<0.2	<0.001

Sample	Pb	Pr	Rb	Sb	Sc	Se	Sm
	µg/L	µg/L	µg/L	µg/L	µg/L	µg/L	µg/L
15-AG-088	<0.002	0.00	2.04	<0.01	<0.1	0.68	<0.001
15-AG-089	0.07	0.05	1.27	0.29	<0.1	<0.2	0.03
15-AG-090	<0.002	0.01	2.97	<0.01	<0.1	<0.2	0.00
15-AG-091	<0.002	0.00	3.54	<0.01	<0.1	1.10	<0.001
15-AG-092	<0.002	<0.0004	<0.005	<0.01	<0.1	<0.2	0.00
15-AG-093	0.60	0.00	8.89	0.86	0.23	0.44	0.00
15-AG-094	0.00	0.00	8.99	0.04	<0.1	<0.2	0.00
15-AG-095	0.01	0.00	5.32	<0.01	<0.1	4.48	<0.001
15-AG-096	0.79	0.00	1.97	0.02	<0.1	0.89	0.00
15-AG-097	0.03	0.01	1.13	0.03	<0.1	0.47	0.01
15-AG-098	0.04	<0.0004	3.42	<0.01	<0.1	3.42	<0.001
15-AG-099	1.36	0.00	2.13	0.02	<0.1	0.79	0.00
15-AG-100	<0.002	0.00	5.82	<0.01	<0.1	19.71	<0.001
15-AG-101	0.01	0.00	3.06	<0.01	<0.1	0.52	<0.001
15-AG-102	0.00	0.00	2.09	<0.01	<0.1	0.98	0.00
15-AG-103	0.00	<0.0004	2.61	<0.01	<0.1	0.63	<0.001
15-AG-104	0.01	0.01	1.61	<0.01	<0.1	0.61	0.01
15-AG-105	0.09	0.00	2.70	0.03	<0.1	9.95	0.00
15-AG-106	<0.002	0.00	1.80	<0.01	<0.1	1.21	0.00
15-AG-107	0.00	<0.0004	0.47	<0.01	<0.1	1.02	<0.001
15-AG-108	0.02	0.00	1.50	0.04	<0.1	0.59	<0.001
15-AG-109	0.21	0.04	2.95	0.02	<0.1	1.72	0.03
15-AG-110	0.28	0.00	0.96	0.12	<0.1	0.95	0.00
15-AG-111	0.01	<0.0004	0.93	<0.01	<0.1	0.34	<0.001
15-AG-112	0.21	0.03	3.17	0.06	<0.1	1.74	0.03
15-AG-113	0.16	0.00	2.18	0.04	<0.1	0.83	0.01
15-AG-114	0.02	<0.0004	0.41	<0.01	<0.1	0.26	<0.001
15-AG-115	0.04	<0.0004	0.57	<0.01	<0.1	0.25	<0.001
15-AG-116	0.00	0.00	2.14	<0.01	<0.1	11.34	<0.001
15-AG-117	<0.002	<0.0004	3.45	<0.01	<0.1	2.29	<0.001
15-AG-118	0.16	0.02	1.97	2.96	0.19	1.98	0.02
15-AG-119	0.11	0.00	2.02	0.02	<0.1	2.37	<0.001
15-AG-120	0.02	0.00	4.31	<0.01	0.32	0.27	0.00
15-AG-121	<0.002	<0.0004	3.95	<0.01	<0.1	12.23	<0.001
15-AG-122	<0.002	0.00	2.92	<0.01	0.32	0.79	<0.001
15-AG-123	0.14	0.00	23.46	0.57	0.19	0.74	0.00
15-AG-124	<0.002	<0.0004	4.76	<0.01	0.25	7.96	<0.001
15-AG-125	0.04	0.00	5.78	0.02	0.25	7.54	<0.001
15-AG-126	<0.002	0.00	5.39	<0.01	0.28	1.80	0.00
15-AG-127	<0.002	0.00	7.12	0.02	0.28	9.22	0.00

Sample	Pb	Pr	Rb	Sb	Sc	Se	Sm
	µg/L	µg/L	µg/L	µg/L	µg/L	µg/L	µg/L
15-AG-128	<0.002	0.00	4.85	<0.01	0.23	8.19	<0.001
15-AG-129	0.07	0.06	1.27	0.34	<0.1	<0.2	0.04
15-AG-130	0.01	<0.0004	3.42	0.31	0.13	5.26	0.00
15-AG-131	<0.002	0.00	3.09	<0.01	0.14	0.88	<0.001
15-AG-132	0.01	<0.0004	3.13	0.05	0.11	0.30	0.00
15-AG-133	0.27	0.00	1.74	0.05	<0.1	0.24	0.00
15-AG-134	0.00	<0.0004	0.42	<0.01	<0.1	<0.2	0.00
15-AG-135	<0.002	<0.0004	3.35	0.01	<0.1	1.00	<0.001
15-AG-136	<0.002	0.00	2.64	<0.01	0.11	1.37	<0.001
15-AG-136	<0.002	0.00	2.64	<0.01	0.11	1.37	<0.001
15-AG-137	<0.002	0.00	9.64	0.02	0.31	1.76	<0.001
15-AG-138	0.01	0.00	2.34	<0.01	<0.1	0.51	<0.001
15-AG-139	0.00	0.00	10.77	0.04	0.37	0.82	<0.001
15-AG-140	<0.002	0.00	2.06	<0.01	<0.1	0.58	<0.001
15-AG-141	0.01	0.00	3.80	0.01	0.22	13.80	<0.001
15-AG-142	<0.002	<0.0004	<0.005	<0.01	<0.1	<0.2	0.00
15-AG-143	<0.002	0.00	6.96	<0.01	0.19	10.94	0.00
15-AG-144	<0.002	0.00	3.94	0.06	<0.1	0.73	0.00
15-AG-145	0.11	0.00	1.24	0.17	<0.1	0.78	0.00
15-AG-146	0.00	0.00	10.69	0.04	0.33	0.79	<0.001
15-AG-147	0.00	0.00	6.25	<0.01	0.20	11.31	<0.001
15-AG-148	0.01	0.00	4.03	<0.01	0.14	2.56	<0.001
15-AG-149	0.00	0.00	3.84	0.07	<0.1	0.73	<0.001
15-AG-150	0.01	0.00	1.69	<0.01	<0.1	0.39	<0.001
15-AG-151	0.01	0.00	2.14	0.04	<0.1	0.32	0.00
15-AG-152	0.22	0.00	4.59	0.04	<0.1	3.86	0.00
15-AG-153	0.03	0.01	4.98	<0.01	<0.1	<0.2	0.02
15-AG-165	0.01	0.00	10.75	0.01	0.49	0.38	0.00
15-AG-166	0.00	0.00	2.70	<0.01	0.11	1.01	<0.001
15-AG-167	0.03	0.00	7.19	0.03	0.17	<0.2	0.00
15-AG-168	0.02	0.00	0.29	0.02	<0.1	<0.2	0.00
15-AG-169	0.08	0.05	1.24	0.31	<0.1	<0.2	0.04
15-AG-170	0.01	0.00	6.23	0.01	0.23	0.25	0.00
15-AG-171	0.01	0.00	7.72	0.02	<0.1	1.42	0.00
15-AG-172	0.01	<0.0004	0.73	<0.01	<0.1	0.75	0.00
15-AG-173	0.01	<0.0004	0.48	<0.01	<0.1	<0.2	<0.001
15-AG-174	0.00	0.00	1.06	<0.01	<0.1	1.13	<0.001
15-AG-175	0.00	0.00	6.78	<0.01	0.28	6.44	0.00
15-AG-176	<0.002	0.00	6.89	<0.01	0.26	18.14	0.00
15-AG-177	0.01	0.00	4.05	0.02	<0.1	26.54	0.00

Sample	Pb	Pr	Rb	Sb	Sc	Se	Sm
	µg/L	µg/L	µg/L	µg/L	µg/L	µg/L	µg/L
15-AG-178	0.00	0.00	6.22	<0.01	<0.1	18.63	0.00
15-AG-179	0.01	0.00	4.25	<0.01	<0.1	27.44	<0.001
15-AG-180	0.00	0.00	2.98	<0.01	<0.1	0.33	0.00
15-AG-181	0.08	0.00	0.87	0.02	<0.1	0.68	0.00
15-AG-182	<0.002	0.00	6.17	<0.01	<0.1	0.68	0.00
15-AG-183	0.01	0.00	1.66	<0.01	<0.1	0.87	0.00
15-AG-184	0.00	0.00	2.63	0.39	<0.1	0.40	<0.001
15-AG-185	0.24	0.00	2.81	0.04	<0.1	1.04	0.00
15-AG-186	0.45	0.01	4.61	0.02	<0.1	0.89	0.00
15-AG-187	0.07	<0.0004	0.74	0.01	<0.1	0.28	<0.001
15-AG-188	0.11	0.03	9.27	0.04	<0.1	<0.2	0.02
15-AG-189	0.13	0.00	1.92	0.02	<0.1	1.79	0.00
15-AG-190	0.01	0.00	6.95	<0.01	<0.1	<0.2	0.00
15-AG-191	0.03	<0.0004	0.42	0.05	<0.1	<0.2	0.00
15-AG-192	0.04	<0.0004	0.71	0.01	<0.1	0.23	<0.001

Appendix M: Trace Constituents – Sn, Ta, Tb, Th, Ti, Tl, Tm

Sample	Sn	Ta	Tb	Th	Ti	Tl	Tm
	µg/L	µg/L	µg/L	µg/L	µg/L	µg/L	µg/L
15-AG-001	<0.01	<0.0003	<0.0001	<0.001	0.42	<0.001	0.00
15-AG-002	<0.01	0.00	<0.0001	<0.001	0.42	0.01	<0.0001
15-AG-003	<0.01	<0.0003	0.00	<0.001	0.54	0.01	0.00
15-AG-004	<0.01	<0.0003	0.00	<0.001	0.21	0.01	0.00
15-AG-005	0.02	<0.0003	0.00	<0.001	0.12	0.06	0.00
15-AG-006	<0.01	<0.0003	0.00	<0.001	0.30	<0.001	0.00
15-AG-007	<0.01	0.00	0.00	0.00	0.99	0.01	0.00
15-AG-008	0.03	<0.0003	0.00	<0.001	0.67	<0.001	0.00
15-AG-009	<0.01	<0.0003	0.00	0.00	2.16	0.00	0.00
15-AG-010	0.01	<0.0003	0.00	0.00	0.47	<0.001	0.00
15-AG-011	<0.01	<0.0003	0.00	<0.001	2.37	<0.001	0.00
15-AG-012	0.02	<0.0003	<0.0001	<0.001	0.12	<0.001	<0.0001
15-AG-013	<0.01	0.00	0.00	<0.001	<0.1	<0.001	<0.0001
15-AG-014	<0.01	<0.0003	0.00	<0.001	0.29	0.01	0.00
15-AG-015	0.02	<0.0003	0.00	<0.001	0.13	0.00	0.00
15-AG-016	<0.01	0.00	0.00	0.00	0.61	<0.001	0.00
15-AG-017	<0.01	<0.0003	0.00	<0.001	0.40	<0.001	0.00
15-AG-018	<0.01	0.00	0.00	0.00	0.69	<0.001	0.00
15-AG-019	0.01	0.00	0.00	0.00	0.68	<0.001	0.00
15-AG-020	0.01	<0.0003	0.00	0.00	0.49	<0.001	0.00

Sample	Sn	Ta	Tb	Th	Ti	Tl	Tm
	µg/L	µg/L	µg/L	µg/L	µg/L	µg/L	µg/L
15-AG-021	0.02	<0.0003	0.00	<0.001	0.14	<0.001	0.00
15-AG-022	0.01	<0.0003	0.00	<0.001	0.14	<0.001	0.00
15-AG-023	<0.01	0.00	0.00	0.01	1.03	<0.001	0.00
15-AG-024	0.02	<0.0003	0.00	0.00	<0.1	0.00	0.00
15-AG-025	<0.01	<0.0003	0.00	<0.001	0.15	0.14	0.00
15-AG-026	<0.01	<0.0003	0.00	<0.001	0.41	<0.001	<0.0001
15-AG-027	0.01	<0.0003	0.00	<0.001	<0.1	<0.001	0.00
15-AG-028	0.04	<0.0003	0.00	0.00	0.56	<0.001	0.00
15-AG-029	<0.01	<0.0003	0.00	<0.001	0.45	0.03	0.00
15-AG-030	<0.01	0.00	0.00	0.00	0.45	0.00	0.00
15-AG-031	<0.01	<0.0003	0.00	<0.001	0.44	0.00	0.00
15-AG-032	0.01	<0.0003	<0.0001	<0.001	0.94	<0.001	0.00
15-AG-033	<0.01	<0.0003	0.00	<0.001	0.73	<0.001	0.00
15-AG-034	0.02	<0.0003	0.00	<0.001	0.49	0.01	0.00
15-AG-035	0.02	<0.0003	0.00	<0.001	0.33	0.06	0.00
15-AG-036	0.01	<0.0003	0.00	<0.001	0.40	<0.001	0.00
15-AG-037	0.05	<0.0003	0.00	<0.001	0.35	0.00	0.00
15-AG-038	0.02	<0.0003	0.00	0.00	1.11	0.04	0.00
15-AG-039	0.07	<0.0003	0.00	0.00	0.68	<0.001	0.00
15-AG-040	0.02	<0.0003	0.00	0.00	0.41	0.04	0.00
15-AG-041	0.02	<0.0003	0.00	<0.001	0.32	<0.001	0.00
15-AG-042	0.01	0.00	0.00	<0.001	0.56	<0.001	0.00
15-AG-043	0.31	0.00	0.00	<0.001	<0.1	<0.001	0.00
15-AG-044	0.05	<0.0003	<0.0001	<0.001	<0.1	<0.001	<0.0001
15-AG-045	0.02	<0.0003	0.00	<0.001	0.19	<0.001	<0.0001
15-AG-046	0.02	<0.0003	0.00	<0.001	0.49	0.02	0.00
15-AG-047	<0.01	<0.0003	0.00	<0.001	0.30	0.01	0.00
15-AG-048	<0.01	0.00	0.00	0.01	0.63	0.09	0.00
15-AG-049	0.02	<0.0003	0.00	0.00	2.10	0.00	0.00
15-AG-050	<0.01	<0.0003	0.00	0.00	1.67	<0.001	0.00
15-AG-051	0.02	<0.0003	<0.0001	<0.001	0.27	0.01	<0.0001
15-AG-052	<0.01	<0.0003	0.00	<0.001	<0.1	<0.001	<0.0001
15-AG-053	0.01	<0.0003	0.01	<0.001	0.20	0.01	0.00
15-AG-054	0.01	<0.0003	<0.0001	<0.001	0.31	<0.001	<0.0001
15-AG-055	0.01	<0.0003	0.00	<0.001	1.01	<0.001	<0.0001
15-AG-056	0.04	<0.0003	0.00	<0.001	1.03	<0.001	0.00
15-AG-057	<0.01	<0.0003	0.00	<0.001	0.62	0.11	0.00
15-AG-058	0.01	<0.0003	<0.0001	<0.001	0.53	<0.001	<0.0001

Sample	Sn	Ta	Tb	Th	Ti	Tl	Tm
	µg/L	µg/L	µg/L	µg/L	µg/L	µg/L	µg/L
15-AG-059	<0.01	<0.0003	<0.0001	<0.001	0.46	<0.001	0.00
15-AG-060	<0.01	0.00	0.00	<0.001	0.55	0.11	0.00
15-AG-061	<0.01	<0.0003	0.00	<0.001	<0.1	<0.001	0.00
15-AG-062	<0.01	<0.0003	0.00	<0.001	<0.1	<0.001	0.00
15-AG-063	<0.01	<0.0003	0.00	<0.001	0.17	0.01	<0.0001
15-AG-064	0.01	<0.0003	0.00	<0.001	0.46	<0.001	0.00
15-AG-065	0.01	0.00	0.00	<0.001	0.65	<0.001	0.00
15-AG-066	<0.01	<0.0003	0.00	<0.001	0.16	0.02	0.00
15-AG-067	0.01	<0.0003	0.00	<0.001	0.37	0.01	0.00
15-AG-068	0.02	<0.0003	<0.0001	<0.001	0.22	0.00	0.00
15-AG-069	0.01	<0.0003	<0.0001	<0.001	0.49	<0.001	<0.0001
15-AG-070	0.02	<0.0003	0.00	0.00	0.61	<0.001	0.00
15-AG-071	0.01	<0.0003	<0.0001	<0.001	0.75	<0.001	<0.0001
15-AG-072	0.01	<0.0003	<0.0001	<0.001	0.27	<0.001	0.00
15-AG-073	0.01	0.00	<0.0001	<0.001	<0.1	<0.001	<0.0001
15-AG-074	0.01	<0.0003	<0.0001	<0.001	<0.1	<0.001	<0.0001
15-AG-075	0.02	<0.0003	<0.0001	<0.001	<0.1	0.06	0.00
15-AG-076	0.01	<0.0003	0.00	<0.001	<0.1	0.01	0.00
15-AG-077	<0.01	<0.0003	0.00	0.00	0.30	<0.001	0.00
15-AG-078	<0.01	<0.0003	0.00	0.00	<0.1	0.01	0.00
15-AG-079	0.04	<0.0003	0.00	0.00	<0.1	<0.001	0.00
15-AG-080	<0.01	0.00	0.00	0.01	<0.1	0.00	0.00
15-AG-081	<0.01	<0.0003	<0.0001	<0.001	<0.1	<0.001	<0.0001
15-AG-082	<0.01	<0.0003	<0.0001	<0.001	<0.1	<0.001	<0.0001
15-AG-083	<0.01	<0.0003	0.00	<0.001	<0.1	0.00	0.00
15-AG-084	<0.01	<0.0003	<0.0001	<0.001	0.14	<0.001	<0.0001
15-AG-085	0.38	<0.0003	0.00	<0.001	<0.1	<0.001	0.00
15-AG-086	0.01	<0.0003	<0.0001	<0.001	<0.1	<0.001	0.00
15-AG-087	0.02	<0.0003	<0.0001	<0.001	0.20	<0.001	<0.0001
15-AG-088	0.01	<0.0003	0.00	<0.001	<0.1	<0.001	0.00
15-AG-089	<0.01	<0.0003	0.00	0.00	1.85	0.00	0.00
15-AG-090	<0.01	<0.0003	0.00	0.00	0.13	<0.001	<0.0001
15-AG-091	<0.01	<0.0003	<0.0001	<0.001	<0.1	<0.001	0.00
15-AG-092	<0.01	<0.0003	<0.0001	<0.001	0.14	<0.001	<0.0001
15-AG-093	0.02	<0.0003	0.00	<0.001	1.30	0.00	<0.0001
15-AG-094	0.02	0.00	0.00	0.00	2.17	<0.001	0.00
15-AG-095	<0.01	0.00	<0.0001	<0.001	<0.1	<0.001	<0.0001
15-AG-096	<0.01	<0.0003	0.00	<0.001	<0.1	0.00	0.00

Sample	Sn	Ta	Tb	Th	Ti	Tl	Tm
	µg/L	µg/L	µg/L	µg/L	µg/L	µg/L	µg/L
15-AG-097	<0.01	0.00	0.00	0.00	<0.1	0.01	0.00
15-AG-098	<0.01	<0.0003	0.00	<0.001	<0.1	0.01	<0.0001
15-AG-099	<0.01	<0.0003	0.00	<0.001	<0.1	0.00	0.00
15-AG-100	<0.01	<0.0003	0.00	<0.001	<0.1	<0.001	<0.0001
15-AG-101	<0.01	<0.0003	0.00	<0.001	<0.1	0.00	0.00
15-AG-102	<0.01	<0.0003	0.00	<0.001	<0.1	<0.001	0.00
15-AG-103	<0.01	<0.0003	<0.0001	<0.001	<0.1	0.00	<0.0001
15-AG-104	<0.01	<0.0003	0.00	0.00	<0.1	<0.001	0.00
15-AG-105	<0.01	<0.0003	0.00	0.00	0.15	<0.001	0.00
15-AG-106	<0.01	0.00	<0.0001	<0.001	<0.1	<0.001	<0.0001
15-AG-107	<0.01	<0.0003	<0.0001	<0.001	<0.1	<0.001	<0.0001
15-AG-108	<0.01	<0.0003	0.00	<0.001	<0.1	0.01	0.00
15-AG-109	<0.01	0.00	0.01	0.02	0.99	0.01	0.00
15-AG-110	0.02	<0.0003	<0.0001	<0.001	<0.1	0.09	0.00
15-AG-111	<0.01	<0.0003	0.00	<0.001	<0.1	<0.001	0.00
15-AG-112	<0.01	<0.0003	0.01	0.02	0.85	0.02	0.00
15-AG-113	<0.01	<0.0003	0.00	<0.001	<0.1	0.12	0.00
15-AG-114	<0.01	<0.0003	<0.0001	<0.001	<0.1	<0.001	<0.0001
15-AG-115	0.01	<0.0003	<0.0001	<0.001	<0.1	0.07	<0.0001
15-AG-116	0.01	0.00	<0.0001	<0.001	<0.1	<0.001	0.00
15-AG-117	<0.01	<0.0003	<0.0001	<0.001	<0.1	<0.001	<0.0001
15-AG-118	0.01	0.00	0.00	0.00	1.13	0.00	0.00
15-AG-119	0.04	<0.0003	0.00	0.00	<0.1	<0.001	0.00
15-AG-120	0.02	<0.0003	0.00	<0.001	0.42	<0.001	0.00
15-AG-121	<0.01	<0.0003	<0.0001	<0.001	<0.1	<0.001	<0.0001
15-AG-122	<0.01	<0.0003	0.00	<0.001	0.49	<0.001	0.00
15-AG-123	<0.01	<0.0003	0.00	<0.001	0.87	0.06	0.00
15-AG-124	<0.01	<0.0003	<0.0001	<0.001	0.72	<0.001	<0.0001
15-AG-125	0.03	0.00	0.00	<0.001	0.68	<0.001	0.00
15-AG-126	0.05	0.00	0.00	<0.001	0.46	<0.001	0.00
15-AG-127	<0.01	0.00	0.00	<0.001	0.76	<0.001	0.00
15-AG-128	0.01	0.00	0.00	<0.001	0.64	<0.001	0.00
15-AG-129	<0.01	<0.0003	0.00	0.01	2.01	0.00	0.00
15-AG-130	0.01	0.00	<0.0001	0.00	0.58	0.00	0.00
15-AG-131	0.01	0.00	0.00	<0.001	0.46	<0.001	<0.0001
15-AG-132	<0.01	<0.0003	<0.0001	<0.001	0.17	0.00	<0.0001
15-AG-133	0.01	0.00	0.00	<0.001	<0.1	0.05	0.00
15-AG-134	<0.01	<0.0003	<0.0001	<0.001	<0.1	<0.001	<0.0001

Sample	Sn	Ta	Tb	Th	Ti	Tl	Tm
	µg/L	µg/L	µg/L	µg/L	µg/L	µg/L	µg/L
15-AG-135	0.03	0.00	<0.0001	<0.001	0.16	<0.001	0.00
15-AG-136	<0.01	<0.0003	<0.0001	<0.001	0.34	<0.001	0.00
15-AG-136	<0.01	<0.0003	<0.0001	<0.001	0.34	<0.001	0.00
15-AG-137	0.01	<0.0003	0.00	<0.001	1.25	<0.001	0.00
15-AG-138	<0.01	<0.0003	0.00	<0.001	0.40	<0.001	0.00
15-AG-139	0.02	<0.0003	<0.0001	<0.001	1.64	<0.001	0.00
15-AG-140	<0.01	<0.0003	<0.0001	<0.001	0.29	<0.001	0.00
15-AG-141	<0.01	<0.0003	0.00	<0.001	0.64	<0.001	0.00
15-AG-142	<0.01	<0.0003	<0.0001	<0.001	0.16	<0.001	<0.0001
15-AG-143	<0.01	<0.0003	0.00	<0.001	0.69	<0.001	0.00
15-AG-144	<0.01	<0.0003	0.00	<0.001	0.45	0.01	<0.0001
15-AG-145	<0.01	<0.0003	0.00	<0.001	<0.1	0.01	0.00
15-AG-146	<0.01	<0.0003	0.00	<0.001	1.66	<0.001	0.00
15-AG-147	<0.01	<0.0003	<0.0001	<0.001	0.77	<0.001	0.00
15-AG-148	<0.01	0.00	0.00	<0.001	0.62	<0.001	<0.0001
15-AG-149	<0.01	<0.0003	<0.0001	<0.001	0.24	0.01	0.00
15-AG-150	0.02	<0.0003	0.00	0.00	0.47	<0.001	0.00
15-AG-151	<0.01	<0.0003	0.00	<0.001	0.19	<0.001	0.00
15-AG-152	0.04	<0.0003	0.00	<0.001	0.31	0.00	0.00
15-AG-153	0.03	<0.0003	0.00	0.01	1.26	<0.001	0.00
15-AG-165	0.03	0.00	0.00	0.00	1.67	<0.001	0.00
15-AG-166	0.05	<0.0003	0.00	<0.001	<0.1	<0.001	0.00
15-AG-167	0.19	<0.0003	0.00	<0.001	0.65	0.00	0.00
15-AG-168	0.02	0.00	0.00	<0.001	<0.1	<0.001	0.00
15-AG-169	<0.01	<0.0003	0.00	0.00	1.87	0.00	0.00
15-AG-170	0.02	0.00	0.00	0.00	0.57	<0.001	0.00
15-AG-171	0.44	0.00	0.00	0.00	0.14	0.00	0.00
15-AG-172	0.01	<0.0003	<0.0001	<0.001	<0.1	<0.001	<0.0001
15-AG-173	<0.01	<0.0003	<0.0001	<0.001	<0.1	<0.001	<0.0001
15-AG-174	0.07	0.00	0.00	<0.001	<0.1	<0.001	0.00
15-AG-175	<0.01	0.00	0.00	<0.001	0.65	<0.001	0.00
15-AG-176	<0.01	0.00	0.00	<0.001	0.50	<0.001	0.00
15-AG-177	0.04	0.00	0.00	<0.001	<0.1	<0.001	0.00
15-AG-178	<0.01	<0.0003	0.00	<0.001	<0.1	<0.001	0.00
15-AG-179	<0.01	<0.0003	<0.0001	<0.001	<0.1	<0.001	0.00
15-AG-180	<0.01	<0.0003	0.00	0.00	<0.1	<0.001	0.00
15-AG-181	<0.01	<0.0003	0.00	<0.001	<0.1	0.00	0.00
15-AG-182	<0.01	<0.0003	0.00	<0.001	0.29	<0.001	0.00

Sample	Sn	Ta	Tb	Th	Ti	Tl	Tm
	µg/L	µg/L	µg/L	µg/L	µg/L	µg/L	µg/L
15-AG-183	<0.01	<0.0003	0.00	<0.001	0.74	<0.001	<0.0001
15-AG-184	13.10	<0.0003	0.00	<0.001	0.34	<0.001	<0.0001
15-AG-185	<0.01	<0.0003	0.00	0.00	<0.1	0.01	0.00
15-AG-186	<0.01	<0.0003	0.00	<0.001	0.76	0.18	0.00
15-AG-187	<0.01	<0.0003	<0.0001	<0.001	<0.1	<0.001	<0.0001
15-AG-188	0.30	0.00	0.00	0.06	3.28	<0.001	0.00
15-AG-189	0.04	<0.0003	0.00	0.00	0.33	<0.001	0.00
15-AG-190	0.02	<0.0003	<0.0001	<0.001	0.97	<0.001	0.00
15-AG-191	0.10	0.00	<0.0001	<0.001	<0.1	<0.001	<0.0001
15-AG-192	<0.01	<0.0003	<0.0001	<0.001	<0.1	<0.001	<0.0001

Appendix N: Trace Constituents – U, V, W, Y, Yb, Zn, Zr

Sample	U	V	W	Y	Yb	Zn	Zr
	µg/L	µg/L	µg/L	µg/L	µg/L	µg/L	µg/L
15-AG-001	0.05	0.01	0.03	0.05	<0.001	3.20	<0.1
15-AG-002	0.46	0.03	0.06	0.03	<0.001	127.40	<0.1
15-AG-003	1.53	0.01	0.02	0.01	<0.001	1.40	<0.1
15-AG-004	13.44	0.05	<0.01	0.01	0.00	2.00	<0.1
15-AG-005	1.58	0.10	<0.01	0.06	<0.001	105.20	<0.1
15-AG-006	1.83	0.09	0.02	0.33	0.01	1.20	0.26
15-AG-007	0.87	0.75	<0.01	0.06	0.01	1.30	0.11
15-AG-008	0.48	0.22	0.01	0.03	0.00	2.80	<0.1
15-AG-009	0.09	0.36	<0.01	0.11	0.01	1.20	<0.1
15-AG-010	0.19	0.14	0.03	0.05	0.00	1.10	<0.1
15-AG-011	0.86	0.40	<0.01	0.03	0.00	<1	<0.1
15-AG-012	0.03	0.05	0.01	0.04	<0.001	17.80	<0.1
15-AG-013	0.00	0.09	0.17	0.01	<0.001	<1	<0.1
15-AG-014	1.09	0.05	<0.01	0.08	<0.001	9.30	<0.1
15-AG-015	6.50	0.13	<0.01	0.04	0.00	4.50	0.22
15-AG-016	3.27	0.29	<0.01	0.09	0.00	6.10	1.70
15-AG-017	0.16	0.17	<0.01	0.05	<0.001	4.10	0.46
15-AG-018	0.09	0.56	0.02	0.30	0.03	<1	0.38
15-AG-019	0.09	0.54	0.02	0.29	0.02	2.70	0.40
15-AG-020	0.13	0.15	0.01	0.12	0.00	3.20	0.86
15-AG-021	0.05	0.10	0.12	0.10	0.00	4.50	<0.1
15-AG-022	1.41	0.18	0.10	0.09	0.00	<1	0.21
15-AG-023	0.77	0.32	<0.01	0.16	0.01	5.50	0.24

Sample	U	V	W	Y	Yb	Zn	Zr
	µg/L	µg/L	µg/L	µg/L	µg/L	µg/L	µg/L
15-AG-024	2.61	0.17	<0.01	0.12	0.01	17.35	0.16
15-AG-025	2.63	0.08	<0.01	0.06	0.00	4.50	<0.1
15-AG-026	0.03	0.02	0.01	0.06	<0.001	3.20	<0.1
15-AG-027	0.58	0.01	<0.01	0.08	<0.001	2.90	<0.1
15-AG-028	0.93	0.12	<0.01	0.07	<0.001	10.50	<0.1
15-AG-029	12.76	0.02	<0.01	0.11	<0.001	5.00	<0.1
15-AG-030	1.19	0.05	<0.01	0.08	0.00	4.60	0.15
15-AG-031	1.17	0.04	<0.01	0.08	0.00	11.20	0.15
15-AG-032	0.00	0.00	<0.01	<0.0005	<0.001	<1	<0.1
15-AG-033	0.47	0.07	0.01	0.03	0.00	5.10	0.13
15-AG-034	3.16	0.16	<0.01	0.10	0.01	3.60	0.17
15-AG-035	1.62	0.11	<0.01	0.06	<0.001	109.30	<0.1
15-AG-036	0.56	0.01	<0.01	0.08	<0.001	3.50	<0.1
15-AG-037	0.41	0.05	<0.01	0.09	0.00	7.60	<0.1
15-AG-038	1.57	0.37	<0.01	0.11	0.00	212.40	0.15
15-AG-039	0.01	0.05	0.12	0.03	0.00	9.90	<0.1
15-AG-040	1.34	0.13	<0.01	0.04	<0.001	10.70	<0.1
15-AG-041	0.02	0.01	<0.01	0.07	0.00	21.00	<0.1
15-AG-042	0.01	<0.003	0.01	0.06	<0.001	4.00	<0.1
15-AG-043	0.01	0.01	0.02	0.07	<0.001	1.85	<0.1
15-AG-044	0.12	0.01	<0.01	0.08	<0.001	2.50	<0.1
15-AG-045	0.11	0.03	0.01	0.05	<0.001	2.60	<0.1
15-AG-046	2.54	0.02	<0.01	0.04	0.00	75.50	<0.1
15-AG-047	0.85	0.03	<0.01	0.05	0.01	9.60	<0.1
15-AG-048	5.91	0.27	<0.01	0.27	0.02	332.90	0.51
15-AG-049	0.09	0.33	0.01	0.11	0.01	1.15	<0.1
15-AG-050	0.71	0.86	0.02	0.09	0.01	3.90	1.07
15-AG-051	1.07	0.02	<0.01	0.09	<0.001	5.50	<0.1
15-AG-052	0.10	0.01	<0.01	0.01	<0.001	1.30	<0.1
15-AG-053	0.70	0.07	<0.01	0.11	0.01	7.40	<0.1
15-AG-054	0.05	0.00	0.02	0.05	<0.001	1.50	<0.1
15-AG-055	0.09	<0.003	<0.01	0.06	<0.001	3.00	<0.1
15-AG-056	0.01	0.02	<0.01	0.06	<0.001	5.60	<0.1
15-AG-057	1.06	0.30	<0.01	0.07	<0.001	34.20	<0.1
15-AG-058	0.01	0.01	<0.01	0.06	<0.001	6.30	<0.1
15-AG-059	0.02	<0.003	0.02	0.06	<0.001	3.90	<0.1
15-AG-060	1.05	0.30	<0.01	0.06	0.00	36.20	<0.1
15-AG-061	0.06	0.01	<0.01	0.08	<0.001	3.60	<0.1

Sample	U	V	W	Y	Yb	Zn	Zr
	µg/L	µg/L	µg/L	µg/L	µg/L	µg/L	µg/L
15-AG-062	2.33	0.04	<0.01	0.05	0.00	1.10	<0.1
15-AG-063	1.43	0.01	<0.01	0.05	<0.001	3.90	<0.1
15-AG-064	0.39	0.16	<0.01	0.11	0.00	7.80	0.21
15-AG-065	0.14	0.05	<0.01	0.10	0.00	5.00	1.47
15-AG-066	4.77	0.04	<0.01	0.01	0.00	26.80	<0.1
15-AG-067	2.17	0.05	<0.01	0.09	0.00	15.00	<0.1
15-AG-068	1.47	0.03	<0.01	0.15	0.00	25.20	<0.1
15-AG-069	0.01	0.02	0.03	0.06	<0.001	4.20	<0.1
15-AG-070	0.01	0.02	0.03	0.06	<0.001	4.10	<0.1
15-AG-071	0.02	0.02	0.03	0.06	<0.001	4.80	<0.1
15-AG-072	0.03	0.04	0.03	0.05	<0.001	3.90	<0.1
15-AG-073	0.13	0.01	0.02	0.10	<0.001	<1	<0.1
15-AG-074	0.02	0.03	0.02	0.07	<0.001	2.00	<0.1
15-AG-075	1.56	0.10	<0.01	0.07	0.00	107.40	<0.1
15-AG-076	9.38	0.02	<0.01	0.12	0.00	5.20	0.38
15-AG-077	1.78	0.55	0.02	0.08	0.01	<1	0.35
15-AG-078	12.85	0.26	<0.01	0.12	0.02	19.60	0.27
15-AG-079	0.01	0.07	0.12	0.03	0.00	9.40	<0.1
15-AG-080	1.99	0.25	<0.01	0.23	0.01	65.10	0.30
15-AG-081	2.11	0.04	<0.01	0.06	<0.001	5.00	<0.1
15-AG-082	0.05	0.03	0.08	0.00	<0.001	1.60	<0.1
15-AG-083	1.01	0.20	0.01	0.06	0.00	4.30	<0.1
15-AG-084	0.01	0.02	0.06	0.05	<0.001	4.40	<0.1
15-AG-085	3.01	0.04	<0.01	0.08	<0.001	7.00	0.27
15-AG-086	0.02	0.17	0.05	0.07	0.00	2.70	<0.1
15-AG-087	0.08	0.01	<0.01	0.06	<0.001	26.30	<0.1
15-AG-088	0.21	0.04	<0.01	0.07	<0.001	2.70	<0.1
15-AG-089	0.09	0.32	<0.01	0.12	0.01	1.20	<0.1
15-AG-090	0.18	0.20	0.03	0.09	<0.001	2.80	<0.1
15-AG-091	0.01	0.04	0.01	0.06	<0.001	4.90	<0.1
15-AG-092	<0.0002	0.01	<0.01	<0.0005	<0.001	<1	<0.1
15-AG-093	0.82	3.71	0.48	0.06	<0.001	8.60	<0.1
15-AG-094	0.25	0.52	0.05	0.08	0.00	5.40	<0.1
15-AG-095	0.07	0.01	0.02	0.06	<0.001	5.20	<0.1
15-AG-096	1.29	0.09	<0.01	0.07	0.00	16.10	<0.1
15-AG-097	1.36	0.22	<0.01	0.10	0.00	153.50	0.38
15-AG-098	0.43	0.02	<0.01	0.02	<0.001	5.20	<0.1
15-AG-099	1.27	0.05	<0.01	0.08	<0.001	23.40	<0.1

Sample	U	V	W	Y	Yb	Zn	Zr
	µg/L	µg/L	µg/L	µg/L	µg/L	µg/L	µg/L
15-AG-100	0.11	0.02	0.02	0.07	<0.001	4.20	<0.1
15-AG-101	0.61	0.02	<0.01	0.05	0.00	4.20	<0.1
15-AG-102	0.17	0.04	<0.01	0.05	0.01	8.10	<0.1
15-AG-103	0.02	0.02	<0.01	0.04	<0.001	1.90	<0.1
15-AG-104	0.16	0.12	<0.01	0.11	0.01	1.60	0.44
15-AG-105	0.16	0.53	0.02	0.09	0.00	13.30	<0.1
15-AG-106	0.07	0.01	0.01	0.06	<0.001	2.90	<0.1
15-AG-107	0.07	0.01	0.02	0.01	<0.001	6.70	<0.1
15-AG-108	10.70	0.07	<0.01	0.08	0.00	84.30	0.19
15-AG-109	3.37	0.40	<0.01	0.39	0.02	45.30	0.92
15-AG-110	3.09	0.15	<0.01	0.02	0.00	28.70	<0.1
15-AG-111	0.18	0.10	<0.01	0.03	0.00	1.60	0.16
15-AG-112	3.54	0.43	<0.01	0.36	0.02	67.60	0.81
15-AG-113	9.55	0.02	<0.01	0.03	0.00	519.20	<0.1
15-AG-114	0.44	0.01	0.02	0.00	<0.001	2.50	<0.1
15-AG-115	1.68	0.11	<0.01	0.07	<0.001	117.40	<0.1
15-AG-116	0.03	0.03	0.04	0.07	<0.001	2.80	<0.1
15-AG-117	0.04	0.01	0.03	0.05	<0.001	3.90	<0.1
15-AG-118	12.65	1.41	0.02	0.10	0.01	3.50	0.19
15-AG-119	0.00	0.05	0.13	0.03	<0.001	10.00	<0.1
15-AG-120	1.58	0.11	0.01	0.24	0.00	60.50	0.74
15-AG-121	0.10	0.01	0.12	0.06	<0.001	4.60	<0.1
15-AG-122	0.02	0.03	0.01	0.07	<0.001	3.40	<0.1
15-AG-123	1.39	2.29	0.02	0.02	0.00	249.55	0.16
15-AG-124	0.03	0.02	<0.01	0.05	<0.001	28.70	<0.1
15-AG-125	0.19	0.02	0.21	0.12	0.00	3.40	<0.1
15-AG-126	0.04	0.03	0.10	0.07	0.00	3.60	<0.1
15-AG-127	0.14	0.03	0.06	0.08	<0.001	2.50	<0.1
15-AG-128	0.34	0.02	0.37	0.07	<0.001	2.50	<0.1
15-AG-129	0.09	0.39	<0.01	0.11	0.01	1.00	<0.1
15-AG-130	3.25	0.28	0.03	0.11	<0.001	2.30	<0.1
15-AG-131	0.05	0.03	0.04	0.05	<0.001	1.80	<0.1
15-AG-132	0.05	0.02	<0.01	0.00	<0.001	21.50	<0.1
15-AG-133	0.54	0.10	0.03	0.06	0.00	63.60	<0.1
15-AG-134	0.12	0.04	0.06	0.01	<0.001	5.50	<0.1
15-AG-135	0.03	0.03	0.05	0.02	<0.001	1.40	<0.1
15-AG-136	0.07	0.01	0.02	0.06	<0.001	3.20	<0.1
15-AG-137	0.02	0.02	0.05	0.07	<0.001	2.20	<0.1

Sample	U	V	W	Y	Yb	Zn	Zr
	µg/L	µg/L	µg/L	µg/L	µg/L	µg/L	µg/L
15-AG-138	0.35	0.02	<0.01	0.11	0.00	3.70	<0.1
15-AG-139	0.01	<0.003	<0.01	0.09	<0.001	2.70	<0.1
15-AG-140	0.12	0.04	<0.01	0.11	<0.001	2.40	0.13
15-AG-141	0.19	<0.003	<0.01	0.06	<0.001	4.70	<0.1
15-AG-142	<0.0002	<0.003	<0.01	<0.0005	<0.001	<1	<0.1
15-AG-143	0.01	0.00	<0.01	0.06	<0.001	3.30	<0.1
15-AG-144	5.14	0.02	0.01	0.11	0.00	2.40	<0.1
15-AG-145	14.36	0.11	<0.01	0.12	0.00	105.20	0.17
15-AG-146	0.02	<0.003	<0.01	0.09	<0.001	2.00	<0.1
15-AG-147	0.02	0.01	0.02	0.06	<0.001	2.60	<0.1
15-AG-148	0.02	0.01	0.02	0.06	<0.001	2.50	<0.1
15-AG-149	5.34	0.02	0.01	0.10	0.00	2.30	<0.1
15-AG-150	0.07	0.20	0.06	0.10	0.00	<1	0.25
15-AG-151	1.06	0.17	0.01	0.04	0.00	1.50	0.58
15-AG-152	0.37	0.24	<0.01	0.07	0.00	26.70	0.25
15-AG-153	0.30	0.61	0.35	0.24	0.01	4.70	0.95
15-AG-165	0.06	0.71	1.04	0.12	0.00	3.00	0.99
15-AG-166	0.38	0.03	0.30	0.06	0.00	3.90	<0.1
15-AG-167	0.80	0.03	0.06	0.07	0.00	9.90	<0.1
15-AG-168	0.32	0.02	0.76	0.02	0.00	1.45	<0.1
15-AG-169	0.09	0.36	0.02	0.11	0.01	<1	<0.1
15-AG-170	0.09	0.01	0.06	0.09	<0.001	4.50	<0.1
15-AG-171	0.13	0.03	0.12	0.03	<0.001	8.80	<0.1
15-AG-172	0.26	0.01	0.10	0.01	<0.001	6.40	<0.1
15-AG-173	2.52	0.01	0.04	0.01	0.00	2.10	<0.1
15-AG-174	0.12	0.01	1.31	0.04	<0.001	1.20	<0.1
15-AG-175	0.05	0.03	0.23	0.08	0.00	2.90	<0.1
15-AG-176	0.10	0.01	0.10	0.07	0.00	2.60	<0.1
15-AG-177	0.61	0.03	0.13	0.04	<0.001	2.35	<0.1
15-AG-178	2.12	0.03	2.94	0.12	0.01	<1	0.52
15-AG-179	0.50	0.03	0.13	0.04	<0.001	<1	<0.1
15-AG-180	0.13	0.16	0.08	0.06	0.01	<1	2.04
15-AG-181	1.74	0.09	0.02	0.03	0.00	<1	<0.1
15-AG-182	0.01	0.02	0.02	0.10	0.00	2.60	<0.1
15-AG-183	0.06	0.66	0.02	0.21	<0.001	<1	0.58
15-AG-184	1.67	0.06	0.56	0.04	<0.001	3.00	<0.1
15-AG-185	0.73	0.08	0.23	0.08	0.00	3.70	<0.1
15-AG-186	17.84	0.06	0.17	0.20	0.01	58.00	0.24

Sample	U	V	W	Y	Yb	Zn	Zr
	µg/L	µg/L	µg/L	µg/L	µg/L	µg/L	µg/L
15-AG-187	0.10	0.06	0.20	0.06	<0.001	<1	<0.1
15-AG-188	0.86	0.27	3.99	0.22	0.01	3.50	0.20
15-AG-189	0.00	0.03	0.13	0.03	<0.001	8.90	<0.1
15-AG-190	0.08	0.04	0.51	0.07	0.00	3.60	<0.1
15-AG-191	0.18	0.07	0.51	0.04	<0.001	<1	<0.1
15-AG-192	0.08	0.04	0.20	0.05	<0.001	<1	<0.1

Appendix O: Isotopic Parameters

Sample	Tritium	d18O	dD	DOC_d13C	DIC_d13C	δ34S_SO4	δ18O_SO4	δ34S_S2-	d13C_CH4
	TU	‰	‰	‰	‰	‰	‰	‰	‰
15-AG-001	<0.8	-10.4	-67	-25.9	-7.3	34.7	17.6		
15-AG-002	1.63	-11.1	-72	-26	-8.7	35.1	18.4		
15-AG-003	<0.8	-10.0	-64	-26.2	-8.6	31.3	18.0		
15-AG-004	9.69	-10.5	-68	-26.9	-11.5	-1.8	-1.4		
15-AG-005	3.05	-11.4	-75	-27	-8	25.6	15.7		
15-AG-006	2.05	-9.3	-59	-26.9	-11	12.7	11.2	-13.4	
15-AG-007	13.00	-8.9	-60	-26.4	-12.8	7.6	4.8		
15-AG-008	9.72	-9.1	-62	-27.7	-13.8	31	13.4	-3.1	
15-AG-009	<0.8	-10.5	-68	-26.6	-9.2	19.2	15.4		
15-AG-010	5.66	-10.7	-72	-27.6	-19.2	41.9	15.8	-3.1	-37
15-AG-011	12.46	-8.7	-61	-27.3	-13	25.4	12.7	-14.8	-55
15-AG-012	2.18	-10.1	-66	-26.6	-11.8	27.4	13.2	6.6	
15-AG-013	<0.8	-9.8	-64	-26.5	-2.7	15.5	-4.3		-68
15-AG-014	8.57	-9.6	-62	-25.3	-12.3	23.4	12.5		
15-AG-015	9.66	-8.9	-57	-27.5	-13	1.5	7.6		
15-AG-016	2.29	-9.1	-58	-26.7	-13.5	-2.2	10.2	-9.0	
15-AG-017	6.35	-9.7	-62	-27.4	-14.2	23.3	14.0		
15-AG-018	9.01	-9.5	-62	-27.7	-15.1	3.8	7.7	-36.1	
15-AG-019	13.28	-9.5	-63	-27.9	-15.1	5.3	7.3	-35.6	
15-AG-020	8.64	-10.0	-66	-27.8	-13.8	23.7	12.5	21.2	
15-AG-021	1.03	-10.1	-65	-27.1	-17.3	29.5	13.6	-8.1	
15-AG-022	2.10	-9.1	-58	-26.1	-14.1	3.6	7.5	2.0	
15-AG-023	10.38	-10.7	-70	-28.4	-14.9	1.7	9.1		
15-AG-024	9.60	-10.0	-64	-28.1	-17.2	3.2	11.4		
15-AG-025	12.22	-10.4	-68	-26.6	-15.1	7.1	3.4		

Sample	Tritium	d18O	dD	DOC_d13C	DIC_d13C	δ34S SO4	δ18O SO4	δ34S S2-	d13C_CH4
	TU	‰	‰	‰	‰	‰	‰	‰	‰
15-AG-026	9.94	-10.6	-68	-28.6	-13	24	12.9	25.7	
15-AG-027	4.74	-9.9	-65	-26.9	-12.8	21	10.6		
15-AG-028	1.10	-9.4	-61	-27.6	-11.3	11.5	4.7		
15-AG-029	8.55	-9.6	-62	-26.3	-13.7	16.6	8.4		
15-AG-030	9.96	-10.2	-66	-26.8	-14.2	20.7	10.7		
15-AG-031	6.99	-10.1	-66	-26.7	-14.1	21.2	10.6		
15-AG-032	0.00	-8.6	-66	0	-15.6	18.7	15.5		
15-AG-033	20.51	-8.2	-60	-25.7	-6.1	2.5	-5.5	-15.4	-61
15-AG-034	13.27	-10.2	-66	-25.3	-11.5	15.6	7.0		
15-AG-035	0.00	-11.5	-75	-26.4	-8	26.4	14.9		
15-AG-036	0.00	-10.3	-66	-25.7	-12.2	31.1	11.1		
15-AG-037	2.97	-9.9	-62	-28.1	-11.5	23.6	10.7	22.0	
15-AG-038	10.69	-9.7	-63	-29	-15.6	24.8	11.1		
15-AG-039	<0.8	-10.7	-69	-25.8	-9	18.6	15.5		
15-AG-040	10.88	-10.1	-65	-26.5	-14.5	19.4	9.1		
15-AG-041	<0.8	-9.9	-63	-26.4	-14.1	21.3	10.3		
15-AG-042	<0.8	-10.3	-67	-26.5	-10.2	28.6	14.7	-9.9	
15-AG-043	<0.8	-9.8	-62	-26.3	-9.8	28.2	15.6		
15-AG-044	<0.8	-9.8	-62	-26.5	-9.8	22.4	12.7		
15-AG-045	<0.8	-9.7	-61	-26.4	-9.8	14.5	11.1		
15-AG-046	30.16	-10.1	-66	-27.7	-14.3	17	6.2		
15-AG-047	23.65	-9.9	-65	-27.8	-14.9	14.3	8.4		
15-AG-048	11.60	-9.6	-61	-27.2	-14.4	2.4	12.1		
15-AG-049	<0.8	-10.6	-68	-26.5	-9.2	18.8	16.2		
15-AG-050	5.27	-10.0	-65	-26.9	-18.8	8.6	7.4	3.5	
15-AG-051	5.59	-9.8	-67	-25.8	-13	27.4	14.9		
15-AG-052	2.92	-9.5	-64	-25.9	-12.5	6.5	1.4		
15-AG-053	14.16	-9.7	-67	-28.3	-15.5	11.4	4.3		
15-AG-054	<0.8	-10.4	-70	-26.2	-8.2	29.5	15.8		-40
15-AG-055	<0.8	-13.3	-89	-26.7	-9.4	27.4	12.5	18.2	
15-AG-056	1.50	-9.6	-63	-26.6	-10.1	25.1	13.4	15.5	
15-AG-057	8.19	-9.5	-62	-27.7	-14.1	26.7	13.7		
15-AG-058	<0.8	-9.7	-63	-24.5	-5	25.2	12.6		
15-AG-059	<0.8	-9.6	-63	-27	-10.4	19.3	8.4		
15-AG-060	9.74	-9.6	-62	-27.6	-14.4	26.9	12.1		
15-AG-061	<0.8	-9.4	-61	-27.1	-13.3	17.3	6.9		
15-AG-062	13.18	-9.3	-59	-26.9	-13.8	-3.3	-0.2		
15-AG-063	15.84	-10.1	-65	-26.7	-14	24.2	11.6		

Sample	Tritium	d18O	dD	DOC_d13C	DIC_d13C	δ34S SO4	δ18O SO4	δ34S S2-	d13C_CH4
	TU	‰	‰	‰	‰	‰	‰	‰	‰
15-AG-064	5.31	-9.6	-62	-27.3	-13.4	16.8	8.0		
15-AG-065	2.32	-9.4	-61	-26.6	-12.9	-1.6	7.0	-16.2	
15-AG-066	<0.8	-10.7	-71	-28.1	-16.5	-1.2	5.5		
15-AG-067	4.68	-9.8	-65	-27.2	-12.7	12.6	7.8		
15-AG-068	12.88	-9.6	-64	-26.7	-13.8	18.8	9.3		
15-AG-069	<0.8	-9.4	-61	-27	-7.5	18.3	11.5	20.5	
15-AG-070	<0.8	-9.5	-62	-26.6	-7.1	20.5	11.8	20.3	
15-AG-071	0.83	-14.8	-101	-27.6	-12.5	40.5	12.9	-12.4	
15-AG-072	1.03	-10.1	-65	-26.4	-6.5	17	11.0		
15-AG-073	<0.8	-10.1	-65	-26.1	-13.8	26.4	13.7		
15-AG-074	<0.8	-10.5	-69	-26.1	-6.3	22.3	10.4		
15-AG-075	13.05	-11.5	-76	-26.5	-7.8	26.1	14.0		
15-AG-076	3.62	-9.4	-64	-27	-13.2	16.9	5.7		
15-AG-077	11.04	-8.8	-58	-27.9	-14.5	9.7	9.7	-14.0	-60
15-AG-078	12.19	-9.0	-58	-27.7	-16	6.8	7.5		
15-AG-079	<0.8	-10.4	-69	-24.9	-8.9	20.7	13.7		
15-AG-080	8.47	-9.8	-64	-26.8	-13.8	7.4	8.4		
15-AG-081	0.82	-9.8	-64	-27.4	-12.2	17.2	9.1		
15-AG-082	1.86	-11.9	-79	-26	-6.6	26.2	15.1		
15-AG-083	16.05	-10.2	-67	-27.6	-15.3	25.6	12.5		
15-AG-084	<0.8	-10.8	-71	-26.2	-7.4	29.9	13.2	22.8	-26
15-AG-085	1.69	-9.5	-62	-26.9	-12.4	11.9	3.9		
15-AG-086	<0.8	-9.9	-65	-26.7	-18.1	14.3	9.2	-13.3	
15-AG-087	<0.8	-9.8	-64	-27.4	-13.4	19.9	8.8		
15-AG-088	<0.8	-9.6	-63	-26.6	-11.7	9.4	7.0		
15-AG-089	18.92	-10.5	-69	-26.6	-9.2	17.2	14.0		
15-AG-090	2.26	-10.9	-73	-27.2	-15.7	28.1	12.9		
15-AG-091	2.87	-9.9	-65	-26.6	-9.9	18.9	10.2	4.4	
15-AG-092	0.00	-8.5	-66	-26.5	-16.4	17.4	14.1		
15-AG-093	9.16	-11.0	-73	-28.9	-12.7	29.5	14.6	21.9	
15-AG-094	<0.8	-12.4	-83	-28.6	-13.1	31.1	13.0	-3.8	
15-AG-095	<0.8	-11.0	-74	-26.4	-7	27.9	12.2		
15-AG-096	16.04	-9.9	-65	-27.5	-15.9	22	12.6		
15-AG-097	13.80	-10.5	-68	-26.6	-14.1	10.5	10.0		
15-AG-098	3.02	-10.4	-67	-26.7	-12.8	26.3	14.2		
15-AG-099	15.56	-9.7	-64	-27.5	-15.5	21.4	13.4		
15-AG-100	2.32	-9.8	-65	-27.8	-13.1	30	15.4	-16.2	-42
15-AG-101	16.07	-9.8	-64	-27	-13.5	12.8	7.5		

Sample	Tritium	d18O	dD	DOC_d13C	DIC_d13C	δ34S SO4	δ18O SO4	δ34S S2-	d13C_CH4
	TU	‰	‰	‰	‰	‰	‰	‰	‰
15-AG-102	14.84	-10.3	-68	-27.8	-14	14.2	8.8		
15-AG-103	<0.8	-10.2	-66	-26.3	-10.9	25.3	14.8		
15-AG-104	17.00	-9.7	-64	-26.5	-14.8	10.5	8.8		
15-AG-105	4.93	-10.7	-71	-28.2	-14.7	19.1	11.7		
15-AG-106	<0.8	-10.6	-72	-26.6	-6.4	15.4	10.6		
15-AG-107	1.02	-8.5	-58	-27.1	-6	4.7	10.7		
15-AG-108	8.54	-9.8	-63	-26.9	-12.6	6.4	4.8		
15-AG-109	3.01	-9.5	-63	-26.5	-14.2	3.8	3.7		
15-AG-110	10.70	-9.9	-66	-27.3	-15.4	14.5	5.1		
15-AG-111	1.20	-9.9	-64	-26.5	-13	20.1	11.3		
15-AG-112	4.11	-9.7	-64	-26.5	-14.3	4.2	3.3		
15-AG-113	13.98	-8.7	-58	-27.3	-14.6	10	10.7		
15-AG-114	7.14	-11.1	-74	-26.6	-9.4	13	2.9		
15-AG-115	20.31	-11.5	-76	-27.1	-8.2	26.7	13.2		
15-AG-116	<0.8	-12.4	-85	-26.7	-22.1	26.2	12.2		
15-AG-117	<0.8	-11.4	-76	-26.7	-8.5	26.4	14.8	2.5	
15-AG-118	13.48	-10.3	-68	-27.9	-15.7	12.7	5.8		
15-AG-119	<0.8	-10.7	-70	-25.1	-9.5	16	14.8		
15-AG-120	8.32	-10.0	-66	-26.6	-14.9	16	10.1		
15-AG-121	<0.8	-13.7	-93	-27.1	-7.5	25.4	11.8	10.7	
15-AG-122	<0.8	-9.6	-63	-26.7	-12.3	15.6	7.7		
15-AG-123	17.83	-8.9	-58	-27	-13.2	22.6	11.1		
15-AG-124	<0.8	-14.8	-101	-26.3	-7.7	27.7	11.7		
15-AG-125	0.90	-13.7	-93	-29.8	-6.8	26.3	11.3		
15-AG-126	4.00	-11.7	-78	-27.2	-14.9	27.5	13.1	21.4	-34
15-AG-127	1.34	-11.8	-78	-28.8	-4.5	28	13.0		
15-AG-128	1.21	-14.0	-95	-29.7	-9	28	11.4	28.9	
15-AG-129	23.18	-10.7	-70	-26.1	-9.1	15.9	14.6		
15-AG-130	10.04	-10.0	-65	-27.5	-13.2	23.4	11.5	20.7	
15-AG-131	1.50	-11.9	-79	-26.3	-6.7	26.1	14.3		
15-AG-132	11.61	-11.9	-79	-25.5	-14.7	26.2	10.7		
15-AG-133	3.47	-10.8	-71	-26.7	-11.9	27.8	15.8		
15-AG-134	1.47	-11.5	-75	-25.8	-9.8	27.2	12.9		
15-AG-135	<0.8	-9.6	-63	-25.7	0.3	45.1	7.0	22.2	-77
15-AG-136	0.98	-9.4	-61	-26.6	-9.5	24.1	12.3		
15-AG-136	0.98	-9.4	-61	-26.6	-9.5	24.1	12.3		
15-AG-137	<0.8	-12.4	-83	-31.5	-13.9	31.2	13.0	26.2	
15-AG-138	12.72	-10.5	-69	-27.1	-13.5	24.2	11.6	23.9	

Sample	Tritium	d18O	dD	DOC_d13C	DIC_d13C	δ34S SO4	δ18O SO4	δ34S S2-	d13C_CH4
	TU	‰	‰	‰	‰	‰	‰	‰	‰
15-AG-139	<0.8	-15.6	-107	-35.1	-6.1	30.1	11.5		
15-AG-140	12.97	-10.7	-69	-26.3	-13.2	23.9	11.3		
15-AG-141	0.88	-11.9	-78	-27.2	-7.5	24.7	13.6		
15-AG-142	0.00	-9.1	-69	-26.9	-18.6	19.7	15.5		
15-AG-143	<0.8	-13.1	-87	-26	-5.4	28.7	12.1		
15-AG-144	13.81	-11.1	-72	-27.4	-12.8	23.5	10.7		
15-AG-145	19.02	-9.4	-60	-26.5	-13.5	5.3	5.8		
15-AG-146	1.43	-15.5	-107	-35.4	-6.2	30.5	11.0		
15-AG-147	1.32	-10.0	-66	-26.9	-12	13.5	8.2		
15-AG-148	1.86	-12.9	-87	-25.9	-8.3	28.7	12.6	28.0	
15-AG-149	16.13	-10.8	-70	-27.3	-13.1	22.7	11.4		
15-AG-150	2.41	-10.3	-66	-27	-14.4	23.5	13.4	4.4	
15-AG-151	15.09	-10.4	-67	-28	-15.1	35	17.9	-11.7	
15-AG-152	5.24	-10.7	-70	0	0	26.1	12.6		
15-AG-153	0.00	0.0	0	-26.8	-15.4	0	0.0		
15-AG-165	1.51	-10.9	-71	-29.2	-12.6	26	12.9	-9.3	-40
15-AG-166	<0.8	-10.4	-69	-27.3	-13.9	35.7	14.5	34.2	-43
15-AG-167	1.18	-11.2	-74	-28.8	-8.2	27.4	12.6		
15-AG-168	<0.8	-11.3	-75	-30.8	-9.3	25.6	13.2		
15-AG-169	15.59	-10.6	-70	-26.3	-9.4	18.5	14.1		
15-AG-170	<0.8	-12.3	-82	-30.3	-9.8	27.1	12.1		
15-AG-171	<0.8	-12.6	-85	-26	-4.4	4.6	5.5		
15-AG-172	2.05	-11.6	-77	-26.2	-9.3	28.3	12.9		
15-AG-173	3.53	-11.5	-76	-26.6	-9.4	17.9	3.9		
15-AG-174	1.64	0.0	0	-30	-6.3	28	14.6		
15-AG-175	1.96	0.0	0	-28.6	-7.8	27.3	12.8		-38
15-AG-176	<0.8	0.0	0	-30	-16.4	35.3	15.5		-28
15-AG-177	2.00	0.0	0	-29.4	-15	15.7	9.3		
15-AG-178	<0.8	0.0	0	-27.9	-13.4	7	-2.0		
15-AG-179	2.56	0.0	0	-29.3	-15	9.4	8.0		
15-AG-180	<0.8	0.0	0	-26.8	-15	7.7	17.0		-72
15-AG-181	12.05	0.0	0	-26.8	-10.1	2.6	-4.2		
15-AG-182	1.24	0.0	0	-26.7	-13.1	9.8	6.9		
15-AG-183	11.62	0.0	0	-27	-14.5	14.6	12.2		-71
15-AG-184	1.67	0.0	0	-25.9	-8.7	19.3	13.9	14.8	
15-AG-185	4.50	0.0	0	-27.9	-11.5	25.4	11.0		
15-AG-186	1.29	0.0	0	-26.3	-12.3	-2	-1.5		
15-AG-187	<0.8	0.0	0	-26.4	-6.9	20.6	11.7		

Sample	Tritium	d18O	dD	DOC_d13C	DIC_d13C	δ34S SO4	δ18O SO4	δ34S S2-	d13C_CH4
	TU	‰	‰	‰	‰	‰	‰	‰	‰
15-AG-188	1.35	0.0	0	-29.6	-11.8	31.9	13.4	24.3	
15-AG-189	<0.8	0.0	0	0	0	18.4	14.4		
15-AG-190	1.02	0.0	0	-26.8	-7.3	25.8	11.0	23.6	
15-AG-191	0.97	0.0	0	-29.8	-13.1	25.3	13.7		
15-AG-192	<0.8	0.0	0	-26.6	-6.9	20.3	12.3		

Appendix P: Water Type and Cl/Br Ratios

Station ID	Cluster	Water Type	Short Water Type	Cl/Br Mass Ratio
15-AG-001	B4	Ca-Na-SO4	Ca-SO4	28.5
15-AG-002	B4	Ca-SO4	Ca-SO4	70.2
15-AG-003	B4	Na-Ca-Mg-HCO3-SO4	Na-HCO3	52.9
15-AG-004	B4	Na-HCO3-SO4	Na-HCO3	1457.9
15-AG-006	B2	Mg-Ca-SO4-HCO3	Mg-SO4	146.7
15-AG-007	B3	Ca-Mg-HCO3-Cl	Ca-HCO3	875.7
15-AG-008	B3	Ca-Mg-HCO3-SO4	Ca-HCO3	290.6
15-AG-010	B4	Ca-Mg-SO4-HCO3	Ca-SO4	148.0
15-AG-011	B4	Ca-Mg-HCO3-Cl	Ca-HCO3	1540.7
15-AG-012	B2	Ca-Mg-SO4-HCO3	Ca-SO4	281.1
15-AG-013	B3	Na-Ca-HCO3	Na-HCO3	26.4
15-AG-014	A3	Ca-SO4	Ca-SO4	58.8
15-AG-015	B1	Mg-Ca-HCO3-SO4-Cl	Mg-HCO3	2986.4
15-AG-016	A2	Mg-SO4	Mg-SO4	135.0
15-AG-017	B1	Ca-Mg-SO4-HCO3	Ca-SO4	157.4
15-AG-018	B1	Mg-Ca-Na-SO4-HCO3-Cl	Mg-SO4	675.4
15-AG-019	B3	Mg-Ca-Na-HCO3-SO4-Cl	Mg-HCO3	963.2
15-AG-020	A3	Ca-SO4	Ca-SO4	179.8
15-AG-021	B2	Ca-Mg-SO4-HCO3	Ca-SO4	209.6
15-AG-022	B1	Mg-SO4-HCO3	Mg-SO4	106.6
15-AG-023	B1	Ca-Mg-HCO3-SO4-Cl	Ca-HCO3	1328.5
15-AG-024	B3	Ca-Mg-HCO3-SO4	Ca-HCO3	498.2
15-AG-025	B3	Ca-Mg-HCO3	Ca-HCO3	1118.9
15-AG-026	A2	Ca-SO4	Ca-SO4	160.9
15-AG-027	A2	Ca-Mg-SO4-HCO3	Ca-SO4	184.3
15-AG-028	A1	Ca-Mg-SO4	Ca-SO4	124.9
15-AG-029	A2	Ca-Mg-SO4	Ca-SO4	115.4
15-AG-030	B1	Ca-SO4-HCO3	Ca-SO4	229.1
15-AG-031	B1	Ca-SO4-HCO3	Ca-SO4	-1352.3
15-AG-033	B3	Ca-HCO3	Ca-HCO3	90.2
15-AG-034	B4	Ca-Mg-HCO3-SO4	Ca-HCO3	-907.3
15-AG-036	A2	Ca-SO4	Ca-SO4	72.7
15-AG-037	A1	Ca-Mg-SO4	Ca-SO4	969.7
15-AG-038	B4	Ca-SO4	Ca-SO4	209.7
15-AG-040	B1	Ca-Mg-SO4-HCO3	Ca-SO4	312.3
15-AG-041	A1	Ca-Mg-SO4	Ca-SO4	63.3

Station ID	Cluster	Water Type	Short Water Type	Cl/Br Mass Ratio
15-AG-042	A1	Ca-Mg-SO4	Ca-SO4	89.2
15-AG-043	B2	Ca-Mg-SO4	Ca-SO4	84.8
15-AG-044	B2	Ca-Mg-Na-SO4	Ca-SO4	68.5
15-AG-045	B2	Ca-Mg-Na-SO4	Ca-SO4	59.9
15-AG-046	B3	Ca-Mg-SO4-HCO3-Cl	Ca-SO4	338.6
15-AG-047	B1	Ca-Na-Mg-Cl-HCO3-SO4	Ca-Cl	2688.3
15-AG-048	B1	Mg-Ca-SO4-HCO3	Mg-SO4	1428.4
15-AG-050	A2	Mg-Ca-SO4	Mg-SO4	200.3
15-AG-051	B4	Ca-Mg-SO4-HCO3	Ca-SO4	292.8
15-AG-052	B1	Mg-Ca-HCO3	Mg-HCO3	825.1
15-AG-053	B3	Na-Ca-Cl-HCO3	Na-Cl	5960.1
15-AG-054	B2	Ca-Na-Mg-SO4	Ca-SO4	82.5
15-AG-055	A1	Ca-Mg-SO4	Ca-SO4	85.4
15-AG-056	A1	Ca-Mg-SO4	Ca-SO4	99.1
15-AG-057	A3	Ca-SO4	Ca-SO4	131.3
15-AG-058	A1	Ca-SO4	Ca-SO4	84.9
15-AG-059	A1	Ca-Mg-SO4	Ca-SO4	88.7
15-AG-060	A3	Ca-SO4	Ca-SO4	138.4
15-AG-061	A1	Ca-Mg-SO4	Ca-SO4	99.1
15-AG-062	B1	Ca-Mg-HCO3-SO4	Ca-HCO3	1401.0
15-AG-063	A2	Ca-SO4-HCO3	Ca-SO4	215.0
15-AG-064	A1	Ca-Mg-SO4	Ca-SO4	206.5
15-AG-065	A2	Mg-Ca-SO4	Mg-SO4	94.6
15-AG-066	B3	Ca-Mg-HCO3-SO4	Ca-HCO3	282.1
15-AG-067	A1	Ca-Mg-SO4	Ca-SO4	94.1
15-AG-068	B1	Ca-Mg-HCO3-SO4	Ca-HCO3	371.2
15-AG-069	A1	Ca-Mg-SO4	Ca-SO4	73.1
15-AG-070	A1	Ca-Mg-SO4	Ca-SO4	72.1
15-AG-071	A3	Ca-Mg-SO4-Cl	Ca-SO4	79.7
15-AG-072	B2	Ca-Mg-Na-SO4	Ca-SO4	74.6
15-AG-073	B4	Na-Mg-Ca-HCO3-SO4	Na-HCO3	56.6
15-AG-074	B2	Ca-Mg-Na-SO4	Ca-SO4	75.5
15-AG-076	A2	Ca-Mg-SO4	Ca-SO4	109.4
15-AG-077	B1	Mg-Ca-HCO3-SO4	Mg-HCO3	380.6
15-AG-078	B1	Mg-Ca-HCO3-SO4	Mg-HCO3	73.0
15-AG-080	B1	Mg-Ca-SO4-HCO3	Mg-SO4	515.8
15-AG-081	A1	Ca-Mg-SO4	Ca-SO4	117.3
15-AG-082	B4	Na-SO4-HCO3	Na-SO4	35.1
15-AG-083	B1	Ca-SO4-HCO3	Ca-SO4	601.5
15-AG-084	A1	Ca-Mg-SO4	Ca-SO4	59.7
15-AG-085	A2	Mg-Ca-SO4	Mg-SO4	140.5
15-AG-086	B4	Mg-Ca-SO4	Mg-SO4	95.7
15-AG-087	A1	Ca-Mg-Na-SO4-Cl	Ca-SO4	87.0
15-AG-088	B2	Ca-Mg-Na-SO4	Ca-SO4	67.5
15-AG-090	B2	Ca-Mg-Na-SO4-Cl	Ca-SO4	94.3
15-AG-091	A3	Ca-Mg-SO4	Ca-SO4	100.7
15-AG-093	A1	Ca-Na-Cl-SO4	Ca-Cl	88.4
15-AG-094	A3	Ca-Mg-Na-SO4-Cl	Ca-SO4	87.2
15-AG-095	A1	Ca-Mg-Na-SO4	Ca-SO4	84.4

Station ID	Cluster	Water Type	Short Water Type	Cl/Br Mass Ratio
15-AG-096	B1	Ca-Mg-SO4-HCO3	Ca-SO4	234.4
15-AG-097	B1	Ca-Mg-HCO3-SO4	Ca-HCO3	1219.3
15-AG-098	A2	Ca-Mg-SO4	Ca-SO4	112.5
15-AG-099	B3	Ca-Mg-SO4-HCO3	Ca-SO4	230.6
15-AG-100	A3	Ca-Mg-SO4-Cl	Ca-SO4	81.7
15-AG-101	B1	Ca-Mg-SO4-HCO3	Ca-SO4	587.0
15-AG-102	B1	Ca-Mg-HCO3-SO4-Cl	Ca-HCO3	709.2
15-AG-103	B1	Ca-Mg-SO4-HCO3	Ca-SO4	82.9
15-AG-104	B1	Ca-Mg-HCO3-Cl-SO4	Ca-HCO3	2501.2
15-AG-105	B2	Ca-Mg-Na-SO4	Ca-SO4	97.8
15-AG-106	B2	Ca-Na-Mg-SO4	Ca-SO4	56.0
15-AG-107	B2	Na-Ca-Mg-SO4	Na-SO4	60.2
15-AG-108	B1	Mg-Ca-SO4-HCO3	Mg-SO4	191.2
15-AG-109	A2	Mg-Ca-SO4	Mg-SO4	134.1
15-AG-110	B3	Ca-Na-HCO3-Cl	Ca-HCO3	2260.6
15-AG-111	B2	Ca-Mg-SO4-HCO3	Ca-SO4	90.4
15-AG-112	A2	Mg-Ca-SO4	Mg-SO4	133.1
15-AG-113	B3	Ca-Mg-SO4-HCO3-Cl	Ca-SO4	1418.1
15-AG-114	B2	Mg-Ca-HCO3-SO4	Mg-HCO3	1232.8
15-AG-116	B2	Ca-Mg-Na-SO4	Ca-SO4	91.0
15-AG-117	A1	Ca-Mg-SO4	Ca-SO4	75.4
15-AG-118	B1	Ca-Mg-HCO3-SO4-Cl	Ca-HCO3	127.6
15-AG-120	A2	Ca-Mg-SO4-HCO3	Ca-SO4	407.0
15-AG-121	A3	Ca-Mg-Na-SO4	Ca-SO4	93.2
15-AG-122	A1	Ca-Mg-SO4	Ca-SO4	97.5
15-AG-123	B3	Ca-SO4-HCO3	Ca-SO4	1118.5
15-AG-124	A1	Ca-Mg-Na-SO4	Ca-SO4	97.7
15-AG-125	A1	Ca-Mg-Na-SO4	Ca-SO4	92.9
15-AG-126	A3	Ca-Mg-SO4	Ca-SO4	91.2
15-AG-127	A1	Ca-Mg-SO4	Ca-SO4	101.4
15-AG-128	A1	Ca-Mg-Na-SO4	Ca-SO4	105.5
15-AG-130	B2	Ca-Mg-SO4-Cl	Ca-SO4	116.2
15-AG-131	B2	Ca-Mg-SO4	Ca-SO4	35.2
15-AG-132	B3	Ca-Mg-HCO3-SO4	Ca-HCO3	91.5
15-AG-133	B3	Ca-Mg-SO4-HCO3	Ca-SO4	251.3
15-AG-134	B2	Mg-Ca-HCO3-SO4	Mg-HCO3	-27.0
15-AG-135	B4	Na-HCO3-SO4	Na-HCO3	54.9
15-AG-136	A1	Ca-Mg-SO4	Ca-SO4	80.3
15-AG-137	A1	Na-Ca-Mg-Cl-SO4	Na-Cl	87.1
15-AG-138	A2	Ca-SO4	Ca-SO4	1147.3
15-AG-139	A1	Na-Ca-Mg-Cl-SO4	Na-Cl	91.2
15-AG-140	A2	Ca-SO4	Ca-SO4	719.3
15-AG-141	A1	Ca-Mg-SO4-Cl	Ca-SO4	89.8
15-AG-143	A1	Ca-Mg-SO4	Ca-SO4	96.1
15-AG-144	A3	Ca-SO4	Ca-SO4	265.3
15-AG-145	B4	Mg-Ca-SO4-HCO3	Mg-SO4	263.0
15-AG-146	A1	Na-Ca-Mg-Cl-SO4	Na-Cl	87.2
15-AG-147	A3	Ca-Mg-SO4	Ca-SO4	92.0
15-AG-148	A1	Ca-Mg-Na-SO4	Ca-SO4	59.4

Station ID	Cluster	Water Type	Short Water Type	Cl/Br Mass Ratio
15-AG-149	A3	Ca-SO4	Ca-SO4	263.0
15-AG-150	B1	Mg-Ca-HCO3	Mg-HCO3	103.5
15-AG-151	B1	Ca-Mg-HCO3-Cl	Ca-HCO3	2918.0
15-AG-152	A2	Ca-SO4	Ca-SO4	146.0
15-AG-153	B3	Mg-Ca-SO4-HCO3	Mg-SO4	132.7
15-AG-165	A3	Ca-Mg-Na-Cl-SO4	Ca-Cl	134.6
15-AG-166	A1	Ca-Mg-SO4	Ca-SO4	81.7
15-AG-167	A1	Ca-Mg-Na-SO4	Ca-SO4	105.2
15-AG-168	B4	Ca-Na-SO4-HCO3	Ca-SO4	-50.0
15-AG-170	A1	Ca-Na-Mg-SO4-Cl	Ca-SO4	100.0
15-AG-171	B2	Na-Ca-SO4	Na-SO4	52.1
15-AG-172	B2	Ca-Mg-HCO3-SO4	Ca-HCO3	104.2
15-AG-173	B2	Mg-Ca-HCO3-SO4	Mg-HCO3	265.0
15-AG-174	B2	Ca-Mg-Na-SO4	Ca-SO4	83.2
15-AG-175	A3	Ca-Mg-SO4	Ca-SO4	140.4
15-AG-176	A3	Ca-Mg-SO4-Cl	Ca-SO4	95.6
15-AG-177	B2	Na-Mg-Ca-Cl-SO4	Na-Cl	122.2
15-AG-178	B1	Mg-Na-Cl-SO4-HCO3	Mg-Cl	85.4
15-AG-179	B2	Na-Mg-Ca-Cl-SO4	Na-Cl	119.7
15-AG-180	B4	Ca-Mg-HCO3-SO4	Ca-HCO3	303.9
15-AG-181	B1	Ca-Mg-HCO3-Cl	Ca-HCO3	1209.3
15-AG-182	A1	Ca-Mg-SO4	Ca-SO4	111.8
15-AG-183	B1	Ca-Mg-HCO3	Ca-HCO3	284.6
15-AG-184	A1	Ca-SO4	Ca-SO4	164.8
15-AG-185	A1	Ca-Mg-SO4	Ca-SO4	99.8
15-AG-186	A2	Mg-SO4	Mg-SO4	119.6
15-AG-187	B4	Na-Ca-Mg-SO4	Na-SO4	43.4
15-AG-188	A1	Ca-Na-Mg-SO4-Cl	Ca-SO4	94.1
15-AG-190	A3	Ca-Na-Mg-SO4-Cl	Ca-SO4	92.9
15-AG-191	B3	Na-Ca-Mg-HCO3-SO4	Na-HCO3	92.0
15-AG-192	B4	Na-Ca-Mg-SO4	Na-SO4	37.5